AVERTISSEMENT

Ce document est le fruit d'un long travail approuvé par le jury de soutenance et mis à disposition de l'ensemble de la communauté universitaire élargie.

Il est soumis à la propriété intellectuelle de l'auteur. Ceci implique une obligation de citation et de référencement lors de l'utilisation de ce document.

D'autre part, toute contrefaçon, plagiat, reproduction illicite encourt une poursuite pénale.

Contact : ddoc-theses-contact@univ-lorraine.fr

LIENS

Code de la Propriété Intellectuelle. articles L 122. 4
Code de la Propriété Intellectuelle. articles L 335.2- L 335.10
http://www.cfcopies.com/V2/leg/leg_droi.php
http://www.culture.gouv.fr/culture/infos-pratiques/droits/protection.htm

INSTITUT NATIONAL POLYTECHNIQUE DE LORRAINE

ÉCOLE DOCTORALE SCIENCE ET INGÉNIERIE RESSOURCES PROCÉDÉS PRODUITS ENVIRONNEMENT

École Nationale Supérieure d'Agronomie et des Industries Alimentaires
Laboratoire de Science et Génie Alimentaires

Thèse

Présentée à l'Institut National Polytechnique de Lorraine

par

Guillaume GILLET

Pour obtenir le grade de Docteur de l'INPL

Spécialité : Procédés Biotechnologiques et Alimentaires

Prévision de la conformité des matériaux d'emballage par intégration de méthodes de déformulation et de modélisation du coefficient de partage

Soutenue publiquement le 14 Novembre 2008 devant la commission d'examen composée de :

Présidente du jury :

Mme Andrée Voilley	Professeur Université de Bourgogne-ENSBANA

Rapporteurs :

Mme Nathalie Gontard	Professeur Université Montpelier II
Mr Bernard Rousseau	Chargé de recherche CNRS - Orsay

Examinateurs :

Mr Carlos de la Cruz Garcia	Spécialiste sécurité et conformité des emballages Nestlé
Mr Stéphane Desobry	Professeur INPL, directeur de thèse
Mr Régis Lebossé	Responsable Division LNE- Trappes
Mr Olivier Vitrac	Chargé de recherche INRA, co-directeur de thèse

Remerciements

Je souhaite tout d'abord remercier l'Association Nationale pour la Recherche Technique d'avoir accepté de financer ce travail de thèse dans le cadre d'un contrat CIFRE au sein du Laboratoire National de métrologie et d'Essai et du Laboratoire de Science et Génie Alimentaires de l'École Nationale Supérieure d'Agronomie et des Industries Alimentaires.

Je remercie Mlle Gaëlle Lebrun, Mr Pierrick Camus et Mr Hervé Marcel de m'avoir accueilli au sein du Laboratoire National de métrologie et d'Essais. Je remercie également Mr Régis Lebossé pour avoir assuré l'encadrement industriel durant la dernière partie de la thèse.

Je remercie tout particulièrement Mr Stéphane Desobry, Professeur de l'Institut National Polytechnique de Lorraine et Directeur du Laboratoire de Science et Génie Alimentaires pour son encadrement, sa confiance et son soutien tout au long de la thèse.

Je tiens à remercier également Mr Olivier Vitrac, Chargé de Recherche INRA, pour sa disponibilité et son implication dans ces travaux.

J'exprime mes sincères remerciements à Mme Nathalie Gontard, Professeur de l'Université Montpellier II, et Mr Bernard Rousseau, Chargé de Recherche CNRS, pour avoir accepté de juger ce travail en qualité de rapporteurs.

Je remercie également Mme Andrée Voilley, Professeur de l'Université de Bourgogne-ENSABANA, et Mr Carlos de la Cruz Garcia, spécialiste sécurité et conformité des emballages, d'avoir accepté de prendre part à ce jury.

Je remercie vivement toutes les personnes du LNE avec lesquelles j'ai travaillé et en particulier celles qui m'ont formé et aidé pour les essais. Je pense surtout à Jacques, Cédric et Xavier, mais aussi à Isa, Véro, Valery, Sandrine, Marie-Claire, Séverine, Marilyn et Françoise. Je n'oublie pas non plus le travail qu'a réalisé Stéphanie durant son stage, merci à elle. Merci également à Natacha et Patrick pour leur aide concernant la règlementation. Merci aux documentalistes pour leur aide, merci à Mr Grolaud pour sa compréhension et sa réactivité.

Je remercie également toutes les personnes du LSGA qui m’ont supporté dans cette période difficile qu’est la rédaction du mémoire de thèse. Merci en particulier à Elmira, Laetitia et Imran.

Je voudrais aussi remercier les amis qui m’ont accompagné tout au long de ce périple. Les "pléiadiens" en particulier se reconnaîtront, mais je pense aussi à tous les autres et notamment à Matthieu qui vit aussi la grande aventure qu’est une thèse.

Je terminerai en remerciant ma famille et surtout mes parents sans qui rien n’aurait été possible. Merci, merci, merci pour m’avoir supporté et surtout aidé toutes ces années. Merci aussi à mon petit-frère Grégory pour me laisser encore le battre sur le playground et à Peyo pour mon éducation ludique.

In theory, there is no difference between theory and practice. But in practice, there is.
Jean L.A. van de Snepscheut

Mais surtout demander pourquoi l'axe de la planète ne germe pas, où va l'amour ou quel bruit fait le jaune.
Terry Pratchett

TABLE DES MATIÈRES

Liste des Figures

Liste des Tableaux

Liste des Équations

Glossaire

Sigles

ABS : Acrylonitrile-Butadiène-Styrène

ACTIA : Association de Coordination Technique pour l'Industrie Agroalimentaire

ANRT : Association Nationale pour la Recherche Technique

CAS : Chemical Abstract Service

CES : Chromatographie d'Exclusion Stérique

CFS : Chromatographie en Fluide Supercritique

CLHP : Chromatographie Liquide Haute Performance

CPG : Chromatographie Phase Gaz

CV : Coefficient de Variation

DEDL : Détecteur Évaporatif à Diffusion de Lumière

DIF : Détecteur à Ionisation de Flamme

DL : Domaine Linéaire

DSC : calorimétrie différentielle à balayage (Differential Scaling Calorimetry)

DST : Détecteur Sélectif Thermo-ionique

EAM : Extraction Assistée par Micro-onde

EFP : Extraction sous Fluide Pressurisé

EFS : Extraction sous Fluide Supercritique

ENSAIA : École Nationale Supérieure d'Agronomie te des Industries Alimentaires

ET : Espace de Tête

EPS : Extraction Phase Solide

EVA : éthylène-acétate de vinyle

EVOH : éthylène-alcool vinylique

INPL : Institut National Polytechnique de Lorraine

INRA : Institut National de la recherche Agronomique

IR : Infra Rouge

IRTF : Infra Rouge à Transformée de Fourier

LMG : Limite de Migration Globale

LMS : Limite de Migration Spécifique

LNE : Laboratoire National de métrologie et d'Essai

LSGA : Laboratoire de Science et Génie Alimentaires

MEPS : Micro-Extraction Phase Solide

MIR : Moyen Infra Rouge

PA : polyamides

PE : Polyéthylène

PEBD : Polyéthylène Basse Densité

PEHD : Polyéthylène Haute Densité

PET : Polyéthylène téréphtalate

PIR : Proche Infra Rouge

PO : Polyoléfine

PP : Polypropylène

PS : Polystyrène

PVC : poly(chlorure de vinyle)

PVdC : poly(chlorure de vinylidène)

Py : injection pyrolyse

RMN : Résonnance Magnétique Nucléaire

SB : Styrène-Butadiène

SM : Spectromètre de Masse

UV = Ultra Violet.

Abréviation relatives aux composés

F : aliment ou simulant de l'aliment

i : molécule de diffusant

P : polymère

Grandeurs physiques

$\underline{C}$: vecteur de concentrations ($mol \cdot L^{-1}$)

$C_{i,F}\big|_t$: concentration au temps t de la molécule *i* dans *F* ($mg \cdot kg^{-1}$)

$C_{i,F/P}$: concentration de *i* dans *F*, à la surface de *P* en contact avec *F*

$C_{i,k}$: Concentration de la molécule *i* dans *k* ($mg \cdot kg^{-1}$)

$C_{i,k}\big|_{eq}$: concentration à l'équilibre de la molécule *i* dans *k* ($mg \cdot kg^{-1}$)

$C_{i,P}\big|_{t=0}$: concentration initiale de la molécule *i* dans le polymère *P* ($mg \cdot kg^{-1}$)

$\underline{\underline{D}}$: matrice dictionnaire ou matrice de calibrage

$D_{i,P}$ = coefficient de diffusion de la molécule *i* dans le polymère *P* ($m^2 \cdot s^{-1}$)

Eta : nombre d'étapes nécessaires à la description de la méthode (formule de complexité)

$\left\{G_{i+k}^{m}\right\}_{k=P,F}$: enthalpie libre de mélange de *i* et *k* (J)

$\left\{H_{i+k}^{m}\right\}_{K=P,A}$: enthalpie de mélange de *i* et *k* (J)

$K_{i,F/P}$: coefficient de partage de la molécule *i* entre l'aliment (le simulant) *F* et le polymère *P*

$L_{F/P}$: coefficient de dilution

M : masse molaire ($g \cdot mol^{-1}$)

Na : nombre d'Avogadro ($6.02 \cdot 10^{23}$ molécules$\cdot mol^{-1}$)

Q_M : Quantité Maximale autorisée dans le polymère pour respecter la LMS

R : constante des gaz parfait ($8.31\ J \cdot K^{-1} \cdot mol^{-1}$)

$\underline{S}$: spectre d'absorption d'un échantillon (vecteur)

$\left\{S_{i+k}^{m}\right\}_{K=P,F}$: entropie de mélange de *i* et *k* ($J \cdot K^{-1}$)

T : température (K)

V_i^H : volume d'une molécule de *i* accessible aux atomes d'hydrogène ($Å^3$)

V_i^p : volume molaire d'une molécule de *i* ($Å^3$)

V_i^{vdw} : volume de Van der Waals d'une molécule de *i* ($Å^3$)

$\left\{V_j\right\}_{j=i,P,F}$: volume de *j* ($Å^3$)

V_{pyc} : volume du pycnomètre (mL)

c : cristallinité (%)

$c_{(x,t)}$: concentration en migrant au temps *t* et à l'abscisse *x*

d : nombre de détecteurs (formule de complexité)

e : nombre total d'éluants (formule de complexité)

ec : nombre d'éluants complexes (formule de complexité)

h : coefficient e convection ($m \cdot s^{-1}$)

k_B : constante de Boltzmann ($1{,}38.10^{-28}\ J \cdot K^{-1}$)

$m_{éthanol}$: masse d'éthanol (g)

m_{pyc} : masse du pycnomètre vide (g)

m_{tot} : masse du pycnomètre plein (g)

n_k : nombre de molécules de k

p : nombre de paramètres évoluant au cours de l'analyse (formule de complexité)

ps : conditions pour lesquelles des valeurs fixes sont ajoutées (formule de complexité) ; 5 pour l'ajout d'un étalon interne, 10 si une extraction est nécessaire avant analyse, 5 si un système d'injection particulier est requis et 10 si une analyse complexe des spectres ou chromatogrammes est nécessaire

r_F^{-1} : contribution entropique, rapport de taille de la molécule *i* et de l'aliment (du simulant) *F*

$\{r_k\}_{k=P,F}$: taille relative de *k*, sur un modèle à grille de type Flory-Huggins, par rapport à la taille de référence (taille des billes)

t : temps

x : abscisse

$x_{ethanol}$: fraction molaire en éthanol

z_{a+b} : nombre de coordination de a et b (nombre de molécules de *b* qui peuvent venir au contact d'une molécule de *a*)

α_i^{ν} : coefficient d'extinction molaire de i au nombre d'onde ν ($L \cdot mol^{-1} \cdot cm^{-1}$)

$\{\gamma_{i,k}^{\nu}\}_{k=P,F}$: coefficient d'activité volumique de *i* dans *k*

$\{\delta_j^d\}_{j=i,P,F}$: contribution dispersive à l'énergie de cohésion ($J \cdot mol^{-1}$)

$\{\delta_j^p\}_{j=i,P,F}$: contribution polaire à l'énergie de cohésion ($J \cdot mol^{-1}$)

$\{\delta_j^h\}_{j=i,P,F}$: contribution à l'énergie de cohésion due aux liaisons hydrogène ($J \cdot mol^{-1}$)

ε_{a+b} : énergie d'interaction entre *a* et *b* ($J \cdot mol^{-1}$)

μ_i : potentiel chimique de *i* ($J \cdot mol^{-1}$)

μ_i^0 : potentiel chimique de référence *i*, ou potentiel chimique de *i* pur ($J \cdot mol^{-1}$)

$\{\mu_{i,k}\}_{k=P,F}$: potentiel chimique de *i* dans *k* ($J \cdot mol^{-1}$)

ρ_e : densité du matériau plastique ($g \cdot cm^{-3}$)

$\rho_{éthanol}$: densité de l'éthanol ($g \cdot cm^{-3}$)

$\phi_{ethanol}$: fraction volumique en éthanol

$\{\phi_{i,k}\}_{k=P,F}$: fraction volumique de *i* dans *k*

χ_{a+b} : coefficient de Flory-Huggins entre *a* et *b*

INTRODUCTION

Les emballages protègent les produits au cours de leur transport, permettent leur conservation et sont un support à la fois marketing et pour les informations au consommateur. Leur développement a induit une forte évolution de nos habitudes de consommation. Les matériaux utilisés dans la conception des emballages alimentaires sont divers : papier, carton, verre, bois, aluminium, acier et matières plastiques. Les matériaux plastiques sont ceux qui ont connus la plus grande diversification et le plus grand nombre de développements (Brydson, 1999). Or, ils contiennent de nombreux additifs de faible masse moléculaire dans leur formulation et présentent par conséquent des risques d'interaction avec les aliments qu'ils contiennent, en libérant dans ceux-ci une partie de leurs additifs ou auxiliaires de fabrication. Alors que jusque dans les années 60 on estimait que ces substances ne quittaient pas les emballages, la contamination d'aliments a été mise en évidence par plusieurs études (Petersen et Breindhal, 2000 ; Sharman *et al.*, 1994 ; Harisson, 1988) et les taux de contaminants (solvants, additifs produits de dégradation et monomères) migrant des polymères dans des aliments ont été étudiés (Downes, 1987 ; Risch, 1988 ; Gilbert *et al.*, 1980 ; Koros et Hopfenberg, 1979). Les risques associés à cette contamination sont encore mal connus et l'exposition des consommateurs ne cesse d'augmenter du fait de l'évolution des habitudes de consommation (nomadisme, portions individuelles, etc.). Parmi les matériaux plastiques, les plus utilisés dans l'industrie agro-alimentaire sont les polyoléfines (PO), le polystyrène (PS) et le polyéthylène téréphtalate (PET), représentant respectivement 54%, 18% et 18% du marché en volume.

Suite à ces différents travaux, une règlementation stricte et harmonisée a été mise en place dans l'Union Européenne pour les matériaux au contact des aliments. Elle repose sur le règlement cadre 1935/2004 (Commission Européenne, 2004) qui impose à la fois un principe d'inertie des matériaux vis-à-vis de l'aliment et engage la responsabilité de l'industrie alimentaire qui met sur le marché l'aliment emballé. Même si elle est toujours en phase de consolidation, une réglementation détaillée, incluant notamment une liste positive des additifs et monomères, a été mise en place pour les matériaux thermoplastiques dans le cadre de la directive 2002/72/CE (Commission Européenne, 2002) et de ses différents amendements successifs. Bien que ces principes d'inertie et de liste positive soient aujourd'hui modulés du fait d'innovations ne pouvant rentrer strictement dans le cadre précédent (matériaux actifs libérant volontairement des substances dans l'aliment, matériaux recyclés incluant des contaminants potentiels n'appartenant pas à la liste positive), ils doivent absolument être vérifiés avant toute mise sur le marché. Le document synoptique de la Commission Européenne (Commission Européenne, 2008) recense aujourd'hui 937 substances (340

monomères et 597 additifs) autorisées pour un contact alimentaire. Parmi celles-ci, 502 (230 monomères et 272 additifs) sont soumis à des limites de migration spécifiques (LMS) du fait de leur toxicité potentielle.

Ainsi, pour démontrer l'aptitude d'un matériau plastique à être utilisé au contact de denrées alimentaires, il doit être prouvé que toutes les substances utilisées font partie de la liste positive. La quantité totale de migrants ne doit pas dépasser 10mg par dm^2 d'emballage ou 60mg par kg d'aliment (la limite de migration globale, LMG). Par ailleurs, le respect du niveau de migration des substances soumises à des LMS doit aussi être contrôlé. Ces tests se font par mise au contact de $1dm^2$ de matériau avec un (ou plusieurs) simulant alimentaire selon la nature de l'aliment emballé. Quatre simulants, respectivement notés A, B, C et D, ont été définis : l'eau pour les aliments aqueux, l'acide acétique 3% (p/v) pour les aliments type jus de fruit, l'éthanol 5, 15 ou 50% (v/v) pour les boissons alcoolisées, selon leur degré d'alcool, et l'huile d'olive pour les aliments gras. En pratique, l'utilisation de l'huile d'olive ne permet pas d'analyses robustes sur des substances spécifiques. Elle est généralement remplacée par des solvants ou mélanges de solvants tels que l'isooctane ou l'éthanol 95% (v/v). Le temps de contact pour les essais est réglementairement de 10j à 40°C. Par ce test de migration la LMG peut aisément être contrôlée mais la mesure des LMS nécessite quand à elle une bonne connaissance de la formulation des polymères. Cette information, nécessaire aussi pour l'application de modèles prédictifs, est répartie le long de la chaîne de production (fabricants, importateurs, transformateurs, utilisateurs, etc.) et est particulièrement difficile à obtenir en raison notamment des secrets de fabrication. Il est donc nécessaire pour les laboratoires d'analyses de disposer de méthodes leur permettant de déterminer les compositions initiales des matériaux testés (déformulation). Si les quantités des substances initialement présentes ne sont pas nécessaires, leur nature au moins doit être connue. Des méthodes globales d'investigation ont été proposées pour les matériaux polymères (Battum et Van Lierop, 1997 ; Bart, 2005). Il s'agit en général de réaliser dans un premier temps un spectre infrarouge du matériau pour en définir la nature, puis d'en extraire les additifs et résidus de fabrication. Ceux-ci sont ensuite identifiés et quantifiés par des méthodes et équipements les plus spécifiques possibles. La maîtrise des principales méthodes d'analyses et de leurs limites, ainsi que le développement d'une méthode de déformulation basée sur l'analyse du spectre infrarouge constituent les premiers objectifs de ce travail de thèse.

Le développement des approches prédictives a quant à lui été favorisé ces dernières années tant au niveau européen par la Direction Générale pour la Santé et la Protection du Consommateur qu'au niveau nord-américain par la Food and Drug Administration. La

multiplication des obligations règlementaires et des situations (matériaux, additifs, résidus de fabrication, aliments, type de contact, etc.) conduit en effet à un nombre très important de tests analytiques. Des outils sont d'ores et déjà publiés et disponibles : le Safe Food Packaging Portal (INRA, 2002) et les conclusions du groupe de travail européen SMT-CT98-7513 (Hinrichs *et al.*, 2002 ; Begley *et al.*, 2005) regroupent les principales informations dans ce domaine. Les résultats du groupe de travail sont à l'origine de l'article 8 de la Directive 2002/72/CE (Commission Européenne, 2002). Ils affirment notamment que la prévision des niveaux de migration est acceptable pour le remplacement des tests de migration dans la mesure où elle surestime de manière sûre la contamination réelle, notion déjà introduite via le calcul des quantités maximales autorisées (Q_M) dans un matériau formulé (Baner, et al., 1996). Ils proposent enfin de nombreuses valeurs expérimentales de coefficients de diffusion ($D_{i,P}$) de substances, notées i, dans les polymères, notés P, et des valeurs estimées pour ce paramètre ainsi que pour les coefficients de partage ($K_{i,F/P}$) entre les aliments (ou les simulants), notés F, et les polymères lorsqu'aucune donnée expérimentale n'est disponible. En effet, pour modéliser les transferts emballage/aliment, il faut non seulement connaître les substances présentes dans le matériau, comme pour les tests de mise en contact, mais aussi savoir en quelles quantités elles sont présentes et quelles sont les valeurs de $D_{i,P}$ et $K_{i,F/P}$ pour chaque additif. Dans le cas où les données manquent, la surestimation de ces paramètres est autorisée mais a toutefois ses limites car elle conduit le plus souvent à l'impossibilité de démontrer la conformité des matériaux, par excès de surestimation (Chatwin et Katan, 1989). Il apparaît donc de plus en plus nécessaire, sinon de déterminer expérimentalement les valeurs de $D_{i,P}$ et $K_{i,F/P}$, au moins de les prévoir le plus justement possible. Si de nombreux travaux ont été développés dans la littérature sur la prévision des coefficients de diffusion, peu ont concernés le coefficient de partage. Ce point particulier constitue un deuxième axe de recherche de cette thèse.

Ce travail de recherche s'est déroulé dans le cadre du projet ACTIA RA 05.22 qui avait pour objectif général de définir, de sélectionner et d'évaluer des outils et des méthodologies pour l'évaluation du risque sanitaire liée à l'utilisation de matériaux d'emballages au contact des aliments, dans une démarche plus particulièrement destinée et adaptée à l'industrie agroalimentaire et aux organismes de contrôle. Ce projet visait plus particulièrement à acquérir des techniques analytiques permettant de pallier la connaissance imparfaite de la formulation des matériaux (additifs utilisés, concentrations initiales) et à générer quelques données de référence de $K_{i,F/P}$, paramètre encore peu caractérisé jusque là. L'étude a porté sur

deux matériaux plastiques en particulier : un polyéthylène haute densité (PEHD), matériau semi-cristallin caoutchoutique et un polystyrène (PS), matériau amorphe vitreux. L'objectif final de ce travail est de proposer un arbre de décision permettant de statuer sur la conformité d'un matériau d'emballage.

Les travaux de thèse ont donné lieu à la rédaction de quatre publications indépendantes et d'une discussion générale sur la robustesse de l'approche complète, qui sont le socle de ce mémoire. Ce mode de rédaction a été choisi afin de faciliter la dissémination de résultats qui sont d'application immédiate à la fois pour la filière emballage et les industries alimentaires. Le mémoire est organisé en trois chapitres. La partie bibliographique présente les éléments qui sont à l'origine des choix retenus dans ce travail à la fois en matériaux d'étude, de méthodes d'extraction et d'analyse ainsi que des choix de modélisation des propriétés de transport. Des éléments bibliographiques plus précis sont donnés dans les différentes publications. Afin de faciliter la reprise de ce travail, le deuxième chapitre, intitulé "Matériels et Méthodes", rassemble tous les éléments expérimentaux utilisés pour les développements initiaux et pour l'analyse de la robustesse finale. Les développements théoriques sont, quant à eux, détaillés dans des parties spécifiques des quatre publications. Le troisième chapitre, "Résultats et Discussion", introduit les publications et reprend les principales conclusions sous la forme d'une discussion générale. Une conclusion résume enfin les principaux résultats et propose des recommandations pour une mise en œuvre rapide des méthodes proposées et des futurs travaux visant à élargir le champ applicatif initial : extensions à d'autres matériaux, application dans une logique de veille sanitaire.

Chapitre 1

BIBLIOGRAPHIE

1. Matériaux plastiques

1.1. Généralités

Les matériaux plastiques, ou matériaux polymères, sont des matériaux constitués de macromolécules obtenues par polymérisation à partir d'un ou plusieurs motifs unitaires. Les motifs les plus simples permettent d'obtenir les plastiques de base que sont le polyéthylène (PE), le polypropylène (PP), le poly(chlorure de vinyle) (PVC) et le polystyrène (PS). Des plastiques techniques sont obtenus par polymérisation à partir de motifs plus complexes ou de plusieurs motifs. C'est le cas par exemple du polyéthylène téréphtalate (PET).

Les matériaux polymères sont dis amorphes ou semi-cristallins selon la forme, amorphe ou semi-cristalline, que présentent leurs chaines. Ces différences sont liées à la capacité du matériau à cristalliser, mais aussi à la façon dont il à été mis en œuvre (refroidissement plus lent pour un matériau plus cristallin). Aux conditions de température d'utilisation, les matériaux polymères thermoplastiques sont constitués de chaînes enchevêtrées pouvant présenter des niveaux d'organisation à des échelles variables comme décrit sur la Figure 1.1 pour un polyéthylène haute-densité (PEHD).Une structure cristallisée est une structure organisée de la matière. Par ailleurs, la température de transition vitreuse (*Tg*) des matériaux plastique permet de distinguer deux états pour la phase amorphe des matériaux polymères : un état dense et cohésif, dit vitreux, en dessous de la *Tg* et un état caoutchoutique au dessus de la *Tg*.

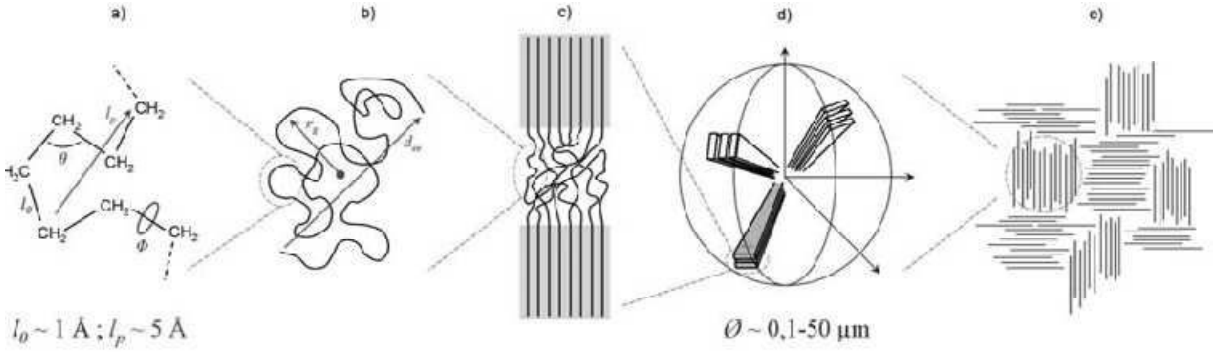

Figure 1.1. Organisation multi-échelle des polymères : exemples d'un PEHD. a) structure chimique, b) chaine gaussienne, c) structure semi-cristalline, d) structure poly-cristalline à symétrie de révolution (sphérulite), e) matériau hétérogène. l_0 : longueur d'une liaison, l_p : longueur de persistance, ϕ : angle de torsion, r_g : rayon de gyration, d_{ee} : distance bout-à-bout. source : Vitrac et Joly (2008).

Des compléments sont disponibles dans les ouvrages généraux sur les matériaux polymères et composites (Brydson, 1999 ; Groupe GPF, 2005 ; Kausch *et al.*, 2005 ; Klenin, 1999).

Dans cette étude, la phase ordonnée, ou zone cristalline, sera considérée inaccessible aux solvants.

1.2. Position des matériaux plastiques dans le secteur de l'emballage alimentaire

Dans le domaine de l'emballage alimentaire, les matériaux plastiques ont pris ces dernières années une part de plus en plus importante du marché. Ils représentent, en répartition des facturations, 33% des matériaux utilisés dans le domaine (Figure 1.2). Le secteur de l'emballage représente en quantité 30% de l'utilisation des matières plastiques (Figure 1.3). Dès leur conception, les polymères plastiques étaient destinés à remplacer les matériaux traditionnels tels que le verre, l'acier ou le bois. Ils ont en effet un poids spécifique plus faible et présentent une mise en forme plus simple et plus flexible que les matériaux qu'ils remplacent (Ehrenstein et Montagne, 2000). Parmi les autres propriétés recherchées, on peut citer le toucher agréable, l'imperméabilité, le comportement aux chocs et aux vibrations, l'isolation thermique ou encore le coût réduit. La transformation des polymères donne, surtout avec l'injection, un produit prêt à l'emploi et multifonctionnel, contrairement aux métaux par exemple qu'il faut assembler ou usiner en plusieurs étapes (Reyne, 1998).

Les principaux polymères utilisés dans le domaine de l'emballage alimentaire sont (Kirwan et Strawbridge, 2003) : PE, PP, PET, éthylène-acétate de vinyle (EVA), éthylène-alcool vinylique (EVOH), polyamides (PA), PVC, poly(chlorure de vinylidène) (PVdC), PS, styrène-butadiène (SB), acrylonitrile-butadiène-styrène (ABS).

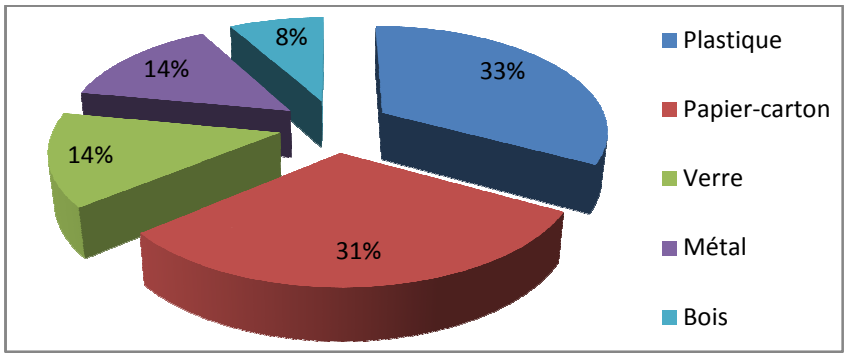

Figure 1.2. Répartition des facturations par matériaux dans le domaine de l'emballage (SESSI, 2005)

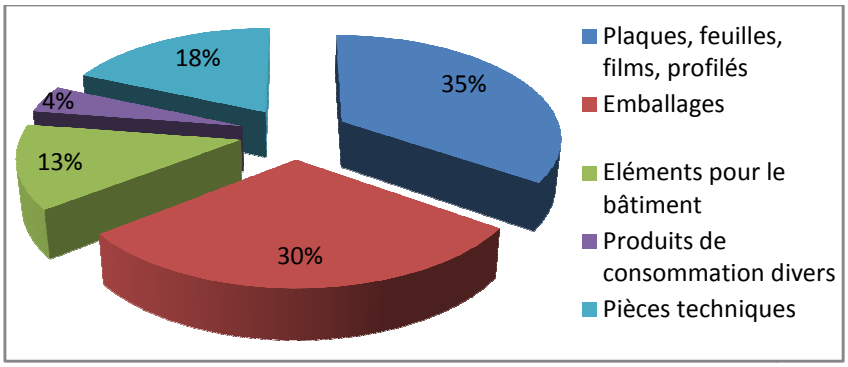

Figure 1.3. Répartition des quantités de plastique livrées par secteur (SESSI, 2004)

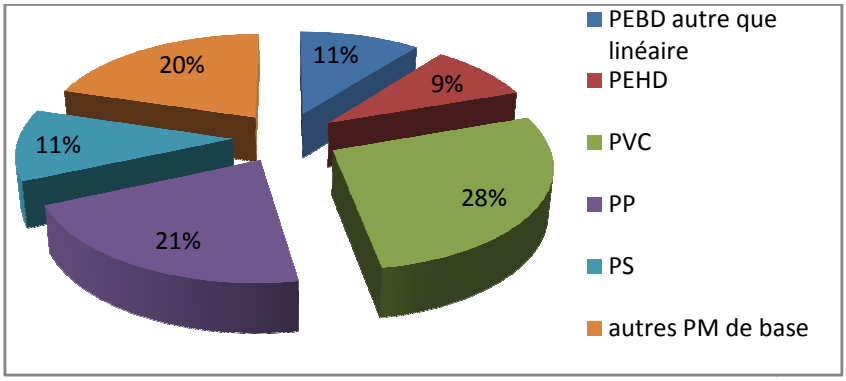

Figure 1.4. Part, en quantités, des différents plastiques de base (SESSI, 2004)

Parmi ceux-ci, nous avons choisi de nous intéresser plus particulièrement au PE et au PS, qui représentent respectivement 20% et 11% des plastiques de base utilisés en 2004 (Figure 1.4). Dans l'emballage en particulier, les PO (PE et PP) et le PS représentent 54% et 18% des matériaux plastiques utilisés.

1.3. Informations spécifiques aux polyéthylènes et polystyrènes

Le PE est le plastique le plus simple du point de vue de la structure (Figure 1.5.a.). Il est fabriqué par polymérisation à partir d'éthylène gazeux dans un réacteur haute température et haute pression (Kirwan et Strawbridge, 2003). Il s'agit d'un matériau plastique semi-cristallin et caoutchoutique à température ambiante. Dans le PS un cycle benzène remplace un atome d'hydrogène (Figure 1.5.b.). Le PS est amorphe et vitreux à température ambiante. Cette opposition amorphe/vitreux et semi-cristallin/caoutchoutique a été déterminante dans le choix de ces deux matériaux comme sujets de l'étude. Le Tableau 1.1 reprend les principales données et caractéristiques relatives à ces deux matériaux.

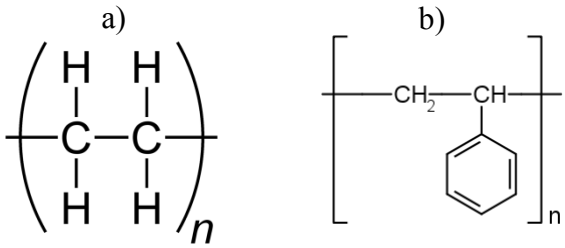

Figure 1.5. Unités de base : a) du PE ; b) du PS.

Tableau 1.1. Principales données relatives aux PE et PS (Ehrenstein et Montagne, 2000 ; Carrega, 2005)

Matériau	Cristallinité	Propriétés	Caractéristiques	Densité ($g.cm^{-3}$)	Tg (°C)
PE	40-55% pour un PEBD ; 60-80% pour un PEHD	Faible masse volumique, faible rigidité, bon marché. Bonne tenue chimique et aptitude au soudage du PEHD, mise en forme aisée et bonnes propriétés d'écoulement pour le PEBD	Brûle avec une flamme jaune (matière qui a tendance à goûter), odeur paraffinique, rayable à l'ongle, flotte sur l'eau. PEHD est blanc laiteux, PEBD est incolore, barrière aux liquides et à la vapeur d'eau	0.855 pour un PE totalement amorphe, 1.003 pour la phase cristalline	< -100
PS	100% amorphe	Rigidité, fragilité, stabilité dimensionnelle, bon marché, surface lisse sensibilité à la fissuration sous contrainte, tenue chimique limitée	Clarté du verre, brûle avec une flamme jaune (formation importante de suie), odeur de styrène à la combustion, barrière aux liquides	1.05	90-100

1.4. Stabilisation des matériaux plastiques

La durée de vie des plastiques est limitée dans le temps. Ceux-ci subissent divers phénomènes de vieillissement qui peuvent être liés à des facteurs physiques ou chimiques tels que des sollicitations mécaniques, des agents chimiques ou la température. Pour éviter ce genre de phénomènes, faciliter la mise en œuvre ou donner des propriétés supplémentaires (brillance, couleur, etc.), les matériaux plastiques sont complémentés au cours de leur fabrication à l'aide de substances appelées additifs.

Tableau 1.2. Principaux types d'additifs utilisés pour stabiliser les matériaux plastiques (Reyne, 1998)

Type de molécules	Effet recherché	Nature des molécules	Taux usuels
Antioxydants	Contre-vieillissement et oxydation (O_2, O_3)	Dérivés phénoliques, amines aromatiques	< 0,5%
Anti-UV	Empêcher ou retarder la dégradation photochimique	Benzophénones, benzotriazoles, complexes organométalliques	< 5%
Charges	Spécifique : tenue choc, thermique, chimique, glissement, abrasion, …	Talc, calcaire, graphite, …	< 50%
Colorants	Donner un aspect coloré	Pigments minéraux (oxydes de Ti, Fe, Cr, Cd, Mb, etc.) et organiques (noir de C)	< 1%
antistatiques	Dissiper l'énergie électrostatique	Dérivés aminés, ammonium quaternaire, alkylphénol, alkylsulfonate	< 2%
Lubrifiants internes	Faciliter le moulage, surfaces brillantes	Stéarate de Ca ou de Zn, oléamines, érucylamines, acides palmitique, stéarique	< 2%
Lubrifiants externes	Faciliter la séparation du moule	Cires, paraffines, stéarates	< 2%

Le Tableau 1.2 présente les principaux types d'additifs utilisés. Les types et taux d'additifs utilisés dans un matériau donné dépendent de sa nature et de son utilisation. Des informations plus détaillées, allant jusqu'à des formulations typiques de polymères, peuvent être trouvées dans la littérature (Zweifel, 2000 ; Sheftel, 2000 ; Flick, 2002).

Une définition des différentes familles d'additifs et des risques toxicologiques associés peut être trouvée dans le livre de Multon *et al.* (1992). Pour éviter l'intoxication des consommateurs, la migration des additifs depuis les matériaux destinés au contact alimentaire vers les aliments est très contrôlée, notamment au niveau européen (Commission Européenne, 2002, 2004, 2005 et 2007). Le respect des LMS et LMG doit être vérifié pour tous les matériaux plastiques destinés au contact alimentaire. Cette vérification ne peut toutefois pas se faire sans une bonne connaissance de l'identité des additifs utilisés dans la fabrication des matériaux. Cette information n'étant généralement pas transmise aux organismes de contrôle et aux utilisateurs des emballages plastiques, responsables des tests, il apparaît nécessaire aujourd'hui de disposer de méthodes de déformulation (détermination de la composition initiale) de ces matériaux pour connaître l'identité des substances utilisées et leurs quantités initiales.

2. Méthodes d'analyse des matériaux plastiques

2.1. Principes généraux

Pour la déformulation des matériaux plastiques, des stratégies globales d'analyses ont été proposées (Battum et Van Lierop, 1997 ; Bart, 2005 ; Lau et Wong, 2000). De manière plus spécifique, le projet AIR (Feigenbaum *et al.*, 1997) présentait dans son rapport final des diagrammes de choix pour valider ou non la conformité d'un matériau plastique destiné au contact alimentaire. La méthode générique consiste en une extraction des additifs de la matrice polymère suivie de leur identification et dosage grâce à des méthodes chromatographiques. Quelques méthodes alternatives d'identification et dosage directement dans les matériaux, telles que la spectroscopie infrarouge (IR), existent aussi. Dans cette partie, nous avons souhaité sélectionner une ou plusieurs méthodes efficaces et utilisables dans une logique d'aide à la décision : temps courts, limites de détections et gammes de concentrations compatibles avec les LMS des composés, sensibilité suffisante et coefficients de variation faible, mise en œuvre aisée et traitement simultané du plus grand nombre possible de substances. Les méthodes d'extraction ou d'identification et dosage proposées dans la littérature étant très nombreuses, nous avons recherché spécifiquement celles appliquées à des

PE ou PS et aux additifs qu'ils sont susceptibles de contenir. L'analyse proposée tient compte également de l'expérience que j'ai pu acquérir préalablement sur ces techniques ainsi que du savoir faire des nombreuses personnes avec qui j'ai pu travailler.

2.2. Identification et dosage des additifs

Les données relatives aux méthodes référencées sont regroupées dans le Tableau 1.3. Un code a été attribué à chaque méthode. Il y sera fait référence, plutôt qu'aux publications associées, dans le texte et les figures.

Nous avons effectué une comparaison sur la base des paramètres jugés les plus pertinents : le temps d'analyse (Figure 1.6), les limites de détection (Figure 1.7), le domaine linéaire de quantification (Figure 1.8), la sensibilité (Figure 1.9) et les coefficients de variation (Figure 1.10). Par ailleurs, nous avons attribué à chaque méthode référencée une valeur de complexité calculée essentiellement sur la base de paramètres liés à la mise en œuvre, tels que le temps nécessaire à la préparation d'un éluant ou à l'ajout systématique d'un étalon interne, mais liés aussi à la nécessité d'un savoir-faire pour interpréter des spectres complexes (spectres de masse ou spectre IR). Cette valeur est envisagée comme une information supplémentaire pour discriminer les méthodes. Par ailleurs, la formule proposée (équation (1.1)) a fait l'objet de discussions et de validations avec des personnes du LNE habituées aux différentes méthodes étudiées.

$$complexité = (e + ec + p) \times Eta + d + ps \tag{1.1}$$

e est le nombre total d'éluants et *ec* est le nombre d'éluants complexes (sels ou solutions stabilisées par exemple). Cette distinction permet une pondération différente selon le temps nécessaire à la préparation des éluants. *p* est le nombre de paramètres évoluant au cours de l'analyse (débit, pression, température, etc.). *Eta* est le nombre d'étapes nécessaires à la description de la méthode (paliers et rampes de variations des paramètres). Par exemple, une méthode isocratique sera décrite en une seule étape (*Eta* =1) alors qu'une méthode utilisant des changements d'éluants au cours du temps sera décrite en plusieurs étapes (*Eta* >1). Enfin, *d* est le nombre de détecteurs et *ps* représente des conditions particulières pour lesquelles des valeurs fixes sont attribuées : 5 pour l'ajout d'un étalon interne, 10 si une extraction est nécessaire avant analyse, 5 si un système d'injection particulier est requis et 10 si une analyse complexe des spectres ou chromatogrammes est nécessaire.

Tableau 1.3. Codes relatifs aux méthodes d'identification et dosage des additifs, références associées et valeurs des paramètres étudiés (DL = domaine linéaire testé ; CV = coefficient de variation). Le tableau continu sur la page suivante.

Code	Séparation	Détection	Référence	Temps (min)	DL (mg/L)	CV (%)	*complexité*
Fa	EFS-CFS	DIF	Ashraf-Khorassani et Levy (1990)	56	1000-4000	/	9
Fb	CFS	DIF	Kithinji *et al.* (1990)	/	/	/	12
Fc	CFS	DIF		/	/	/	12
Fd	CFS	DIF		/	/	/	12
Fe	CFS	DIF		/	/	/	12
Ff	CFS	SM	Arpino *et al.* (1990)	80	/	/	23
Fg	CFS	DIF		80	/	/	33
Fh	CFS	SM	Bücherl *et al.* (1994)	68.5	/	/	23
Fi	CFS	DIF	Ryan *et al.* (1990)	30	/	/	17
Fj	CFS	IR	Wiebolt *et al.* (1990)	52	/	/	21
Fk	CFS	DIF	Zhou *et al.* (1999)	15	/	/	17
Fl	CFS	IR	Raynor *et al.* (1988)	90	/	/	24
Ga	ET-MEPS-CPG	SM	Ezquerro *et al.* (2003)	24.5	/	11,6	24
Gb	Py-CPG	SM	Coulier *et al.* (2005)	29	/	/	20
Gc	CPG	SM	Philo *et al.* (1997)	12.2	5.10^{-4}-$1,1.10^{-2}$	/	27
Gd	CPG	DIF		14.8	5.10^{-4}-$1,1.10^{-2}$	/	17
Ge	Py-CPG	DIF	Wang (200) et Wang *et al.* (2000)	10	/	/	34
Gf	Py-CPG	SM		50	/	/	20
Gg	CFS-CPG	SM	Carrott *et al.* (1998)	16	0,05-25	/	24
Gh	CPG	DIF	Frisina *et al.* (1979)	120	/	/	12
Gi	MEPS-CPG	DIF	Burman *et al.* (2005)	34	/	4,5	14
Gj	ET-MEPS-CPG	SM		34	/	17,3	15
Gk	CES-Py-CPG	SM	Kaal *et al.* (2007)	16	/	/	29
Gl	CPG	DIF	Garrido-López *et al.* (2007a)	19	9,7-61,5	2,1	19
Gm	CPG	DST		19	10,7-61,5	2,2	19
Gn	CPG	SM		19	22,5-41	14	29
Go	ET-CPG	SM	Lickly *et al.* (1995)	/	/	/	34
Gp	ET-CPG	SM	Krzymien *et al.* (2001)	43.5	/	/	22
Gq	ET-CPG	SM	Skjevrak *et al.* (2003)	/	/	/	27
Gr	Py-CPG	SM	Manabe *et al.* (1999)	30	/	3	22
Gs	CPG	DIF	Tan *et al.* (1988)	9	/	/	17
La	CLHP	UV	Dopico-Garcia *et al.* (2003)	17	2,5-20	/	19
Laa	CLHP	UV	Zhou *et al.* (1999)	38	/	/	24
Lab	CLHP	IR	Somsen *et al.* (1996)	32	/	/	23
Lac	CLHP	UV	Tan *et al.* (1988)	30	/	/	23
Lad	CLHP	UV-SM	Garrido-López *et al.* 2007b	27	/	/	18
Lae	CLHP	UV-SM		80	/	/	23
Laf	CLHP	DEDL	Schaefer *et al.* (2003)	55	6,25-93,75	/	23
Lag	CLHP-	UV-Fluo	García *et al.* (2004)	55	0,1-10	/	23
Lah	CLHP	UV	Lickly *et al.* (1995)	/	/	/	13
Lai	CLHP	UV	O'Brien *et al.* (1997)	/	0,5-20	/	18
Laj	CLHP	DEDL	Leselier et Tchapla (1993)	35	/	/	44
Lal	CLHP	UV	Smith (1998)	/	50-280	/	12
Lak	CLHP	UV	Macko *et al.* (1996)	10	/	1,8	14
Lb	CLHP	SM	Garrido-Lopez et Tena (2005)	45	1-24,8	7,09	34
Lc	CLHP	SM		80	/	/	31

Code	Séparation	Détection	Référence	Temps (min)	DL (mg/L)	CV (%)	*complexité*
Ld	CLHP	UV-DEDL	Coulier *et al.* (2005)	41	0,1- ?	/	41
Le	CLHP	UV	Lundbäck *et al.* (2005)	8	/	/	18
Lf	CLHP	UV	Camacho et Karlsson (2001)	30	212,5-975	5,55	12
Lg	CLHP	UV	Haider et Karlsson (1999a)	30	/	2	12
Lh	CLHP	UV	Tawfik et Huyghebaert (1999)	/	/	/	/
Li	CLHP	UV	Marcato et Vianello (2000)	18	/	/	24
Lj	CLHP	UV	Marcato *et al.* (2003)	16	/	/	23
Lk	CLHP	UV	Ashraf-Khorassani *et al.* (1999)	/	/	/	17
Ll	CLHP	UV	Nielson (1991)	25	/	/	17
Lm	CLHP	UV	Nielson (1993)	22	/	/	17
Ln	CLHP	UV	Caceres *et al.* (1996)	10	25-500	/	13
Lo	CLHP	IR	Jordan et Taylor (1997)	22	/	/	32
Lp	CLHP	UV	Hodgeman (1981)	40	/	/	18
Lq	CLHP	UV	Arpino *et al.* (1990)	35	/	/	19
Lr	CES-CLHP	UV	Nerin *et al.* (1995)	30	2-200	3,4	18
Ls	CLHP	UV-SM	Vargo et Olson (1986)	32	/	5,43	21
Lt	EPS-CLHP	UV	Burman *et al.* (2005)	85	/	3,8	40
Lu	CLHP	UV	Haider, et Karlsson (2002)	30	/	/	12
Lv	CLHP	UV	Marcato *et al.* (1991)	22	/	3	13
Lw	CLHP	UV	Matuska *et al.* (1992)	15	40-2000	10	12
Lx	CLHP	UV	Molander *et al.* (1999)	65	/	1,2	19
Ly	CLHP	UV	Schabron et Fenska (1980)	30	/	1,5	13
Lz	CLHP	UV	Vandenburg *et al.* (1999)	/	/	/	22
Ma	/	MALDI-ToF-SM	Hsiao *et al.* (2001)	/	/	/	22
Ra	/	IR	Vitali (2001)	5	10-40	/	12
Rb	/	IR		5	10-40	/	12
Rc	/	IR	Möller *et al.* (2001)	5	/	/	17
Rd	/	IR	Carlsson *et al.* (2001)	5	/	/	11
Re	/	IR	Karstang et Henriksen (1992)	5	/	/	11
Rf	/	IR	Földes *et al.* (2006)	5	/	/	11
Ua	/	UV	Haider et Karlsson 1999b	5	27,5-105	/	12
Ub	/	UV	Haider et Karlsson 1999a	5	30-100	2	12
Uc	/	UV	Bermudez *et al.* (2002)	/	/	/	12
Ud	/	UV	Haider et Karlsson (2001)	5	/	/	12

CES = chromatographie d'exclusion stérique, CFS = chromatographie en fluide supercritique, CLHP = chromatographie liquide haute performance, CPG = chromatographie phase gaz, DEDL = détecteur évaporatif à diffusion de lumière, DIF = détecteur à ionisation de flamme, DST = détecteur sélectif thermo-ionique, ET = espace de tête, EPS = extraction phase solide, IR = spectroscopie infrarouge, MEPS = micro-extraction phase solide, Py = injection pyrolyse, SM = spectromètre de masse, UV = spectroscopie UV.

Nous nous sommes intéressés dans un premier temps à la durée des méthodes, à leur complexité et aux nombres de substances simultanément traitées. Ces trois paramètres sont regroupés sur la Figure 1.6 dont les méthodes de durée supérieure à 1h ont été écartées dès le départ. La considération conjuguée de ces trois paramètres nous a amené à définir quatre classes principales de méthodes, présentées dans le Tableau 1.4.

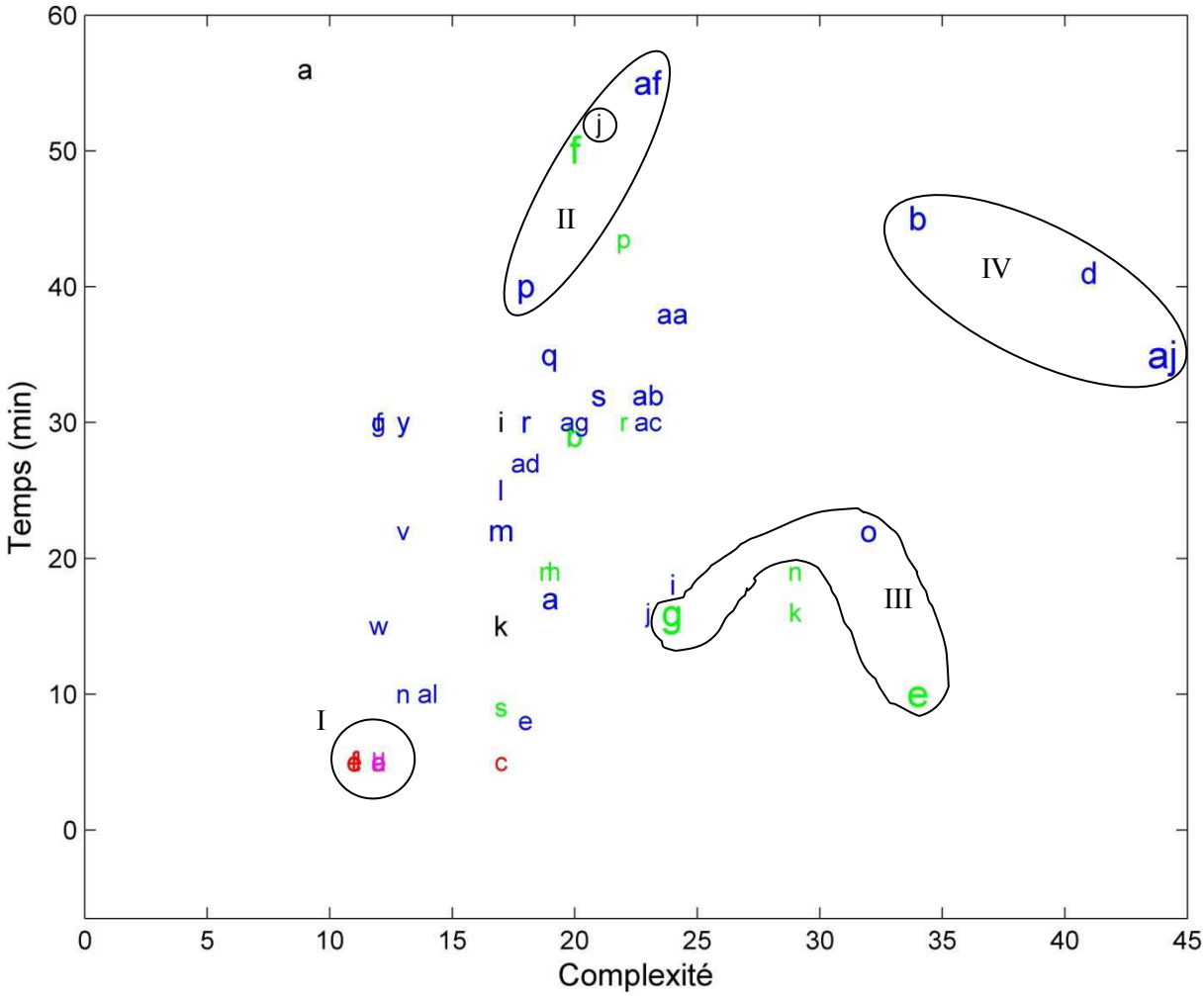

Figure 1.6. Temps nécessaire à la séparation pour les différentes méthodes référencées dont la durée est inférieure à 60 min. Une figure présentant toutes les méthodes est disponible en annexe 2. Noir = CFS (F), bleu = CLHP (L), vert = CPG (G), rouge = IR (R), violet = UV (U). La taille du texte est proportionnelle au nombre de substances analysées par la méthode. Les méthodes les plus intéressantes sont regroupées en 4 classes (Tableau 1.4).

Tableau 1.4. Principales classes de méthodes analytiques étudiées.

Classe	Durée	Complexité	Nombre de substances traitées simultanément
I	Très courte (<10min)	Très faible (<15)	Faible (<5)
II	Longue (>30min)	Faible (<30)	Elevé (>10)
III	Courte (<30min)	Intermédiaire	Elevé (>10)
IV	Longue (>30min)	Elevée (>30)	Elevé (>10)

Les méthodes situées en dehors des classes ont été rapidement écartées car présentant des rapports durée-complexité/molécules traitées peu intéressants (trop peu d'additifs traités simultanément au regard d'une complexité et/ou d'une durée trop élevées). Les méthodes de la classe I sont celles basées sur la réalisation de spectres sans séparation préalable. Les principales techniques sont la spectroscopie IR et la spectroscopie Ultraviolet (UV). Hsiao *et al.* (2001) ont aussi proposé une méthode d'identification et de dosage des additifs en utilisant

la technique d'ionisation MALDI (Matrix-Assisted Laser Desorption Ionization) couplée à de la spectrométrie de masse à temps de vol (ToF-MS). Toutes ces méthodes permettent une identification et une quantification rapides d'additifs dans les cas simples de matériaux peu formulés, c'est-à-dire dans lesquels peu d'additifs différents sont présents. Ces méthodes ont donc elles aussi été écartées dans un premier temps de celle potentiellement intéressantes dans le cadre de cette étude. Les applications de la spectroscopie IR combinées aux outils chimiométriques seront explorées dans une partie dédiée.

Toutes les méthodes des classes II, III et IV se rapportent aux deux techniques les plus générales et majoritairement utilisées de part leurs champs d'application larges et variés : la CLHP et la CPG.

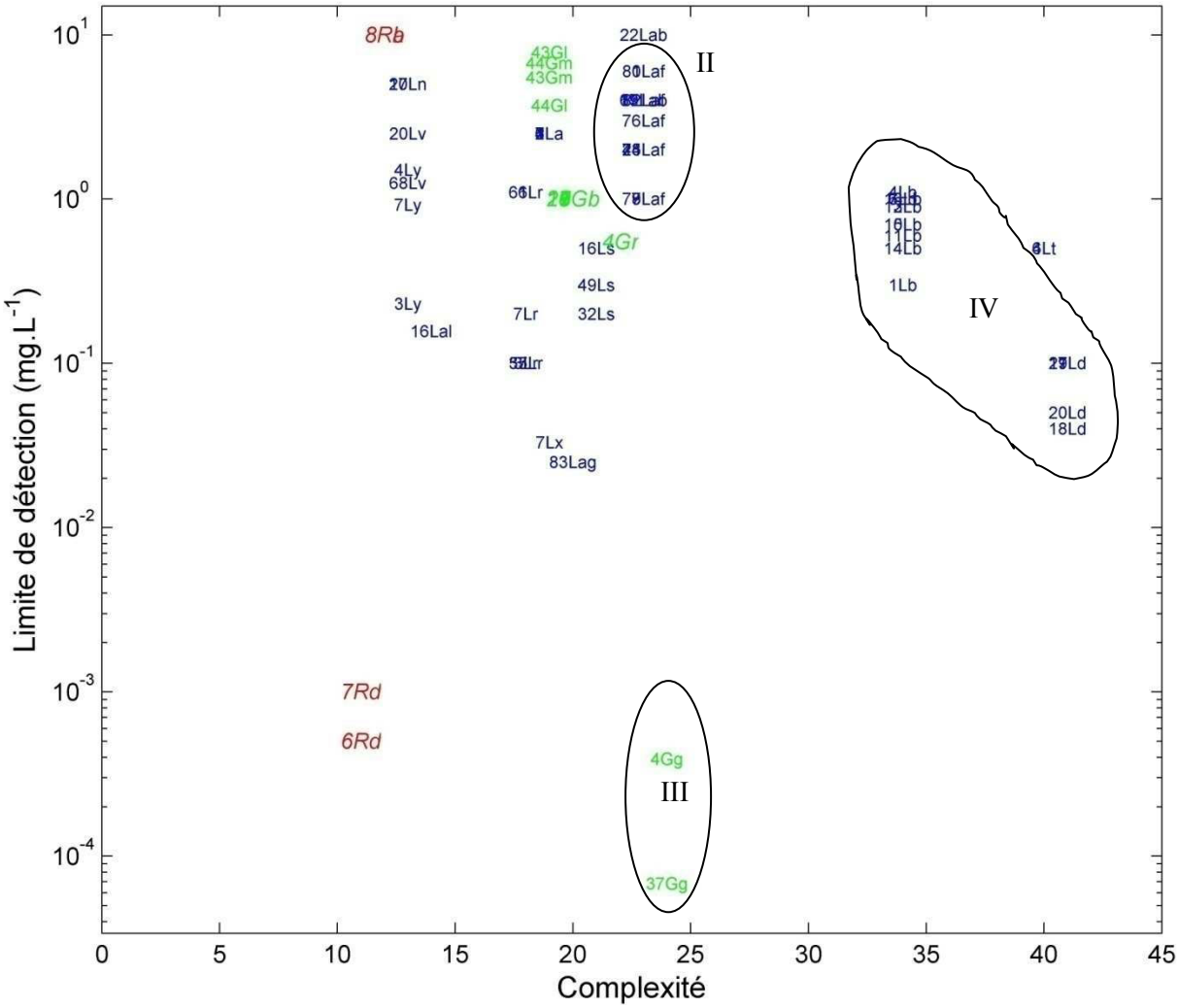

Figure 1.7. Limites de détection des additifs (cf annexe 1 pour les codes relatifs aux additifs). Les limites de détection pour le dosage directement dans les matériaux sont indiquées en gras et en italique. Seules les limites de détections inférieures à 10mg/L sont représentées, une figure complète est disponible en annexe 2. Noir = CFS (F), bleu = CLHP (L), vert = CPG (G), rouge = IR (R), violet = UV (U).

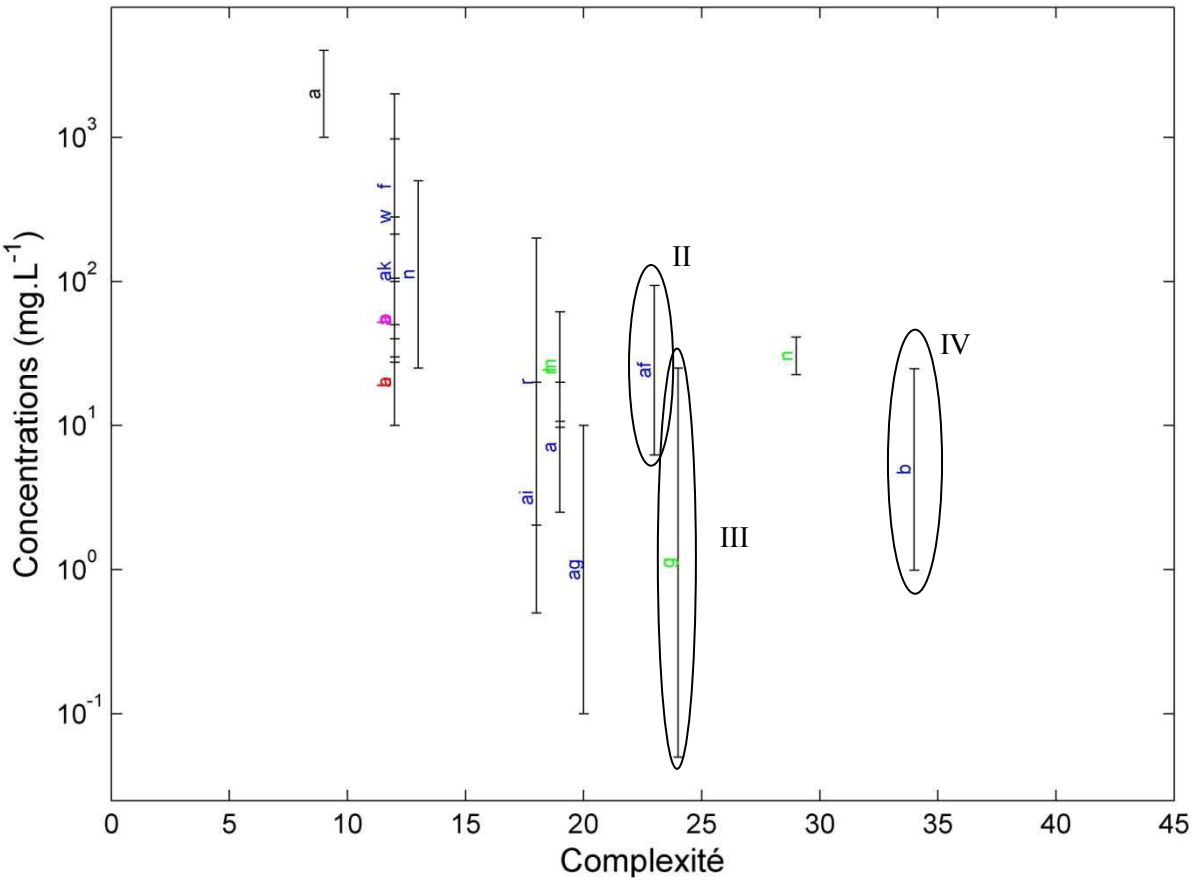

Figure 1.8. Domaines linéaires de quantification. Noir = CFS (F), bleu = CLHP (L), vert = CPG (G), rouge = IR (R), violet = UV (U). La taille du texte est proportionnelle au nombre de substances analysées par la méthode.

Pour affiner notre sélection de méthodes, nous avons malheureusement dû nous appuyer sur des données tronquées. En effet, les limites de détections, domaines linéaires, sensibilités et coefficients de variation des méthodes proposées ne sont généralement pas donnés et ne peuvent que rarement être recalculés. Les limites de détections supérieures à 10 $mg \cdot kg^{-1}$ ont été jugées inintéressantes pour nos applications car les LMS sont généralement inférieures à 10 $mg \cdot kg^{-1}$ d'aliment. Des sensibilités supérieures à 1000 unités et des domaines linéaires les plus larges possibles sont généralement recherchés.

La méthode Gg, pour laquelle quelques seuils de détection (Figure 1.7) et domaines de linéarité (Figure 1.8) sont donnés, peut convenir au dosage de substances soumises à LMS. Les seuils de détection notamment sont particulièrement bas. La limite à la CPG reste la nécessité que les substances à doser soient suffisamment volatiles pour être vaporisées dans l'injecteur. Elle est donc limitée aux additifs de faible à moyen poids moléculaires.

Une alternative au problème de poids moléculaire des substances est donnée par la Py-CPG. Elle consiste à pyrolyser les échantillons et à injecter les pyrolysats dans la colonne de chromatographie gazeuse. L'intérêt de cette technique est double : i) elle permet d'analyser

les substances de forts poids moléculaires ; ii) elle permet de travailler directement sur les matériaux polymères sans extraction préalable. Les méthodes Ge (classe III) et Gf (classe II) utilisent cette technique. On peut regretter toutefois que l'application de ces deux méthodes ait été limitée aux lubrifiants et antioxydants.

La CLHP est particulièrement intéressante pour analyser simultanément des substances de tous types et tous poids moléculaire. Deux méthodes semblent particulièrement intéressantes : Ld et Laj (classe IV), développées toutes deux pour obtenir une séparation efficace d'antioxydants et d'anti-UV avec une seule et même méthode. Un certain nombre d'anti-UV ont un poids moléculaire trop élevé pour permettre leur séparation par CPG. Les auteurs ont utilisé deux détecteurs pour chaque méthode : un détecteur UV pour les additifs présentant des groupements chromophores (répondant à une excitation UV) et un DEDL pour les additifs de moyen à fort poids moléculaire. Ils ont aussi utilisé une élution par gradient (modification dans le temps des quantités de solvant composant le mélange éluant), des solvants stabilisés et/ou complexes et des variations de débits, faisant des deux méthodes ainsi obtenues les plus complexes d'après nos critères (Figure 1.6). Pour la méthode Ld, les seuils de détection (Figure 1.7) et le domaine linéaire de quantification (Figure 1.8) présentés sont tout à fait compatibles avec l'analyse d'additifs soumis à LMS. La méthode Laf (classe II) n'utilise quant à elle qu'un DEDL, ce qui peut expliquer la faible sensibilité observée pour cette méthode (Figure 1.9).

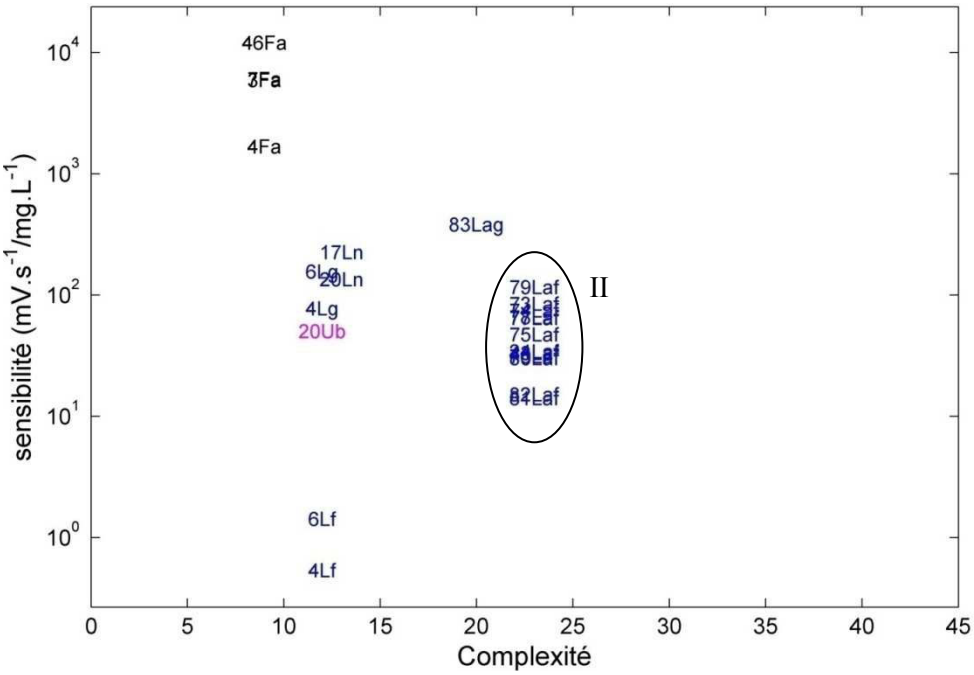

Figure 1.9. Sensibilité des méthodes de dosage. Noir = CFS (F), bleu = CLHP (L), vert = CPG (G), rouge = IR (R), violet = UV (U). La taille du texte est proportionnelle au nombre de substances analysées par la méthode.

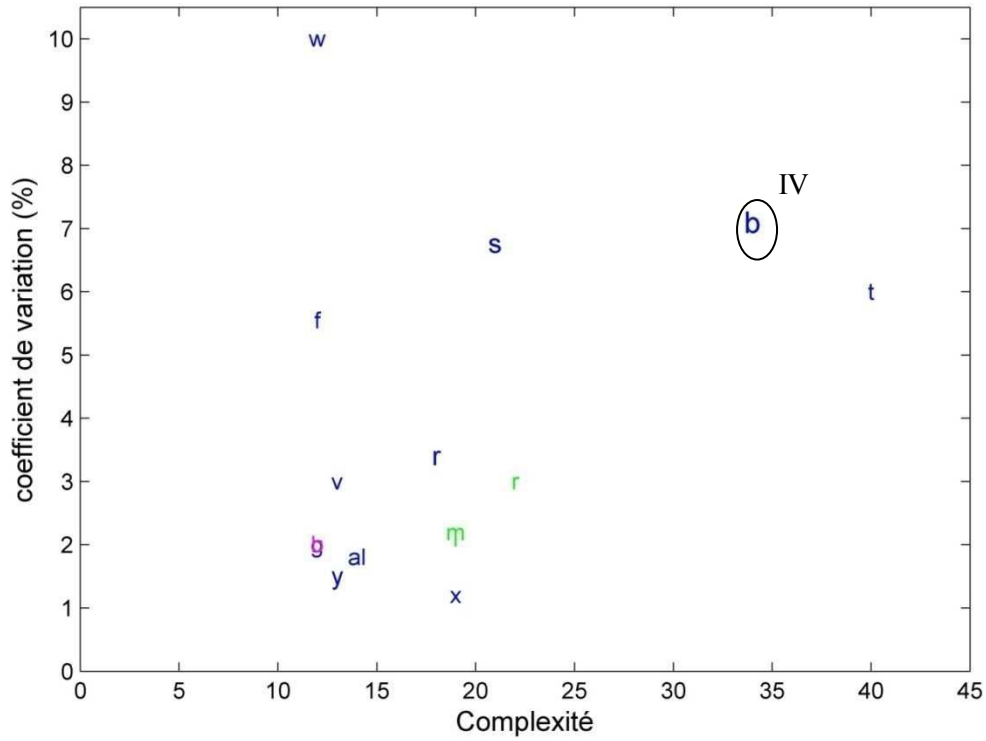

Figure 1.10. Coefficients de variation des méthodes (CV<10, une figure présentant l'ensemble des méthodes est disponible en annexe 2). Noir = CFS (F), bleu = CLHP (L), vert = CPG (G), rouge = IR (R), violet = UV (U). La taille du texte est proportionnelle au nombre de substances analysées par la méthode.

L'identification des substances n'est que peu ou pas discutée dans les publications de méthodes d'analyse. Dans la plupart des cas, les détecteurs utilisés sont non spécifiques de manière à pouvoir obtenir un signal pour le plus grand nombre possible de substances. C'est le cas par exemple du DEDL ou du DIF. L'identification ne peut se faire avec ce type de détection que par comparaison du temps de rétention du produit avec celui d'un étalon et elle n'est donc jamais absolue. A contrario, l'utilisation de détecteurs SM ou IR permet d'obtenir une identification stricte des substances en mesurant respectivement leur spectre de masse ou leur spectre IR. L'utilisation de tels détecteurs permet aussi l'identification des éventuels produits de dégradation des additifs ou des polymères. Un certain nombre d'études a été réalisé à ce sujet, que ce soit sur les produits de dégradation des additifs (Philo *et al.*, 1997 ; Haider et Karlsson, 2001 ; Skjevrak *et al.*, 2003 ; Burman *et al.*, 2005) ou sur les produits issus de traitements ionisants (Buchalla *et al.*, 1999 ; Buchalla *et al.*, 2000 ; Pacáková et Leclercq, 1991 ; Carlsson *et al.*, 2001 ; Krzymien *et al.*, 2001), thermiques (Piao *et al.*, 1999 ; Burman et Albertsson, 2005 ; Font *et al.*, 2004; Breen *et al.*, 2000; Wallis et Bhatia, 2007) ou même catalytiques (Park *et al.*, 1999) des polymères.

Enfin, des méthodes analytiques existent pour doser des additifs de matériaux plastiques directement dans les simulants alimentaires définis par la règlementation européenne

(Dopico-Garcia *et al.*, 2003 ; Philo *et al.*, 1997 ; Lickly *et al.*, 1995 ; O'Brien *et al.*, 1997 ; Salafranca *et al.*, 1999 ; Leepipatpiboon *et al.*, 2005). La CLHP est particulièrement indiquée pour ce genre de dosage car elle permet l'injection de tout liquide soluble dans la phase mobile (éluants).

Pour conclure, l'analyse de substances contenues dans un matériau plastique destiné au contact alimentaire peut se faire de manière assez simple si l'on sait quelles sont les substances recherchées. Des méthodes spécifiques à des familles de molécules ou même à des molécules particulières existent en effet dans la littérature. Dans le cas de tests en aveugle, il faut préférer des méthodes plus génériques et plus robustes. La CFS couplée à un détecteur IR (Fl) semble prometteuse, mais les techniques plus classiques que sont la CPG et la CLHP permettent d'obtenir de très bons résultats avec des méthodes certes un peu plus complexes. Pour le développement de méthodes CLHP, les méthodes Ld et Laj semblent être un bon point de départ. Torres-Lapasió et García-Álvarez-Coque (2006) proposent par ailleurs des techniques d'optimisation de méthodes CLHP, expliquant que les paramètres les plus important sont la colonne (en particulier la nature de la phase stationnaire), le mode d'élution, les modificateurs organiques et la nature des tampons et qu'il faut suivre l'évolution des limites de détection, des coefficients de variation et de la sensibilité. La détection doit se faire idéalement par SM ou IR pour permettre une identification stricte des additifs. La CLHP-SM notamment va certainement devenir une méthode indispensable dans les analyses de simulants ou polymères destinés au contact alimentaire, combinant avantageusement les avantages de la CLHP (phases mobiles et stationnaires diverses, élution de composés de grande masse moléculaire) et de la SM (identification) (Simal-Gandara *et al.*, 2002). Un autre avantage de la CLHP est la possibilité d'analyser directement les simulants alimentaires. Pour les additifs de faible à moyen poids moléculaire, la CPG, et particulièrement la Py-CPG, offre la possibilité d'analyses simples et rapides avec de bons résultats. Étant par ailleurs plus facilement couplée à de la SM, elle pourra être préférée à la CLHP pour l'identification et le dosage de produits de dégradation.

2.3. Extraction des additifs des matériaux polymères

Nous avons effectué une comparaison sur la base des informations disponibles : le temps d'extraction (Figure 1.11 et Figure 1.12), le rendement d'extraction (Figure 1.11) et les coefficients de variation (Figure 1.12). Nous nous sommes plus particulièrement intéressés aux méthodes les plus rapides, permettant des temps de réaction plus courts en cas de crise sanitaire par exemple. Les extractions en reflux avec ou sans soxhlet bien que très répandues et efficaces, ne seront que très peu abordées dans ce travail car elles nécessitent des temps de contact de l'ordre de 5 à 40h en fonction des matériaux et des additifs.

Le Tableau 1.5 présente les méthodes référencées dans les figures qui vont suivre. De la même manière que pour les méthodes analytiques, il sera fait référence aux codes des méthodes dans le texte et les figures, plutôt qu'aux publications associées.

La plupart des méthodes proposées dans la littérature présentent des rendements d'extraction proches de 90% ou supérieurs (Figure 1.11). Les rendements des méthodes Oa et Uh n'ont pas pu être déterminés car elles n'ont pas abouti à une extraction suffisante des anti-UV étudiés pour permettre leur quantification (Caceres *et al.,* 1996). Il apparaît ainsi que les méthodes d'extraction simple (diffusion par mise en contact avec un solvant dans un récipient) et par ultrasons ne sont pas efficaces pour l'extraction des additifs de type polymérique. La grande taille de ces additifs nécessite l'emploie de méthodes d'extraction plus complexes pour les extraire des polymères en des temps raisonnables.

Tableau 1.5. Codes relatifs aux méthodes d'extraction des additifs de PE et PS

Code	Méthode	Matériau	Référence	Temps (h)	Rendement (%)	CV (%)
Da	Dissolution / précipitation	HDPE	Coulier *et al.* (2005)	/	/	/
Db	Dissolution / précipitation	PS	Philo *et al.* (1997)	/	/	/
Dc	Dissolution / précipitation	PE	Wang et Buzanowski (2000)	/	/	/
Dd	Dissolution / précipitation	HDPE	Caceres *et al.* (1996)	1	67.5	/
De	Dissolution / précipitation	LDPE, HDPE	Frisina *et al.* (1979)	0.5	96	8.3
Df	Dissolution / précipitation	MDPE	Macko *et al.* (1996)	2	95	/
Dg	Dissolution / précipitation	PE	Schabron et Fenska (1980)	/	/	3.93
Dh	Dissolution / précipitation	PS	(Lickly *et al.* (1995)	/	102.83	/
Di	Dissolution / précipitation	LDPE, HDPE	O'Brien *et al.* (1997)	/	/	/
Dj	Dissolution / précipitation	PS	Smith (1998)	3	91	5.82
Fa	EFS	PS	Bermudez *et al.* (2002)	/	/	/
Fb	EFS	LDPE	Carrott *et al.* (1998)	1.5	/	/
Fc	EFS	Films commerciaux	Bücherl *et al.* (1994)	0.5	/	/
Fd	EFS	PE	Ryan *et al.* (1990)	0.25	95	/
Fe	EFS	PE	Wiebolt *et al.* (1990)	5	/	/
Ff	EFS	LDPE	Zhou *et al.* (1999)	1	86.75	/

Code	Méthode	Matériau	Référence	Temps (h)	Rendement (%)	CV (%)
Fg	EFS	PS	Smith (1998)	2	95.5	10.73
Ma	EAM	LDPE	Lundbäck *et al.* (2005)	0.66	76	/
Mb	EAM	HDPE,MDPE	Camacho et Karlsson (2001)	0.5	91	/
Mc	EAM	HDPE, LLDPE	Marcato et Vianello (2000)	0.25	92.67	/
Md	EAM	HDPE	Marcato *et al.* (2003)	0.25	/	/
Me	EAM	LDPE, HDPE	Nielson (1991)	0.33	92.3	1.8
Mf	EAM	LDPE, HDPE		0.33	92.67	1.8
Mg	EAM	LDPE, HDPE		0.33	92.43	2.82
Mh	EAM	LDPE	Molander *et al.* (1999)	1	90	/
Oa	Simple	HDPE	Caceres *et al.* (1996)	672	0	/
Pa	EFP	LDPE	Garrido-Lopez et Tena (2005)	0.67	101.9	/
Pb	EFP	LDPE	Ashraf-Khorassani *et al.* (1999)	0.67	99.4	1.3
Pc	EFP	LDPE	Zhou *et al.* (1999)	0.5	63.8	/
Pd	EFP	PE	Garrido-López *et al.* (2007b)	0.3	/	/
Pe	EFP	PE	Garrido-López *et al.* (2007a)	0.6	97.2	/
Ra	Reflux	HDPE	Caceres *et al.* (1996)	2	95	/
Rb	Reflux	LDPE	Hsiao *et al.* (2001)	3	/	/
Sa	Soxhlet	LDPE	Lundbäck *et al.* (2005)	5	92	/
Sb	Soxhlet	PS	Tawfik et Huyghebaert (1999)	12	76.5	/
Sc	Soxhlet	PS	Bermudez *et al.* (2002)	/	/	/
Sd	Soxhlet	LDPE	Molander *et al.* (1999)	3	90	/
Se	Soxhlet	PE	Tan *et al.* (1988)	8	/	/
Sf	Soxhlet	LDPE, HDPE	O'Brien *et al.* (1997)	32	/	/
Ua	Ultrasons	LDPE	Haider et Karlsson (1999b)	55	100	/
Ub	Ultrasons	LDPE	Haider et Karlsson (1999a)	0.75	100	/
Uc	Ultrasons	LDPE, HDPE	Nielson (1991)	1	92.3	1.9
Ud	Ultrasons	LDPE, HDPE		1	92.67	1.9
Ue	Ultrasons	LDPE, HDPE		1	90.85	2.57
Uf	Ultrasons	HDPE	Nielson (1993)	1	90.92	3.96
Ug	Ultrasons	HDPE		1	94	2.93
Uh	Ultrasons	HDPE	Caceres *et al.* (1996)	5	0	/
Ui	Ultrasons	MDPE	Haider et Karlsson 2002	0.75	/	/
Uj	Ultrasons	LDPE	Haider et Karlsson 2001	1	/	/
Xa	Soxtec	HDPE	Caceres *et al.* (1996)	/	50	/

EAM = extraction assistée par micro-onde, EFP = extraction sous fluide pressurisé, EFS = extraction sous fluide supercritique.

Les méthodes donnant des rendements supérieurs à 90% pour des temps d'extraction inférieurs à 1h ont été retenues dans un premier temps sur la Figure 1.11. Parmi celles-ci, on trouve essentiellement des méthodes EFP ou EAM. On trouve aussi 5 méthodes ultrasons pour lesquelles le temps d'extraction est d'une heure.

Contrairement aux deux premiers systèmes, l'extraction en utilisant un bain à ultrasons nécessite une intervention manuelle constante au cours de l'expérimentation. Il a en effet été démontré qu'une agitation manuelle est nécessaire pour obtenir une extraction suffisante en des temps courts (Nielson, 1991 et 1993). Les systèmes d'EFP ou d'EAM semblent donc plus intéressants puisqu'ils permettent respectivement une automatisation d'extractions en série et le lancement de plusieurs extractions simultanées, sans aucune intervention manuelle au cours du procédé. Deux méthodes en particulier, Pa et Mg, ont attiré notre attention car elles ont permis l'extraction d'un plus grand nombre d'additif. La méthode Pa a permis une extraction totale de 11 additifs. Les rendements présentés avoisinent les 100% et il est dommage de ne pas disposer d'information sur les erreurs liées à cette technique. La Figure 1.12 présente les

coefficients de variation associés aux méthodes d'extraction. La méthode Mg a quant à elle permit une bonne extraction de 6 additifs en entrainant de faibles erreurs sur les mesures.

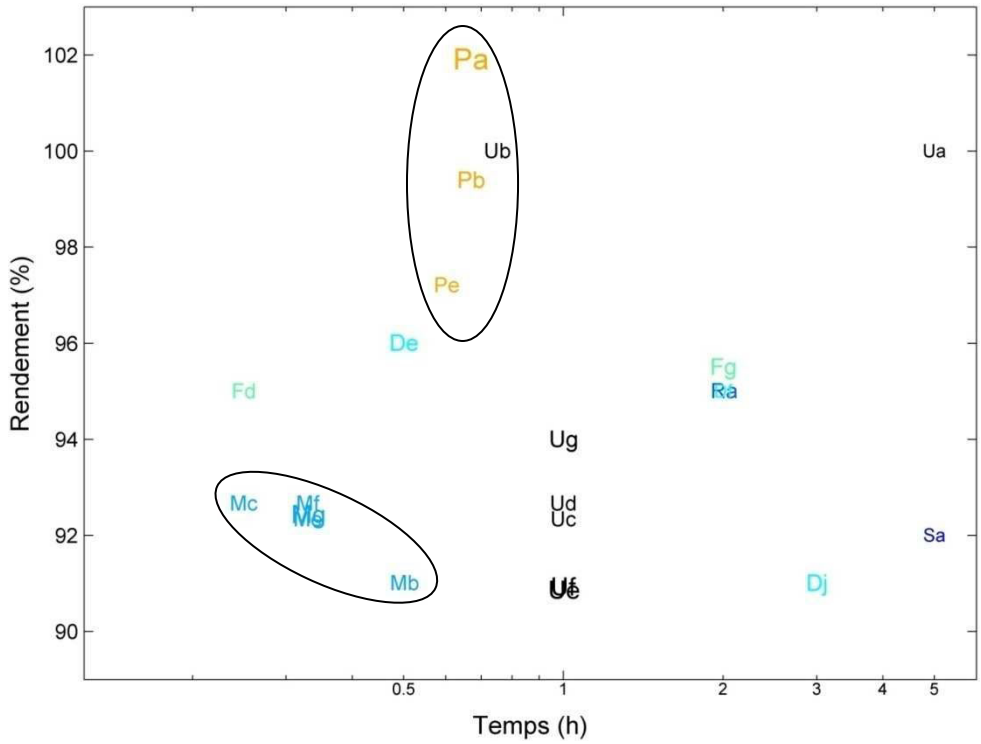

Figure 1.11. Rendements et temps d'extraction des différentes méthodes référencées. La taille du texte est proportionnelle au nombre de substances extraites par la méthode. Seules les méthodes présentant des rendements supérieurs à 90% en moins de 6h ont été représentées, une figure présentant l'ensemble des méthodes est disponible en annexe 3.

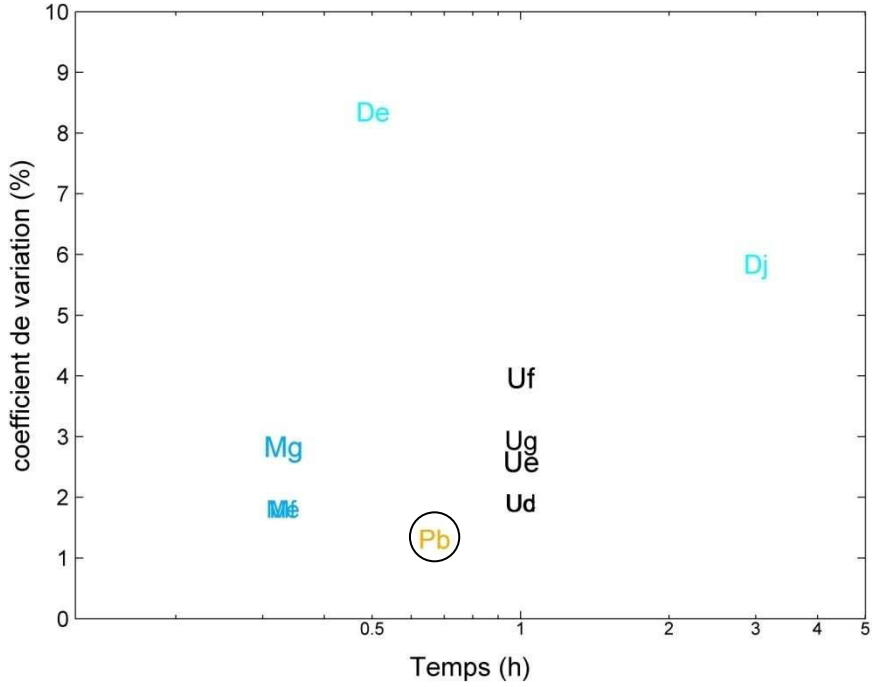

Figure 1.12. Coefficients de variation et temps d'extraction des différentes méthodes référencées. La taille du texte est proportionnelle au nombre de substances extraites par la méthode. Seules les méthodes présentant des coefficients de variation inférieurs à 10% pour des durées de moins de 6h ont été représentées, une figure présentant l'ensemble des méthodes est disponible en annexe 3.

La dissolution/précipitation (De) et l'EFS (Fd) semblent aussi potentiellement intéressantes (Figure 1.11). La première est la plus répandue pour les extractions d'additifs du polystyrène, car ce dernier est soluble dans un grand nombre de solvants du fait de sa cristallinité nulle. Dissoudre un polyéthylène demande en revanche d'utiliser un solvant agressif (Xylène) et de chauffer, ce qui explique que cette méthode soit peu utilisée pour ce matériau. Par ailleurs, dissoudre puis précipiter un polymère ne permet pas de contrôler un éventuel emprisonnement d'additifs dans la matrice nouvellement formée. Cela peut notamment expliquer que de telles méthodes présentent en général des coefficients de variation plus élevés (Figure 1.12). De même que pour la méthode Pa, il est regrettable que peu de données sur les erreurs soient disponibles pour l'EFS. Les coefficients de variations n'ont pu être calculés que pour la méthode Fg, qui donne des rendements similaires à Fd en des temps plus importants, et ils ne sont pas très encourageants (supérieurs à 10%).

Concernant le choix des solvants d'extraction, le dichlorométhane est très largement utilisé pour les essais sur le polyéthylène. Pour extraire les additifs du polystyrène, le toluène est plus généralement utilisé pour dissoudre la matrice avant de la reprécipiter dans un alcool (méthanol ou éthanol le plus souvent).

Pour conclure sur les méthodes d'extraction, les ultrasons et la dissolution/précipitation nous semblent être des méthodes à éviter car respectivement trop contraignante et trop peu robuste. L'EFP et l'EAM semblent être les méthodes les plus indiquées pour obtenir un résultat rapide. Toutes deux nécessitent toutefois un équipement particulier qui n'est pas disponible dans tous les laboratoires et ne peuvent donc pas être considérées comme des méthodes de référence. Les méthodes Pa et Mg semblent être de bons points de départ pour l'utilisation respective de systèmes d'EFP ou d'EAM. L'extraction en reflux avec ou sans soxhlet est une méthode robuste qui n'a pas été traitée. Elle est la méthode de référence actuellement et elle pourra être utilisée si aucun matériel spécifique n'est disponible ou venir en complément des méthodes rapides pour confirmer les résultats obtenus.

2.4. Utilisation de la spectrométrie infrarouge pour la déformulation rapide

Pour la déformulation rapide de matériaux polymères, des méthodes basées sur les spectroscopies Raman ou RMN (Résonnance Magnétique Nulcléaire) ont été proposées respectivement par Bart (2005) et Begley *et al.* (2005). Ces deux techniques sont toutefois difficilement utilisables dans un contexte industriel et nous avons choisi pour cela de nous intéresser plutôt à la spectroscopie IR, plus accessible.

La spectrométrie IR est très largement utilisée car elle permet de réaliser des mesures avec peu de préparation d'échantillons. Elle permet d'obtenir un spectre d'absorption lié à la vibration des liaisons chimiques des molécules. Ainsi, des molécules présentant des structures différentes auront a priori des spectres différents. La spectrométrie IR est principalement utilisée en transmission (le rayonnement IR traverse directement l'échantillon) ou en réflexion (le rayonnement IR est réfléchie par l'échantillon) dans les domaines du proche infrarouge (PIR) ou du moyen infrarouge (MIR).

Tableau 1.6. Régions du visible et de l'infrarouge (Lachenal, 1998)

Région	**f (Hz)**	**υ (cm^{-1})**
Visible	$7.9 \cdot 10^{14}$ à $3.8 \cdot 10^{14}$	26300 à 12800
PIR	$3.8 \cdot 10^{14}$ à $1.2 \cdot 10^{14}$	12800 à 4000
MIR	$1.2 \cdot 10^{14}$ à $6 \cdot 10^{12}$	4000 à 200

La spectroscopie infrarouge à transformée de Fourier (IRTF) est préférentiellement utilisée. Au lieu d'enregistrer la quantité d'énergie absorbée par l'échantillon en fonction de la fréquence, les ondes IR passent au travers d'un interféromètre. L'opération mathématique de transformation de Fourier est ensuite appliquée au signal pour redonner un spectre identique à celui que l'on aurait obtenu par la méthode conventionnelle. La spectroscopie IRTF est moins chère et plus rapide que les anciennes méthodes. Elle permet notamment de collecter et moyenner plusieurs spectres d'un échantillon en un temps très court, augmentant ainsi la sensibilité de la mesure.

Dans le domaine des polymères, on peut citer comme exemple d'applications (Lachenal, 1998) : estimation du poids moléculaire, conformation de chaine ou configuration, taux de cristallinité, anisotropie, influence des traitements thermiques ou mécaniques, suivi de polymérisation, nombre d'hydroxyle, masse molaire, contrôle de procédés en ligne, contrôle de l'épaisseur de films ou d'enductions, viscosité, identification d'emballages et recyclage, contrôle de routine d'ester de cellulose et mesure d'additifs ou de charge.

La spectroscopie IR peut être utilisée comme détecteur consécutif à une technique de séparation (Wiebolt *et al.*, 1990 ; Schunk *et al.*, 1994 ; Somsen *et al.*, 1996 ; Raynor *et al.*, 1988). Ces méthodes sont très pratiques car elles permettent d'obtenir de bons spectres des substances et donc une identification robuste des composés.

Plusieurs méthodes ont été proposées et appliquées pour l'identification et la quantification d'additifs directement dans des matériaux plastique. L'intérêt est d'éviter l'étape d'extraction des additifs de la matrice plastique car elle n'est pas toujours complète et certains composés se dégradent rapidement dans les solvants (Carlsson *et al.*, 2001). L'identification se fait généralement par recherche d'un pic caractéristique (Möller *et al.*, 2001 ; Yagoubi *et al.*, 1996 ; Földes *et al.*, 2006 ; Vitali, 2001). La quantification est alors réalisée par calibrage de la concentration en chaque additif sur les intensités des pics caractéristiques correspondants. Des rapports d'aires de pics par rapport à une référence peuvent être faits (Vitali, 2001). Ces méthodes sont toutefois limitées à de petits nombres de substances pour éviter que les pics caractéristiques ne se confondent avec d'autres pics de l'échantillon.

Une autre méthode d'identification et de quantification possible résulte de l'utilisation des outils chimiométriques. Dans le spectre d'un échantillon, les concentrations correspondantes à chaque contribution résultent de l'application de la loi de Beer-Lambert généralisée (Kramer, 1998) :

$$\underline{S} = \underline{\underline{D}} \cdot \underline{C} \tag{1.2}$$

$\underline{S}$ est le spectre de l'échantillon, $\underline{\underline{D}}$ est la matrice dictionnaire ou matrice de calibrage (matrice des coefficients d'extinction de toutes les molécules testées) et $\underline{C}$ est le vecteur contenant les concentrations (inconnues) des composés. Après calibrage de la matrice $\underline{\underline{D}}$, un vecteur $\underline{C}$ peut être calculé pour chaque échantillon à partir de son spectre IR. Cette méthode a été appliquée à l'identification et la quantification d'additifs des polymères directement dans un PE (Crine *et al.*, 1988). Le couplage à un apprentissage type réseau de neurone a aussi été testé sur des mélanges de xylène (o, m, p) et d'ethylbenzène (Li *et al.*, 1999).

Dans l'application de ces outils, une normalisation des spectres des échantillons est nécessaire pour tenir compte de la contribution du matériau plastique. Une première solution consiste à soustraire au spectre de l'échantillon le spectre du film non additivé (c'est-à-dire dans lequel aucune autre substance n'est présente). L'obtention de ce spectre peut se faire par extraction totale des additifs de la matrice (Carlsson *et al.*, 2001). Une correction plus fine peut être réalisée en tenant compte de l'épaisseur du matériau (Karstang et Henriksen, 1992).

Dans ce dernier cas les auteurs proposent d'ailleurs plusieurs modèles de correction : une normalisation basée sur des régions sélectives, une multiplication corrective du signal et une mise à l'échelle optimisée.

Pour le contrôle des matières plastiques destinées au contact alimentaire, l'utilisation des outils chimiométriques permettrait d'obtenir rapidement l'identité et la quantité des substances potentiellement migrantes contenues dans les matériaux. La principale difficulté de telles pratiques provient du grand nombre de substances à rechercher en même temps, rendant les résolutions mathématiques incertaines. Par ailleurs, l'absence d'une molécule présente dans l'échantillon de la matrice dictionnaire $\underline{\underline{D}}$ est aussi un point critique de la méthode car cela fausse la résolution mathématique. Ainsi, les cas étudiés jusque là ne comportent pas plus de 3 additifs dans un polymère (Crine *et al.*, 1988) et quatre en solution (Li *et al.*, 1999). Une généralisation de ces méthodes à un plus grand nombre de substances pourrait toutefois être intéressante à envisager à condition de palier aux difficultés mentionnées.

3. Modélisation de la migration des additifs

3.1. Définition de la diffusion moléculaire

3.1.1. Mécanisme de la diffusion

Le mécanisme de dispersion moléculaire du fait de la seule agitation brownienne des molécules est appelé diffusion moléculaire. Ce mécanisme est le processus responsable des mouvements de matière d'un compartiment d'un système vers un autre compartiment (Crank, 1975). La diffusion dépend entre autre de la température, de la pression et de la taille du migrant. La première loi de Fick postule que la densité de flux de matière, $J(x)$ est proportionnelle au gradient de concentration :

$$\begin{cases} J\left(x\right) = -D_{i,P} \cdot \left.\dfrac{\partial c_{(x,t)}}{\partial x}\right|_{(x)} \\ \dfrac{\partial c_{(x,t)}}{\partial t} = D_{i,P} \cdot \dfrac{\partial^2 c_{(x,t)}}{\partial x^2} \end{cases} \tag{1.3}$$

$D_{i,P}$ est le coefficient de diffusion moléculaire. $c_{(x,t)}$ est la concentration en migrant au temps t et à l'abscisse x dans le matériau. En remarquant que chaque molécule est animée d'un mouvement propre aléatoire du fait de l'agitation brownienne, le flux net J(x) résulte de la marche au hasard (sans direction privilégiée) des molécules à partir d'une distribution initiale

non uniforme (Einstein, 1905). Pour des molécules dispersées dans un réseau dense de chaînes longues (Figure 1.13), la translation des molécules d'additif requiert des mouvements coopératifs des segments du polymère. Ainsi, seule une fraction des déplacements des atomes du diffusant conduit à une translation du centre de gravité sur de longues échelles de temps.

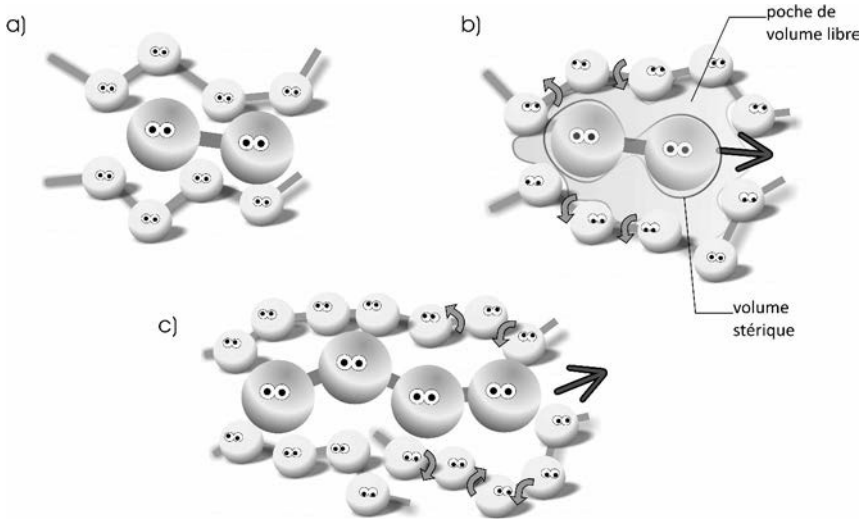

Figure 1.13. a) Encapsulation ou piégeage temporaire d'une molécule d'additif entre les segments du polymère. b) Translation de la molécule d'additif rendue possible par la relaxation locale du polymère ; elle est elle-même favorisée par le volume libre créé autour de l'additif. c) Illustration du volume libre requis pour une molécule allongée flexible ; relativement à la taille de la molécule, la poche de volume libre requise pour la translation est plus faible que pour une grosse molécule de type additif que pour une molécule de plus petite taille. Adapté de Mauritz *et al.* (1990). Source : Vitrac et Joly (2008)

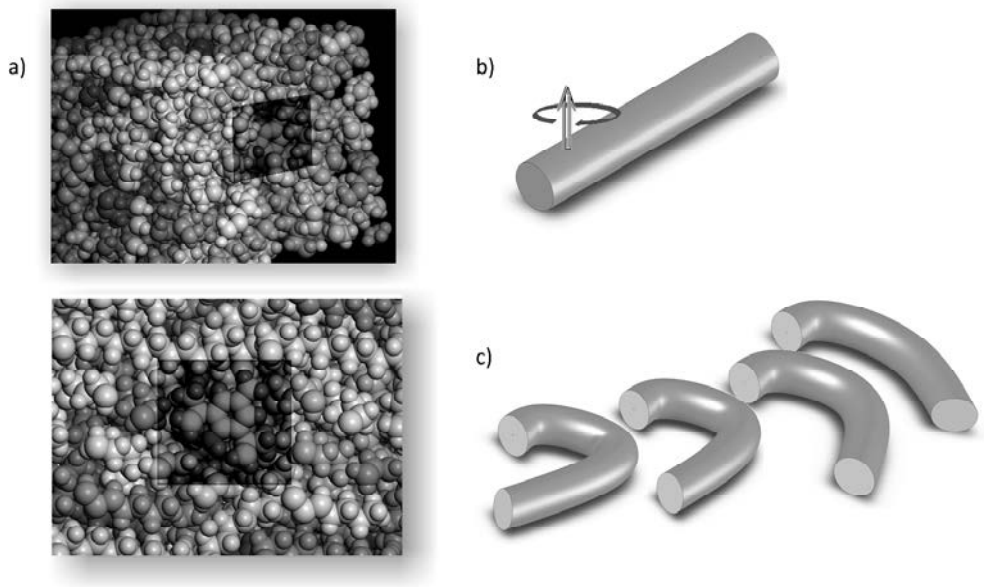

Figure 1.14. Mécanismes de translation d'un additif dans une matrice thermoplastique. a) Illustration du confinement d'un antioxydant (BHT) dans une matrice de polyéthylène (les chaînes qui masquaient l'additif ont été partiellement éliminées ou coupées). La région contenant l'additif a été noircie. b) Translation du centre de gravité d'un corps rigide par réorientation (rotation autour d'une position distincte de centre de gravité). c) translation d'un corps déformable par fluctuation du contour. Source : Vitrac et Joly (2008)

Les mesures réalisées à partir de molécules sondes chromophores (Deschesnes et Vanden Bout, 2001) ou de sondes paramagnétiques (Kovarski, 1997 ; Medick *et al.*, 2002), confirment que les molécules de type additif translatent essentiellement par réorientation. Une illustration des processus de translation par réorientation et fluctuation du contour est donnée sur la Figure 1.14.

3.1.2. Condition limite

La condition limite exprime la concentration du migrant à la surface du solide, c'est-à-dire à la surface du polymère dans le cas qui nous intéresse. Elle est obtenue en écrivant que le flux de migrant qui quitte le polymère est à tout moment égal au flux qui amène le migrant au niveau de la surface par diffusion au travers du polymère (Vergnaud, 1993 ; Rosca et Vergnaud, 2006) :

$$-D_{i,P} \cdot \frac{\partial C_{i,P}}{\partial x} = h \cdot \left(C_{i,F/P} - C_{i,F} \right) \tag{1.4}$$

$C_{i,P}$ est la concentration en migrant *i* dans le polymère à l'abscisse *x*, $C_{i,F/P}$ est la concentration de *i* dans *F*, à la surface de *P* en contact avec *F*, et $C_{i,F}$ est la concentration de *i* dans *F* au temps *t*. *h* est le coefficient de convection de *i* dans *F*.

3.1.3. Équilibre thermodynamique

L'équilibre thermodynamique est atteint lorsque le flux de molécules de *i* qui migrent de *P* vers *F* est égal au flux de molécules de *i* qui migrent de *F* vers *P*. Le coefficient de partage $K_{i,F/P}$ est défini à partir des concentrations volumiques à l'équilibre $\left\{C_{i,k}^{eq}\right\}_{k=P,F}$ dans *F* et *P* :

$$K_{i,F/P} = \frac{C_{i,F}\Big|_{eq}}{C_{i,P}\Big|_{eq}} \tag{1.5}$$

Par ailleurs, le bilan de matière à l'équilibre s'écrit :

$$C_{i,P}\Big|_{t=0} = C_{i,P}\Big|_{eq} + L_{F/P} \cdot C_{i,F}\Big|_{eq} \tag{1.6}$$

$L_{F/P} = V_F / V_P$ est le coefficient de dilution volumique (V_F et V_P sont les volumes respectifs de *F* et *P* mis en contact), $C_{i,P}\Big|_{t=0}$ est la concentration initiale de *i* dans *P*, supposée homogène.

La combinaison des équations (1.5) et (1.6) permet d'exprimer $C_{i,F}\Big|_{eq}$ en fonction de $C_{i,P}\Big|_{t=0}$:

$$C_{i,F}\Big|_{eq} = \frac{C_{i,P}\Big|_{t=0}}{\frac{1}{K_{i,F/P}} + L_{F/P}} \tag{1.7}$$

Dans le cadre d'évaluation de la contamination d'un aliment par un migrant, l'équation (1.7) est utilisée pour calculer le risque maximum de contamination. Connaissant la quantité de substance initialement présente dans le matériau, elle permet de calculer la quantité maximale de cette même substance pouvant migrer dans l'aliment. A l'inverse, il est possible de calculer une concentration maximale autorisée dans le polymère, $C_{i,P}\Big|_{t=0}^{\max}$, si l'on veut être sûr de ne pas dépasser un seuil de migration (une LMS par exemple) donné par $C_{i,F}\Big|_{eq}^{\max}$:

$$C_{i,P}\Big|_{t=0}^{\max} = C_{i,F}\Big|_{eq}^{\max} \cdot \left(\frac{1}{K_{i,F/P}} + L_{F/P} \right) \tag{1.8}$$

3.2. Démarche de modélisation et modèles associés

3.2.1. Solutions analytiques aux équations de transport

Pour la démonstration de la conformité d'un matériau plastique *P* vis-à-vis du contact avec les aliments, des modèles peuvent être utilisés pour prévoir quelle sera la quantité d'une substance qui migrera dans un aliment (ou un simulant) *F*, après un temps donné.

Les modèles de migration sont basés sur des propositions de solutions analytiques aux équations de conservation et de transport (équations (1.3), (1.4) et (1.8)).

$$C_{i,F}(t) = C_{i,F}(t=0) + \frac{A}{V_F} \cdot \int_0^t j\Big|_I \cdot dt \tag{1.9}$$

De nombreuses solutions approchées, c'est-à-dire basées sur des approximations simples ont été proposées par le passé. Citons entre autres des modèles sans partage proposés par Crank (1975) et Baner *et al.* (1996), des modèles de diffusion en aliment infini proposés par Till *et al.* (1982) et Lau et Wong (1997) ou encore des modèles de surestimation de la migration proposés par Crank (1975), Baner *et al.* (1996), Limm et Hollifield (1996) et Begley (1997). Il existe par ailleurs une famille de solutions analytiques exactes. Les plus récentes, proposées par Goujot et Vitrac (2008), généralisent les solutions proposées initialement par Sagiv (2001) qui s'appuie sur une base de fonctions propres différentes de celles répertoriées par Crank (1975) et Vergnaud (1993).

Il existe aussi des modèles spécifiques de migration multicouches appliqués aux barrières fonctionnelles (Franz, 1997) et des modèles de migration de substances de l'air dans un aliment à travers un matériau plastique (Lau *et al.*, 1995).

Les équations relatives à tous ces modèles sont généralement très complexes et ne seront pas présentées ici car elles ne seront pas discutées dans ce travail.

Elles ont par ailleurs été implémentées dans des logiciels de prévision, libres ou commerciaux qui permettent généralement de calculer quelle sera la quantité de migrant passée de P dans F en un temps t. Ces différents logiciels sont exploités aujourd'hui pour la prévision de la contamination des aliments par des emballages plastiques. La principale limitation à leur utilisation reste la non disponibilité de données d'entrée robustes ($K_{i,F/P}$ en particulier). Les surestimateurs disponibles empêchent le plus souvent d'aboutir à une conclusion en termes de conformité sur la seule base de la modélisation (Chatwin et Katan, 1989). En effet, un excès de surestimation entraine le plus souvent l'obtention du résultat "non conforme" car la migration devient alors trop importante.

3.3. Prévision des coefficients de diffusion

Sur la base de la première loi de Fick (équation (1.3)), Jost (1960), Skelland (1974), Sherwood *et al.* (1975), Crank (1975) et Hines et Maddox (1985), entre autres, ont modélisé la diffusion d'un composé dans des systèmes variés. Elle est le point de départ de nombreux modèles de diffusion dans les polymères. Les coefficients de diffusion dans les matériaux en particulier ont été largement étudiés. L'ensemble des modèles qui décrivent ce paramètre a été recensé dans une revue bibliographique (Masaro et Zhu, 1999) et ils ne seront donc pas tous énumérés ici. Dans les solides, les valeurs de $D_{i,P}$ varient d'un facteur supérieur à 10^{10}, ce qui y rend la diffusion difficile à estimer (Cussler, 1997).

Les corrélations entre la migration des substances et leur taille ont été considérées depuis de nombreuses années. Elles sont données par la formule générale :

$$D_{i,P} \approx M^{-\alpha} \tag{1.10}$$

M est la masse molaire de la substance i. Le Tableau 1.7 présente les différentes valeurs de α possibles, en fonction des mécanismes de diffusion qui y sont associés.

Tableau 1.7. Valeurs de α en fonction des mécanismes de diffusion associés.

α	Mécanisme de diffusion associé	source
½	Molécule constituée d'une bille de rayon ρ_0 (Stokes-Einstein) en solution	Einstein (1905)
1	Molécule constituée de N billes de rayon ρ_0 (Rousse) en solution	Rouse (1953)
2	Molécule constituée de N billes enchevêtrées et de rayon de giration ρ avec ses semblables, elle ne peut translater que le long de ses contours (reptation)	De Gennes (1971), Doi, et Edwards (1978)
>2	Reptation avec relâchement des contraintes	Bueche (1968), Lodge (1999)

Tableau 1.8. Modèles de surestimation des coefficients de diffusion dans les polymères.

<table>
<tr><th>Catégorie</th><th>Modèle</th><th>Source</th></tr>
<tr><td>Approche déterministe, corrélation empirique</td><td>$$\ln(D_P) = \ln(A) + a\cdot(M_W)^{1/2} - \frac{K\cdot(M_W)^{1/3}}{T} \quad (1.11)$$
D_P : coefficient de diffusion
T : température
M_W : masse molaire
a et K : constante calculées à partir des données expérimentales</td><td>Limm et Hollifield, (1996)</td></tr>
<tr><td>Approche déterministe, corrélation empirique, surestimation, approche pire des cas</td><td>$$D_P < D_P^* = 10^4 \cdot \exp\left(A_P - a\cdot M_W - b\cdot T^{-1}\right) \quad (1.12)$$
D_P : coefficient de diffusion
D_P^* : coefficient de diffusion estimé
a : coefficient de corrélation = 0.010
b : coefficient de corrélation = 10450
T : température
M_W : masse molaire
A_P : effet du polymère sur la diffusivité
<table>
<tr><th>Type de polymère</th><th>A_P</th></tr>
<tr><td>LDPE</td><td>9</td></tr>
<tr><td>LLDPE</td><td>9</td></tr>
<tr><td>HDPE</td><td>5.4, 8</td></tr>
<tr><td>PP</td><td>6.5</td></tr>
<tr><td>Non polyoléfine</td><td>0</td></tr>
<tr><td>PET, PC</td><td>-3</td></tr>
<tr><td>PVC (rigide)</td><td>-7</td></tr>
</table></td><td>Baner et al. (1996)</td></tr>
<tr><td>Approche probabiliste</td><td>$$D = a\cdot\exp\left[-\left(\frac{M}{M_0}\right)^b\right] \quad (1.13)$$
M : masse molaire
M_0 : valeur de référence de 1g/mol
a et b : paramètres dépendants du polymère et de la température
s : écart type de la distribution
<table>
<tr><th>Polymères</th><th>a</th><th>b</th><th>s</th></tr>
<tr><td>LDPE etLLDPE</td><td>$1.2\cdot10^{-6}$</td><td>0.37</td><td>1.3</td></tr>
<tr><td>MDPE et HDPE</td><td>$7.2\cdot10^{-7}$</td><td>0.39</td><td>1.6</td></tr>
<tr><td>PP</td><td>$1.9\cdot10^{-8}$</td><td>0.36</td><td>2.0</td></tr>
</table></td><td>Helmroth et al. (2002), Helmroth et al. (2005)</td></tr>
<tr><td>Approche probabiliste</td><td>Prévision des coefficients de partage en utilisant un arbre de décision basé sur 3 descripteurs topologiques des molécules.
V^{VdW} : volume de Van der Waals
ρ : rayon de gyration
I_Z/I_X : facteur de forme</td><td>Vitrac et al. (2006)</td></tr>
</table>

<table>
<tr><th>Catégorie</th><th>Modèle</th><th>Source</th></tr>
<tr><td>Corrélation empirique, surestimation, approche pire des cas</td><td>
$$D_P < D_P^* = D_0 \cdot \exp\left(A_P' - 0.1351 \cdot \left(M_i\right)^{2/3} + 0.003 \cdot M_i - \frac{10454 + \tau}{T} \right) \quad (1.14)$$
D_P : coefficient de diffusion
D_P^* : coefficient de diffusion estimé
D_0 : 10^4 cm^2/s
T : température
M_i : poids moléculaire relatif (dalton)
0.1351 : résulte de la corrélation entre les volumes molaires et masses molaires des n-alcanes
10454 : résulte de l'énergie d'activation de référence (86.9kJ/mol)
A_P' : effet du polymère sur la diffusivité
τ : correction tenant compte de la différence d'énergie d'activation entre les polymères
<table>
<tr><th>Type de polymère</th><th>A_P</th><th>τ</th></tr>
<tr><td>LDPE</td><td>11.5</td><td>0</td></tr>
<tr><td>HDPE</td><td>14.5</td><td>1577</td></tr>
<tr><td>PP (homo et random)</td><td>13/1</td><td>1577</td></tr>
<tr><td>PP (caoutchouc)</td><td>11.5</td><td>0</td></tr>
<tr><td>PS</td><td>-1</td><td>0</td></tr>
<tr><td>HIPS</td><td>1</td><td>0</td></tr>
<tr><td>SBS</td><td>10.5</td><td>0</td></tr>
<tr><td>PET, T>Tg (70°C)</td><td>6.4</td><td>1577</td></tr>
<tr><td>PET, T<Tg (70°C)</td><td>3.1</td><td>1577</td></tr>
<tr><td>PA6</td><td>0</td><td>0</td></tr>
<tr><td>PA6.6</td><td>2.0</td><td>0</td></tr>
<tr><td>PA12</td><td>2.6</td><td>0</td></tr>
<tr><td>PEN</td><td>5.0</td><td>1577</td></tr>
<tr><td>PVC (rigide)</td><td>-1.0</td><td>0</td></tr>
</table>
</td><td>Piringer et Baner (2000)</td></tr>
</table>

Aucun de ces modèles n'est toutefois applicable aux additifs des matériaux plastiques. Aussi, d'autres travaux ont été réalisés pour proposer des modèles applicables aux substances de poids moléculaire élevés, de type additifs. Pour les applications au domaine de la sécurité alimentaire, elles sont basées sur des corrélations empiriques ou des approches probabilistes permettant de surestimer $D_{i,P}$ pour ne pas sous-estimer le risque de contamination des aliments. Les principaux modèles de surestimation des coefficients de diffusion d'additifs dans les matériaux plastiques sont regroupés dans le Tableau 1.8 avec les références associées et les principales informations les concernant.

Le modèle de surestimation communément admis pour la surestimation de la migration dans les aliments est le modèle dit de Piringer (Piringer et Baner, 2000)

Le coefficient de diffusion des additifs dans les polymères a largement été étudié par le passé et des modèles de prévision ou de surestimation robustes existent. Nous avons souhaité utiliser ces modèles dans cette étude, sans essayer de contribuer aux modèles eux-mêmes.

3.4. Prévision des coefficients de partage

Des recherches expérimentales sur les coefficients de partage ont été menées entre autres par Gavara *et al.* (1996), Hernandez-Munoz *et al.* (2001), Kinigakis *et al.* (1987) et Pushpa *et al.* (1996). Peu de données expérimentales sont toutefois disponibles à ce jour pour les additifs des matériaux plastiques de part la difficulté de réalisation des mesures (solubilités, seuils de détection, dégradation des migrants dans les simulants, etc.). Des méthodes RQSP (Relation Quantitative Structure-Propriété) et RQSA (Relation Quantitative Structure-Activité) ont été utilisées pour essayer de prévoir les valeurs de $K_{i,F/P}$, en particulier pour des flaveurs alimentaires. La théorie régulière des solutions a été développée par Hildebrand et Scott (1936) et est basée sur les densités d'énergie cohésive. Son équation est simple mais les faibles corrélations entre ses prévisions et les valeurs expérimentales indiquent que la contribution entropique ne peut pas être négligée (Paik et Tigani, 1993). Les modèles de contribution de groupe sont efficaces pour décrire les propriétés thermodynamiques des mélanges de liquides (Fredenslund *et al.*, 1977 ; Voutsas et Tassios, 1997). Le modèle le plus largement utilisé est le modèle UNIFAC (UNIQUAC Functional group Activity Coefficient) qui combine le concept de groupes fonctionnels avec les résultats analytiques du modèle UNIQUAC (UNIversal, QUAsi-chemical Activity Coefficient). Ce dernier est basé sur la théorie quasi-chimique de Guggenheim qui contient une part combinatoire, due aux différences de taille et de forme des molécules dans les mélanges, et une part résiduelle, due aux énergies d'interaction. Une approche semi-empirique de prévision directe des coefficients de partage, sans prévoir les coefficients d'activité a aussi été proposée par Arab Tehrany et collaborateurs (2005, 2006 et 2007). Les propriétés les plus influentes sur le partage y sont recherchées et des valeurs de $K_{i,F/P}$ sont calculées à partir de ces propriétés grâce à une équation optimisée à l'aide de données expérimentales. Enfin, la théorie de Flory-Huggins permet a priori de prévoir indifféremment les coefficients d'activité dans les polymères et les solvants (Mougharbel, 2005). Les coefficients de Flory, qui peuvent être calculés à l'aide d'outils de modélisation moléculaire, restent toutefois à affiner pour que les prévisions obtenues par cette méthode soient acceptables. Cette théorie nous a semblé particulièrement intéressante et elle sera développée plus particulièrement dans ce travail.

3.4.1. Définition du coefficient de partage à partir des coefficients d'activité

Pour un aliment *F* en contact avec un polymère *P* contenant un migrant *i* (Figure 1.15.a), l'équilibre thermodynamique se traduit par l'égalité des potentiels chimiques :

$$\underbrace{\mu_i^0 + RT\ln\left(\gamma_{i,P}^v \cdot \phi_{i,P}\right)}_{\mu_{i,P}} = \underbrace{\mu_i^0 + RT\ln\left(\gamma_{i,F}^v \cdot \phi_{i,F}\right)}_{\mu_{i,F}} \tag{1.15}$$

Soit :

$$\frac{\phi_{i,F}}{\phi_{i,P}} = \frac{\gamma_{i,P}^v}{\gamma_{i,F}^v} \tag{1.16}$$

μ_i^0 est le potentiel chimique de *i* pur (potentiel chimique de référence), $\left\{\mu_{\mathrm{i,k}}\right\}_{\mathrm{k=P,F}}$ est le potentiel chimique de *i* dans *k*, $\left\{\phi_{i,k}\right\}_{k=P,F}$ est la fraction volumique de *i* dans *k* et $\left\{\gamma_{i,k}^v\right\}_{k=P,F}$ est le coefficient d'activité défini à partir des fractions volumiques en substances *i* dans *k*.

Le coefficient de partage $K_{i,F/P}$ défini à partir des concentrations volumiques à l'équilibre $\left\{C_{i,k}\big|_{eq}\right\}_{k=P,F}$ de *i* dans chacun des compartiments *k* peut alors s'exprimer à partir des coefficients d'activité volumiques :

$$K_{i,F/P} = \frac{C_{i,F}\big|_{eq}}{C_{i,P}\big|_{eq}} = \frac{V_i \cdot \phi_{i,F}}{V_i \cdot \phi_{i,P}} = \frac{\gamma_{i,P}^v}{\gamma_{i,F}^v} \tag{1.17}$$

Où V_i est le volume molaire de *i*.

3.4.2. Théorie de Flory-Huggins

Le modèle à grille de Flory-Huggins (Flory, 1953) est une extension de la théorie des solutions régulières pour les mélanges de polymères. Il est basé sur 3 hypothèses :

- pas de changement de volume pendant le mélange (modèle incompressible) ;
- l'enthalpie de mélange est due aux interactions entre les différents segments après élimination des interactions entre les segments de même type ;
- l'entropie de mélange est entièrement déterminée par le nombre de réarrangements possibles au cours du mélange.

Ce modèle est à champs moyen, c'est-à-dire que seules les interactions paires-à-paires sont prises en considération.

Pour des mélanges simples de molécules dont les structures chimiques sont proches (n-alcanes et PE par exemple), la théorie de Flory-Huggins, qui calcule l'entropie positionnelle

sur une grille rigide, permet une bonne estimation des grandeurs thermodynamiques (Luettmer-Strathmann *et al.*, 1998). La condition nécessaire est que le volume par mole de sites de la grille soit fixé.

Il a été démontré (Elbro *et al.*, 1990) qu'une expression peut être dérivée sans considérer la forme des molécules (c'est-à-dire sans devoir fixer une taille de référence des sites) mais plutôt les fractions volumiques et volumes libres de chaque substance du mélange. Un dérivé du modèle de Flory-Huggins a été développé pour tenir compte des espaces libres entre les molécules (Bawendi et collaborateurs, 1986, 1987 et 1988).

D'un point de vue énergétique, l'approximation de champ moyen semble trop grossière pour décrire les interactions entre molécules très dissemblables ou de flexibilités différentes (Sariban et Binder, 1987). Des arguments similaires ont été utilisés pour expliquer les divergences entre les données expérimentales et les prévisions faites à partir des coefficients de solubilité (Hansen, 2007). La principale raison est que toutes les configurations paires à paires n'ont pas la même probabilité à l'échelle atomique. L'entropie résiduelle devrait par ailleurs être incluse dans l'approximation de champ moyen. De ce fait, la description des interactions à l'échelle atomique et l'approximation hors-réseau des énergies d'interaction tenant compte du regroupement des atomes sont toutes deux nécessaires pour une estimation robuste de la contribution enthalpique (Schweizer et Curro, 1988).

La Figure 1.15 est une représentation du modèle à grille de Flory-Huggins appliqué au partage du BHT entre un PE et du méthanol. La taille des billes est définie comme étant la taille de *i*. Ainsi, une bille de *F* contient plusieurs molécules alors qu'une chaine de *P* est représentée par plusieurs billes (deux chaines sont représentées dans la Figure 1.15).

Pour un mélange aléatoire de 2 molécules, l'entropie de mélange est obtenue par la relation de Van't Hoff appliquée aux billes de *k* et *i* (représentant *P* ou *F*). Pour n_i molécules de *i* de taille 1 et n_k molécules de *k* de taille relative (par rapport à *i*) r_k :

$$\begin{aligned} S_{i+k}^{m} &= k_B \cdot \left[n_k \cdot \ln\left(\frac{n_i + n_k r_k}{n_k r_k} \right) + n_i \cdot \ln\left(\frac{n_i + n_k r_k}{n_i} \right) \right] \\ &= -k_B \cdot \left[n_k \cdot \ln\left(\phi_k\right) + n_i \cdot \ln\left(1-\phi_k\right) \right] \end{aligned} \tag{1.18}$$

où k_B est la constante de Boltzmann.

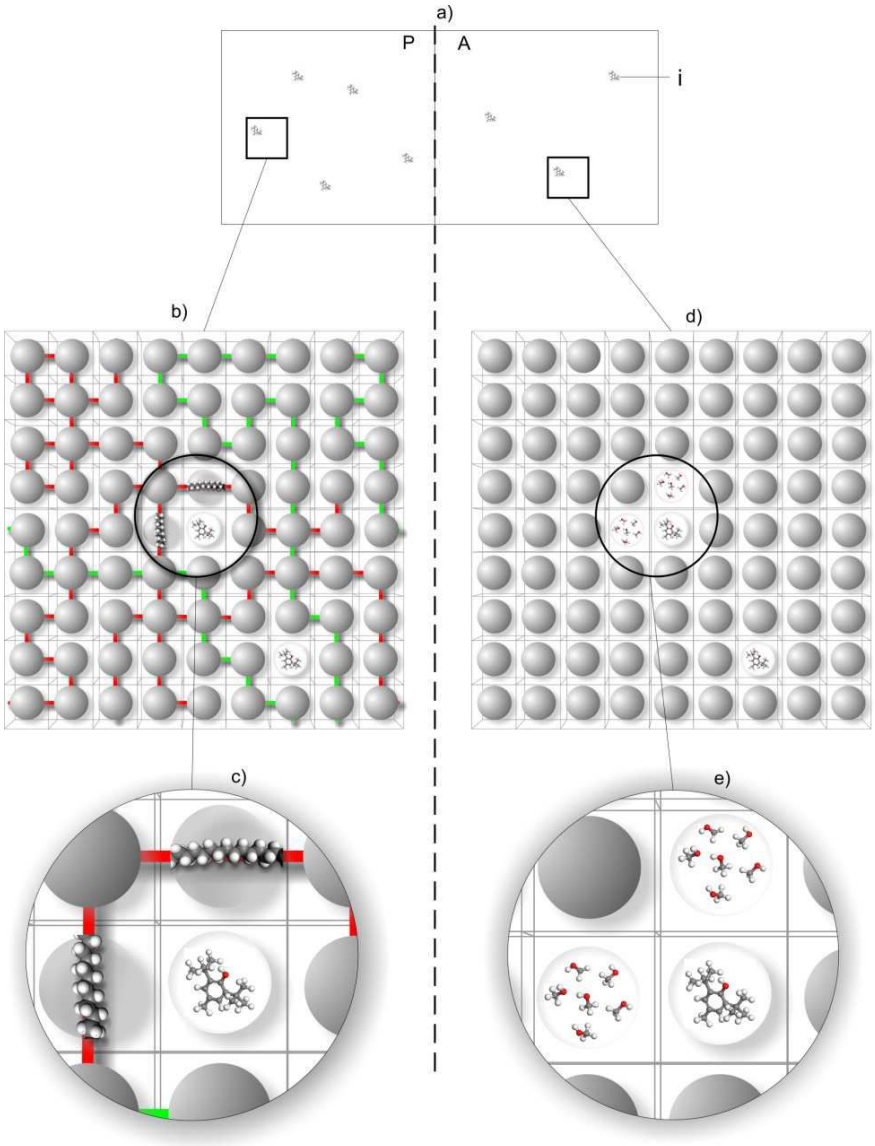

Figure 1.15. a) représentation du contact entre le polymère *P* et l'aliment *F* en présence du contaminant *i* ; b) représentation mésoscopique de *P*, 2 chaines sont représentées ; c) approximation du mélange polymère-migrant en champs moyen ; d) représentation mésoscopique de *F* ; e) approximation du mélange aliment-migrant en champs moyen.

L'enthalpie de mélange est quant à elle définie en appliquant les concepts de la théorie régulière des solutions par :

$$\Delta H_{i+k}^{m} = k_B \cdot T \cdot \chi_{i+k} \cdot n_i \cdot \phi_k \tag{1.19}$$

T est la température et $\chi_{i,k}$ est un nombre adimensionné défini à partir des énergies d'interaction paires à paires $\{\varepsilon_{a+b}\}_{a,b=i,P,F}$ et du nombre de coordination *z* qui rend compte du nombre de voisin de chaque molécule (4 sur une grille en 2 dimensions, 6 sur une grille en 3 dimensions) :

$$\chi_{i+k} = \frac{z}{2} \cdot \frac{\left[\varepsilon_{i+k} + \varepsilon_{k+i} - \left(\varepsilon_{i+i} + \varepsilon_{k+k} \right) \right]}{k_B \cdot T} \tag{1.20}$$

En utilisant les équations (1.18) et (1.19) l'énergie libre de mélange peut être exprimée par :

$$\begin{aligned} \Delta G^m_{i+k} &= \Delta H^m_{i+k} - T \cdot \Delta S^m_{i+k} \\ &= k_B \cdot T \cdot \left[n_k \cdot \ln\left(\phi_k\right) + n_i \cdot \ln\left(1-\phi_k\right) + \chi_{i+k} \cdot n_i \cdot \phi_k \right] \end{aligned} \tag{1.21}$$

Les coefficients d'activités sont alors donnés par :

$$\begin{aligned} \ln\left(\gamma^v_{i,k}\right) &= \frac{\mu^m_{i,k}}{k_B \cdot T} = \frac{1}{k_B \cdot T} \cdot \left. \frac{\partial G^m_{i+k}}{\partial n_i} \right|_{P,T,n_k} \\ &= \left(1 - \frac{1}{r_k}\right) \cdot \phi_k + \chi_{i,k} \cdot \phi_k^2 \approx \left(1 - \frac{1}{r_k}\right) + \chi_{i,k} \end{aligned} \tag{1.22}$$

D'où finalement, en supposant que la taille de *P* est très grande devant celle de *i*, c'est-à-dire que $\frac{1}{r_P} \to 0$, le coefficient de partage de *i* entre *F* et *P* devient :

$$\ln\left(K_{i,F/P}\right) = \underbrace{r_F^{-1}}_{\substack{\text{contribution} \\ \text{entropique}}} - \underbrace{\chi_{i+F} + \chi_{i+P}}_{\substack{\text{contribution} \\ \text{enthalpique}}} \tag{1.23}$$

3.4.3. Evaluation de $\left\{\chi_{i,k}\right\}_{k=P,F}$ par le biais des coefficients de solubilité

Les paramètres d'interaction de Flory-Huggins sont généralement calculés à partir des énergies de cohésion (Hildebrand et Scott, 1936) et plus particulièrement de leur séparation en une contribution dispersive $\left\{\delta^d_j\right\}_{j=i,P,F}$, une contribution polaire $\left\{\delta^p_j\right\}_{j=i,P,F}$ et une contribution due aux liaisons hydrogène $\left\{\delta^h_j\right\}_{j=i,P,F}$, (Van Krevelen et Hoftyzer, 1976 ; Barton, 1983) :

$$\chi_{i,k} = \frac{V_i \cdot \left[\left(\delta^d_i - \delta^d_k\right)^2 + \left(\delta^p_i - \delta^p_k\right)^2 + \left(\delta^h_i - \delta^h_k\right)^2 \right]}{R \cdot T} \tag{1.24}$$

Où *R* est la constante des gaz parfaits.

Baner et Piringer (1991) ont réalisé une première estimation des coefficients de partage en utilisant ce type d'approche. Pour que leur modèle soit corrélé aux données expérimentales, ils ont introduit un facteur empirique dépendant de la taille et de la forme des molécules pour corriger les valeurs prévues. Leurs résultats sont reportés sur la Figure 1.16 et la Figure 1.17.

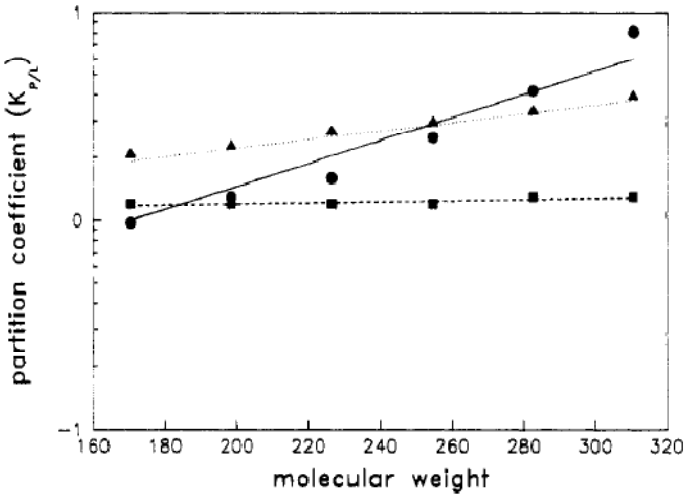

Figure 1.16. Régressions linéaires de données de coefficients de partage expérimentaux et calculés de n-alcanes entre un PEBD et de l'éthanol, en fonction de la masse molaire des n-alcanes à 25°C : (●) données expérimentales (Koszinowski, 1986a) ; (▲) coefficients de solubilité de Hoy (1985) ; (■) coefficients de solubilité de Van Krevelen et Hoftyzer (1976). Source : Baner et Piringer (1991).

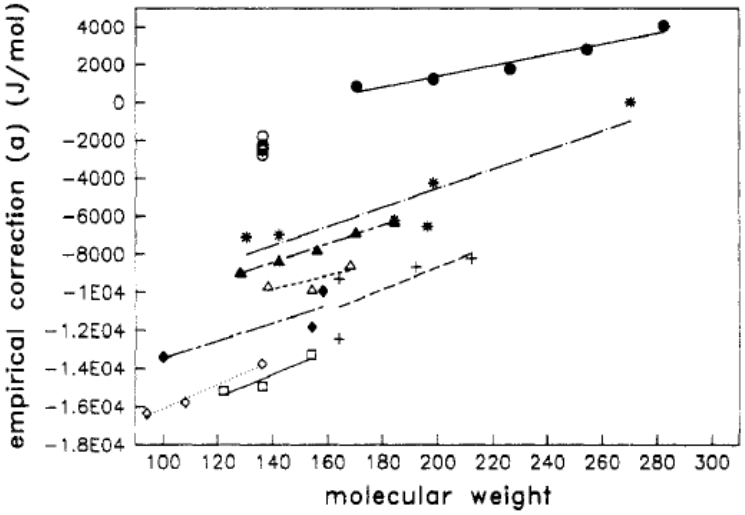

Figure 1.17. Régression linéaire du facteur empirique (*a*) en fonction de la masse molaire de solutés polaires et apolaires partagés entre un PEBD et du méthanol. *a* est calculé à partir des coefficients de solubilité de Hoy (1985) et des données expérimentales de Koszinowski (1986b) et de Koszinowski et Piringer (1990): (●) n-alcanes ; (○) hydrocarbures insaturés ; (Δ) aldéhydes insaturés ; (*) esters linéaires ; (▲) n-aldéhydes; (+) esters de phényle; (♦) alcools primaires ; (□) alcools phényliques ; (◊) phénols (solvant éthanol). Source : Baner et Piringer (1991).

Les corrélations entre le modèle proposé et les données expérimentales sont bonnes. Il faut noter toutefois que cette approche ne tient pas compte du calcul de l'entropie non configurationelle, qui pourrait peut-être être associée au coefficient empirique introduit. En effet, le terme correctif *a* introduit par Baner et Piringer apparaît corrélé à la masse moléculaire des additifs, tout comme l'entropie non configurationelle qui est un effet de taille.

Des revues bibliographiques récentes (Lindvig *et al.*, 2002 ; Hansen, 2007), sur la prévision des coefficients d'activité dans les polymères ont montré que : i) l'évaluation par les coefficients de solubilité amène une forte surestimation systématique et ii) la décomposition des coefficients de solubilité doit être pondérée empiriquement par des valeurs inférieures à 1. L'équation proposée est la suivante :

$$\chi_{i,k} = \alpha \frac{V_i \cdot \left[\left(\delta_i^d - \delta_k^d \right)^2 + 0.25 \left(\delta_i^p - \delta_k^p \right)^2 + 0.25 \left(\delta_i^h - \delta_k^h \right)^2 \right]}{R \cdot T} \quad (1.25)$$

α est un facteur correctif empirique que Hansen (2007) propose de laisser égal à 1. Il peut toutefois être estimé à partir de données expérimentales pour prévoir au mieux les coefficients de partage.

3.4.4. Prévision par la modélisation moléculaire

Une méthode alternative pour prévoir les coefficients de solubilité est issue de la modélisation moléculaire (Frenkel et Smit 2002 ; Ben-Naim, 2006). La méthode la plus répandue consiste à mesurer l'excès d'énergie libre en dynamique moléculaire lorsque l'on ajoute (Widom, 1963) ou retire (Boulougouris *et al.*, 2001) un soluté à une phase de référence. Les méthodes d'insertion et de délétion ne sont robustes que si la dynamique de réorganisation de la phase de référence n'est pas limitante.

Du fait que les temps nécessaires à la relaxation des polymères sont relativement longs devant les périodes de vibration des atomes, la différence d'énergie libre peut être avantageusement remplacée par une intégration thermodynamique (van der Vegt et Briels, 1998). Une réduction supplémentaire des temps de calculs peut être obtenue en remplaçant les dynamiques moléculaires (longues) par des techniques d'échantillonnage Monte-Carlo dans un ensemble de Gibbs (Nath *et al.*, 2001).

Toutes ces méthodes ont été appliquées à des mélanges de grandes molécules (polymères) avec de petits solutés, mais elles n'ont jamais été appliquées à de gros solutés tels que des additifs phénoliques ou des anti-UV polymériques utilisés comme stabilisants des matières plastiques.

Pour conclure, des outils sont d'ores et déjà disponibles pour la modélisation de la migration de substances contenues dans un emballage vers un aliment. Des logiciels sont même disponibles pour une utilisation plus directe des concepts qui ont été développés. Deux paramètres en particulier sont nécessaires à l'utilisation des modèles et ne sont pas mesurables

simplement : le coefficient de diffusion, $D_{i,P}$, et le coefficient de partage, $K_{i,F/P}$. si des modèles de prévision robuste de $D_{i,P}$ existent aujourd'hui, ce n'est pas le cas pour $K_{i,F/P}$ qui n'a encore été que peu étudié, particulièrement pour des molécules telles que des additifs des matériaux plastiques et leur partage entre des simulants alimentaires et des polymères. Relativement peu de données expérimentales de ce dernier sont disponibles et les modèles proposés jusque là sont encore trop peu robustes. Le recours à des surestimateurs grossiers (1 ou 1000) est la solution la plus répandue pour le moment.

4. Synthèse de la bibliographie : objectifs et démarche du travail

4.1. Objectifs

A la suite de cette étude bibliographique, il apparaît que, pour pouvoir prévoir la conformité d'un matériau d'emballage plastique au contact alimentaire, certains aspects ont été peu traités dans la littérature. La Figure 1.18 présente de façon très schématique le processus de vérification de la conformité d'un emballage et met en évidence les connaissances nécessaires. Les parties grisées du schéma présentent les données peu disponibles dans la littérature sur lesquelles nous avons concentré nos efforts de recherche.

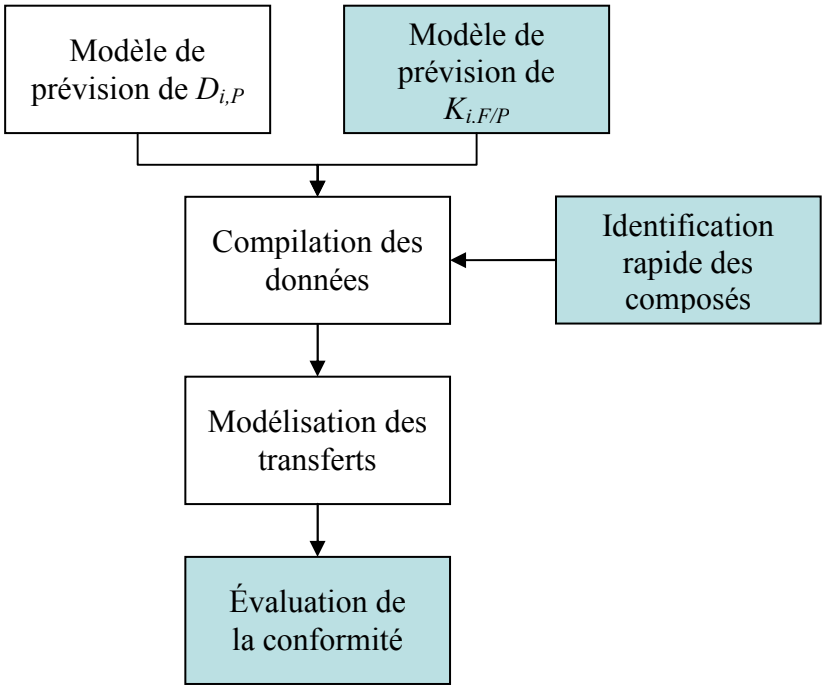

Figure 1.18. Représentation schématique des outils nécessaires à l'évaluation de la conformité des matériaux d'emballage. Les besoins de recherche apparaissent en grisé.

Nous voulons apporter une contribution aux nombreux travaux réalisés pour permettre la maîtrise des transferts de contaminant, assurer une évaluation robuste et plus précise des contaminants et finalement optimiser la formulation des emballages pour accroître les performances sans mettre en cause la sécurité du consommateur.

En effet, des méthodes robustes d'identification et de quantification des substances dans les solvants et simulants existent aujourd'hui, rendant la vérification de la conformité des matériaux plastiques vis-à-vis du contact alimentaire théoriquement possible. Toutefois, ces méthodes sont souvent lourdes à mettre en œuvre et restent incompatibles avec le besoin de prendre des décisions rapides en cas de crise sanitaire. Le manque d'informations accessibles concernant la formulation des matériaux empêche les utilisateurs d'emballage et les laboratoires de contrôle de vérifier réellement la conformité. Les méthodes analytiques ne sont par ailleurs pas bien intégrées dans une démarche globale de prévision du risque de contamination. Il semble donc nécessaire de réévaluer ces techniques pour les intégrer dans la démarche globale et de tester l'aptitude de méthodes plus simples et plus rapides à mettre en œuvre, telles que la spectroscopie IR, pour l'identification, voire la quantification des substances.

Le manque de données de types coefficients de partage expérimentaux ou de modèles robustes limite encore l'utilisation des outils prédictifs. La génération de données expérimentales est aujourd'hui nécessaire d'une part pour l'utilisation des outils de prévision de la contamination et, d'autre part, pour le développement de modèles de prévision de $K_{i,F/P}$. Une prévision robuste de ce paramètre permettrait en effet de palier les difficultés de mesures expérimentales. L'application du modèle de Flory-Huggins à la fois au polymère et à l'aliment (ou à un simulant de l'aliment) semble être une bonne alternative aux modèles actuels de prévision des coefficients d'activité.

L'objectif général de ce travail est de contribuer au développement des méthodes rapides, analytiques ou de type modélisation, pour la vérification de l'aptitude des matériaux plastiques au contact alimentaire et de les intégrer dans une démarche globale de prévision de la conformité des matériaux plastiques vis-à-vis du contact alimentaire. Ces méthodes devront être utilisables par les différents acteurs de la filière et notamment les industriels de l'agroalimentaire et les laboratoires de contrôle.

Les objectifs plus particuliers sont :

- de réévaluer les techniques analytiques existantes pour les intégrer dans la démarche d'évaluation de la conformité ;

- de tester la possibilité d'identifier les substances contenues dans un matériau plastique par étude du spectre infrarouge issu du matériau (transmission directe à travers le polymère ou spectre d'un extrait) ;
- de générer des valeurs expérimentales de coefficients de partage de molécules de type additifs entre des polymères (PEHD ou PS) et des simulants alimentaires.
- de proposer un modèle de prévision des coefficients d'activités en appliquant la théorie de Flory-Huggins à la fois au polymère et au simulant alimentaire et de le confronter aux données expérimentales de la littérature et à celles acquises au cours de l'étude ;
- de proposer des règles simples, basées sur des arbres de décisions, d'utilisation des outils prédictifs existant en fonction des informations de formulation connues et des paramètres disponibles.

4.2. Démarche

De part leur utilisation répandue et leurs différences de propriétés à température ambiante, un PEHD (caoutchoutique) et un PS (vitreux) ont été sélectionnés comme matériaux d'études. Les additifs choisis doivent couvrir les principales classes d'additifs (antioxydants primaires et secondaires, stabilisants UV, agent glissants, charges) tout en présentant des structures chimiques les plus différentes possibles (phénol, benzotriazoles, thio-esters, triazine, etc.).

Si les modèles de prévision peuvent s'appliquer au PEHD et au PS, la quantité de données de références disponibles, de type coefficient de diffusion ou coefficient de partage, n'est pas comparable. Il existe très peu de données concernant le PS. De manière générale, peu de travaux ont été réalisés sur ce matériau et le Tableau 1.5 montre par exemple que peu de méthodes d'extraction ont été proposées. Seule la dissolution/reprécipitation est utilisée aujourd'hui.

Nous avons donc choisi d'axer particulièrement notre étude sur un PEHD, de manière à être le plus exhaustif possible dans la démarche globale intégrant analyses et prévisions. Du fait de la diffusivité des molécules de poids moléculaires élevés dans ce matériau ($D_{i,P}$ élevés), la contamination est surtout contrôlée par les coefficients de partage. C'est pourquoi nous avons décidé de mesurer expérimentalement cette grandeur pour obtenir de nouvelles données de référence. Nous nous sommes notamment intéressés à des mélanges eau/éthanol, de fractions volumiques différentes, pour essayer de déterminer par extrapolation des valeurs de $K_{i,F/P}$

entre un PEHD et l'eau. En effet, les mesures directes dans l'eau sont rendues très difficiles par les faibles solubilités des molécules de types additifs dans ce simulant d'une part, et par leur hydrolyse d'autre part. L'équation (1.26) montre les différents biais potentiels pour la mesure de $K_{i,F/P}$:

$$K_{i,F/P} = \frac{C_{i,F}\Big|_{eq}}{C_{i,P}\Big|_{eq}^{a}} = (1-c)\cdot \frac{\frac{1}{a_{i,F}}\cdot \hat{C}_{i,F}\Big|_{eq}}{\frac{1}{a_{i,P}}\cdot \hat{C}_{i,P}\Big|_{eq} - b_i \cdot C_{i,P}\Big|_{t=0}} \tag{1.26}$$

$C_{i,F}\Big|_{eq}$ et $C_{i,P}\Big|_{eq}^{a}$ sont les concentrations à l'équilibre dans l'aliment (le simulant) et le polymère respectivement. $\left\{\hat{C}_{i,k}\Big|_{eq}\right\}_{k=P,F}$ sont les concentrations correspondantes mesurées expérimentalement, chacune pondérée d'un rendement $\left\{a_{i,k}\right\}_{k=P,F}$ lié à l'hydrolyse ou à l'extraction par exemple. c est la cristallinité du polymère (fraction volumique en phase cristalline). Par ailleurs, les additifs de grande taille ont parfois des points de fusion supérieurs aux températures de mise en forme des matériaux, c'est pourquoi l'équation (1.26) tient aussi compte d'une éventuelle proportion b_i d'additif qui resterait cristallisée (ou serait piégée dans la phase cristalline du polymère) et ne participerait pas aux échanges.

Les $\left\{a_{i,k}\right\}_{k=F,P}$ peuvent être évalués et contrôlés par l'utilisation de méthodes d'analyses robustes, ce qui obligera une phase de calibrage fine des méthodes. Les b_i quant à eux peuvent être déterminés à partir de la mesure des $\left\{\hat{C}_{i,k}\Big|_{eq}\right\}_{k=F,P}$ pour différents ratios massiques de polymère et de simulant comme la déviation de l'isotherme de Henry de l'idéalité (ordonnée à l'origine négative).

La méthode d'extrapolation a déjà été utilisée par le passé (Piringer et Baner, 2000) avec un modèle linéaire (premier degré) qui ne nous semble pas raisonnable du fait des considérations thermodynamiques issues du modèle de Flory-Huggins (Young, et al., 2002), indiquant qu'un modèle du troisième degré serait a priori plus approprié. La mesure expérimentale de données de partage de référence reste toutefois une démarche lourde et peu robuste quand la concentration dans l'un des deux milieux (polymère ou simulant) est très faible. Nous avons donc aussi choisi de développer et d'évaluer un modèle de prévision des coefficients de

partage à partir d'un modèle à grille de type Flory-Huggins. Ce modèle sera appliqué à quelques simulants simples mais aussi aux mélanges binaires de type eau-éthanol.

Les travaux sur le PS seront quant à eux amorcés. La dissolution/reprécipitation ne permettant pas de contrôler le piégeage de substances au cours de la phase de précipitation, nous avons souhaité développer une autre méthode, rapide, d'extraction des additifs d'une matrice PS. Les techniques d'identification et de dosage dans les solvants utilisées ensuite sont inchangées. Nous avons aussi décidé de mesurer expérimentalement de coefficients de partage entre le PS et divers simulants, conjointement aux mesures réalisées sur le PEHD.

Chapitre 2

Matériels et Méthodes

La rédaction de la partie résultats et discussion étant réalisée sous forme de publications, les matériels et méthodes relatifs à chaque sous-partie des résultats de la thèse sont détaillés dans la ou les publication(s) associée(s). Bien que traitant tous les points, le matériel et méthodes présenté dans cette partie est donc volontairement succinct. La théorie relative à la prévision des coefficients de partage en particulier, et notamment les démonstrations et équations intermédiaires, sera détaillé dans les publications.

1. Choix des formulations étudiées

De part leur utilisation répandue et leurs différences de propriétés à température ambiante, un PEHD (caoutchoutique) et un PS (vitreux) ont été sélectionnés comme matériaux d'études. Quatre formulations ont été définies pour chaque polymère : 2 formulations simples permettant le développement et la validation de méthodes de référence pour l'identification et le dosage des additifs ; 2 formulations proches de formulations industrielles, définies en collaboration avec des professionnels du domaine (TOTAL, BP) pour tester les méthodes développées sur des échantillons les plus proches possible d'échantillons réels. Les données relatives aux substances étudiées sont regroupées en annexe 3. Le Tableau 2.1 regroupe les formulations de HDPE étudiées alors que le Tableau 2.2 regroupe les formulations de PS étudiées.

Tableau 2.1. Compositions des films de PEHD étudiés.

Additif	PE1 (mg/kg)	PE2 (mg/kg)	PE3 (mg/kg)	PE4 (mg/kg)
Irganox 1076	467 ± 23	/	156 ± 3	159 ± 27
Irgafos 168	2497 ± 167	/	626 ± 40	/
Erucamide	3436 ± 116	/	1523 ± 152	/
Chimassorb 81	/	3293 ± 370	668 ± 46	/
Chimassorb 944	/	3327 ± 237	/	545 ± 26
Tinuvin 622	/	3416 ± 960	/	427 ± 120
Irganox 3114	/	/	463 ± 42	/
Tinuvin 326	/	/	626 ± 61	/
Irganox PS 802	/	/	/	502 ± 17

Tableau 2.2. Compositions des films de PS étudiés.

Additif	PS1 (mg/kg)	PS2 (mg/kg)	PS3 (mg/kg)	PS4 (mg/kg)
Irganox 1076	443 ± 44	/	/	/
Irgafos 168	3418 ± 340	/	/	873 ± 87
Erucamide	4110 ± 410	/	/	920 ± 92
Chimassorb 81	/	3233 ± 320	/	/
Chimassorb 944	/	3326 ± 336	/	/
Tinuvin 622	/	/	/	/
Irganox 245	/	/	322 ± 32	/
Irganox PS 802	/	/	467 ± 47	/
Acide stéarique	/	/	615 ± 62	/
Irganox 1035	/	/	/	423 ±42

Les additifs ont été fournis par CIBA (Suisse), à l'exception de l'Erucamide, fourni par CRODA (Italy) et de l'acide stéarique fourni par MERCK (Allemagne). Les polymères non additivés ont été fournis par ATOCHEM (France).

Des granulés de polymères ont tout d'abord été formulés avec les additifs avant la mise en forme finale. La Figure 2.1 présente l'ensemble du processus de mise en forme des films étudiés. Les deux extrusions ont été réalisées à 200°C sur une extrudeuse double-vis (model BC-21 CLEXTRAL, France) et les matériaux ont finalement été calandrés en rouleaux de 0.15 m de large.

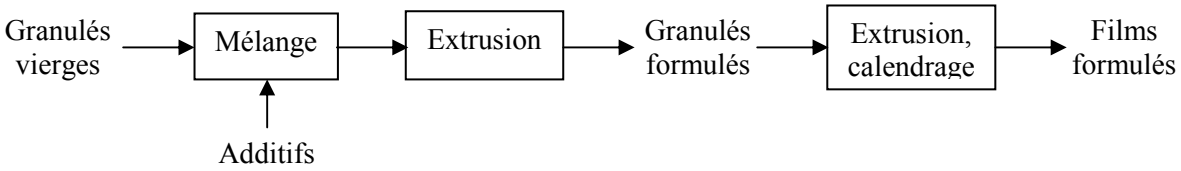

Figure 2.1. Schéma du processus de mise en forme des films formulés étudiés.

La densité et la cristallinité du PEHD obtenu sont respectivement 940 $kg \cdot m^{-3}$ et 70 %, avec un point de fusion à 136°C. La densité et la température de transition vitreuse du PS obtenu sont respectivement 1030 $kg \cdot m^{-3}$ et 98°C.

La densité des matériaux a été déterminée par la méthode du pycnomètre (norme ISO 1183-1:2004). Les mesures ont été réalisées dans un laboratoire thermo-régulé à 23°C ± 0.5°C à l'aide de pycnomètres de Gay-Lussac de 25mL (Figure 2.2).

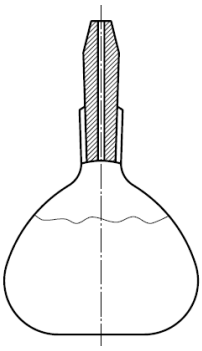

Figure 2.2. Pycnomètre de Gay-Lussac

La densité de l'éthanol a été déterminée dans un premier temps : le pycnomètre est rempli d'éthanol et pesé sur une balance préalablement tarée à l'aide du pycnomètre vide,

La densité des matériaux est ensuite déterminée par immersion : environ 1g de polymère (pesé précisément) est placé dans le pycnomètre dont le volume est ensuite complété par de l'éthanol. La masse du pycnomètre est alors mesurée et la densité de l'échantillon est donnée par la formule suivante :

$$\rho_e = \frac{m_{tot} - (m_{pyc} + m_{éthanol})}{V_{pyc} - \frac{m_{EtOH}}{\rho_{éthanol}}} \tag{2.1}$$

Où ρ_e est la densité de l'échantillon, $\rho_{éthanol}$ est la densité de l'éthanol, m_{tot} est la masse du pycnomètre plein (contenant l'éthanol et le matériau), m_{pyc} est la masse du pycnomètre vide, $m_{éthanol}$ est la masse d'éthanol, V_{pyc} est le volume du pycnomètre (25mL).

Les propriétés thermiques des matériaux et la cristallinité du PEHD ont été déterminées par calorimétrie différentielle à balayage (DSC modèle 2920, TA instrument, France). Deux cycles successifs sont réalisés. Dans chaque cycle, une rampe à raison de 10°C/min jusqu'à 150°C a été appliquée.

2. Techniques d'analyse

2.1. Extractions des additifs d'un polystyrène

Trois méthodes d'extractions différentes ont été testées sur les matériaux polymères étudiés.

L'EFP (modèle ASE 200, DIONEX, USA) a été utilisée pour extraire les additifs contenus dans les formulations de PS. Le solvant utilisé est un mélange isopropanol-dichlorométhane (75:25, v/v). Les deux solvants sont fournis par SIGMA-ALDRICH (USA). Le protocole utilisé est similaire à celui décrit par Garrido-Lopez et Tena (2007). 600 mg d'échantillon découpé en carrés de 5 mm de côté sont placés dans une cellule d'extraction de 11mL. L'extraction est réalisée à 105°C et 10.3MPa en deux phases statiques successives de 15min chacune. Pour éviter la dégradation des additifs, 100 $\mu L \cdot L^{-1}$ de tri-éthylphosphite (SIGMA-ALDRICH, USA) sont ajoutées préalablement dans le solvant d'extraction. L'extrait est récupéré dans un flacon approprié puis volumé à 20mL avant dosage des substances extraites. Cette méthode a été appliquée au PEHD et au PS.

L'extraction par simple reflux a été réalisée en plaçant 10g d'échantillon découpé en carrés de 5 mm de côté dans 100mL de mélange isopropanol-dichlorométhane (75:25, v/v) pendant 40h à 40°C. L'extrait est ensuite complété à 100mL avant le dosage des substances extraites. Cette méthode a été appliquée au PEHD et au PS.

L'extraction par dissolution / reprécipitation a été réalisée en dissolvant les poudres de PS dans le dichlorométhane puis en précipitant ensuite le polymère dans l'isopropanol. L'extrait obtenu est alors quasi totalement évaporé puis revolumé dans 100mL de mélange isopropanol-dichlorométhane (75:25, v/v).

2.2. Identification et quantification des additifs

2.2.1. Chromatographie liquide haute performance

L'identification et la quantification des additifs s'est essentiellement faite par CLHP couplée à deux détecteurs : une barrette de diode (UV) et un DEDL. La chaine consiste en un Autosampler Waters 717plus, un contrôleur Waters 600, un four de colonne et dégazeur en ligne AF, tous fournis par WATERS (USA). Les détecteurs utilisés sont un PDA 2996

(WATERS, USA) et un DDL 31 (EUROSEP, France), respectivement comme détecteur UV et DEDL. La séparation s'est faite sur une colonne Xterra C8 (150mm×3.0mm; 5µm; WATERS, USA) chauffée à 60°C. La méthode de séparation est dérivée de celle développée par Coulier *et al.* (2005). Le Tableau 2.3 présente le détail du gradient de concentration au cours du temps. Le débit est maintenu à 0.8 $mL \cdot min^{-1}$ tout au long de la séparation et le volume d'injection est de 30 µL.

Tableau 2.3. Gradient de solvants appliqué pour la séparation des composés en CLHP.

Temps (min)	Solvent A (%)	Solvent B (%)	Solvent C (%)
0	40	60	0
2	40	60	0
30	0	100	0
32	0	0	100
37	0	0	100
42	40	60	0
53	40	60	0

Solvant A : NH_4Ac (VWR, France) 10mM, pH ajusté à 9.5 avec du NH_4OH à 25% (ACROS organics, Belgium), ajout de 500µL/L de *n*-hexylamine (SIGMA-ALDRICH, USA) ; Solvant B: acétonitrile (HPLC grade, CARLO ERBA, France), ajout de 500µL/L de *n*-hexylamine ; Solvant C: isopropanol, ajout de 500µL/L de *n*-hexylamine.

2.2.2. Chromatographie Phase Gaz

L'identification et la quantification de certains additifs a été réalisée par CPG- DIF à l'aide d'un AutoSystem XL (Perkin Elmer, USA) utilisé en mode "on-column". 1µL de solution est injecté dans un injecteur maintenu à 45°C pendant 2min puis chauffé à 320°C à raison de 100°C/min. Une colonne capillaire BPX5 (30m×0,25mm×0,25µm; SGE Europe, France). Est utilisée dans un four maintenu à 50°C pendant une minute, puis chauffé jusqu'à 330°C à raison de 15°C/min. La température est enfin maintenu à 330°C pendant 5min.

2.2.3. Infra-rouge à transformée de Fourrier

Les spectres IRTF ont été réalisés à 23°C à l'aide d'un spectromètre spectrum one (Perkin-Elmer, USA). Les spectres des films ont été réalisés par transmission directe alors que les spectres des extraits (ou des solutions étalons) ont été réalisés par transmission dans une cellule omni-cell de 100µm (Eurolab, Allemagne).

Tous les spectres ont été réalisés entre 550 et 4000 cm^{-1}. 16 spectres ont été mesurés et moyennés par l'appareil pour chaque échantillon.

2.3. Mesure expérimentale de coefficients de partage

Les coefficients de partage de 7 additifs entre des simulants et du PEHD ont été mesurés. Il a été choisi de travailler avec quatre ratios massiques PEHD/simulant pour vérifier le respect des isothermes de Henry. Le Tableau 2.4 regroupe les choix de ratios et les conditions de mise en contact correspondantes. Les ratios ont été choisis de manière à faciliter les mesures de concentrations à l'équilibre. Les mises en contact ont été réalisée à 40°C.

Ratio choisi	Volume de fiole (mL)	Masse de PEHD (g)
50	100	2.0
40	100	2.5
30	100	3.3
20	100	5.0

Tableau 2.4. Ratios et conditions de mises en contact du PEHD avec les simulants

Les coefficients de partage de 2 additifs entre des simulants et du PS ont été mesurés en plaçant 2.5 cm^3 de polymère réduit en poudre par cryobroyage (Broyeur à azote liquide, DELTALABO, France) au contact de 25 mL de simulant à 40°C.

Quatre simulants différents ont été testés : l'isopropanol et trois mélanges d'éthanol (MERCK, Allemagne) et d'eau (eau MilliQ, MILLIPORE, USA) de fractions volumiques en éthanol respectives égales à 95%, 75% et 50%. Les concentrations à l'équilibre dans le simulant et dans le polymère ont été mesurée en utilisant les méthodes précédemment décrites. L'extraction des substances présentes dans le PEHD à l'équilibre a été réalisée par la méthode d'EFP. L'extraction des substances présentes dans le PS à l'équilibre a été réalisée par la méthode de dissolution / reprécipitation.

3. Outils de simulation : prévision des coefficients de partage

3.1. Théorie de prévision des coefficients de partage

La théorie développée pour la prévision de $K_{i,F/P}$ a été testée dans un premier temps sur les PE pour lesquels des données expérimentales sont disponibles. Nous avons souhaité par la suite étendre les résultats au PS, en appliquant à ceux-ci strictement les mêmes méthodes que celles développées pour les PE. Ainsi, la théorie calculatoire est très largement détaillée dans les publications et ne sera reprise que succinctement dans cette partie. Seules les principales équations sont présentées, le détail des démonstrations pourra être retrouvé dans les publications de la partie résultats et discussion.

Sur un modèle à grille de type Flory-Huggins, l'équation (1.23) permet de calculer $K_{i,F/P}$ pour un contact entre un polymère et un simulant, alors que l'équation (2.2) permet de calculer $K_{i,F/P}$ pour un contact entre un polymère et un mélange binaire de simulants F_1 et F_2:

$$\begin{aligned}\ln K_{i,(F_1+F_2)/P} &= 1+\chi_{i,P}-\ln\gamma^{v}_{i,F_1+F_2}\approx \\ &\underbrace{-2\frac{V_i^{vdw}}{V_{F_2}^{P}}\frac{\partial\chi_{F_1,F_2}}{\partial\phi_{F_2}}}_{enthalpic}\cdot\phi_{F_2}^{3} \\ &+\underbrace{\frac{V_i^{vdw}}{V_{F_2}^{P}}\cdot\left(\chi_{F_1,F_2}+3\frac{\partial\chi_{F_1,F_2}}{\partial\phi_{F_2}}\right)}_{enthalpic}\cdot\phi_{F_2}^{2} \\ &+\left(\underbrace{r_{i,F_2}^{-1}-r_{i,F_2}^{-1}}_{entropic}+\underbrace{\chi_{i,F_1}-\frac{V_i^{vdw}}{V_{F_2}^{P}}\chi_{i,F_2}+\frac{V_i^{vdw}}{V_{F_2}^{P}}\chi_{F_1,F_2}-\frac{V_i^{vdw}}{V_{F_2}^{P}}\frac{\partial\chi_{F_1,F_2}}{\partial\phi_{F_2}}}_{enthalpic}\right)\cdot\phi_{F_2} \\ &\underbrace{+r_{i,F_1}^{-1}}_{entropic}+\underbrace{\chi_{i,P}-\chi_{i,F_1}}_{enthalpic}\end{aligned} \tag{2.2}$$

Du fait que la taille des mailles et le nombre de voisins sont fixés sur un modèle à grille, le coefficient de Flory-Huggins peut être calculé à partir des énergies d'interaction paires à paires. Une représentation continue a été utilisée :

$$2\cdot k_B\cdot T\cdot\left\{\chi_{i,k}(T)\right\}_{k=P,F}=\left\langle z_{i+k}\right\rangle\cdot\left\langle\varepsilon_{i+k}\right\rangle_T+\left\langle z_{k+i}\right\rangle\cdot\left\langle\varepsilon_{k+i}\right\rangle_T-\left\langle z_{k+k}\right\rangle\cdot\left\langle\varepsilon_{k+k}\right\rangle_T-\left\langle z_{i+i}\right\rangle\cdot\left\langle\varepsilon_{i+i}\right\rangle_T \tag{2.3}$$

$\langle\ \rangle$ and $\langle\ \rangle_T$ sont respectivement les opérateurs moyenne et moyenne thermalisée. Cette dernière est calculée en pondérant la distribution d'énergies $p_{a+b}(\varepsilon)$ par le facteur de Boltzmann, définie par $\exp(-\varepsilon/k_B\cdot T)$:

$$\left\langle\varepsilon_{a+b}\right\rangle_T=\frac{\int_{-\infty}^{+\infty}p_{a+b}(\varepsilon)\cdot e^{-\frac{\varepsilon}{k_B\cdot T}}\cdot\varepsilon\cdot d\varepsilon}{\int_{-\infty}^{+\infty}p_{a+b}(\varepsilon)\cdot e^{-\frac{\varepsilon}{k_B\cdot T}}\cdot d\varepsilon} \tag{2.4}$$

L'échantillonnage de $p_{a+b}(\varepsilon)$ est basé sur un grand nombre (10^4) de conformères de molécule sonde et de molécule au contact et sur tous les contacts possibles entre leurs enveloppes de Van der Waals en tenant compte des possibles symétries (jusqu'à 10^9 configurations). Les nombres de voisins, aussi appelés nombres de coordination, sont calculés de la même manière sur un grand nombre de configurations possibles (jusqu'à 10^4) pour lesquelles les sphères de Van der Waals sont en contact sans se chevaucher. Tous ces

échantillonnages ont été réalisés à l'aide de l'environnement logiciel Material Studio 4.1 (ACCELRYS, USA). Tous les calculs à l'échelle atomique ont été réalisés en utilisant le champ de force commercial COMPASS (ACCELRYS, USA).

3.2. Paramètre d'interaction entre l'eau et l'éthanol

Le paramètre d'interaction de Flory-Huggins entre l'eau et l'éthanol $\chi_{eau,éthanol}$ a été calculé à partir des enthalpies de mélange, $\Delta H^{m}_{eau+éthanol}$, tabulées par Boyne et Williamson (1967) :

$$\chi_{eau,éthanol} = x_{éthanol} \cdot (1 - \phi_{éthanol}) \cdot \frac{\Delta H^{m}_{eau+éthanol}}{RT} \qquad (2.5)$$

Où $x_{ethanol}$ et $\phi_{ethanol}$ sont respectivement la fraction molaire et la fraction volumique en éthanol. R est la constante des gaz parfaits.

3.3. Volumes des molécules

3.3.1. Volumes de Van der Waals

Les volumes de Van der Waals V_i^{vdw} correspondent au volume des atomes et de leurs nuages électroniques. Ils ont été calculés en moyennant les résultats obtenus pour trente configurations moléculaires différentes. Tous ces échantillonnages ont été réalisés à l'aide de l'environnement logiciel Material Studio 4.1 (ACCELRYS, USA) et du champ de force commercial COMPASS (ACCELRYS, USA).

3.3.2. Volumes molaires partiels

Les volumes molaires partiels V_i^p ont été calculés à partir des densités des substances, ρ_i, et de leurs masses molaires, M_i, à 313K :

$$V_i^p = \frac{M_i}{\rho_i \cdot Na} \times 1 \cdot 10^{24} \qquad (2.6)$$

Où Na est le nombre d'Avogadro et V_i^p est calculé en Å^3.

Les masses molaires des substances ont été obtenues sur les fiches techniques fournies par les fabricants des produits. Les densités ont été obtenues en moyennant, interpolant ou extrapolant selon le cas les données disponibles sur la base du données du CAS (Chemical Abstract Service).

3.3.3. Volumes accessibles aux atomes d'hydrogène

Les volumes accessibles aux atomes d'hydrogènes V_i^H sont échantillonnés par déplacement autour d'une molécule de *i* d'une sonde de rayon comparable à celui d'un atome d'hydrogène, comme représenté sur la Figure 2.3. Le volume est calculé par tesselation de Delaunay. Tous ces échantillonnages ont été réalisés à l'aide de l'environnement logiciel Material Studio 4.1 (ACCELRYS, USA) et du champ de force commercial COMPASS (ACCELRYS, USA).

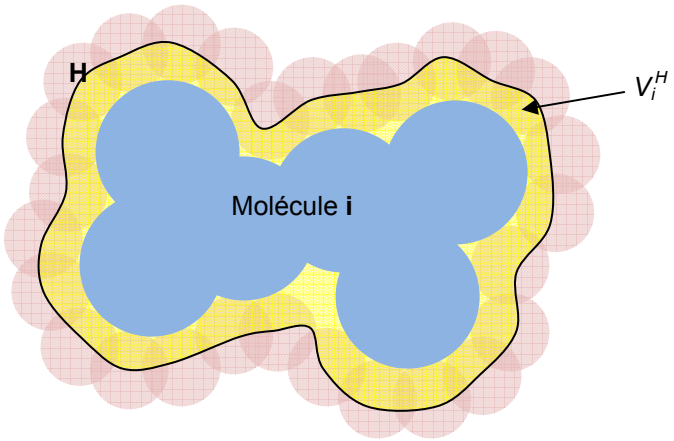

Figure 2.3. Représentation de la méthode de calcul du volume accessible à un atome d'hydrogène (représenté en jaune). Les atomes d'hydrogène sont représentés en violet et la molécule de i en bleu.

Chapitre 3

Résultats et Discussion

Ce travail a donné lieu à quatre publications qui constituent le corps principal de ce chapitre. Les deux premières publications concernent la prévision des coefficients de partage et ont été soumises au journal *Industrial and Engineering Chemistry Research*. En outre, la première publication présentée dans ce travail a été acceptée dans le journal alors que la seconde est encore au stade de la soumission. La troisième publication concerne une méthode rapide de déformulation des PO basée sur l'utilisation de méthodes chimiométriques. Cette publication a été soumise à la revue scientifique *Journal of Applied Polymer Science*. Enfin, la quatrième et dernière publication présente une combinaison des deux approches, prédictive et expérimentale, dans le but d'établir des règles de décision concernant l'aptitude des matériaux à être utilisés au contact des aliments. Cette publication a été soumise au journal *Food Additives and Contaminants*.

Ainsi, ce chapitre est subdivisé en quatre parties. Les résultats et les deux publications associés à la prévision des coefficients de partage sont présentés dans la première partie. La deuxième partie présente les résultats et la publication associés à la déformulation rapide des matériaux sur la base d'une analyse des spectres IRTF de PO. La quatrième publication, qui combine les deux approches dans une logique d'aide à la décision est présentée dans la troisième partie. Une discussion plus générale, concernant notamment l'application des méthodes développées à d'autres matériaux que les PO, au PS en particulier, est proposée dans la quatrième partie.

1. Prévision des coefficients de partage entre un PE et des simulants alimentaires

Les données concernant les coefficients de partage manquent cruellement dans la littérature internationale pour plusieurs raisons : i) les données expérimentales sont difficiles à obtenir car les équilibres sont dépendants des conditions expérimentales ; ii) les méthodes de dosages du composé à l'équilibre doivent être très précises car les concentrations dans les deux milieux sont souvent très différentes (facteur 1000 voire plus entre les deux concentrations) ; iii) le financement de ces travaux de fond est difficile à obtenir. Ces données sont toutefois nécessaires à la prévision de la migration des additifs des matériaux plastiques vers les aliments (ou simulants alimentaires). La Figure 3.1 présente les cinétiques de deux additifs migrant d'un PEHD dans le simulant éthanol 50%. Dans le cas du BHT, on observe que l'équilibre, qui dépend essentiellement du coefficient de partage (équation (1.7)), est atteint très rapidement. La contamination des aliments par cette substance dépend donc

principalement de son coefficient de partage et non de son coefficient de diffusion. A contrario, la migration de l'Irganox 3114, un additif de poids moléculaire très élevé, est lente et l'équilibre n'est pas atteint après 10j de migration.

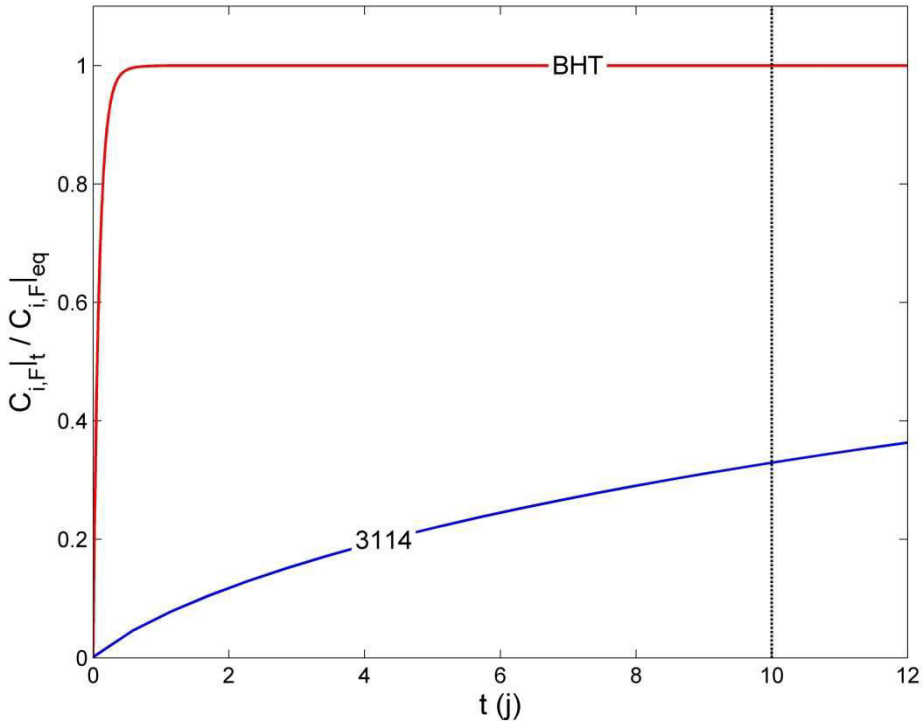

Figure 3.1. Cinétiques de migration à 313K de deux additifs entre un PEHD et le simulant éthanol 50%. BHT = Butylated HydroxyToluene ; 3114 = Irganox 3114 (CIBA, Suisse)

Plus les molécules migrent rapidement, plus la connaissance des coefficients de partage est nécessaire pour prédire la quantité de substance migrant dans les simulants alimentaires.

La mesure des coefficients de partage étant le plus souvent difficile (seuils de détection, faibles limites de solubilité dans les milieux, hydrolyse dans les simulants, etc.), la prévision de ce coefficient est donc une alternative à considérer pour limiter le nombre d'expérimentations à la validation des modèles de migration. Dans ce chapitre, nous proposons une approche de modélisation du coefficient de partage entre emballage et aliment. Plusieurs travaux expérimentaux ont été publiés par Arab-Tehrany et collaborateurs en 2006 et 2007, proposant un modèle de prédiction semi-empirique basé sur une approche RQSP et un grand nombre de données expérimentales concernant la migration de petits solutés. D'autre part, les premiers essais de prévision en utilisant un modèle à grille de type Flory-Huggins (Mougharbel, 2007) ont montré que l'application de cette approche est possible dans les simulants, le calcul des coefficients de Flory restant toutefois à affiner. Ces travaux ont traité des polyoléfines et des développements sont encore nécessaires pour pouvoir évaluer rapidement le coefficient de partage de migrants de type additifs entre un emballage et un

simulant alimentaire. La seconde approche nous a semblé plus appropriée à la prédiction du partage des substances de type additifs.

Nous nous sommes concentrés dans le présent travail sur les polyoléfines qui représentent 54% des matériaux plastiques utilisés dans des applications industrielles liées à l'emballage alimentaire et qui contiennent des oligomères et un grand nombre d'additifs. En particulier nous nous sommes intéressés au polyéthylène (PE) qui est le plus utilisé des matériaux.

Ainsi, dans une première partie de la thèse, nous avons choisi de nous intéresser tout particulièrement aux coefficients de partage. La mesure expérimentale de ce paramètre étant le plus souvent délicate (faible solubilité dans un des milieux, hydrolyse des additifs, etc.), nous avons également choisi d'axer notre travail sur les méthodes de prévision des coefficients de partage. Les premiers essais de prévision en utilisant un modèle à grille de type Flory-Huggins (Mougharbel, 2007) ont montré que l'application de cette approche est possible dans les simulants, le calcul des coefficients de Flory restant toutefois à affiner. Nous avons donc essayé de prévoir $K_{i,A/P}$ par cette approche en affinant la méthode de calcul. Ces travaux sont développés dans les deux publications qui suivent.

La première publication introduit la prévision de coefficients de partage entre des LDPE et des simulants alimentaires en appliquant la théorie de Flory-Huggins indifféremment aux deux compartiments. La contribution entropique, due aux différentes configurations et aux réorientations possibles des molécules, a été échantillonnée à l'échelle atomique à l'aide d'outils de modélisation moléculaire. Une analyse des biais d'échantillonnage des molécules non sphériques a aussi été réalisée et des corrections proposées. Le biais observé sur les valeurs prédites est finalement du même ordre de grandeur que celui observé sur les données expérimentales. Un modèle général a aussi été proposé à partir des coefficients de solubilité.

La seconde publication présente deux extensions particulières de la méthode décrite dans le premier travail. Un calcul des volumes molaires partiels des migrants dans les simulants a été réalisé à partir de simulations moléculaires en milieu isobare pour évaluer de manière plus précise la contribution entropique dans ces simulants. Un volume alternatif nécessitant moins de temps de calcul a aussi été proposé : le volume accessible aux atomes d'hydrogène. La deuxième extension concerne une application de la méthode à l'eau et aux mélanges eau/éthanol. Les limitations intrinsèques au modèle de Flory-Huggins, qui néglige la coopérativité des liaisons hydrogène, ont été compensées par une repondération des énergies de contact.

Prediction of solute partition coefficients between polyolefins and alcohols using a generalized Flory-Huggins approach

Guillaume Gillet[a,b], *Olivier Vitrac**[c], *Stéphane Desobry*[b]

(a) Laboratoire National de métrologie et d'Essais, Centre Energie, Matériaux et Emballage, 29 avenue Roger Hennequin, 78197 Trappes CEDEX, France.

(b) Nancy Université, LSGA-ENSAIA-INPL, 2 avenue de la forêt de Haye, BP 172, 54505 Vandoeuvre lès Nancy, France.

(c) Institut National de la Recherche Agronomique, UMR 1145 Génie Industriel Alimentaire, 1 avenue des Olympiades, 91300 Massy, France

* Corresponding author: olivier.vitrac@agroparistech.fr

The partition coefficients of n-alkanes, n-alcohols, volatiles and typical antioxidants between a low density polyethylene and several alcohols (methanol and ethanol) were predicted without fitting variables using an off-lattice Flory-Huggins approach. The main advantage of the proposed excluded volume constraint method was to sample at atomistic scale pairwise contact energies and the residual entropic contribution due to possible different conformers and reorientations. The positional entropy was considered both in the polymer and in the liquid as in the original Flory-Huggins theory. Possible biases due to the formulation and conformational sampling were analyzed for molecules different in size, in shape and in stiffness. The predictions were close to the experimental uncertainty on the partition coefficients between the amorphous part of the polymer and the tested liquids. The present work confirmed that plastic additives, which are by design highly compatible with the polymer, had also a significant chemical affinity with polar liquids consisting in smaller molecules. Finally, a general predictive model of partition coefficients based on solubility coefficients was proposed.

KEYWORDS: thermodynamics, polymer, desorption, chemical potential, Flory theory

1. Introduction

Solute partition coefficients between thermoplastics and liquids are used to predict mass diffusion[1-5] in various fields including: protective clothing[6], biomedical studies[7], separation techniques[8-10] and food packaging[11-13]. Several recent regulations in EU[14] regarding the safety of chemicals, so-called REACH directives, urge the development of predictive approaches on the migration of chemicals into the environment or through the food chain. This work was motivated by the EU regulation 1935/2004/EC[15] specific for food contact materials, which enforces a safety assessment and risk management decision for all starting substances and possible degradation products coming from the material. For plastic materials, article 14 of directive 2002/72/EC[16] introduces diffusion modeling as an alternative to time-consuming and costly experiments for both compliance testing and risk assessment. The principles for probabilistic modeling of packaging substances desorption into food was previously analyzed[17] and applied to different situations[18-20]. The main limitation in predictive approaches for both compliance testing and risk assessment is the availability of physicochemical properties for a wide range of substances and polymers under particular thermodynamical conditions (temperature, swelling). Whereas robust approaches have been developed for the prediction[21-24] or overestimation[25-27] of diffusion coefficients in polyolefins, no appropriate method

exists to predict partition coefficients between a polyolefin and a food product or simulated food[8]. A first significant attempt was made by Baner and Piringer[28] using an approach mixing both the regular solution theory on the food side and Flory-Huggins approach on the polymer side. To fit experimental results, the predictions were corrected by an empirical factor, which was found to be dependent on the size and the shape of the considered substance. On polymer side, Flory-Huggins interactions parameters are conventionally derived from the separation of the square root of the polymer cohesive energy[29] into a dispersive contribution (short-range dispersion forces) and a long-range Coulombic contribution, which encompasses arbitrary a polar term and a term due to hydrogen bonding[30,31]. Recent reviews[32,33] on predictions of activity coefficients in polymer solutions showed that i) evaluations from solubility coefficients led systematically to strong overestimations and ii) consequently solubility coefficients decomposition should be empirically reweighted by factors lower than 1. Alternative methods to predict solute activity coefficients rely on Metropolis Monte-Carlo (MC)[34] or molecular dynamics (MD)[35,36]. Conventional strategies consist in measuring the excess in free energy by molecular dynamics when the guest solute is inserted[37] or removed[38] into the host phase. Such methods converge rapidly for solutes smaller than accessible voids but may be prohibitive when the reordering dynamics of the host phase is required to accommodate the solute insertion/deletion. As the complete relaxation of entangled polymer segments is not tractable, the free energy difference before and after insertion/deletion can be advantageously replaced by a thermodynamic integration (TI) along an arbitrary path[39,40] possibly combined with a perturbation protocol[41,42]. In complex solute mixtures, MC techniques working in the Gibbs ensemble[43] may alternatively be used. Although recent developments in MC and MD sampling methods are promising for large solutes, no study has been published on a large set of bulky and hindered solutes in polymers and in liquids. In particular, all methods require ad-hoc equilibration steps via molecular dynamics, which are computationally expensive for large systems involving few solutes and a much larger number of host molecules.

The current work examines a tailored MC sampling methodology based on contact energies instead of an explicit description of the binary mixture to assess, at a reasonable computational cost, excess chemical potential in polyethylene amorphous regions and in food simulants with increasing polarity (ethanol and methanol). Because reference data on excess chemical potentials are very scarce, predictions were compared with macroscopic partition coefficients previously measured on different classes of solutes: volatile compounds[28], homologous series of n-alkanes and n-alcohols[44,45] and small phenolic antioxidants[45]. In this context and due to inherent biases in heterogeneous experimental data, our objective was to achieve predictions not far off the marks and within typical experimental errors on partitioning while taking into account the effects of crystallinity and the density of the polymer. The choice of a generalized Flory-Huggins approach was motivated by the apparent symmetry between a bulky solute dispersed among much larger segments and a bulky solute dispersed among much smaller molecules constituting the liquid simulant. In both cases, the positional and the configurational entropy is expected to spread the mixed-segment and the mixed-simulant interaction energies. For simple mixtures of molecules, such as n-alkanes in polyethylene, with similar chemical structures (i.e. with no significant van Laar enthalpy) but different shapes, the Flory-Huggins [46,47] theory, which calculates the positional entropy on a rigid lattice,

describes remarkably their thermodynamics[48]. The necessary condition is that the volume per mole of lattice sites is fixed. Elbro et al.[49] demonstrated that an expression – analogous to the Flory-Huggins combinatorial term – can be derived irrespectively to the considered substance shape (i.e. independent of any lattice frame of reference) by considering the volume fraction and free volumes of each substance in the mixture. A systematic derivation of the Flory-Huggins theory, which takes the free volumes into account, has been proposed by Bawendi *et al.*[50-52]. In non-ideal mixtures, the heat of mixing can be approximated by the van Laar expression of first neighbor contact energies. Because the original Flory theory captures pair interaction terms only on a coarse grain scale, the corresponding mean field approximation may appear too coarse to describe the interactions with very dissimilar species or presenting different flexibilities[53]. Similar arguments have been used to explain the large discrepancy in predictions by solubility coefficients derived from different group-contributions (atomistic, group-based, and blob-based)[33]. The main reason is that all pair-configurations will not have equal probability at atomic scale; moreover, the residual entropy should be included in the mean field approximation. From these considerations, both atomistic description of interactions and off-lattice approximation of energetic interactions taking into account the packing of atoms are expected to provide more accurate estimate of the enthalpic contribution[54].

The paper is organized as follows. The theoretical section introduces the concepts used to derive estimates of solute partition coefficients between a semi-crystalline polymer and a liquid in the framework of Flory-Huggins theory at atomistic scale. The conditions of simulation and validation are detailed in a third section. In the two subsequent sections, the simulation results are analyzed: first, by comparing the sampling biases calculated for homologous or typical solutes; second, by comparing with experimental partition coefficients between alcoholic simulants and a low density polyethylene. Since our results provide independent estimates of Flory-Huggins parameters, the weighted sum of solubility coefficients proposed by Lindvig et al.[32] is validated on data described by Baner and Piringer[28]. In the last section, we summarize our conclusions.

2. Theoretical background

Before we introduce the concepts of the computational method used in this work, we briefly summarize the general assumptions, which support the definition of a thermodynamical equilibrium between a thermoplastic packaging, denoted *P*, and a liquid in contact, denoted *L*. For concision, the initial definition assumes that *P* is amorphous (no crystalline phase) and that the solute, denoted *i*, is initially well dispersed in *P*. A more general definition is subsequently proposed.

2.1. Thermodynamical equilibrium between the packaging material and the liquid in contact

The thermodynamical equilibrium between *P* and *L* is reached when the cumulated free energy between *P* and *L*, G_{P+L}, is minimal. At constant temperature and pressure, the evolution towards equilibrium is accompanied by a mass transport between *P* and *L*. In this work, only the solute molecules are assumed to migrate (Fig. 1a). These assumptions are particularly well satisfied when *i* migrates in an aqueous food or polar simulant. For an isolated system *P*+*L*, G_{P+L} is:

$$\begin{aligned} G_{P+L} &= G_{i+P} + G_{i+L} \\ &= \underbrace{N_P \cdot \overbrace{\mu_P}^{\mu_P^{id}+\mu_P^{excess}} + N_{i,P} \cdot \overbrace{\mu_{i,P}}^{\mu_i^0+\mu_i^{id}+\mu_{i,P}^{excess}}}_{G_{i+P}=G_{i+P}^{id}+G_{i+P}^{excess}} \\ &+ \underbrace{N_L \cdot \overbrace{\mu_L}^{\mu_L^{id}+\mu_L^{excess}} + N_{i,L} \cdot \overbrace{\mu_{i,L}}^{\mu_i^0+\mu_i^{id}+\mu_{i,L}^{excess}}}_{G_{i+L}=G_{i+L}^{id}+G_{i+L}^{excess}} \end{aligned} \quad (1)$$

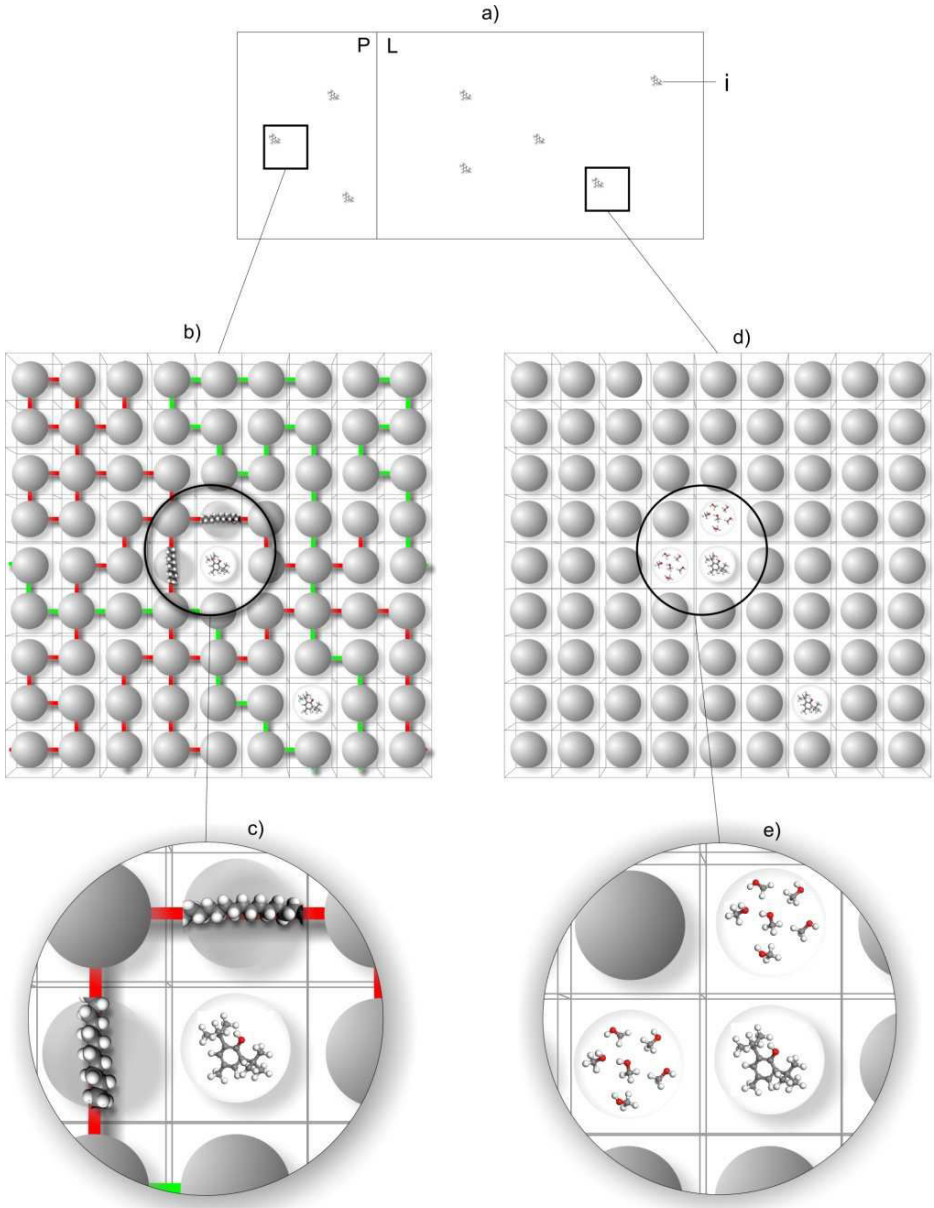

Figure 1. Multiscale description of interactions b-c) between *P* and *i*, and d-e) between *L* and *i*; b,d) mean-field approximation on a lattice; c,d) description of interactions between first neighbors.

where $\{N_j\}_{j=P,L}$ and $\{N_{i,j}\}_{j=P,L}$ are the number of molecules *j* and the number of molecules *i* in *j* respectively. Their corresponding chemical potentials are $\{\mu_j\}_{j=P,L}$ and $\{\mu_{i,j}\}_{j=P,L}$ respectively. All energetic terms are further decomposed into an ideal, ^{id}, and an excess part, ^{excess}. From a microscopic point of view, the detailed mass balance at the interface enforces that the partition coefficient at the interface between *P* and *L*, noted $K_{i,L/P}$, is equal to the ratio of presence probabilities from each side of interface, $\left\{ p_{i,j}\Big|_{eq} \right\}_{j=P,L}$, and to the ratio of frequencies of crossing the interface: $k_{i,P\to L}$ and $k_{i,L\to P}$. By introducing the free energy of the barrier to cross the interface, $G_i^{\dagger}$, the transition state theory defines $K_{i,L/P}$ in the canonical ensemble as:

$$\begin{aligned} K_{i,L/P} &= \frac{p_{i,L}\Big|_{eq}}{p_{i,P}\Big|_{eq}} = \frac{k_{i,P\to L}}{k_{i,L\to P}} \\ &= \frac{\dfrac{k_B\cdot T}{h}\exp\left(-\dfrac{G_i^{\dagger}-G_{i+P}}{k_B\cdot T}\right)}{\dfrac{k_B\cdot T}{h}\exp\left(-\dfrac{G_i^{\dagger}-G_{i+L}}{k_B\cdot T}\right)} \\ &= \exp\left(\frac{G_{i+P}-G_{i+L}}{k_B\cdot T}\right) \end{aligned} \qquad (2)$$

with h the Planck's constant, k_B the Boltzmann's constant and T the absolute temperature. Eq. (2) can be used to estimate $K_{i,L/P}$ in the Gibbs Ensemble[55] but it requires calculating the energy of each subsystem after equilibration. An alternative relies on a macroscopic description of equilibrium ($dG_{P+L}=0$) for a closed system ($dN_{i,L}=-dN_{i,P}$), which leads to: $\mu_{i,L}=\mu_{i,P}$. By choosing the state of pure i as reference and by expressing the activities of both non ideal mixtures from their volume fractions in i, $\{\phi_{i,j}\}_{j=P,L}$, $K_{i,L/P}$ is approximated as:

$$K_{i,L/P} \approx \frac{V_i \cdot \phi_{i,L}}{V_i \cdot \phi_{i,P}} = \exp\left(\frac{\mu_{i,P}^{excess} - \mu_{i,L}^{excess}}{k_B \cdot T}\right) = \frac{\gamma_{i,P}^{v}}{\gamma_{i,L}^{v}} \quad (3)$$

with $\left\{\gamma_{i,j}^{v}\right\}_{j=P,L}$ the activity coefficient of i in j and V_i the partial specific volume of solute i.

Solutes tend to concentrate in the phase, for which they have the greatest chemical affinity. From the mixing point of view and irrespectively to specific molecular interactions, solutes tend to migrate in the phase where diluting the system with solutes causes a largest gain in entropy (i.e. largest increase in the number of micro-configurations). This "attractive" effect is expected higher for the phase consisting in molecules smaller than the solute i (i.e. L rather than P). It is however counterbalanced by the cohesive energy associated to the creation of a cavity with a similar volume as the solute. Indeed increasing the cohesion of one phase (e.g. due to hydrogen bonding) generates a resistance to the insertion of the solute and decreases consequently its frequency of occurring. For a rubber amorphous phase, the cohesive energy of the system is expected to be lower and the partitioning to small solutes controlled mainly by the entropic contribution.

2.2. Additional assumptions

Since the diffusion of a substance i, such as a plastic additive, requires polymer cooperative motions[23], the substance i is assumed to diffuse only in the amorphous phase of the polymer. The partition coefficient between L and the polymer amorphous phase, $K_{i,L/P}$, is therefore:

$$K_{i,L/P} = \frac{C_{i,L}\big|_{eq}}{C_{i,P}\big|_{eq}^{a}} = (1-c)\cdot\frac{\hat{C}_{i,L}\big|_{eq}}{\frac{1}{a_i}\cdot\hat{C}_{i,P}\big|_{eq} - b_i \cdot C_{i,P}\big|_{t=0}} \quad (4)$$

where $C_{i,L}\big|_{eq}$ is the concentration in L at equilibrium; $C_{i,P}\big|_{eq}^{a}$ is the concentration in the amorphous phase of P at equilibrium; $\left\{\hat{C}_{i,j}\big|_{eq}\right\}_{j=L,P}$ is the macroscopic concentration in each phase as experimentally assessed; $C_{i,P}\big|_{t=0}$ is the initial concentration in P (i.e. before contact with L); c is the polymer crystallinity (volume fraction of crystalline phase); a_i is the extraction yield of i from P; b_i is the amount of substance i, which is not "well-dispersed" in P. Additives with a melting point higher than the extrusion temperature (i.e. "low melting additives") or any process of hygroscopic additives (e.g. phenolic and phosphate antioxidants) or of any nucleating substance are known to lead to incomplete dispersion in the polymer matrix[56]. From the thermodynamical point of view, substances, which are not or poorly dispersed, have a much higher chemical potential than well dispersed substances (i.e. their activity is closer to pure substance chemical potential, that is 1 by definition). The driving force associated to their migration is consequently higher but desorption occurs less rapidly due to kinetic limitations (melting, trapping, and strong hydrogen bonding). As a result, thermodynamical equilibrium described in Eq. (3)is assumed only related to the "well-dispersed" substance (at infinite dilution).

From previous considerations, it is expected that the current definition of the partitioning may differ from the apparent or macroscopic partition coefficient, $\hat{K}_{i,L/P}$, and assessed macroscopically:

$$\hat{K}_{i,L/P} = \frac{\hat{C}_{i,L}\big|_{eq}}{\hat{C}_{i,P}\big|_{eq}} \qquad (5)$$

Definitions of partitioning derived from Eqs. (4) and (5) are related through the macroscopic mass balance between *L* and *P*:

$$C_{i,P}\big|_{t=0} = \frac{1}{a_i}\hat{C}_{i,P}\big|_{eq} + l^{-1}\cdot\hat{C}_{i,L}\big|_{eq} \qquad (6)$$

where *l* is the dilution factor or equivalently the ratio between the volume of *P* and the volume of *L*. The relationship between $K_{i,L/P}$ and $\hat{K}_{i,L/P}$ is given by:

$$\frac{K_{i,L/P}}{\hat{K}_{i,L/P}} = \left(1-c\right)\cdot\frac{1}{\frac{1-b_i}{a_i} - \frac{\hat{K}_{i,L/P}}{l}\cdot b_i} = \frac{a_i}{1-b_i}\cdot\left(1-c+\frac{K_{i,L/P}}{l}\cdot b_i\right) \qquad (7)$$

Since most of authors assess $\hat{K}_{i,L/P}$ instead of $K_{i,L/P}$, comparisons between experimental and predictions from several sources must take into account the variability in the polymer material (crystallinity and density), its formulation (estimate of b_i) and experimental conditions (l and a_i). When they are not available, they must be estimated from reasonable assumptions including a sensitivity analysis on these parameters. For a practical use, two extreme behaviors are worth to be identified. When $b_i\cdot K_{i,L/P}/l << 1$ (e.g. $K_{i,L/P} << 2.5$ for common experimental conditions: l=1/20 and b_i=0.02), $\left(1-c\right)^{-1}\cdot K_{i,L/P}/\hat{K}_{i,L/P}$ is a constant (higher than 1), which does not depend on the true value $\hat{K}_{i,L/P}$. Trends for homologous molecules series and ratios obtained in similar experimental conditions can therefore be directly compared to predictions. By contrast when $K_{i,L/P} \geq L/b_i$ (e.g. 2.5), the discrepancy between $K_{i,L/P}$ and $\hat{K}_{i,L/P}$ tends to be maximum. For $\hat{K}_{i,L/P}$ values larger than 1, $\left(1-c\right)\cdot\hat{K}_{i,L/P}$ provides an underestimate of $K_{i,L/P}$, whose bias $K_{i,L/P} - \left(1-c\right)\cdot\hat{K}_{i,L/P}$ increases as the root of $K_{i,L/P}$. For these conditions, reference data are required to provide valuable comparisons with predictions. In other words, previously published partition coefficients with values much lower than 1 are more valuable to validate a predictive model than larger values. Similarly, underestimating the "true" $K_{i,L/P}$ may lead to significant risk underestimation for liquid contamination.

2.3. Flory-Huggins theory of mixing

According to the Flory-Huggins theory[46,47,57,58], the expression of excess chemical potentials can be derived from local interactions between neighboring molecules since the conformations of both polymer segments and liquid medium molecules are not perturbed by surroundings ones beyond a critical distance. In the polymer, it is therefore assumed that excluded volume among non-connected monomers (belonging to the same chain or not) do not affect the overall chain conformations. A more general discussion can be found[59]. In this framework, the entropies of mixing corresponding to mixtures *P*+*i* and *L*+*i* are defined as the sums of a combinatorial term and a residual term. The combinatorial term is assessed at a coarse grain level, so-called blob size. The residual term depends on the detailed conformations of each molecule and on the dispersion of the number of contacts between pairs of molecules. When *L* is a non-interacting liquid, the equilibration of chemical potentials between *P* and *L* may be complicated by a secondary transport of *L* in *P*, so that the ternary mixture *P*+*L*+*i* is involved with additional constraints release in *P*. This secondary transport of *L* in *P* was neglected in this study, since only fluids (i.e. polar liquids) with high cohesive energies[60] were considered.

The equivalent representation of interactions between *P* and *i* on the first hand and between *L* and *i* on the other hand are illustrated on Fig. 1. The reference mesh size or blob size corresponds either to the partial specific volume of the solute, V_i , or to a volume which exposes a similar contact surface. *P* is represented by many interconnected lattice sites (Figs. 1b and 1c), whereas a single site represents many *L* molecules (Figs. 1d and 1e). Because the end-chain effects are neglected, *P* or *L* sites are supposed randomly dispersed on the lattice without taking into account their real connectivity. We can thus notice that the same argument and mathematical expressions can be used in *P* as well as in *F*. On simple lattices, the number of neighbors does not depend on the blob size. Following the arguments in[61], two different values of V_i were compared in this work: the volume of van der Waals, denoted V_i^{vdw}, calculated as the volume enclosed within the Connolly surface[62] for a spherical probe of 0.1 Å with a grid step of 0.15 Å and the molar volume V_i^M. For molecules *j* with a volume fraction ϕ_j and consisting in r_j blobs of volume V_i, one gets at infinite dilution of *i*[63]:

$$\begin{aligned}\frac{\left\{\mu_{i,j}^{excess}\right\}_{j=P,L}}{k_B\cdot T} &= \ln\gamma_{i,j}^{v}\\ &= \left(1-\frac{1}{r_j}\right)\cdot\phi_j+\chi_{i,j}\cdot\phi_j^2 \\ &\approx \left(1-\frac{1}{r_j}\right)+\chi_{i,j}^{H}\end{aligned} \quad (8)$$

where $\chi_{i,j}\cdot n_i\cdot\phi_j = H_{i+j}^{excess}\big/k_B\cdot T$ is the heat of mixing. The first term represents the effect of the configurational entropy associated to the increase of microstates due to the distribution of *j* around *i*. The absolute value of the first term is expected to be small in polymers (r_j>>1) while it is expected to be significant in liquids consisting in molecules much smaller than *i*. The term r_j^{-1} is equivalent to the cavity dimensionless size (relative to the size of *j*) required to insert one molecule *i*. Since the size of *P* is large comparing to *i* ($r_P \gg 1$), then the simplification $1/r_P \to 0$ is reasonable. Eqs. (3) and (8) lead to the following model for the partition coefficient:

$$\begin{aligned}\ln K_{i,L/P} &= \ln\gamma_{i,P}^{v}-\ln\gamma_{i,L}^{v}\\ &= \underbrace{r_L^{-1}}_{\substack{entropic\\ contribution}} + \underbrace{\chi_{i,P}-\chi_{i,L}}_{\substack{enthalpic\\ contribution}}\end{aligned} \quad (9)$$

It is worth to notice that the exact meaning of r_L^{-1} is difficult to establish as it may varies according to the nature of the host *L*. The lower bound is necessarily the number (possibly fractional) of *L* molecules to be displaced to insert a volume corresponding to the van-der-Waals volume of *i*. In interacting liquids, the upper bond depends on the pressure-volume work done by the bulk liquid when it loses one or several hydrogen bonds at the interface with the solute. As an example in water, a study showed that the reordering of *L* was dependent on the solute and led to low-density ordered water in the vicinity of the solute[64].

2.4. Estimation of $\chi_{i,k}$ from pairwise contact energies

Our off-lattice method to calculate excess chemical potentials in *P* and *L* is derived from the methodology described by Fan et al.[65]. Its main advantage is to take into consideration the excluded-volume in pairwise interactions and in the coordination number. Indeed, the blob size and the coordination number cannot be modified in original lattice methods, so that the lattice approximation is less accurate for estimating the interactions between structures dissimilar in size and in shape[61]. A continuous representation of the binary interaction parameter was used instead:

$$\begin{aligned}&2\cdot k_B\cdot T\cdot\left\{\chi_{i,j}(T)\right\}_{j=P,L}\\ &= g_{i+j}+g_{j+i}-g_{j+j}-g_{i+i}\\ &\approx \left\langle z_{i+j}\right\rangle\cdot\left\langle\varepsilon_{i+j}\right\rangle_T+\left\langle z_{j+i}\right\rangle\cdot\left\langle\varepsilon_{j+i}\right\rangle_T\\ &\quad -\left\langle z_{j+j}\right\rangle\cdot\left\langle\varepsilon_{j+j}\right\rangle_T-\left\langle z_{i+i}\right\rangle\cdot\left\langle\varepsilon_{i+i}\right\rangle_T\end{aligned} \quad (10)$$

For any pair of molecules A (denoted seed molecule) and B (denoted contact molecule), possibly equivalent but with non symmetric roles, $g_{A+B} = \langle z_{A+B} \cdot \varepsilon_{A+B} \rangle_T$ represents the ensemble-averaged potential energy associated to a set of molecules B in contact with a single molecule A. z_{A+B} is the coordination number of the arrangement when A is surrounded by molecules B (i.e. number of neighbors B) and ε_{A+B} is the contact energy associated to the contact(s) between a molecule A and a molecule B. $\langle\ \rangle$ and $\langle\ \rangle_T$ denote averaging on the sampled configurational space and Boltzmann-weighted ensemble averaging respectively. By introducing the Boltzmann weight, $\exp(-\varepsilon/k_B \cdot T)$, the expectation of the distribution of contact energies $p_{A+B}(\varepsilon)$ becomes

$$\langle \varepsilon_{A+B} \rangle_T = \frac{\int_{-\infty}^{+\infty} p_{A+B}(\varepsilon) \cdot e^{-\frac{\varepsilon}{k_B \cdot T}} \cdot \varepsilon \cdot d\varepsilon}{\int_{-\infty}^{+\infty} p_{A+B}(\varepsilon) \cdot e^{-\frac{\varepsilon}{k_B \cdot T}} \cdot d\varepsilon} \quad (11)$$

The sampling of $p_{A+B}(\varepsilon)$ was based on a large set of conformers set A and B representative of their condensed state at temperature T and based on all possible contacts of their van der Waals envelopes with elliptical symmetric probability around their centers of mass. The coordination number was determined similarly on a large number of packed configurations, where van der Waals envelopes were put in contact without overlapping. Polymers based on few monomers were idealized by discarding all configurations where head and tail atoms were in contact with any surface. Because the radii of all exposed atoms were chosen equal to their van der Waals radii at their fundamental states (incompressible mixtures), the higher packing related to hydrogen bonding was locally underestimated.

3. Simulation details

3.1. MC sampling

The sampling of conformers and pairwise contact energies was performed using the client/server Materials Studio environment version 4.1 (Accelrys, San Diego, USA), its scripting features and the atom-based COMPASS forcefield. All van der Waals and Coulombic interactions were calculated without any cutoff since the computational cost of pairwise interactions was not limiting. The commercial implementation of Eqs. (10) and (11) in Materials Studio via the package Blends was not privileged as the sampling method is mainly optimized for small and spherical solutes. The excluded-volume constraint method was instead implemented using an importance sampling optimized for aspherical and bulky solutes. The algorithm to retrieve configurations representative of the condensed state of the mixture A+B is summarized hereafter.

1) Two configurations are randomly picked for A (seed molecule) and B (contact molecule).

2) A is oriented along the referential R_A formed by its principal axes; the principal axes of B are also oriented along R_A.

3) A random position, O, was assigned with a normal radial distribution centered on the center of mass of A and with a standard deviation equal to the gyration radius of A.

4) A random direction starting from the center of mass of A, D_A, is chosen. The angular distribution was chosen to match the differential cross-section per unit solid angle of the ellipsoid enclosing A. A random direction D_B is similarly chosen from the ellipsoid enclosing B.

5) The main axis of B is oriented along D_B while a random rotation around D_B is applied.

6) B is translated from O along D_A until the van der Waals surfaces are in contact (multiple contacts are permitted) while minimizing the overlapping volume.

Non feasible displacements or configurations are discarded.

7) ε_{A+B} is calculated.

For conformers presenting an internal cavity and small contact molecules, step 6 was modified to minimize the risk of oversampling of internal cavities. The initial position of *B* was chosen along the straight line defined by *O* and D_A either outside *A* or in *O*. The displacement of *B* proceeded subsequently by a contraction (displacement towards *O*) or by an expansion (displacement from *O*). The modifications introduced made it possible to sample efficiently the configuration space associated to two conformers of *A* and *B* in contact. Usually 10^2 to 10^3 samples were sufficient to achieve a convergence for two particular conformers. Because the whole procedure was repeated for a random pairs of 10^4 to 10^6 of conformers, $\langle \varepsilon_{A+B} \rangle_T$ was calculated from the distribution of 10^6 to 10^9 estimates of contact energies.

To generate conformers realistic at the desired temperature *T* while minimizing the computational cost of their generations, 10^3 to 10^4 conformers were extracted as first guess from 20 ns MD simulations in vacuum. The two first ns were discarded. For flexible chains much shorter than their persistence length, this protocol was in particular assumed compatible with the real configuration of tested molecules in a theta solvent. All molecular dynamics were simulated with Discover (Accelrys, USA) and the same COMPASS forcefield. The temperature *T* was set to 298 K or 313 K in Eq. (11) and MD simulations to match experimental tests recommended by the EU regulation of plastics materials in contact with food.

3.2. Biases associated to configurational space sampling

In lattice methods, the coordination number depends only on the lattice and not on the considered seed molecule so that z_{A+B} and ε_{A+B} remain uncorrelated. In the off-lattice formulation proposed in Eq.(10), approximating the enthalpic terms $g_{A+B} = \langle z_{A+B} \cdot \varepsilon_{A+B} \rangle_T$ by the product of their averages reduced drastically the overall computational method cost but introduced a bias, denoted β_{A+B}, which was equal to the covariance between z_{A+B} and ε_{A+B}:

$$\beta_{A+B} = \langle z_{A+B} \cdot \varepsilon_{A+B} \rangle_T - \langle z_{A+B} \rangle \langle \varepsilon_{A+B} \rangle_T \quad (12)$$

In presence of biases, the potential energy of *i* in *P* might depend on the length of the polymer segment chosen to represent *P*. The optimal length would therefore correspond to a minimal bias. Since it was too expensive to calculate $g_{A+B} = \langle z_{A+B} \cdot \varepsilon_{A+B} \rangle_T$ for all possible pairs *A* and *B* by MD simulations, biases were estimated from the neighborhood-based local covariance for a set of homologous series of molecules:

$$\begin{aligned} \beta_{A+B} &\approx 2 \cdot s^2_{\varepsilon_{A+B}} \cdot s^2_{z_{A+B}} \cdot \frac{\Delta_{A+B}}{s^2_{\varepsilon_{A+B}} \cdot \Delta^2_{A+B} + s^2_{z_{A+B}}} \\ &\leq s_{\varepsilon_{A+B}} \cdot s_{z_{A+B}} \end{aligned} \quad (13)$$

where s^2_X is the variance estimate of *X* within the considered sample of homologous molecules and Δ_{A+B} is referred as the derivative of z_{A+B} with ε_{A+B}. Δ_{A+B} was approximated by the gradient assessed when either *A* or *B* is replaced by a similar molecule:

$$\begin{aligned} \Delta_{A+B} &= \left. \frac{\partial z_{A+B}}{\partial \varepsilon_{A+B}} \right|_{A,B} \\ &\approx \frac{1}{2} \cdot \left(\left. \frac{\partial z_{A+B}}{\partial \varepsilon_{A+B}} \right|_{\text{A,homologous } B} + \left. \frac{\partial z_{A+B}}{\partial \varepsilon_{A+B}} \right|_{\text{B,homologous } A} \right) \end{aligned} \quad (14)$$

Estimating β_{A+B} on homologous molecules instead on conformers, made it possible to keep similar ensemble averages on a large number of conformers.

According to Eqs. (10) and (12), the estimation of $\{\chi_{i,j}\}_{j=P,L}$ becomes:

$$\begin{aligned} 2 \cdot k_B \cdot T \cdot \{\chi_{i,j}(T)\}_{j=P,L} = & \langle z_{i+j} \rangle \cdot \langle \varepsilon_{i+j} \rangle_T \\ & + \langle z_{j+i} \rangle \cdot \langle \varepsilon_{j+i} \rangle_T \\ & - \langle z_{j+j} \rangle \cdot \langle \varepsilon_{j+j} \rangle_T \\ & - \langle z_{i+i} \rangle \cdot \langle \varepsilon_{i+i} \rangle_T \\ & + \beta_{i+j} + \beta_{j+i} \\ & - \beta_{j+j} - \beta_{i+i} \end{aligned} \quad (15)$$

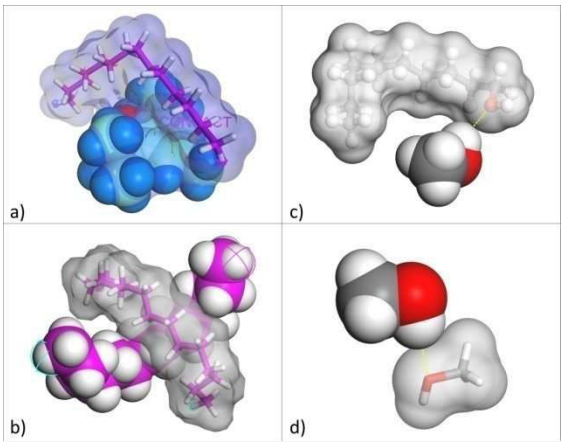

Figure 2. Typical configurations with minimal pair contact energies: a) BHT + PE segment idealized as 7 monomers, denoted PE_7; b) PE_7+PE_7; c) decanol+methanol; d) methanol+methanol.

According to Eqs. (9) and (15), the estimate of the partition coefficient between *L* and *P* becomes:

$$\begin{aligned} 2\cdot k_B\cdot T\cdot \ln K_{i,L/P} \approx\ & 2\cdot k_B\cdot T\cdot r_L^{-1} \\ & +\left(\left\langle z_{i+P}\right\rangle+\left\langle z_{P+i}\right\rangle\right)\cdot\left\langle \varepsilon_{i+P}\right\rangle_T \\ & -\left(\left\langle z_{i+L}\right\rangle+\left\langle z_{L+i}\right\rangle\right)\cdot\left\langle \varepsilon_{i+L}\right\rangle_T \\ & -\left\langle z_{P+P}\right\rangle\cdot\left\langle \varepsilon_{P+P}\right\rangle_T \\ & +\left\langle z_{L+L}\right\rangle\cdot\left\langle \varepsilon_{L+L}\right\rangle_T \\ & +\beta_{i+P}+\beta_{P+i}-\beta_{i+L} \\ & -\beta_{L+i}-\beta_{P+P}+\beta_{L+L} \end{aligned} \quad (16)$$

It is worth to notice that the final result did not depend on reference chemical potential g_{i+i}. Besides, some symmetric biases (*i*+*P* and *P*+*i*, *i*+*L* and *L*+*i*) were expected to balance each other due to a possible exchange of roles between the seed and the contact molecule.

3.3. Reference partition coefficients

A set of experimental partition coefficients around our targeted temperature (313 K) was collected from the literature. The corresponding values of $K_{i,L/P}$ are gathered in table 1 along with estimates of V_i^{vdw}, V_i^M, melting ranges and b_i. It is worth to notice that a significant uncertainty exist on $K_{i,L/P}$ values derived from apparent partitioning $\hat{K}_{i,L/P}$ (via Eq. (7)), since the data were obtained on different polyethylenes with different formulations and for temperatures ranging between 298 K and 313 K. When data on

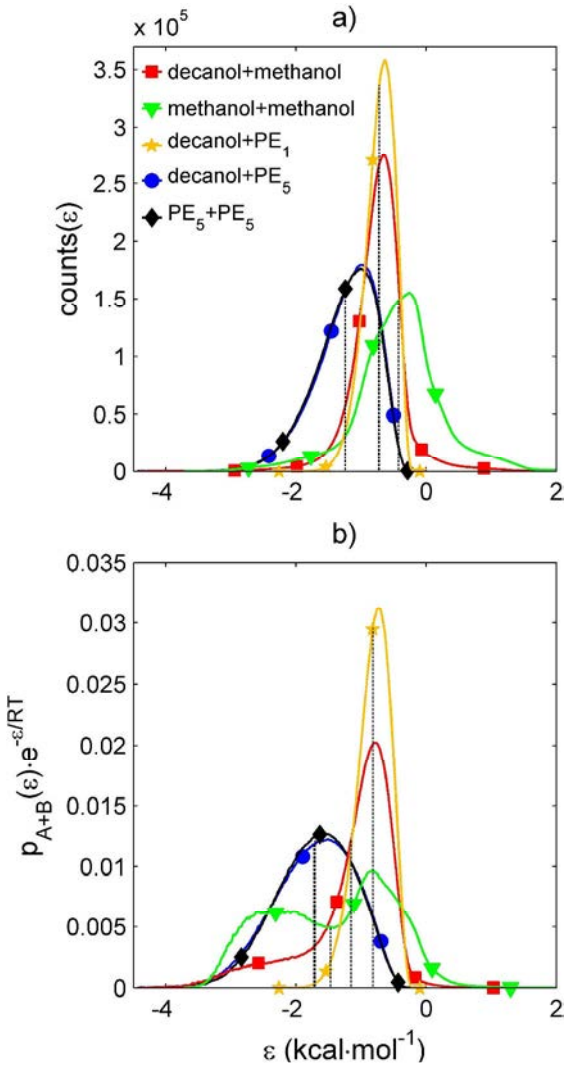

Figure 3. Typical distributions of pair contact energies: a) as sampled, b) after reweighting with the Boltzmann factor. PE_1 and PE_5 are PE segments idealized as 1 and 5 monomers respectively.

polymer crystallinity and density were missing, likely values were applied.

4. Results and discussion

In Eq. (9), $\chi_{i,P}$-$\chi_{i,L}$, encompasses both the enthalpic contribution (four pairwise terms) and the residual entropy. For convenience, the usual terminology of enthalpic contribution will be used for $\chi_{i,P}$-$\chi_{i,L}$. Similarly, r_L^{-1} will be related to the entropic contribution, whereas it accounted only for the positional entropy. In the perspective to develop a tailored computational method, we detail firstly important steps in calculation of terms of Eq. (16) and analyze possible sampling biases according to statistics and

Table 1. Main characteristics of tested solutes and corresponding partition coefficients between *L* (methanol or ethanol) and amorphous regions of PE

Solute *i*	CAS number	V_i^{vdw} (Å^3)	V_i^M (Å^3)	Melting range (°C)	b_i (%)	$K_{methanol/PE}$	$K_{ethanol/PE}$
Camphor	8022-77-3	172 ±5.2	320	179.8[d]	0.3	353[a]	168[a]
Diphenyl oxide	101-84-8	168 ±3.9	266	27-30[d]	0	2.78[a]	4.57[a]
Diphenylmethane	101-77-9	179 ±3.8	279	25.3[d]	0	2.37[a]	2.56[a]
D-limonene	5989-27-5	170 ±4.0	271	-95.5[d]	0	0.955[a]	1.52[a]
DL-menthol	89-78-1	188 ±3.6	292	34-35[d]	0	32.0[a]	73.6[a]
Eugenol	97-53-0	170 ±3.8	256	-7.5[d]	0	21.3[a]	49.2[a]
Isoamyl acetate	123-92-2	149 ±2.9	287	-78[d]	0	14.9[a]	13.9[a]
Linalyl acetate	115-95-7	229 ±4.7	362	<0[d]	0	11.0[a]	9.85[a]
Phenylethyl alcohol	60-12-8	131 ±3.7	199	-27[d]	0	66.0[a]	267[a]
Decane	124-18-5	192 ±5.0	324	-29.7[d]	0		1.16[b] / 0.548[c]
Undecane	1120-21-4	212 ±12	351	-25.6[d]	0.1		
Dodecane	112-40-3	230 ±5.8	378	-9.6[d]	0.2		0.722[b] / 0.510[c]
Tridecane	629-50-5	246 ±5.0	405	-5.5[d]	0.3		
Tetradecane	69-59-4	268 ±8.2	432	5.9[d]	0.4	0.254	0.567[b] / 0.400[c]
Pentadecane	629-62-9	283 ±5.4	459	10[d]	0.5		
Hexadecane	544-76-3	301 ±10	486	18.2[d]	0.6	0.146	0.477[b] / 0.358[c]
Heptadecane	629-78-7	321 ±7.5	513	22[d]	0.7		
Octadecane	593-45-3	339 ±5.9	544	28.2[d]	0.8	0.0768	0.299[b] / 0.216[c]
Nonadecane	629-92-5	357 ±7.3	568	32.1[d]	0.9		
Eicosane	112-95-8	377 ±6.3	595	36.8[d]	1		0.172[b]
Docosane	629-97-0	415 ±13	649	44.4[d]	1.2	0.0358	0.150[c]
Tetracosane	646-31-1	452 ±14	704	54[d]	1.4	0.0124	0.0773[c]
Octacosane	630-02-4	529 ±29	813	64.5[d]	1.6	0.0110	0.0197[c]
Decanol	112-30-1	201 ±5.0	318	6.9[d]	0		
Undecanol	112-42-5	220 ±6.6	345	19[d]	0. 1		
Dodecanol	112-53-8	239 ±5.5	374	30[d]	0.2		30.5[b] / 1.25[c]
Tridecanol	112-70-9	257 ±4.9	405	32-33[d]	0.3		
Tetradecanol	27106-00-5	274 ±4.6	432	39-40[d]	0.4		22.1[b] / 1.12[c]
Pentadecanol	629-76-5	294 ±7.6	456	35[d]	0.5		
Hexadecanol	36653-82-4	311 ±5.9	493	50[d]	0.6		19.4[b] / 1.12[c]
Heptadecanol	1454-85-9	330 ±4.1	503	54[d]	0.7		
Octadecanol	112-92-5	346 ±8.8	553	59-60[d]	0.8		12.1[b] / 0.836[c]
Nonadecanol	1454-84-8	365 ±4.1	583	62-63[d]	0.9		
Eicosanol	629-96-9	385 ±6.3	590	72-73[d]	1		
BHT	128-37-0	251 ±6.6	349	70[d]	0		1.18[c]
Irganox 1076	2082-79-3	647 ±12	949	50-55[e]	0		0.563[c]

[a]: calculated from experimental values at 298K with $c = 0.4$ [28]; [b]: calculated from experimental values at 298K with $c = 0.4$ [44]; [c]: calculated from experimental values at 313K with $c = 0.3$ [45]; [d]: extracted from Handbook[66]; [e]: CIBA (Basel, Switzerland) technical datasheet; V_i^M were calculated at 298K or 313K with densities (averaged or extrapolated at the good temperature) from CAS database or Handbook[66].

mechanical arguments. The results obtained in polyethylene with our methodology are secondly compared with classical results of Flory-Huggins theory as a first validation step. As the partial specific volume of a given solute *i* in an alcoholic solution *L* in relation to its size, shape and polarity is not known a priori, the choice of a simple approximation will be discussed by comparing predictions of Eq. (16) with experimental values. Finally, the best approximation in *L* will be applied without fitting to predict partitioning between *P* and *L* for all tested solutes.

4.1. Sampling of contact energies

For a given solute *i* in *P* and in *L*, the default strategy consisted in applying the same sample of conformers of *i* to the calculation of all pairs $\{i+j\}_{j=i,P,L}$. Each conformer was subsequently weighted via the Boltzmann factor according to $\varepsilon_{i+j} = \varepsilon_{j+i}$ values (see Eq. (11)). By contrast, real configurations are weighted by the packing energy of each structure $\{i+j\}_{j=i,P,L}$, formally $z_{j+i} \cdot \varepsilon_{j+i}$ and $z_{i+j} \cdot \varepsilon_{i+j}$. Since we started as a first guess from a set of conformers *i* representative of their configurations in a gas phase rather than in their respective condensed phase, the effects of the contact method together with the set of conformers were particularly investigated.

Fig. 2 presents some typical pair configurations with very low interactions energies and representative of the different pairs tested in this work. One molecule is outlined by its trace embedded inside its van der Waals envelope, while the other is plotted as a calotte model with atoms radii matching their van der Waals ones. Both representations led to very similar results and the determination of contacts was determined for efficiency from the van der Waals radii of atoms. The depicted configurations with minimal potential energy are known to be not necessarily privileged at high temperature and required an appropriate weighting. They illustrate however two significant trends respectively for large molecules and for a mixture of H donor and H acceptor molecules.

For flexible molecules without strong attractive interactions, the configurations of minimal energies correspond to a crossing over of molecules on their concave surfaces (Figs. 2a and 2b). This crossover configuration is very likely for isolated molecules but not very realistic in packed systems since all curved molecules expose both an intrados and an extrados to the contact with their neighbors. For large molecules such as polymers, the configuration depicted in Fig. 2b is very similar to the one envisioned for an entanglement. In the case of polyethylene, the persistence length imposes an entanglement every about 30 monomers[63]. As a result, the depicted situation has a relative weight about 7/30.

When hydrogen bonding exists, the importance of large molecule configuration is much less important and the proximity between the H donor and the H acceptor is favored irrespectively of the length of the molecule (Fig. 2c and 2d). The frequency of such a contact depends however on the size and shape of the molecule and on the strategy used to sample the contacts. Since the configurational space was weighted according to pair interactions instead of packing energies, the default method could not describe a possible alteration of the configuration of the gross side chain due to a long-lived hydrogen bonding (see Fig. 2c as an example). The probability to sample a contact with the oxygen atom of decanol (denoted *A*) depicted in Fig. 2c was in turn proportional to its solid angle when it is observed from the center of mass of the contact molecule (methanol, denoted *B*). Since the solid angle was inversely proportional to square of the distance between *A* and *B*, d_{AB}, or equivalently inversely proportional to the gyration radius of *A*, the probability to put in contact *B* with a terminal atom of a linear

molecule A (here an oxygen), denoted p^{O}_{A+B}, depended on its length, n_A, and on its considered configuration, according to following scaling relationship:

$$\frac{p^{o}_{A+B}\big|_{rigid}}{p^{o}_{A+B}\big|_{random}} = \left(\frac{d_{AB}\big|_{random}}{d_{AB}\big|_{rigid}}\right)^2 \propto \left(\frac{n_A^{0.5}}{n_A}\right)^2 = \frac{1}{n_A} \quad (17)$$

where subscripts "rigid" and "random" indicate a rigid configuration (as in good solvent) and a random configuration close to a Gaussian (as in a theta solvent).

It is emphasized that the bias identified for linear molecules with Eq. (17) was not associated to accessibility effects but to our isotropic sampling of pair interactions. To minimize this effect for oblong molecules, the initial expansion/contraction method was modified as follows. The space around the molecule was randomly cut into two half-spaces around its center of mass, the center of mass of atoms belonging to one of the half space was chosen as the new center of expansion/contraction. Previous considerations suggested that n-alcohols represented a particular worst-case to validate our whole strategy of sampling of pair contact energies.

The distributions of pair contact energies, ε_{A+B}, corresponding to pairs similar to those depicted in Fig. 2 are plotted in Fig. 3. In absence of significant polar interactions, the raw sampled distributions had a negative skew, which was characteristic of dispersive van-de-Waals forces (induced dipole-dipole forces). The associated contact energies were negative since all atoms were separated by a distance equal or greater than their van der Walls radii. By contrast, pair molecules with strong dipolar interactions created almost symmetric distributions with a high kurtosis including a sharp maximum and fat tails. The pair potential could be significantly positive due to possible repulsions between close partial charges with same signs. It is worth to emphasize that partial overlapping of atoms in the case of significant attractive Coulombic interactions was not allowed by the sampling algorithm.

Weighting previous distributions with the Boltzmann factor (see Eq. (11)) determined the relative probability of each sampled pair configuration as if the system was in thermodynamic equilibrium with a thermostat at the desired temperature (Fig. 3a). Further details on the distinction between so-called global and local equilibrium states can be found[67]. In absence of dipolar interactions, the thermalization process decreased the average interaction energy of few dozen percents without changing the overall distribution shape. By contrast, the distributions including dipolar interactions were drastically modified after thermalization. A sharp secondary mode associated to hydrogen bonding was noticed for values lower than -2 kcal·mol^{-1}. Although the potential associated to a hydrogen bond is about 10 times the potential of London forces[68], its importance decreases rapidly with the size of linear alcohols. For small molecules, such as methanol, distributions presented several maxima.

For non-convex molecules, there was a risk to oversample internal cavities larger than the contact molecule. The situation is depicted in Figs. 4a and 4b for heptadecanol in contact with methanol. Such configurations promoted the creation of a hydrogen bond. As result, the expansion method starting from a position close to the center of the cavity yielded probabilities of hydrogen bonding much higher than observed for shorted molecules such as decanol, which was not realistic. By contrast, the contraction method minimized the contribution of hydrogen bonding in long n-alcohols. The behavior of both methods was systematically studied for all n-alcohols used as seed molecules, A, in contact with small alcohols, B, with

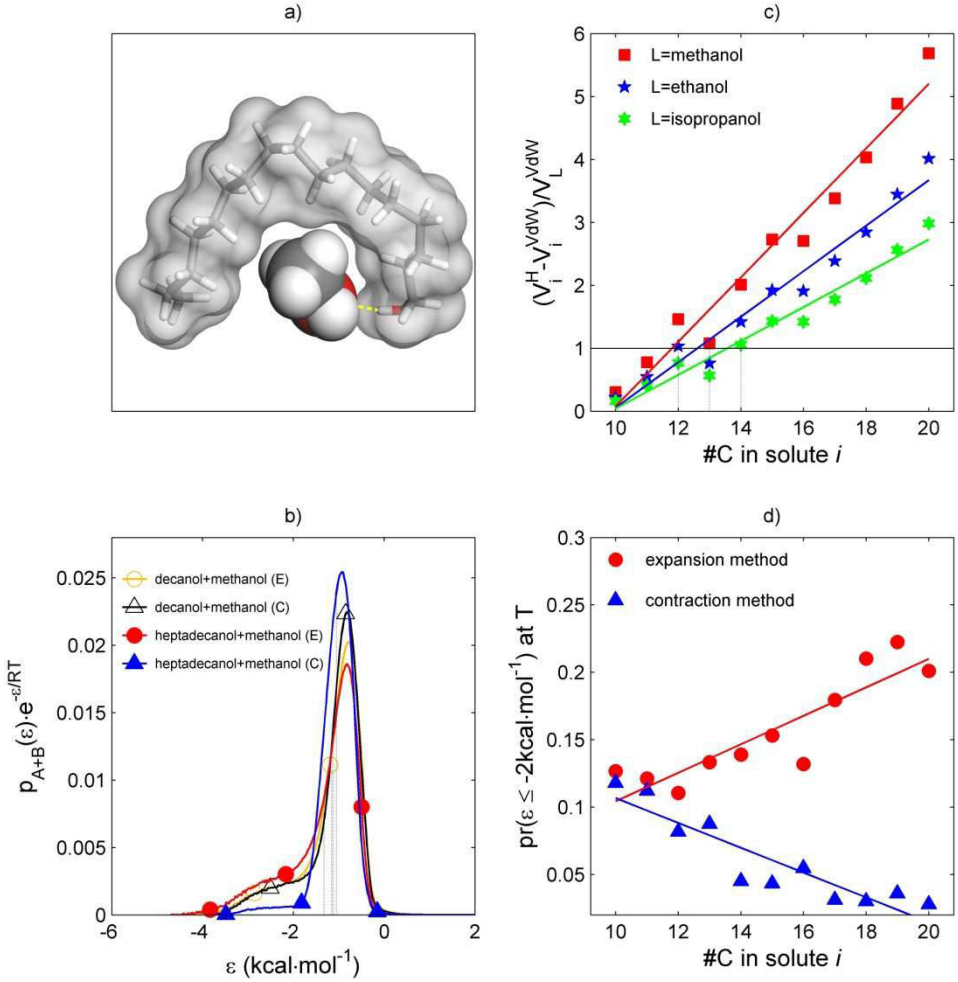

Figure 4. Illustrations of possible biases during the sampling of contact energies between n-alcohols and alcohols. a) example of cavity between a methanol in contact with heptadecanol; b) distributions of thermalized contact energies sampled with the expansion method (E) and the contraction method (C); c) variation of the cavity criterion according to the length of n-alcohols and the considered contact alcohol; d) probability of sampling a hydrogen bond, assessed as the cumulative probability to sample a thermalized contact energy lower than -2 kcal·mol^{-1}.

increasing size. The criterion to create an internal cavity was defined as:

$$\frac{V_A^H - V_A^{VdW}}{V_B^{VdW}} > 1 \qquad (18)$$

where V_A^H is the hydrodynamic volume occupied by the molecule A; V_A^{VdW} and V_B^{VdW} are the van-der-Waals volume of molecules A and B respectively. The values of the criterion (18) averaged over more than 50 conformers are plotted for all tested n-alcohols and liquids in Fig. 4c. The critical size to create a cavity for tested n-alcohols appeared between dodecanol and tetradecanol. The corresponding contribution of hydrogen bonding was assessed by calculating the cumulative probability to sample, at temperature T, a contact energy lower than -2 kcal·mol^{-1}. Beyond the critical size, both contacting methods led to dramatically dissimilar results and only the contraction method gave the expected trend: the contribution of hydrogen bonding should decrease linearly with the number of carbons in the chain.

Additional error due to the number of conformers is illustrated in Table 2 while keeping the same number of MC trials. For the same reasons as discussed previously, it was significant for flexible molecules due to the large extent of the conformation phase space. To minimize this error, up to

Table 2. Effect of the number of conformers on the pair contact energies and first contact neighbors while keeping the same MCsampling method (i.e. similar numbers of pair contact trials and of contact neighbors trials) for *i*=decanol and *L*=methanol.

# conformers of *i*	$<\varepsilon_{i,i}>_T$	$<\varepsilon_{i,L}>_T$	$z_{i,i}$	$z_{i,L}$	$z_{L,i}$
4000	-1.86 ±0.01	-1.16 ±0.01	5.54 ±0.03	8.89 ±0.06	3.45 ±0.02
5	-1.90 ±0.13	-1.31 ±0.18	5.57 ±0.01	8.90 ±0.03	3.49 ±0.04

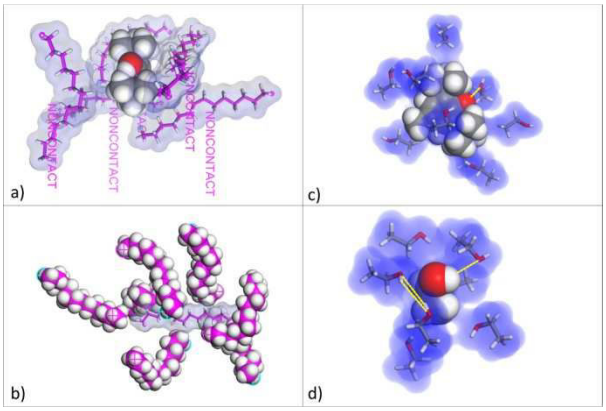

Figure 5. Typical packing configurations to sample the number of first neighbors in contact with a seed molecule: a) BHT + polyethylene segment consisting in 7 monomers, denoted PE_7; b) PE_7+PE_7; c) BHT+ethanol; d) ethanol+ethanol.

10^4 conformers were sampled to achieve an appropriate convergence..

4.2. Sampling of the number of first neighbors

The number of neighbors in contact with a seed molecule was assigned only on the basis of packing considerations as illustrated in Fig. 5. The convergence was faster for molecules with similar size and shapes. To ensure that the configuration space of each molecule was conveniently sampled 10^4 packing samples were at least performed. Infinite long molecule such as polymer were simulating by preventing the head and tail atoms to be in contact with any other molecule (Fig. 5a and 5b). In case of associating molecules, multiple hydrogen bonding could be achieved (Fig. 5d), but since no thermalization process was applied this configuration was not favored in the sample. Thus the packing of associating liquids such as methanol or ethanol are expected to differ from their real structure as they could be assessed using molecular dynamics. As we were interested in the average number of neighbors and not in the structure factor of the liquid, this approximation was hence not limiting. Nevertheless, it is worth to notice that since packaging and enthalpic considerations were treated separately, it was not possible to account for possible multiple hydrogen bonds involving more than 2 molecules. Thus, in ethanol at 298 K, about 79% of molecules have 2 hydrogen bonds against 15% that have a single hydrogen bond[69]. The approximation introduced by the Flory-Huggins theory is however partly compensated by the highest lifetime (or equivalently the lowest free energy) of simple hydrogen bonds or double hydrogen bonds involving only two molecules.

The effect of the number of sampled conformers on the contact neighbors are presented in Table 2. The effect was much lower than for pair interaction energies.

4.3. A first attempt of the validation of the Flory-Huggins approximation

The mean-field theory of Flory-Huggins relies on two important assumptions, which should be verified by our simulation results. i) The interactions in *P* do not depend on the length of polymer segments used to represent the polymer. ii) The pair contact energies and the number of neighbors are not correlated together and consequently the average of the product can be approximated efficiently by the product of the averages. According to Fig. 5a, the first assumption seemed unrealistic in our simulations when the size of polymer segments was much smaller than

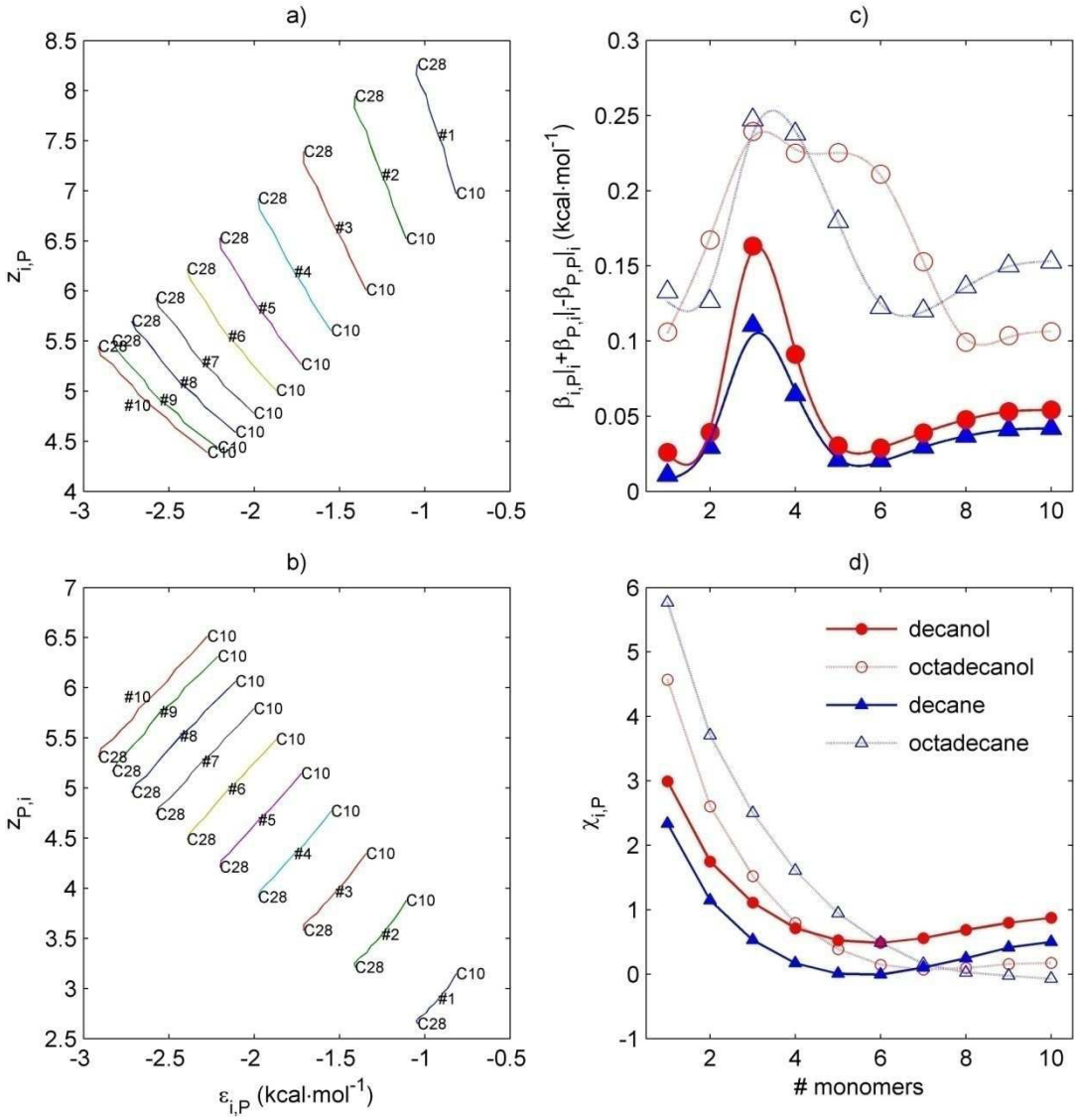

Figure 6. Estimation of biases due to the sampling procedure of excess contact energies with direct neighbors in *P*: a-b) number of neighbors when PE segments idealized by 1 (denoted #1) to 10 monomers (denoted #10) are in contact with n-alcohols (from decanol, denoted C_{10}, to octacosanol, denoted C28) versus the corresponding sampled thermalized pair contact energy; c) overall bias calculated with equations (12-14); d) effects of the number of monomers to idealize PE segments on the estimation of $\chi_{i,P}$.

the solute size. Indeed, the non-contact condition of head and tail atoms in *P* tended to underestimate the real number of contacts and neighbors. The violation of the second assumption was more obvious as all calculations demonstrated that z_{A+B} was always highly correlated to ε_{A+B}. The subtle correction was provided by the off-lattice approach, which preserved the asymmetry between z_{A+B} and z_{B+A} (i.e. their variations are opposite). This condition was almost sufficient to ensure a minimum covariance between the random variable ε_{A+B} and the random variable $z_{A+B} + z_{B+A}$. It is underlined that the conventional Flory-Huggins description on a lattice is by construction symmetric (Fig. 1), because the size of the blob increases with the volume of *i* while the number of neighbors remains imposed by the lattice coordination number.

Since our Monte-Carlo approach of pair interactions sampled both the conformation and the reorientation phase space, the non-combinatory entropic contribution was accounted in the estimate of $\left\{\chi_{i,j}\right\}_{j=P,L}$. Nevertheless, to be physically consistent, the whole approach required $\chi_{i,P}$ estimates

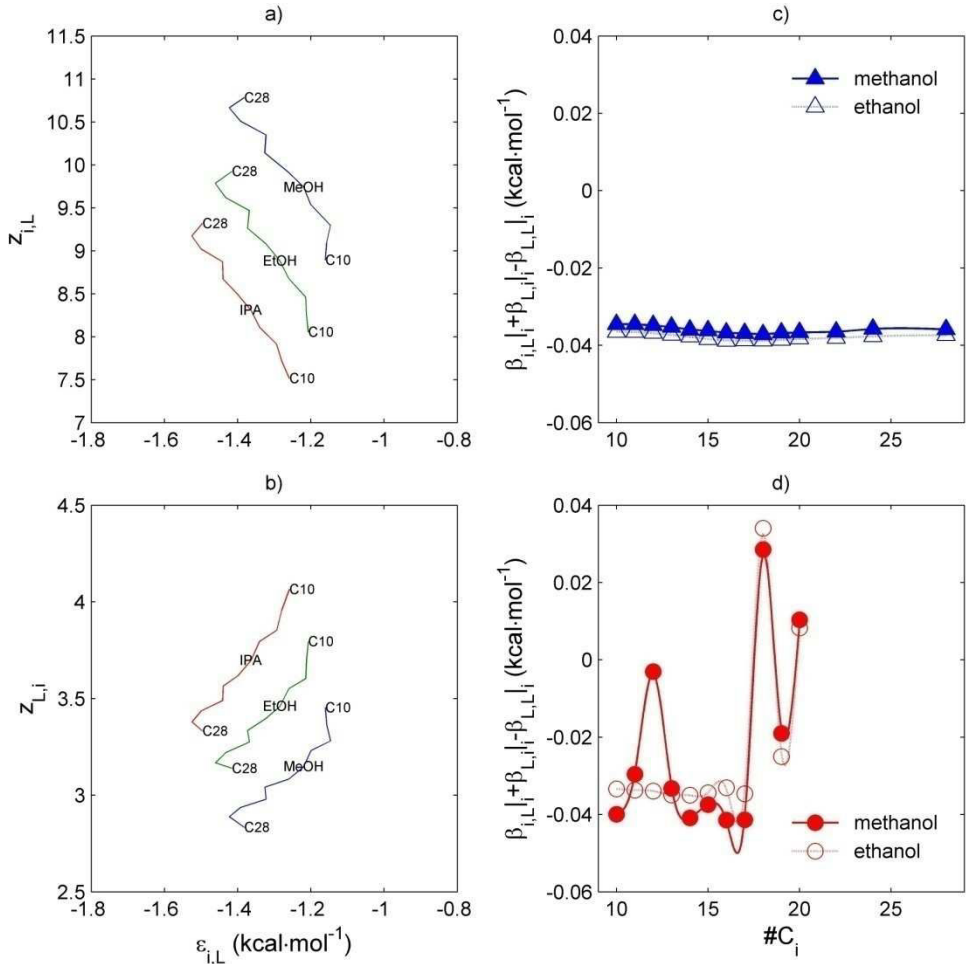

Figure 7. Estimation of biases due to the sampling procedure of excess contact energies with direct neighbors in *L*: a-b) number of neighbors when small alcohols (MeOH=methanol, EtOH=ethanol, IPA=isopropanol) are in contact with n-alcohols (from decanol, denoted C_{10}, to octacosanol, denoted C28) versus the corresponding sampled thermalized pair contact energy; c) overall bias calculated with equations (12-14) for n-alkanes; d) idem for n-alcohols.

not to depend on the number of monomers, *m*, used to represent the polymer. For a same solute *i* and according to Eq. (10), this condition implied that the variation in the pair interaction energy $g_{i+P}+g_{P+i}$ was exactly balanced by a similar variation of g_{P+P} when *m* was increasing. The best suitable number of monomers, *m*, was chosen to minimize the criterion $C_{P+i}^{(m)}$:

$$C_{P+i}^{(m)} = \left| 1 - \frac{\partial g_{i+P}^{(m)}}{\partial g_{P+P}^{(m)}}\bigg|_i - \frac{\partial g_{P+i}^{(m)}}{\partial g_{P+P}^{(m)}}\bigg|_i \right| \quad (19)$$

Because the configuration sampling of large polymer systems was computationally more expensive, the optimal *m* value was expected to occur for an intermediate value of *m* as the best trade-off between convergence costs and sampling biases. Fig. 6 plots the correlations between z_{i+P}, z_{P+i} and ε_{i+P}, the associated cumulated biases, $\beta_{i+P}\big|_i + \beta_{P+i}\big|_i - \beta_{P+P}\big|_i$ as defined in Eq. (16), and their consequences on the estimate of $\chi_{i,P}$ when *m* was increasing. The antisymmetry between the role of the polymer used as seed molecule or as contact molecule was best illustrated in Figs 6a and 6b when it was in contact with aliphatic molecules, which resembled it. When *P* was the contact molecule (Fig. 6a), the number of *P* segments increased around the solute *i* while the contact energy was increasing (i.e. the number of contact per molecule of *P* decreased). Linear solutes behaved symmetrically when they were placed around a single segment of *P* (Fig. 6b). Corresponding biases are listed in Table 3 for all tested

Table 3. Estimation of typical biases ($\times 10^3$) due to the sampling pair contact procedure as assessed with Eqs (12-14).

Solute *i*	$\beta_{i,P}$	$\beta_{P,i}$	$\beta_{P,P}$	$\beta_{i,L}^{MeOH}$	$\beta_{L,i}^{MeOH}$	$\beta_{L,L}^{MeOH}$	β_{tot}^{MeOH} [a]	$\beta_{i,L}^{EtOH}$	$\beta_{L,i}^{EtOH}$	$\beta_{L,L}^{EtOH}$	β_{tot}^{EtOH} [b]
Decane	380	-480	-244	45.2	-20.8	0.1	132	45.6	-209.0	-0.1	308
Undecane	406	-491	-245	47.5	-21.0	0.1	133	47.8	-21.0	-0.1	132
Dodecane	429	-508	-245	49.8	-21.3	0.1	138	50.2	-21.3	-0.1	137
Tridecane	451	-514	-218	51.7	-21.3	0.1	126	52.1	-21.3	-0.1	124
Tetradecane	472	-522	-173	53.8	-21.5	0.1	91	54.2	-21.5	-0.1	90.6
Pentadecane	483	-533	-193	53.9	-21.5	0.1	111	54.2	-21.5	-0.1	111
Hexadecane	502	-534	-209	56.2	-21.3	-0.1	141	56.7	-21.3	0.1	141
Heptadecane	512	-539	-177	57.0	-21.2	-0.1	114	57.4	-21.3	0.1	114
Octadecane	527	-543	-270	58.2	-21.3	-0.1	217	58.5	-21.3	0.1	217
Nonadecane	548	-542	-286	61.1	-21.6	0.3	252	61.5	-21.7	-0.2	252
Eicosane	552	-542	-282	60.6	-21.2	-0.1	253	61.0	-21.2	0.1	253
Decanol	397	-488	-244	22.4	-10.0	0.1	141	22.7	-10.1	-0.1	141
Undecanol	422	-498	-245	27.7	-12.1	0.1	153	28.4	-12.2	-0.1	152
Dodecanol	449	-509	-245	33.5	-14.0	0.1	165	34.1	-14.1	-0.1	165
Tridecanol	468	-505	-218	32.6	-13.1	0.1	161	33.6	-13.3	-0.1	160
Tetradecanol	492	-513	-173	34.0	-13.2	0.1	131	34.6	-13.3	-0.1	130
Pentadecanol	508	-514	-193	32.6	-12.3	0.1	167	33.0	-12.4	-0.1	167
Hexadecanol	521	-505	-209	27.0	-9.8	-0.1	208	28.2	-10.0	0.1	207
Heptadecanol	541	-507	-177	27.8	-9.7	-0.1	193	29.5	-10.2	0.1	193
Octadecanol	548	-500	-270	25.3	-8.7	-0.1	301	27.0	-8.3	0.1	299
Nonadecanol	563	-502	-286	24.0	-8.0	0.3	331	25.6	-8.4	-0.2	330
Eicosanol	577	-501	-282	24.3	-8.3	-0.1	342	27.4	-9.4	0.1	341

[a]: $\beta_{tot}^{MeOH} = \beta_{i,P} + \beta_{P,i} - \beta_{P,P} - \beta_{i,L}^{MeOH} - \beta_{L,i}^{MeOH} + \beta_{L,L}^{MeOH}$;

[b]: $\beta_{tot}^{EtOH} = \beta_{i,P} + \beta_{P,i} - \beta_{P,P} - \beta_{i,L}^{EtOH} - \beta_{L,i}^{EtOH} + \beta_{L,L}^{EtOH}$

molecules. Despite significant biases introduced by the separation of the calculation of z_{A+B}, z_{B+A} and ε_{A+B}, a minimum global bias was finally achieved by considering the sum $z_{A+B} + z_{B+A}$. The cumulative biases were in particular minimal when the roles of seed and contact molecule were exactly interchangeable, that is when there sizes were similar (Fig. 6c). When the solute did not resemble the polymer, the bias was higher. The consequence was that $\chi_{i,P}^{(m)}$ calculated from Eq. (15) admitted a minimum value close to the value, which was responsible for the minimal overall bias (Fig. 6d). For too small m values, head and tails effects dominated leading to overestimations of $\chi_{i,P}$. For large m values, end effects vanished and the dependence to m was lower, as expected in the Flory-Huggins theory. The accuracy of results was more sensitive to the quality of sampling: all biases increased with m and in particular the contribution of $\beta_{P+P|i}$. It is worth to notice that the asymptotic bias estimated in our simulations (between $0.14 \cdot k_B \cdot T$ and $0.31 \cdot k_B \cdot T$) was close to the theoretical correction of $0.35 \cdot k_B \cdot T$ conventionally applied to fit the Flory-Huggins theory to the solubility of linear n-alkanes in polyethylene[33]. The minimum value of $\chi_{i,P}^{(m)}$ over a likely range of m values coincided with the minimum of criterion (19) and was chosen to estimate $K_{i,L/P}$ in Eq. (9). For an arbitrary solute, the examined range of m values was chosen to mimic a polymer segment with a hydrodynamic volume ranging between half and twice the hydrodynamic volume of *i*.

Previous biases associated to our off-lattice approach of polymer-solute

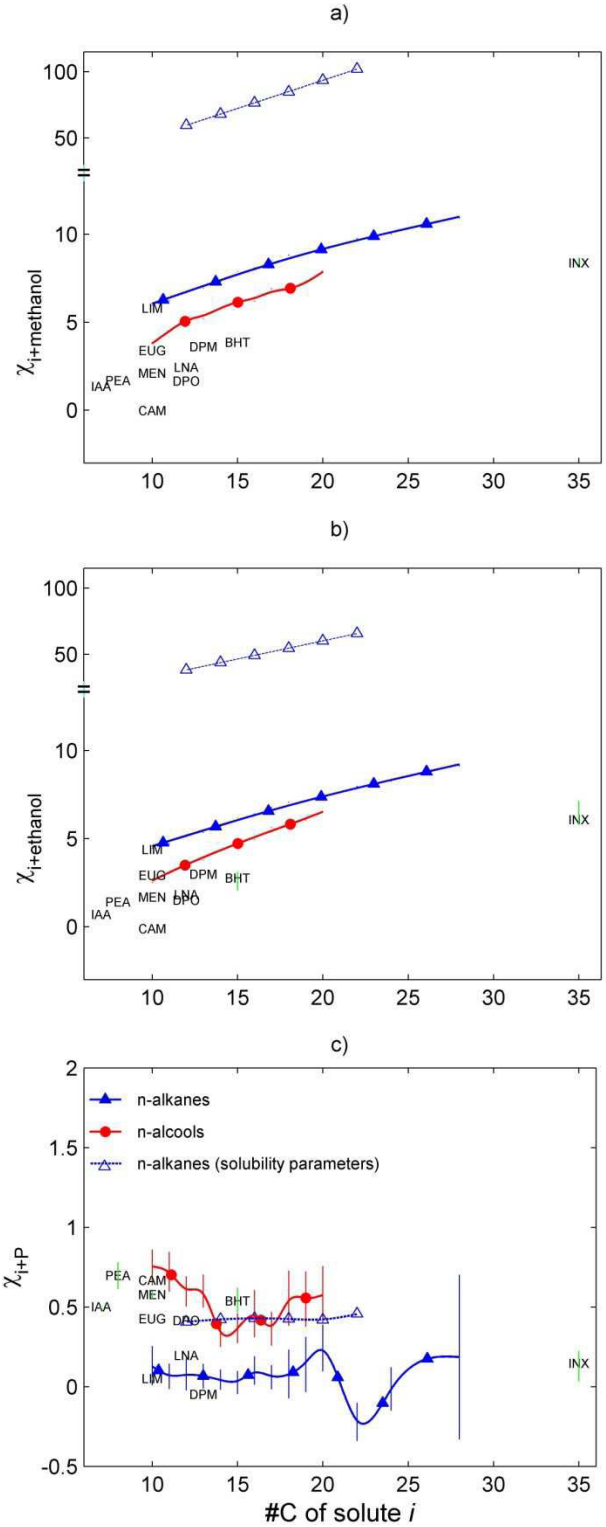

Figure 8. Flory-Huggins parameters versus the number of carbon atoms in i: a) L=methanol; b) L=ethanol; c) P = polyethylene segment with optimal length. CAM=camphor; DPM=diphenylmethane; DPO=diphenyl oxide; EUG = eugenol; IAA=isoamyl acetate; INX = Irganox 1076; LIM=d-limonene; LNA=linalyl acetate; MEN=DL-menthol; PEA=phenylethylalcohol.

interactions were observed also in L (Figs. 7a and 7b). By contrast with P, there was however no degree of freedom (i.e. m)

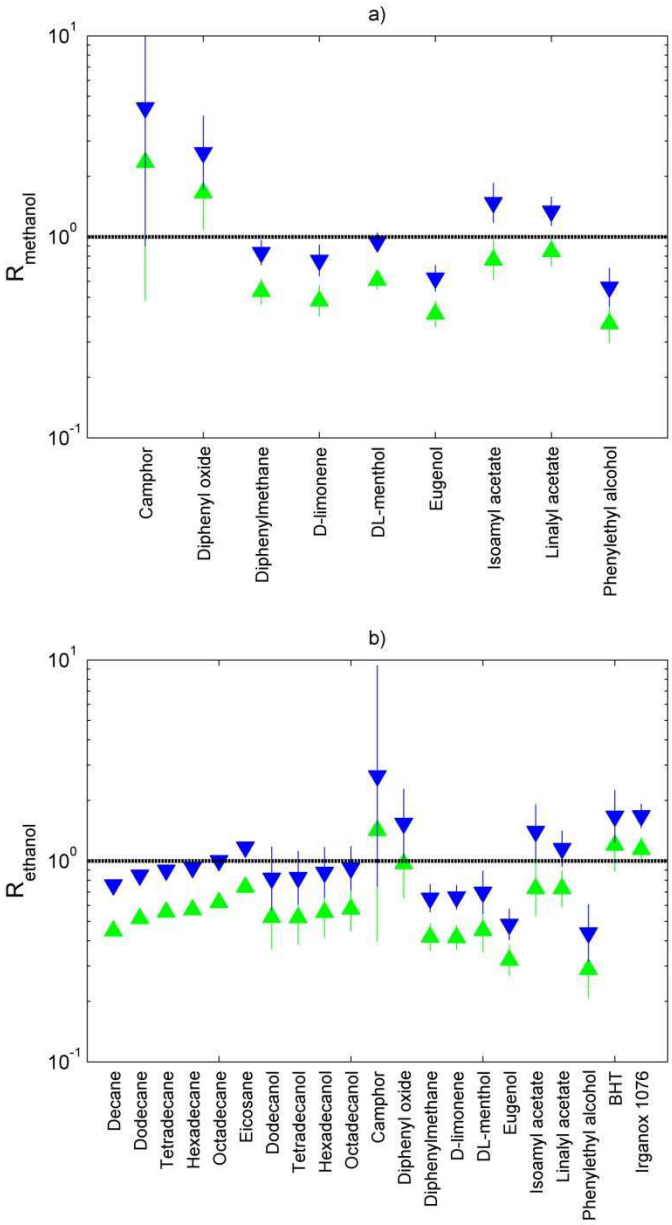

Figure 9. Ratio of cavity sizes to insert a solute i in L defined in Eq. (20) a) partition between methanol and PE; b) partition between ethanol and PE. Vertical pars represent the dispersion index of the ratio due to experimental errors in experimental $K_{i,P/L}$ values.

available to control the overall bias. As L molecules were much smaller than solute ones, the cumulated biases appeared mainly negative. It is nevertheless underlined that it was almost constant for linear solutes (Figs. 7c and 7d).

$\chi_{i,P}$ and $\chi_{i,L}$ values calculated with our off-lattice Flory-Huggins approach are gathered in Fig. 8 versus the number of solute carbons and are compared along with conventional values derived from van Krevelen solubility coefficients[70]. The

Table 4. Calculated Flory-Huggins interaction parameters.

Solute	$\chi_{i,methanol}$	$\chi_{i,ethanol}$	$\chi_{i,isopropanol}$	$\chi_{i,P}$
Decane	5.89 ± 0.01 [b]	4.40 ± 0.01 [b]	3.28 ± 0.002 [b]	0.3 ± 0.05 [b]
Undecane	6.17 ± 0.005 [b]	4.65 ± 0.003 [b]	3.50 ± 0.001 [b]	0.30 ± 0.001 [b]
Dodecane	6.62 ± 0.001 [b]	5.06 ± 0.003 [b]	3.87 ± 0.001 [b]	0.31 ± 0.02 [b]
Tridecane	6.90 ± 0.005 [b]	5.31 ± 0.003 [b]	4.10 ± 0.01 [b]	0.30 ± 0.01 [b]
Tetradecane	7.26 ± 0.01 [b]	5.64 ± 0.01 [b]	4.38 ± 0.02 [b]	0.23 ± 0.003 [b]
Pentadecane	7.84 ± 0.02 [b]	6.16 ± 0.01 [b]	4.85 ± 0.01 [b]	0.24 ± 0.01 [b]
Hexadecane	8.03 ± 0.05 [b]	6.35 ± 0.05 [b]	5.03 ± 0.04 [b]	0.37 ± 0.04 [b]
Heptadecane	8.44 ± 0.05 [b]	6.72 ± 0.05 [b]	5.36 ± 0.04 [b]	0.28 ± 0.04 [b]
Octadecane	8.76 ± 0.05 [b]	7.01 ± 0.05 [b]	5.62 ± 0.04 [b]	0.44 ± 0.04 [b]
Nonadecane	8.82 ± 0.05 [b]	7.09 ± 0.05 [b]	5.66 ± 0.04 [b]	0.55 ± 0.04 [b]
Eicosane	9.15 ± 0.02 [b]	7.38 ± 0.02 [b]	5.93 ± 0.01 [b]	0.68 ± 0.01 [b]
Docosane	9.71 ± 0.02 [b]	7.91 ± 0.01 [b]	6.40 ± 0.01 [b]	0.11 ± 0.01 [b]
Tetracosane	9.96 ± 0.6 [b]	8.21 ± 0.06 [b]	6.68 ± 0.05 [b]	0.39 ± 0.05 [b]
Octacosane	10.87 ± 0.7 [b]	9.08 ± 0.6 [b]	7.48 ± 0.5 [b]	0.35 ± 0.5 [b]
Decanol	3.77 ± 0.05 [b]	2.49 ± 0.04 [b]	1.86 ± 0.04 [b]	0.79 ± 0.03 [b]
Undecanol	4.43 ± 0.05 [b]	3.03 ± 0.04 [b]	2.09 ± 0.04 [b]	0.77 ± 0.04 [b]
Dodecanol	5.29 ± 0.01 [b]	3.71 ± 0.005 [b]	2.47 ± 0.001 [b]	0.69 ± 0.002 [b]
Tridecanol	5.19 ± 0.04 [b]	3.77 ± 0.03 [b]	2.27 ± 0.03 [b]	0.68 ± 0.01 [b]
Tetradecanol	5.81 ± 0.03 [b]	4.35 ± 0.03 [b]	2.49 ± 0.03 [b]	0.40 ± 0.003 [b]
Pentadecanol	6.21 ± 0.02 [b]	4.80 ± 0.02 [b]	2.52 ± 0.01 [b]	0.46 ± 0.01 [b]
Hexadecanol	6.18 ± 0.06 [b]	4.92 ± 0.06 [b]	2.37 ± 0.05 [b]	0.54 ± 0.05 [b]
Heptadecanol	6.89 ± 0.06 [b]	5.62 ± 0.06 [b]	2.70 ± 0.05 [b]	0.47 ± 0.04 [b]
Octadecanol	6.76 ± 0.03 [b]	5.71 ± 0.03 [b]	2.34 ± 0.02 [b]	0.70 ± 0.02 [b]
Nonadecanol	7.22 ± 0.06 [b]	6.04 ± 0.06 [b]	2.49 ± 0.05 [b]	0.72 ± 0.05 [b]
Eicosanol	7.95 ± 0.02 [b]	6.68 ± 0.02 [b]	2.94 ± 0.01 [b]	0.76 ± 0.01 [b]
Camphor	-0.54 ± 0.005 [a]	-0.81 ± 0.005 [a]	-1.02 ± 0.005 [a]	0.67 ± 0.002 [a]
Diphenyl oxide	-1.05 ± 0.005 [a]	-0.78 ± 0.005 [a]	-0.55 ± 0.005 [a]	0.42 ± 0.002 [a]
Diphenylmethane	3.37 ± 0.02 [a]	2.73 ± 0.01 [a]	2.12 ± 0.01 [a]	-0.05 ± 0.01 [a]
D-limonene	5.12 ± 0.03 [a]	3.80 ± 0.01 [a]	2.73 ± 0.01 [a]	0.04 ± 0.01 [a]
DL-menthol	2.02 ± 0.03 [a]	1.55 ± 0.03 [a]	1.09 ± 0.03 [a]	0.56 ± 0.03 [a]
Eugenol	3.07 ± 0.02 [a]	2.59 ± 0.01 [a]	2.02 ± 0.04 [a]	0.43 ± 0.03 [a]
Isoamyl acetate	1.36 ± 0.02 [a]	0.71 ± 0.01 [a]	0.21 ± 0.01 [a]	0.49 ± 0.01 [a]
Linalyl acetate	2.40 ± 0.03 [a]	1.77 ± 0.02 [a]	1.19 ± 0.02 [a]	0.20 ± 0.02 [a]
Phenylethyl alcohol	1.62 ± 0.02 [a]	1.30 ± 0.01 [a]	0.93 ± 0.01 [a]	0.62 ± 0.01 [a]
BHT	3.85 ± 0.003 [b]	3.12 ± 0.61 [b]	2.30 ± 0.1 [b]	0.51 ± 0.06 [b]
Irganox 1076	8.65 ± 0.13 [b]	7.14 ± 0.48 [b]	6.03 ± 0.1 [b]	0.15 ± 0.1 [b]

[a]: values at 298K, [b]: values at 313K.

interesting feature was that both $\chi_{i,L}$ curves were parallel but with values 9 to 11 times lower when they were calculated with the our off-lattice approach. This result confirmed indirectly the bad solubility coefficients weighting for the prediction of activity coefficients in interacting liquids[32]. Since almost all tested molecules appeared to be highly compatible with the polymer, with $\chi_{i,P}$ values close to or lower than 1, errors and biases on $\chi_{i,P}$ impacted a few on on $\chi_{i,P}$-$\chi_{i,L}$ differences (see Eqs. (15) and (16)) and only for molecules with a good or a moderate affinity for L, that is mainly for volatiles and phenolic compounds.

4.4. Combinatorial entropic contribution

The volume of the cavity required to insert a molecule i in the medium L, also called partial specific volume, affected significantly the prediction of partitioning (see Eq. (8)). In particular, increasing the volume of the cavity in L increased the affinity for L due to a higher entropic contribution. In polar media, the introduction of a hydrophobic substance i is expected to modify the network of hydrogen bonding so that the orientation of L molecules may not be random around i and may increase the size of the effective cavity. On the opposite, the possibility of hydrogen bonding between i and L may lead to a contraction of the cavity. Because our objective was to keep within the simplified framework of the Flory-Huggins theory, we argue that the expected size of the cavity was comprised between the van-der-Waals volume of i (hard core volume) and its molar volume. This assumption has been studied in a companion work to be published by isobarc molecular dynamics for different fractions in solutes. A dimensionless size of the cavity, r_L^{-1} (as used in Eq. (9)), is obtained by dividing the previous volume with the molar volume of pure L at the considered temperature. The choice of the molar volume to normalize the typical blob size was consistent with the assumption that no modification of bulk properties occurs at infinite solute dilution. Conversely, the choice of the molar volume for pure solutes i, that are solid at the considered temperature (see Table 1) might be questionable since they did not correspond to a disordered state as i was dispersed among L molecules. To check which dimensionless cavity size matched best the experimental partition coefficients between L and the amorphous phase of the polymer, the following ratio, R, was calculated at T=298 K and T=313 K:

$$R = \frac{r_L^{-1}\left(T\right)}{\left(\ln K_{i,L/P}^{(T)}\right) - \left(\chi_{i,P}^{(T)} - \chi_{i,L}^{(T)}\right)} \qquad (20)$$

R values for both assumptions are compared for all tested solutes and liquids in Fig. 9. A ratio lower than 1 indicated an underestimated cavity volume. In agreement with conventional approaches based on cohesive energy densities, solute molar volumes tended to lead more accurate results and in particular for all linear molecules. The significant discrepancy among experimental results made however not possible to confirm the assumption for all tested molecules. As a result, both definitions were used to estimate $K_{i,L/P}$ with Eq. (9) and a likely value was proposed as the geometric mean of possible bonds. Besides, calculated R values confirmed unambiguously the predominant role of the positional entropic contribution in L for the prediction of the partitioning. This effect was neglected in the pioneer work of Baner and Piringer[28].

4.5. Predictions of partitioning

The comparisons between predicted and experimental values for all tested molecules are presented in Fig. 10. Experimental values corresponded to those listed in Table 1. Predicted values were calculated with Eq. (16) using ε_{A+B} and z_{A+B} values obtained from out MC sampling . The corresponding $\left\{\chi_{i,j}\right\}_{j=P,L}$ and β_{A+B} values are gathered in Table 4 and in Table 3 respectively. The vertical error

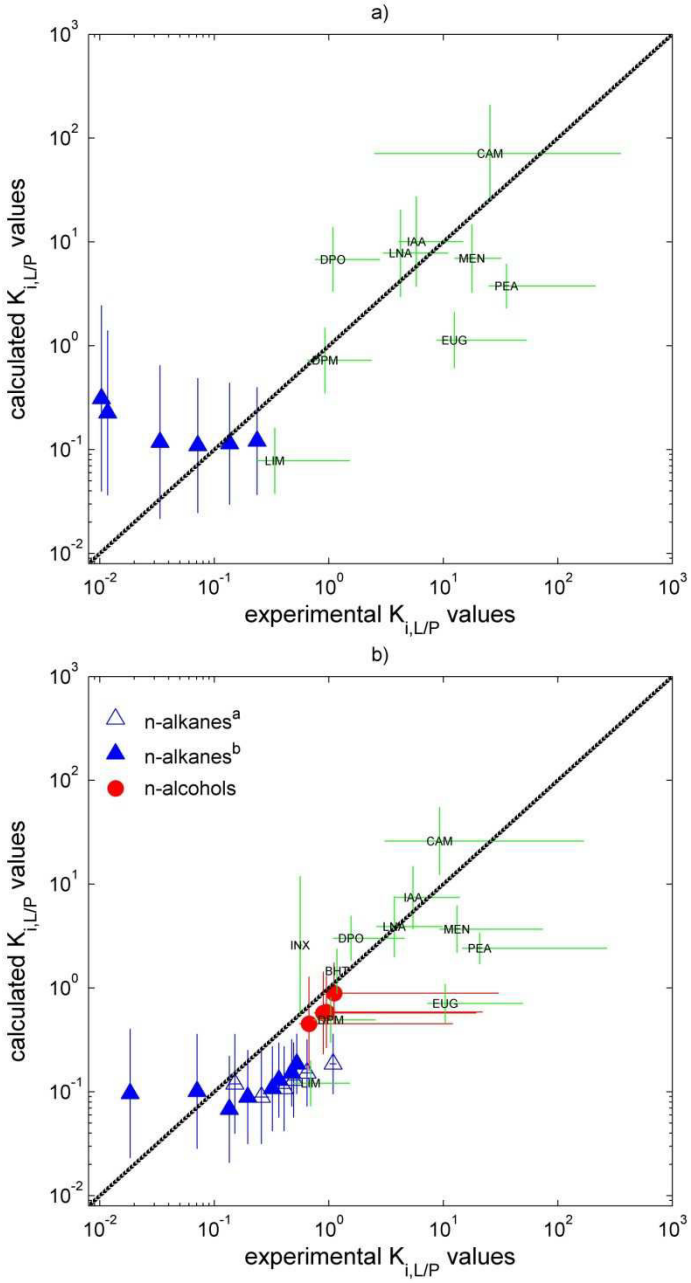

Figure 10. Comparison between calculated (with Eq. (16)) and experimental $K_{i,P/L}$ values for a large set of solutes: a) *L*=methanol; b) L=ethanol. CAM=camphor; DPM=diphenylmethane; DPO=diphenyl oxide; EUG = eugenol; IAA=isoamyl acetate; INX = Irganox 1076; LIM=d-limonene; LNA=linalyl acetate; MEN=DL-menthol; PEA=phenylethylalcohol. [a]: experimental values given in[28]; [b]: experimental values given in[45].

bars are related to the choice of V_i^{vdw} or V_i^M to estimate r_L^{-1}, whereas the horizontal bars include the uncertainty on polymer crystallinity and on solute dispersion in the matrix, as described in Eq. (7). The predictions were in very satisfactory agreement with measurements for a wide range of molecules highly different in size, shape, stiffness and polarity. The higher discrepancy observed for linear aliphatic chains in contact with small polar liquids (methanol) was related to the deviation of their conformations in a poor solvent from the one sampled in a gas phase.

Since our description of partitioning was consistent with previously published values, we tried to modify the solubility coefficients-based approach of Baner and Piringer[28] to match our findings and in particular to fit the values of $\chi_{i,P}$ and $\chi_{i,L}$ estimated by our Monte-Carlo approach. The first modification consisted in introducing a weighting sum of the solubility coefficients as described by Lindwig *et al.*[32]:

$$\left\{\chi_{i,j}\right\}_{j=P,L} = \alpha \cdot \frac{V_i}{RT}\left[\left(\delta_i^d - \delta_j^d\right)^2 + 0.25 \cdot \left(\delta_i^p - \delta_j^p\right)^2 + 0.25 \cdot \left(\delta_i^h - \delta_j^h\right)^2\right] \quad (21)$$

where $\left\{\delta_k^d\right\}_{k=i,P,L}$, $\left\{\delta_k^p\right\}_{k=i,P,L}$ and $\left\{\delta_k^h\right\}_{k=i,P,L}$ are respectively the dispersive, the polar and the hydrogen contribution to the solubility coefficients. The main advantage of such a model is that it uses coefficients, which have been extensively tabulated by group contribution for a wide range of substances[31,33]. As suggested, we used the solubility coefficients of van Krevelen[70] compared with results for low density polyethylene[28]. The scaling coefficient α was set to 0.35 to match our $\chi_{i,L}$ values for n-alkanes. This choice was consistent with the suggested values between 0.25 and 0.3 assessed for mixtures including polymer and hydrogen bonding solvents[32]. The second modification relied on partition-coefficient estimate defined in Eq. (7). The results plotted in Fig. 11 showed a good agreement between predictions and measurements. The proposed improvement made it possible to use solubility coefficients without using a

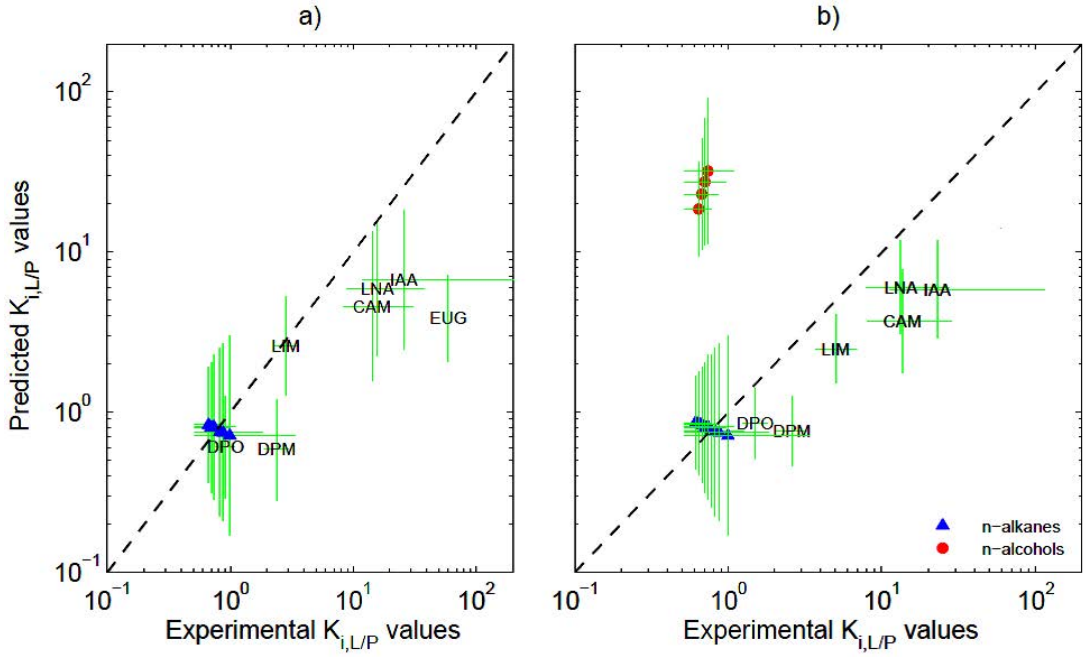

Figure 11. Comparison between $K_{i,P/L}$ values calculated with the weighted sum of solubility coefficients proposed by Lindvig et al.[32] and experimental ones[28]: a) partition between methanol and PE; b) partition between ethanol and PE. CAM=camphor; DPM=diphenylmethane; DPO=diphenyl oxide; EUG = eugenol; HXO=cis-hexenol; IAA=isoamyl acetate; LIM=d-limonene; LNA=linalyl acetate; MEN=DL-menthol; PEA=phenylethylalcohol.

correction, which depends on the considered solute or liquid medium as initially proposed by Baner and Piringer[28]. It emphasized that the chosen value of α is almost universal and it is not expected to depend on either *i* or *L*. Indeed, as it was previously mentioned in Figs. 8a and 8b, the overestimation of the non-weighted sum of solubility coefficients would be mainly related to an inappropriate scaling relationship of the "enthalpic" interactions. The overall correction 0.35x0.25 = 0.09 for the polar and hydrogen contributions, which dominated the final $\chi_{i,L}$ value, acted as a scaling correction factor without changing the general trends. The same scaling relationship was also required for $\chi_{i,P}$ since the non-weighted sum overestimated the values obtained by our Monte-Carlo method.

5. Conclusions

An off-lattice generalized Flory-Huggins approach has been proposed to predict the partitioning of solutes between polymer and liquid amorphous phase. As in the original Flory-Huggins approach, it takes into account interactions only with nearest neighbors and consequently does not require an explicit representation of the whole polymer. The molecular interactions are calculated at atomistic scale using a generic forcefield optimized on quantum mechanics results. Leaving the mean-field approximation of polymer interactions used in conventional Flory-Huggins approach made it possible to sample directly the entropic contribution due to conformers and reorientations. However, the separation of the calculations corresponding to the number of neighbors and the pair interaction energies introduced systematic biases in the sampling, which has also been shown in the original version. They could be minimized in the polymer by choosing a segment length that match the hydrodynamic solute volume. Additionally, it was demonstrated that isotropic sampling of pair interactions might induce additional biases for non-spherical molecules: either linear or including a cavity. By both performing a cautious sampling and by taking into account the positional entropy in the polymer and in the liquid, it has been demonstrated that partition coefficients

could be predicted without any fitting. These results were used to adapt a predictive model of partition coefficients based on solubility coefficients and on the weighted sum[32].

Additionally, the simulations demonstrated that even if plastic additives have a good solubility in polymers, they have also a significant chemical affinity for liquids consisting in small molecules. The high affinity of bulky solutes for liquids was related to the significant contribution of the positional entropy in *L*. This effect was either neglected or underestimated in previous studies. As a result, the migration assessment of large additives such as hindered phenolic antioxidants in alcohols and possibly in water should be revised, in particular in conditions where diffusion in *P* is not limiting (e.g. at high temperature). A companion work is dedicated to generalize the proposed approach of partitioning to water-ethanol mixtures, while providing a reliable estimate of r_F^{-1} in poor and theta solvents.

Acknowledgments

The authors would like to thank the Association de Coordination Technique pour l'Industrie Agroalimentaire and the Association Nationale pour la Recherche Technique (ANRT) for their financial support.

List of symbols

Roman symbols

A: any molecule with a seed role.

B: any molecule with a contact role.

$\left\{ \hat{C}_{i,j} \big|_{eq} \right\}_{j=L,P}$: macroscopic concentration at equilibrium of solute *i* in *j=L,P* as experimentally assessed (kg·m^{-3}).

$C_{i,L} \big|_{eq}$: concentration of solute *i* in liquid *L* at equilibrium (kg·m^{-3}).

$C_{i,P} \big|_{eq}^{a}$: concentration of solute *i* in the amorphous phase of polymer *P* at equilibrium (kg·m^{-3}).

$C_{i,P} \big|_{t=0}$: initial concentration of solute *i* in polymer *P* (i.e. before contact with *L*) (kg·m^{-3}).

$C_{P+i}^{(m)}$: criterion defined in Eq. (19).

$G_i^{\dagger}$: free energy to cross the interface (J).

G_{j+k}: free energy between *j=L,P,i* and *k=L,P,i, j≠k* (J).

H_{i+j} : enthalpy between solute *i* and *j=L,P* (J).

$K_{i,L/P}$: partition coefficient of solute *i* between *L* and the amorphous region of *P*.

$\hat{K}_{i,L/P}$: apparent partition coefficient of solute *i* between *L* and a semi-crystalline polymer *P*.

L: liquid

N_j : number of molecules *j=L,P*.

$N_{i,j}$: number of solute *i* in *j=L,P*.

P: polymer

R: cavity size criterion defined in Eq. (20).

T: absolute temperature (K).

V_A^H: hydrodynamic volume occupied by the molecule *A* (m^3).

V_i: partial specific volume solute *i* (m^3).

V_j^{VdW} : van-der-Waals volume of molecule *j=A,L,i* (m^3).

V_i^M : molar volume of the solute *i* (m^3).

a_i: extraction yield of solute *i* from polymer *P*.

b_i: amount of solute *i*, which is not "well-dispersed" in polymer *P*.

c: polymer crystallinity (volume fraction of crystalline phase).

g_{A+B} : ensemble-averaged potential energy associated to a set of molecules *B* in contact with a single molecule *A*.

i: solute index.

h: Plank's constant (6.63·10^{-34} J·s^{-1}).

k_B: Boltzmann's constant (1.38·10^{-23} J·K^{-1}).

$k_{i,j\to k}$: frequency of *i* crossing the interface from *j=L,P* to *k=L,P* with *j≠k* (s^{-1}).

l: dilution factor, or equivalently the ratio between the volume of polymer *P* and the volume of liquid *L*.

m: number of monomers.

n_j: length of molecule *j=A,B*.

$p_{A+B}(\varepsilon)$: distribution of contact energies between *A* and *B*.

p^{O}_{A+B}: probability to put in contact a molecule *B* with a terminal atom of a linear molecule *A*.

$p_{i,j}\big|_{eq}$: presence probability at equilibrium of solute i from side of *j=L,P* at the interface.

r_j: number of blobs of volume V_i for molecule *j= L,P,i*.

z_{A+B}: coordination number of the arrangement when *A* is surrounded by molecules *B*.

Greek symbols

β_{A+B}: covariance between z_{A+B} and ε_{A+B}.

$\gamma^{v}_{i,j}$: activity coefficient of solute *i* in *j=L,P*.

δ^{d}_{j}: dispersive contribution to the solubility coefficients for *j=L,P,i* ($J \cdot mol^{-1}$).

δ^{p}_{j}: polar contribution to the solubility coefficients for *j=L,P,i* ($J \cdot mol^{-1}$).

δ^{h}_{j}: hydrogen contribution to the solubility coefficients for *j=L,P,i* ($J \cdot mol^{-1}$).

Δ_{A+B}: derivative of z_{A+B} with ε_{A+B} (see Eq. (14)).

ε_{j+k}: contact energy associated to the contact(s) between a molecule *j=A,B,L,P,i* and a molecule *k=A,B,L,P,i, j≠k* ($J \cdot mol^{-1}$).

μ_j: chemical potential of *j=P,L*.

$\mu_{i,j}$: chemical potential of molecules solute *i* in *j=L,P*.

ϕ_j: volume fraction of *j=L,P*.

$\phi_{i,j}$: volume fraction of solute *i* in *j=L,P*.

$\{\chi_{i,j}\}_{j,P,L}$: Flory-Huggins parameter.

Subscripts

$X|_{eq}$: *X* value at equilibrium.

X^{excess}: excess part of *X*.

X^{id}: ideal part of *X*.

Mathematical operators

pr(X ≤ x): probability that variable *X* was lower or equal to value *x*.

s^2_X: variance estimate of *X*.

$\langle\ \rangle$: averaging on the sampled configurational space.

$\langle\ \rangle_T$: Boltzmann-weighted ensemble averaging on the sampled configurational space.

References

(1) Crank, J. *Mathematics of Diffusion*. 2nd Ed.; Oxford University: Oxford, 1979.

(2) Vieth, W. R. *Diffusion in and Through Polymers: Principles and Applications*; Oxford University: Oxford, 1991.

(3) Vergnaud, J. M. *Liquid Transport Processes in Polymeric Materials. Modelling and Industrial Applications*; Prentice Hall: Englewood Cliffs, 1991.

(4) Cussler, E. L. *Diffusion: Mass transfer in Fluid Systems*, 2nd Ed.; Cambridge University: Cambridge, 1997.

(5) Tosun, I. *Modeling in Transport Phenomena: a Conceptual Approach*, 2nd Ed; Elsevier Science & Technology: Amsterdam, 2007.

(6) Goydan, R; Schwope, A. D.; Reid, R. C.; Krishnamurthy, S.; Wong, K. Approaches to Predicting the Cumulative Permeation of Chemicals Through Protective Clothing Polymers. In *Performance of Protective Clothing: Second Symposium*; Mansdorf, S. Z., Sager, R., Nielson, A. P., Eds.; ASTM STP 989: ASTM Philadelphia, PA, 1988.

(7) Dunn, W. J., Block, J. H., Pearlman, R. S., Eds. *Partition Coefficients: Determination and Estimation*; Pergamon: New York, 1986.

(8) Sagiv, A. Theoretical Formulation of the Diffusion Through a Slab – Theory Validation. *J. membr. Sci.* **2002**, 199, 125-134.

(9) Lee, Y. M.; Bourgeois, D.; Belfort, G. Sorption, Diffusion and Pervaporation of Organics in Polymer Membrane. *J. Membr. Sci.* **1989**, 41, 161-181.

(10) Kohl, A.; Nielsen, R. *Gas Purification*. 5th Ed.; Gulf Publishing: Houston, 1997.

(11) DeLassus, P. T.;Tou, J. C.; Babinec, M. A.; Rulf, D. C.; Karp, B.K.; Howell, B. A. Transport of Applae Aromas in Polymer Films. In *Food and Packaging Interaction*; Hotchkiss, J. H., Ed.; American Chemical Society: Washington, DC, 1988.

(12) Bart, J. C. J. *Polymer Additive Analytics. Industrial Practice and Case Studies*; Firenze University: Firenze, 2006; Chapter 5, pp 249-316.

(13) Vitrac, O.; Hayert, M. Identification of Diffusion Transport Properties from Desorption/Sorption Kinetics: an Analysis Based on a New Approximation of Fick

Equation During Solid-Liquid Contact. *Ind. Eng. Chem. Res.* **2006**, 45, 7941-7956.

(14) European Community. Regulation (EC) No 1907/2006 of the European Parliament and of the Council of 18 December 2006 concerning the Registration, Evaluation, Authorisation and Restriction of Chemicals (REACH), establishing a European Chemicals Agency, amending Directive 1999/45/EC and repealing Council Regulation (EEC) No 793/93 and Commission Regulation (EC) No 1488/94 as well as Council Directive 76/769/EEC and Commission Directives 91/155/EEC, 93/67/EEC, 93/105/EC and 2000/21/EC. *Off. J. Eur. Union.* **2006**, L396, 1-849.

(15) European Community. Regulation (EC) No 1935/2004 of the European Parliament and of the Council of 27 October 2004 on materials and articles intended to come into contact with food and repealing Directives 80/590/EEC and 89/109/EEC. *Off. J. Eur. Union.* **2004**, L338, 4-17.

(16) European Community. Commission Directive 2002/72/EC of 6 August 2002 relating to plastic materials and articles intended to come into contact with foodstuffs. *Off. J. Eur. Communities.* **2002**, L220, 18-58.

(17) Vitrac, O.; Hayert, M. Risk Assessment of Migration from Packaging Materials into Foodstuffs. *AIChE J.* **2005**, 51, 4, 1080-1095.

(18) Vitrac, O., Challe, B., Leblanc, J.-C. and Feigenbaum, A. Contamination of Packaged Food by Substances Migrating from a Direct-Contact Plastic Layer: Assessment Using a Generic Quantitative Household Scale Methodology. *Food Addit. Contam*. **2007**. 24, 75-94.

(19) Vitrac, O.; Leblanc, J.-C. Exposure of Consumers to Plastic Packaging Materials: Assessment of the Contribution of Styrene from Yoghurt Pots. *Food Addit. Contam*. **2007**, 24, 194–215.

(20) Vitrac, O.; Hayert, M. Design of Safe Packaging Materials Under Uncertainty; In *New Trends Chemical Engineering Research*, Berton, L.P., Ed.; Nova Science: New York, 2007; pp 251-292.

(21) Reynier, A.; Dole, P.; Feigenbaum, A.; Humbel, S. Diffusion Coefficients of Additives in Polymers. I. Correlation with Geometric Parameters. *J. Appl. Polym. Sci*. **2001**, 82, 2422-2433.

(22) Reynier, A.; Dole, P.; Feigenbaum, A.; Humbel, S. Diffusion Coefficients of Additives in Polyolefins. II. Effect of Swelling and Temperature on the D = f(M) Correlation. *J. Appl. Polym. Sci*. **2001**, 82, 2434-2443.

(23) Vitrac, O.; Lézervant, J.; Feigenbaum, A. Application of Decision Trees to the Robust Estimation of Diffusion Coefficients in Polyolefines. *J. Appl. Polymer Sci*. **2006**, 101, 2167-2186.

(24) Vitrac, O.; Hayert, M. Effect of the Distribution of Sorption Sites on Transport Diffusivities: a Contribution to the Transport of Medium-Weight-Molecules in Polymeric Materials. *Chem. Eng. Sci*. **2007**, 62, 9, 2503-2521.

(25) Limm, W.; Hollifield, H.C. 1996. Modelling of Additive Diffusion in Polymers. *Food Addit. Contam*. **1996**, 13, 949-967.

(26) Baner, A. L.; Brandsch, J.; Frantz, R.; Piringer, O. The Application of a Predictive Migration Model for Evaluationg the Compliance of Plastic Materials with European Food Regulations. *Food Addit. Contam.* **1996**, 13, 587-601.

(27) Begley, T.; Castle, L.; Feigenbaum, A.; Frantz, R.; Hinrichs, K.; Liclmy, T.; Mercea, P.; Milana, M.; O'Brien, A.; Rebre, S.; Rijk, R.; Piringer, O. Evaluation of Migration Models that Might be Used in Support of Regulations for Food-Contact Plastics. *Food Addit. Contam*. **2005**, 22, 73-90.

(28) Baner, A. L.; Piringer, O. G. Prediction of Solute Partition coefficients Between Polyolefins and Alcohols Using the Regular Solution Theory and Group Contribution Methods. *Ind. Eng. Chem. Res.* **1991**, 30, 1506-1515.

(29) Hildebrand, J. H. *The Solubility of Non-Electrolytes*. Reinhold: New York, 1936

(30) Van Krevelen, D. W.; Hoftyzer, P. J. *Properties of Polymers: Their Estimation and Correlation with Chemical Structure*; Elsevier: Amsterdam, 1976.

(31) Barton, A. F. M. *CRC Handbook of Solubility Parameters and Other Cohesion Parameters*; CRC: Boca Raton, 1983.

(32) Lindvig, T.; Michelsen, M. L.; Kontogeorgis, G. M. A Flory-Huggins Model Based on the Hansen Solubility Parameters. *Fluid Phase Equilibr*. **2002**, 203, 247-260.

(33) Hansen, C. M. *Hansen Solubility Parameters. A User's Handbook, 2nd Ed.*; CRC: Boca Raton, 2007.

(34) Metropolis, N.; Rosenbluth A. W., Rosenbluth M. N., Teller A. H., Teller E. Equation of State Calculations by Fast Computing Machines. *J. Chem. Phys*. **1953**, 21, 1087-1092.

(35) Frenkel, D.; Smit, B. *Understanding Molecular Simulation. From Algorithms to Applications*; Academic press: New York, 2002; Vol. 1.

(36) Ben-Naim, A. *Molecular Theory of Solutions*; Oxford university: Oxford, 2006.
(37) Widom, B. Some Topics in the Theory of Fluids. *J. Chem. Phys*. **1963**, 39, 2808-2812.
(38) Boulougouris, G. C.; Economou, I. G.; Theodorou, D. N. Calculation of the Chemical Potential of Chain Molecules Using the Staged Particle Deletion Scheme, *J. Chem. Phys*. **2001**, 115, 8231-8237.
(39) Kirkwood, J. Statistical Mechanics of Fluid Mixtures. *J. Chem. Phys*. 1935, 3:300-313.
(40) van der Vegt, F. F. A.; Briels, W. J. Efficient Sampling of Solvent Free Energies in Polymers. *J. Chem. Phys*. **1998**, 109, 7578-7582.
(41) Hess, B.; Peter, C.; Ozal, T.; van der Vegt, N. F. A. Fast-Groth Thermodynamic Integration: Calculating Excess Chemical Potentials of Additive Molecules in Polymer Structures. *Macromol*. **2008**, 41, 2283-2289.
(42) Özal, T.; Peter, C.; Hess, B.; van der Vegt, N. F. A. Modeling Solubilities of Additives in Polymer Microstructures: Single-Step Perturbation Method Based on a Soft-Cavity Reference State. *Macromol*. **2008**. 41, 5055-5061.
(43) Nath, S. K.; Banaszak, B. J.; de Pablo, J. J. Simulation of Ternary Mixtures of Ethylene, 1-Hexene, and Polyethylene, *Macromol*. **2001**, 34, 7841-7848.
(44) Piringer, O. G.; Baner, A. L. *Plastic Packaging Materials for Food. Barrier Function, Mass Transport, Quality Assurance, and Legislation*; Wiley-VCH Verlag GmbH: Germany, 2000.
(45) Vitrac, O.; Mougharbel, A.; Feigenbaum, A. Interfacial Mass Transport Properties Which Control the Migration of Packaging Constituents into Foodstuffs. *J. Food Eng.* **2007**, 79, 3, 1048-1064
(46) Huggins M. L. Derivation of Molecular Relaxation Parameters of an Isomeric Relaxation. *J. Chem. Phys.* **1942**, 46, 151-153.
(47) Flory P. J. Thermodynamics of High Polymer Solutions. *J. Chem. Phys*. **1942**. 10, 51-61.
(48) Luettmer-Strathmann, J.; Schoenhard, J. A.; Lipson, J. E. G. Thermodynamics of n-alkane Mixtures and Polyethylene-n-Alkane Solutions: Comparison of Theory and Experiment, *Macromol*. **1998**, 31, 9231-9237.
(49) Elbro, H. S.; Fredenslund, Aa; Rasmussen, P. A New Simple Equation for the Prediction of Solvent Activities in Polymer Solutions, *Macromol*. **1990**, 23, 4707-4714.
(50) Bawendi, M. G.; Freed, K. F.; Mohanty, U. A Lattice Model for Self-Avoiding Polymers with Controlled Length Distributions. II. Corrections to Flory-Huggins Mean Field. *J. Chem. Phys*. **1986**, 84, 7036-7047.
(51) Bawendi, M. G.; Freed, K. F.; Mohanty, U. A Lattice Field Theory for Polymer Systems with Nearest-Neighbor Interaction Energies. *J. Chem. Phys*. **1987**, 87, 5534-5540.
(52) Bawendi, M. G.; Freed, K. F. Systematic Corrections to Flory-Huggins theory: Polymer-Solvent-Void Systems and Binary Blend-Void Systems. *J. Chem. Phys*. **1988**, 88, 2741-2756.
(53) Sariban, A.; Binder, K. Critical Properties of the Flory–Huggins Lattice Model of Polymer Mixtures. *J. Chem. Phys*. **1987**, 86, 5859-5873.
(54) Schweizer, K. S.; Curro, J. G. Microscopic Theory of the Structure, Thermodynamics, and Apparent χ Parameter of Polymer Blends. *Phys. Rev. Lett*. **1988**, 60, 809-812.
(55) Panagiotopoulos, A. Z. Direct Simulation of Fluid Phase Equilibria by Simulation in the Gibbs Ensemble: A Review, *Mol. Simul.* **1992**, 9, 1-23.
(56) Bart, J. C. J. *Physical Chemistry of Additives in Polymers*; Firenze University: Firenze, Italy, 2006.
(57) Flory, P. J. Thermodynamics of High Polymer Solutions. *J. Chem. Phys.* **1941**, 9, 660-661.
(58) Huggins, M. L. Theory of Solutions of High Polymers. *J. AM. Chem. Soc.* **1942**, 64, 1712-1719.
(59) Fill, K. A., Bromberg S. *Molecular Driving Forces: Statistical Thermodynamics in Chemistry and in Biology*. Garland Science: New-York, 2003; Chapter 31, pp593-608.
(60) Poling, B. E.; Prausnitz, J. M.; O'Conell J. P. *The Properties of Gases and Liquids, 5th Ed.*; McGraw-Hill: New-York, 2004; Chapter 4, pp4-1-4-52.
(61) Lichtenthaledre, R. N., Abrams, D. S. Prausnitz J. M. Combinatorial Entropy of Mixing for Molecules Differing in Size and Shape. *Can. J. Chem*. **1973**, 51. 3071-3080.
(62) Silla, E.; Arnau, A.; Tuñón, I. Solvent Effects on Chemical Systems. In *Handbook of Solvents*; Wypych, I., Ed; ChemTec: Toronto, 2001; pp 7-63.
(63) Klenin, V. J. *Thermodynamics of Systems Containing Flexible-Chain Polymers*; Elsevier Science: Amsterdam, 1999.
(64) Chalikian, T.V. Structural Thermodynamics of Hydration. *J. Phys. Chem*. **2001**, B 105, 12566-12578
(65) Fan., C. F.; Olafson, B. D.; and Blanco, M.; Hsu, S. L. Application of Molecular Simulation to Derive Phase Diagrams of

Binary Mixtures, *Macromol*. **1992**, 25, 3667-3676.
(66) Lide, D. R., Ed. *CRC Handbook of Chemistry and Physics*; CRC: Boca Raton, 2006.
(67) Peters, M. H. *Molecular Thermodynamics and Transport Phenomena. Complexities of Scales in Space and Time*; McGraw-Hill: New-York, 2005; Chapter 4, pp77-137.
(68) Gillespie, R. J.; Popelier, P. L. A. *Chemical Bonding and Molecular Geometry. From Lewis to Electron Densities*; Oxford university: New York, 2001.
(69) Saiz, L.; Padro, J. A.; Guardia, E. Dynamics and Hydrogen Bonding in Liquid Ethanol. *Molec. Phys.* **1999**, 97, 897-905.
(70) Van Krevelen, D.W. *Cohesive Properties and Solubility. Properties of Polymer, the Correlation with Chemical Structure; their Numerical Estimation and Prediction from Additive Group Contributions*, 3rd edition, Elsevier: Amsterdam), 1990; pp 189-225.

Prediction of partition coefficients of plastic additives between packaging materials and food simulants

Guillaume Gillet[a,b], *Olivier Vitrac**[c], *Stéphane Desobry*[b]
(a) Laboratoire National de métrologie et d'Essais, Centre Energie, Matériaux et Emballage, 29 avenue Roger Hennequin, 78197 Trappes CEDEX, France.
(b) Nancy Université, LSGA-ENSAIA-INPL, 2 avenue de la forêt de Haye, BP 172, 54505 Vandoeuvre lès Nancy, France.
(c) Institut National de la Recherche Agronomique, UMR 1145 Génie Industriel Alimentaire, 1 avenue des Olympiades, 91300 Massy, France
* Corresponding author: olivier.vitrac@agroparistech.fr

Partition coefficients, $K_{i,F/P,}$ between liquids, F, and amorphous regions of polymers, P, are important quantities to predict the sorption or desorption kinetics in various areas and in particular to predict the contamination of food by substances originating from food contact materials. This work extends an atomistic Flory-Huggins approach previously developed by us to predict $K_{i,F/P}$ values for large solutes such as antioxidants, light stabilizers and surface agents. Two extensions were particularly considered. To predict accurately the contribution of the positional entropy in F, molar volumes were determined by isobaric molecular simulations in liquids with increasing electric dipolar moment (isopropanol, ethanol, methanol, ethyl acetate, water). It was found to be higher than the molar volume and almost independent of the considered alcohol. A simple estimator was therefore proposed as the volume enclosed within the surface accessible to hydrogen atoms. The effect of conformers in poor solvent was in particular highlighted. The last improvement concerned the extension of the whole methodology to water and water-ethanol mixtures, while including non-idealities. Intrinsic limitations of the Flory-Huggins approximation to handle hydrogen bond cooperativity were overcame by reweighting contact energies in water and by introducing tabulated properties of water-ethanol mixtures. All predictions agreed well previously published partitioning data as well as those generated by this study. From experimental values and theoretical conditions, the possibility to predict the contamination of food emulsions with water-ethanol mixtures is finally discussed.

KEYWORDS: thermodynamics, polymer, desorption, chemical potential, Flory-Huggins theory

1. Introduction

In Europe, all materials intended to be in contact with food must comply with the recently introduced framework regulation 2004/1935/EC[1] specific for food contact materials, which enforces a safety assessment and risk management decision for all starting substances and possible degradation products coming from the material. For plastic materials, article 14 of the directive 2002/72/EC[2] allows the use of mathematical modeling of desorption to demonstrate the compliance of these materials according to the specific migration limits (SML). Due to toxicological concern, among the 937 substances (including 340 monomers and 597 additives) positively listed in EU directives on plastics in contact with food[3], 502 substances (including 230 monomers and 272 additives) are subjected to migration limits. As a result, the development of migration modeling is expected to contribute significantly to an increase of the safety of food products, while reducing significantly the cost of this

safety. In other related areas, the recently introduced EU regulation on the safety of chemicals, so-called REACH directives[4], encourages the development of similar predictive approaches to assess the migration of chemicals into the environment or through the food chain. The principles of robust desorption modeling in presence of uncertainty on composition, contact condition and physicochemical properties has been detailed for monolayer and multilayer materials[5]. In particular, probabilistic modeling[6] has been applied to evaluate the contamination of 12 retailed food products by a ubiquitous antioxidant[7] and to assess the exposure of French consumers to styrene originating from yogurt pots[8]. It is argued that a similar methodology could be used by all involved stakeholders (packaging industry, food industry, regulation authorities, food safety agencies…) and updated according to the information available and the followed objective: compliance testing, tier assessment, sanitary survey... Its dissemination and application to a wide range of substances, contact conditions (temperature, interactions with food) and materials (monolayer and multilayer materials, active materials) is currently limited by either the span of confidence intervals or safety margins mainly due to a large uncertainty on the partitioning of plastic additives with food or food simulants. Indeed, several predictive estimators of diffusion coefficients of additives including uncertainty estimates have been proposed for common polymers such as polyolefins[9-13] but only rough approximations have been proposed to predict their chemical affinity for common food simulants. The current "practical guide" for the application of European directives[14] advises that the concentrations at equilibrium are equal between the contact material and a fatty product whereas they are 10^3 times lower when the same material is in contact with an aqueous food. No recommendation is proposed to estimate partition coefficients between layered materials. The complications in measuring partitioning of plastic additives such as hindered phenolic antioxidants or hindered amine light stabilizers arise for their low affinity for polar media (food simulant or polymer) and to their possible reactivity during migration or extraction[15]. Alternative methods based on the prediction of activity coefficients are scarce and rarely applied to molecules as large as polymeric plastic additives. Group contribution methods and other semi-empirical methods have been recently reviewed[16]. The most extensive study was performed by Baner *et al*[17] and concerned volatiles and solutes with intermediate molecular weights. By mixing both the regular solution theory and a Flory-Huggins approach, a correlation model was proposed for partition coefficients between polyethylene materials and alcohols. Because the introduced correction factor was dependent on the size and the shape of the solute, the approach cannot however be extended reliably to plastic additives.

To overcome previous limitations, we recently devised an off-lattice generalized Flory-Huggins approach at atomistic scale to predict without any adjustment the partition coefficient of solutes, noted K, between the amorphous phase of a polyolefin, noted P, and a liquid simulant[18], noted F. As in the original Flory-Huggins approach, the interactions with P are accounted only with the neighbors in contact so that an explicit representation of the entangled polymer is not required. A similar approach has been applied to assess the activity coefficient in F. The total cost of the method was low since the distributions of interactions were calculated on molecule pairs and averaged over the number of neighbors. Since a full detailed forcefield at atomistic scale was applied, the method is expected to be applicable to any molecule (of solute, of P or of F) even if they generate strong attractive interactions such as hydrogen bonding. The method was satisfactory

applied to all molecules analyzed by Baner *et al.*[17], to series of flexible molecules (n-alkanes and n-alcohols) and to two prototypes of phenolic antioxidants, with a prediction error of a same magnitude order as the overall experimental error. Additionally, the simulations demonstrated that even if low polar molecules including plastic additives have by design a good solubility in P, they have also a significant chemical affinity for polar simulants such as small alcohols (methanol, ethanol). This effect, which was neglected in previous studies, was related to the significant contribution of the positional entropy in liquids consisting of molecules much smaller than the solute. Its contribution was associated to the size of the cavity to insert the solute and equivalently to the number of F molecules to be rearranged when the solute *i* was displaced; it was denoted $r_{i,F}^{-1}$. Only rough estimates of $r_{i,F}^{-1}$ were suggested with values ranged between the hardcore volume and the molar volume of *i*. For large additives with a melting point much higher than the common migration temperature (i.e. 40°C), both bounds seem particularly unrealistic as they correspond respectively to a state where all the van-der-Waals surface of the solute is in contact with F and to an ordered state. Besides, this description in interacting liquids neglected non-ideal effects associated to the perturbation of the network of hydrogen bonds around the solute.

The current work extends the previous study to large hindered antioxidants and analyzes the tradeoff between the size and polarity of different F molecules, including: isopropanol, ethanol, methanol and water. Since hydrolysis avoids direct measurements of *K* in water, the predictions will be compared with different mixtures of ethanol in water. It is emphasized that the mixture 50:50 v/v water and ethanol is also the new food simulant, which has been proposed to assess the migration of plastic additives in milk[19], after a significant amount of a photoinitiator (2-isopropylthioxanthone) for printing inks has been found in baby milk[20] and of other packaged drinks[21]. In presence of long range Coulombic interactions, our approach based on Flory-Huggins theory was however expected to minimize significantly the contribution of hydrogen bonding because: only molecules in contact could interact and a single molecule participated at maximum in two long-lived hydrogen bonds through a head and tail arrangement pattern. A number of hydrogen-bonded neighbors ranged between 1 and 2 was acceptable for ethanol[22] but was unrealistic for water, where a single molecule is involved in up to 6 hydrogen bonds[23]. We extended our approach by including a geometrical model of water derived from the 5 sites transferable intermolecular potential function[24]. This description was shown to be able to predict various properties of liquid water[25].

The paper is organized as follows. Section 2 recapitulates the theoretical principles of calculation of *K* from a Monte-Carlo sampling of pair contact interactions at atomistic scale. Section 3 details the experimental and simulation conditions that were used to generate reference data and predictions. The computational cost associated to direct calculations of partial molar volumes of additives in several simulants by isobaric molecular dynamics simulations was in particular significantly reduced by comparing with their volumes enclosed to surface accessible to hydrogen atoms. Section 4 summarizes the predictions of *K* in all tested conditions for large plastic additives. The improvements induced by new $r_{i,F}^{-1}$ estimates were analyzed against *K* values previously collected for homologous series of solutes[15,26]. Previous allegations of partitioning of additives in water and in water-ethanol mixtures were discussed according to a sensitivity analysis to non-idealities and according to experimental values generated by this study in mixtures and the values

extrapolated by Gandek[27] in pure water. Section 5 summarizes the findings and suggests how the current predictions could be used to assess consumer exposure to ubiquitous hindered phenolic antioxidants and to select an appropriate food simulant of aqueous food for compliance testing.

2. Theory

2.1. Definition of partition coefficients

Since the diffusion of a solute *i*, such as a plastic additive, requires the cooperative motions of the polymer[28], the substance *i* is assumed to diffuse only in the amorphous phase of the polymer. The partition coefficient between F and the amorphous phase of the polymer, P, denoted $K_{i,\mathrm{F/P}}$, is assessed as[18]:

$$K_{i,F/P} = \frac{C_{i,F}\big|_{eq}}{C_{i,P}\big|_{eq}^{a}} = (1-c)\cdot\frac{\hat{C}_{i,F}\big|_{eq}}{\frac{1}{a_i}\cdot\hat{C}_{i,P}\big|_{eq} - b_i\cdot C_{i,P}\big|_{t=0}} \quad (1)$$

where $C_{i,F}\big|_{eq}$ and $C_{i,P}\big|_{eq}^{a}$ are the concentrations at equilibrium in F and P respectively. $\left\{\hat{C}_{i,k}\big|_{eq}\right\}_{k=F,P}$ are the corresponding concentrations as experimentally-assessed. The concentration in P is in particular associated with a concentration yield a_i lower than 1. In addition, since large additives have a melting point much higher than the extrusion temperature of polyolefins, Eq. (1) takes also into account that a significant fraction b_i of the initial additives content, $C_{i,P}\big|_{t=0}$, could be crystallized and does not participate to the apparent equilibrium due to kinetic limitations. c is the crystallinity of the polymer (volume fraction of crystalline phase), which varies according to the considered sample.

2.2. Partition coefficient estimates in alcohols

According to the Flory-Huggins theory[29-32], the activity coefficients relative to volume fractions in solute, denoted $\{\gamma^{v}_{i,k}\}_{k=\mathrm{P,F}}$, can be derived on a rigid lattice, whose mesh size is commensurable to the volume of the penetrant V_i. In this work, we used a similar approach without lattice by sampling explicitly at atomistic scale the molecular pair interactions. The method was similar as the one used in our previous work[18]. By neglecting the sampling biases as discussed previously[18], $K_{F/P}$ was approximated as:

$$\begin{aligned}\ln K_{F/P} = \ln\gamma^{v}_{i,P} - \ln\gamma^{v}_{i,F} = &\underbrace{r_F^{-1}}_{\substack{enthalpic\\ contribution}} + \underbrace{\chi^{H}_{i,P} - \chi^{H}_{i,F}}_{\substack{entropic\\ contribution}} \\ \approx &\frac{1}{2k_BT}\Big[\big(\langle z_{i+P}\rangle + \langle z_{P+i}\rangle\big)\cdot\langle\varepsilon_{i+P}\rangle_T \\ &-\big(\langle z_{i+F}\rangle + \langle z_{F+i}\rangle\big)\cdot\langle\varepsilon_{i+F}\rangle_T \\ &-\langle z_{P+P}\rangle\cdot\langle\varepsilon_{P+P}\rangle_T \\ &+\langle z_{F+F}\rangle\cdot\langle\varepsilon_{F+F}\rangle_T\Big] + r_{i,F}^{-1}\end{aligned} \quad (2)$$

$\left\{\chi^{H}_{i,k}\right\}_{k=P,F}$ is the Flory-Huggins parameter, k_B is the Boltzmann constant, T is the absolute temperature. The enthalpies associated to all binary mixtures P+*i*, F+*i*, P+P and F+F were calculated as the product of the average number of neighbors, $\{z_{A+B}\}_{A,B=i,\mathrm{F,P}}$, times the average enthalpy associated to a single pair $\{\varepsilon_{A+B}\}_{A,B=i,\mathrm{F,P}}$ at the temperature T. The temperature was chosen comparable to the one used in reference data, commonly 313 K as prescribed in EU regulation[2]. $\langle\ \rangle$ and $\langle\ \rangle_T$ are the average operator and the temperature ensemble average operator respectively. The latter was obtained by weighting the sampled distribution of energies $p_{A+B}(\varepsilon)$ with the Boltzmann factor, defined as $\exp(-\varepsilon/k_B\cdot T)$:

$$\langle\varepsilon_{A+B}\rangle_T = \frac{\int_{-\infty}^{+\infty} p_{A+B}(\varepsilon)\cdot e^{-\frac{\varepsilon}{k_B\cdot T}}\cdot\varepsilon\cdot d\varepsilon}{\int_{-\infty}^{+\infty} p_{A+B}(\varepsilon)\cdot e^{-\frac{\varepsilon}{k_B\cdot T}}\cdot d\varepsilon} \quad (3)$$

The sampling of $p_{A+B}(\varepsilon)$ was based on a large conformers set of *A* (seed molecule) and *B* (contact molecule) representative of their condensed state (up to 10^4 configurations) and based on all possible contacts of their van der Waals envelopes with spherical symmetric probability (up to

10^{11} configurations). As previously discussed[18], contacting was performed either by expansion or contraction to avoid an oversampling of cavities in large or flexible molecules. An infinite long polymer was simulated by replacing with an oligomer, where head and tail atoms were non-contact. For each solute, the optimal number of monomers was set to minimize the overestimation of non-contact "head and tail effects" while preserving the overall convergence of the sampling. It was demonstrated that the overall bias was minimal when the test oligomer was commensurable to the solute[18].

The choice of V_i controls in particular the magnitude of the entropic contribution in F, denoted $r_{i,F}^{-1}$, and defined as the ratio between V_i and the molar volume of F. The van-der-Waals volume and the molar volume were proposed as likely bounds of the true size of the cavity to insert a solute *i* in F[18]. In this work, we introduce the partial molar volume of *i* in F, V_i^P, and the volume accessible to protons, V_i^H, to calculate more accurate estimates of $r_{i,F}^{-1}$. In particular, it was argued that close contacts between *i* and F were performed via hydrogen atoms of F rather than by any other heavy atoms.

2.3. Partition coefficient estimates in water and in ethanol-water mixtures

The estimate of $\gamma_{i,F}^{v}$ introduced in Eq. (2) is only valid in binary mixtures. The extension of the Flory-Huggins theory to ternary mixtures, including a solute *i* and a simulant with two components F_1 and F_2, leads to a bilinear equation system[33-35]. We a used a formulation similar to[35] with an equivalent lattice size equal to the van-der-Waals volume of the solute, V_i^{vdw}. This assumption was consistent with our off-lattice sampling of pair interactions. The non-ideal character of the water-ethanol mixture was considered by taking into account the partial molar volume of F_1 and F_2, $V_{F_1}^P$ and $V_{F_2}^P$ respectively. The excess in chemical potential was consequently expressed as:

$$\begin{aligned}\ln\gamma_{i,F_1+F_2}^{v} &= (1-\phi_i) - r_{i,F_1}^{-1}\cdot\phi_{F_1} - r_{i,F_2}^{-1}\cdot\phi_{F_2} \\ &+\left[\left(\chi_{i,F_1}\cdot\phi_{F_1}+\chi_{i,F_2}\cdot\phi_{F_2}\right)\cdot\left(\phi_{F_1}+\phi_{F_2}\right)\right] \\ &-\chi_{F_1,F_2}\cdot\left(\frac{V_i^{vdw}}{V_{F_2}^P}\right)\cdot\phi_{F_1}\cdot\phi_{F_2} \\ &-h_i\cdot h_{F_2}\cdot\phi_{F_2}\cdot\left(\frac{d\chi_{i,F_2}}{dh_{F_2}}\right) \\ &-\phi_i\cdot\phi_{F_1}\cdot\phi_{F_2}\cdot\left(\frac{\partial\chi_{i,F_1}}{\partial\phi_{F_2}}\right) \\ &-\phi_i\cdot\phi_{F_1}^2\cdot\left(\frac{\partial\chi_{i,F_1}}{\partial\phi_{F_2}}\right)-\phi_i\cdot\phi_{F_1}^2\cdot\left(\frac{\partial\chi_{i,F_1}}{\partial\phi_{F_1}}\right) \\ &-\left(\frac{V_i^{vdw}}{V_{F_2}^m}\right)\cdot\phi_{F_1}\cdot\phi_{F_2}^2\cdot\left(\frac{\partial\chi_{F_1,F_2}}{\partial\phi_{F_2}}\right) \\ &-\left(\frac{V_i^{vdw}}{V_{F_2}^P}\right)\cdot\phi_{F_1}^2\cdot\phi_{F_2}\cdot\left(\frac{\partial\chi_{F_1,F_2}}{\partial\phi_{F_1}}\right) \\ &-\phi_i\cdot\phi_{F_1}^2\cdot\phi_{F_2}\cdot\left(\frac{\partial\chi_{i,F_1,F_2}}{\partial\phi_{F_1}}\right) \\ &-\phi_i\cdot\phi_{F_1}\cdot\phi_{F_2}^2\cdot\left(\frac{\partial\chi_{i,F_1,F_2}}{\partial\phi_{F_2}}\right) \\ &-\chi_{i,F_1,F_2}\cdot\phi_{F_1}\cdot\phi_{F_2}\cdot\left(1-2\phi_i\right)\end{aligned} \quad (4)$$

where $\{\phi_k\}_{k=i,F_1,F_2}$ is the volume fraction in *k* in the mixture so that $\phi_i+\phi_{F_1}+\phi_{F_2}=1$; $h_i=\phi_i/\left(\phi_i+\phi_{F_2}\right)$ and $h_{F_2}=\phi_{F_2}/\left(\phi_i+\phi_{F_2}\right)$. At infinite dilution in solute *i*, $\phi_i\to 0$, the ternary Flory-Huggins interaction parameter χ_{i,F_1,F_2} was reasonably supposed negligible. The entropic contribution was related to the size of the cavity to insert the solute *i* in F_1 and in F_2, $r_{F_1}^{-1}$ and r_{F2}^{-1} respectively.

By noticing that $\phi_{F_1}\approx\left(1-\phi_{F_2}\right)$ when $\phi_i\approx 0$, the practical estimate of $K_{F,\mathrm{P}}$ was finally rearranged as a third degree polynomial in ϕ_2, while separating enthalpic and entropic (related to positions) contributions:

$$\ln K_{i,(F_1+F_2)/P} = 1 + \chi_{i,P} - \ln \gamma^{v}_{i,F_1+F_2} \approx$$
$$\underbrace{-2\frac{V_i^{vdw}}{V_{F_2}^{P}}\frac{\partial \chi_{F_1,F_2}}{\partial \phi_{F_2}}}_{enthalpic}\cdot \phi_{F_2}^3$$
$$+\underbrace{\frac{V_i^{vdw}}{V_{F_2}^{P}}\cdot\left(\chi_{F_1,F_2}+3\frac{\partial \chi_{F_1,F_2}}{\partial \phi_{F_2}}\right)}_{enthalpic}\cdot \phi_{F_2}^2$$
$$+\left(\underbrace{r_{i,F_2}^{-1}-r_{i,F_2}^{-1}}_{entropic}+\underbrace{\chi_{i,F_1}-\frac{V_i^{vdw}}{V_{F_2}^{P}}\chi_{i,F_2}}_{enthalpic}\right.$$
$$\left.+\underbrace{\frac{V_i^{vdw}}{V_{F_2}^{P}}\chi_{F_1,F_2}-\frac{V_i^{vdw}}{V_{F_2}^{P}}\frac{\partial \chi_{F_1,F_2}}{\partial \phi_{F_2}}}_{enthalpic}\right)\cdot \phi_{F_2}$$
$$+\underbrace{r_{i,F_1}^{-1}}_{entropic}+\underbrace{\chi_{i,P}-\chi_{i,F_1}}_{enthalpic} \quad (5)$$

Eq. (5) is continuous in ϕ_{F_2}, with values equal to $r_{F_1}^{-1}+\chi_{i,P}-\chi_{i,F_1}$ and $r_{F_2}^{-1}+\chi_{i,P}-\chi_{i,F_2}$ for binary mixtures corresponding to $\phi_{F_2}=0$ and $\phi_{F_2}=1$ respectively. It is emphasized that the nonlinear terms depend only on enthalpic contributions of F_1 and F_2, that is related to the non ideal character of the mixture F_1 and F_2. Since the water-ethanol mixture is known to be non ideal, $\ln K_{i,(F_1+F_2)/P}$ was expected to be a nonlinear function of the concentration in ethanol. To avoid an overestimation of nonlinearities, the properties of water-ethanol were derived from literature data and models instead to be estimated with molecular simulation. Flory-Huggins interaction parameter between water and ethanol, $\chi_{water,ethanol}$, was derived from the polynomial approximation of molar heat of mixing, $\Delta H^{m}_{water+ethanol}$, proposed in[36] via:

$$\chi_{water,ethanol} = x_{ethanol}\cdot(1-\phi_{ethanol})\cdot\frac{\Delta H^{m}_{water+ethanol}}{RT} \quad (6)$$

where $x_{ethanol}$ and $\phi_{ethanol}$ are the molar fraction and the volume fraction in ethanol respectively. R is the universal gas

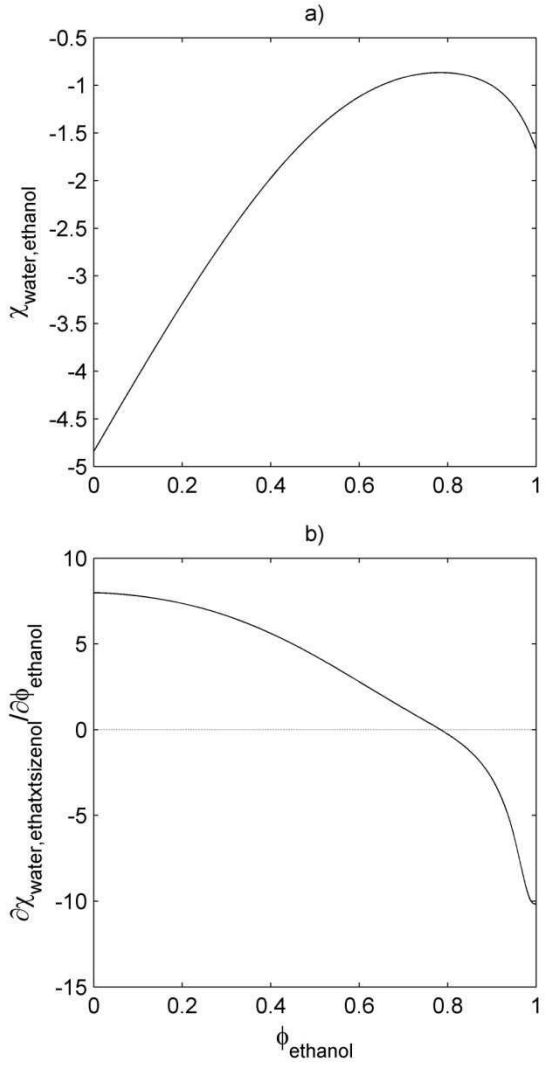

Fig. 1. Flory-Huggins interaction parameter between water and ethanol: a) polynomial model derived from heat of mixing at 25°C[36]; b) its derivative with $\phi_{ethanol}$.

constant. As depicted in Fig. 1, $\chi_{water,ethanol}$ was found to vary nonlinearly between -4.8 and -0.87 with an average value, $\int_0^1 \chi_{water,ethanol}\cdot d\phi_{ethanol}$, about -2. By choosing F_2=ethanol and a constant $\chi_{water,ethanol}$ equal to is average, Eq. (5) becomes a second degree polynomial in $\phi_{ethanol}$ the second degree term in Eq. (5) predicts a convex variation of $\ln K_{i,(F_1+F_2)/P}$ with $\phi_{ethanol}$. In particular, it is highlighted that the decrease of $\ln K_{i,(F_1+F_2)/P}$ with $\phi_{ethanol}$ was expected to be higher in a mixture enriched in ethanol. In this work, additional nonlinearities were accounted

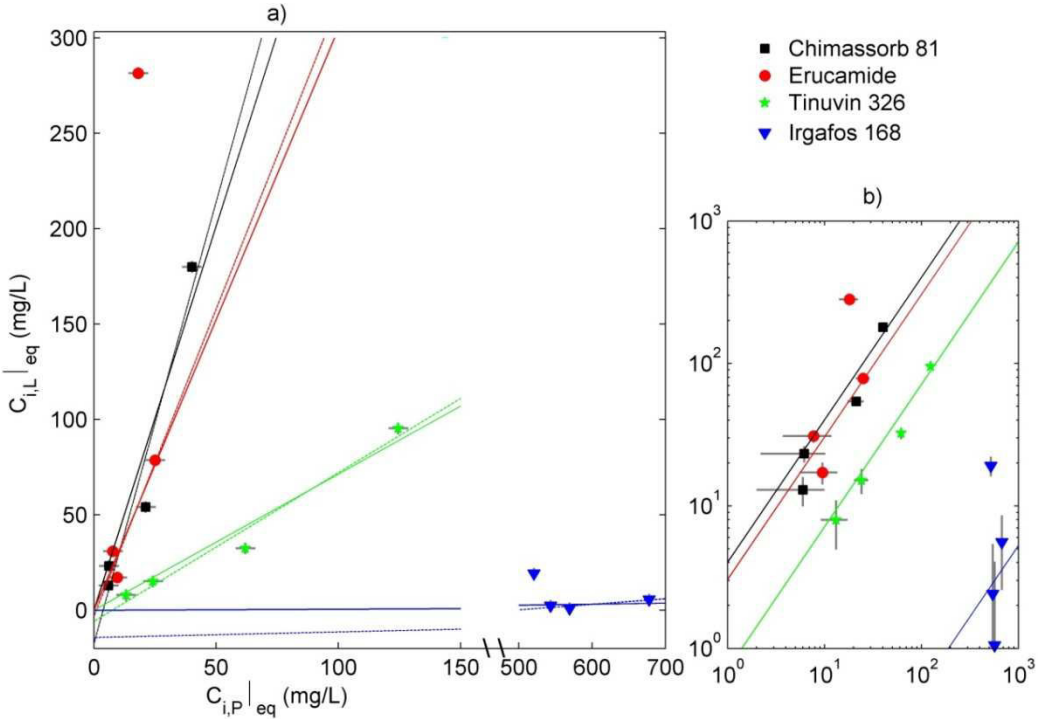

Fig. 2. Desorption isotherms of typical additives in ethanol 95%: a) linear scale; b) log-log scale. Vertical and horizontal bars represent 95% confidence intervals due to experimental errors. The regression line with zero intercept and the normal regression line are plotted in continuous and dashed line respectively. Outliers are removed from the regression for Erucamide and Irgafos 168.

Table 1. Main characteristics of additives.

Additive	CAS number	V_i^{vdw} (Å^3)	V_i^M (Å^3)	Melting range (°C)	b_i (%)
Irganox 1076	2082-79-3	647 ±12	949	50-55[e]	0.002
Irganox PS802	00693-36-7	850 ± 30	1235	64-67	0
Irgafos 168	31570-04-4	747 ± 3	1043	183-186	0.03
Chimassorb 81	01843-05-6	344 ± 2	508	48-49	0.007
Tinuvin 326	03896-11-5	285 ± 3	416	138-141	0.008
Erucamide	00112-84-5	424 ± 6	642	79	0

V_i^M was calculated at 313K with densities from CAS database; Melting ranges were obtained from technical datasheet of products; b_i were estimated with results of Fig. 2.

by introducing for each water-ethanol mixture an estimate of $\partial\chi_{water,ethanol}/\partial\phi_{ethanol}$ (Fig. 1b) and $V_{ethanol}^P$ values derived from experimental densities of water-ethanol mixtures[37]. Non-idealities were also integrated in entropic terms by calculating r_{i,F_1}^{-1} and r_{i,F_2}^{-1} with partial molar volumes of F_1 and F_2, instead of their molar volumes.

By choosing F_1=water, the interaction between solute and water, $\chi_{i,water}$ was inferred almost similarly as $\chi_{i,ethanol}$. Nevertheless, hydrogen bond cooperativity could not be sampled, because our generalized Flory-Huggins formulation averaged interactions only between dimers of water and not on the likely structure of liquid water at room temperature involving

tetramers[38]. In other words, the current Monte-Carlo method allowed only random contacts (i.e. with no preferred orientations) but not long-lived contacts as it should be assessed in the bulk. Indeed, the lifetime of hydrogen bonds in bulk water was estimated between 10^{-12} s and $20 \cdot 10^{-12}$ s, while the lifetime of broken hydrogen bonds was about 10^{-13} s[39]. To extend naturally the current formulation, a tetrahedral coordination of pair interactions, derived from the TIP5P forcefield[24], was introduced. By neglecting the number of "dangling" hydrogen bonds, a factor ¼ was expected between the conventional sampled potential energy $\langle z_{water+water} \rangle \cdot \langle \varepsilon_{water+water} \rangle_T$ and the true one:

$$\chi_{i,water} \approx \frac{1}{2k_BT} \cdot \left[\left(\langle z_{i+water} \rangle + \langle z_{water+i} \rangle \right) \cdot \langle \varepsilon_{i+water} \rangle_T - \langle z_{i+i} \rangle \cdot \langle \varepsilon_{i+i} \rangle_T - 4 \cdot \langle z_{water+water} \rangle \cdot \langle \varepsilon_{water+water} \rangle_T \right] \quad (7)$$

It is emphasized that an almost similar derivation can be derived with the conventional Flory-Huggins description on a 3D cubic lattice. On a 3×3×3 lattice, a seed molecule is in direct contact with 6 neighbors (lattice coordination number) and surrounded by 3^3-1=26 molecules with possible long range interactions. The discrepancy between a short-range sampling and a long-range sampling of interactions is about 6/26≈1/4.33. From these considerations, water in clusters appeared as a prototype of branched molecules, whose interactions on a lattice are discussed in[40].

Eq. (7) made it possible the use of the same computational procedure for all solutes and simulants including water.

3. Materials and methods

3.1. Polymer formulation

Plastic additives were provided by CIBA (Basel, Switzerland) except for Erucamide, which was obtained from CRODA (Vimodrone, Italy). Their main characteristics are summarized in Table 1. Virgin high density polyethylene (PE) was obtained from ATOCHEM (Paris, France). Dried polymer flakes were formulated with the 6 tested additives during a first extrusion step prior to final processing at semi-industrial scale. Both extrusions were performed at 200°C in bi-screw extruder (model BC-21 Clextral, France) and the material was finally calendered as 0.15 m wide ribbons. The final density and the crystallinity were of 940 $kg \cdot m^{-3}$ and 70 % respectively, with a melting point of 136°C.

3.2. Experimental determination of partition coefficients

Partition coefficients of 6 plastic additives were assessed by putting 10 cm^3 of polymer samples cut in small 5mm×5mm pieces in contact with 100 ml of simulant. Tested simulants included isopropanol (SIGMA-ALDRICH, USA) and 3 mixtures of ethanol (MERCK, Germany) and water (MilliQ water, MILLIPORE, USA) with volume fractions of 95%, 75% and 50%.

The amount of non-desorbable substances, denoted b_i in Eq. (1), was estimated from the intercept of desorption linear isotherm (expressing the concentration in P versus the concentration in F) obtained with different volume ratios of ethanol:P (50, 35, 20, 10, 5).

3.3. Extraction of additives from polymer materials

Initial concentrations, $C_{i,P}|_{t=0}$, and residual concentrations after contact, $C_{i,P}|_{eq}$, were assessed after pressurized solid-liquid extraction (model ASE 200, Dionex, USA) in a 75:25 v/v mixture of isopropanol-dichloromethane at 105°C and 10.3 MPa. The protocol was similar to the one described by Coulier et al.[41] and applied to 600 mg of samples mixed with sand in 11 ml extraction cells. Two static cycles of 15 min each were applied to achieve complete extraction. To prevent the degradation of additives during extraction, 100 ppm ($\mu L \cdot L^{-1}$) /L of tri-

ethylphosphite (Sigma-Aldrich, USA) was added to solvents. It was verified that this methodology gave similar results than extraction by reflux during 40 h.

3.4. Concentration measurements of additives in solvents and simulants

The 6 additives were separated and detected either using High Performance Liquid Chromatography (HPLC) associated to an UV Diode Array Detector (DAD) and an Evaporative Light Scattering Detector (ELSD) in series or using Gaz Chromatography (GC) associated to a flame ionization detector (FID). ESLD was only applied to PS802. GC was not applied to Irganox 3114 due to its insufficient volatility. The HPLC protocol was similar to the one described by Garrido-López et al.[42]. The HPLC system consisted in a Waters 717plus autosampler, a Waters 600 controller equipped with a thermostatted column compartment and an in-line degasser AF (Waters, USA). Separation was achieved on a Xterra C8 column (150mm×3.0mm; 5µm particles; Waters , USA) operated at 60°C. The linear solvent gradient is described in Table 2. The flow rate was of 0.8mL/min and the injection volume was of 30µL. UV detection was performed between 200 and 300 nm with a PDA model 2996 (Waters, USA). Light scattering was assessed with a DDL 31 detector (Eurosep, France) using a nebulization temperature of 110°C and a air gas flow of 1.5L/min. The GC system comprised an AutoSystem XL (Perkin Elmer, USA) used in on-column mode. The injector temperature was kept at 45°C during 2 min followed by a linear increase up to 320°C with an heating rate of 100°C/min. Separation was carried out on a BPX5 capillary column (30m×0,25mm×0,25µm; SGE Europe, , France). After injection of 1 µL, the temperature was kept at 50°C during 1min, increased up to 330°C at 15°C/min and was at 330°C for 5 min. Detector was permanently held to 340°C. Because similar results were obtained with GC and HPLC methods, there are not distinguished in the remainder of this work.

Table 2. Linear solvent gradient of HPLC method

Time (min)	Solvent A (%)	Solvent B (%)	Solvent C (%)
0	40	60	0
2	40	60	0
30	0	100	0
32	0	0	100
37	0	0	100
42	40	60	0
53	40	60	0

Solvent A: aqueous 10mM NH4Ac (VWR, France) solution adjusted to pH 9.5 with 25% aqueous NH4OH (ACROS organics, Geel, Belgium) to which 500µL/L *n*-hexylamine (SIGMA-ALDRICH, USA) was added; Solvent B: acetonitrile (HPLC grade, CARLO ERBA, France) to which 500µL/L *n*-hexylamine was added; Solvent C: isopropanol to which 500µL/L *n*-hexylamine was added.

3.5. Monte Carlo sampling and Molecular simulations

All calculations were performed at atomistic scale by using the commercially available COMPASS forcefield (Accelrys, USA). The main interests of this forcefield are that it is optimized for condensed phases as reproduced by our Monte-Carlo sampling and that it incorporates all the parameters required for the study of polymers, additives and simulant properties including water.

As previously described[18], Monte Carlo sampling of pair interaction energies was performed by combining both scripting features of Material Studio 4.2 (Accelrys, USA) and the classical simulation software Discover (Accelrys, USA). All conformers of additives were generated from long term molecular dynamics (MD) simulation at the requested temperature. Conformers of simulant molecules were by contrast extracted from isobaric MD simulations of large boxes (including up to 200 molecules). All sets included between 10^3 and 10^4 conformers. Pair contact energies relied on 10^7 samples for simulant molecules and up to 10^{11} samples for large additives. Potential energies were applied

without any cutoff. The number of neighbors was based on up to 10^4 trials of packing of contact molecules around a seed molecule. The contact surface corresponded to the van-der-Waals determined from the gyration radius of each atom.

Partial molar volumes, V_i^P, were inferred from isobaric MD at T=313K and a pressure p=10^5 Pa by varying the number of solute molecules, n_i, dispersed among a constant number of F molecules, n_F:

$$V_i^P = \left(\frac{\partial V_{F+i}}{\partial n_i} \right)_{T,p,n_F} \quad (8)$$

Initial random mixtures of *i* and F molecules were obtained by a compression technique so as to obtain a final density, which was about 8 % lower than the density of the corresponding ideal mixture. This stage was performed with Amorphous Cell (Accelrys, USA). Each cell was subsequently submitted to a long term MD in the canonical NPT ensemble with an integration time step of 10^{-15} s. Temperature and pressure were kept constant by coupling the simulated cell with an infinite external heat bath (Andersen thermostat) and with an isotropic pressure bath (Berensen barostat). MD simulations between 3 and 5 ns were repeated on 5 initial cell configurations. V_i^P was finally calculated as the regression line between the volume of equilibrated cell with n_i when n_i was increased from 1 to 4. Possible biases introduced by MD simulations were detected by comparing the intercept of the regression line with the theoretical volume of pure F. n_F was chosen equal to 100 for alcohols and up to 800 for water. It was verified that doubling n_F or changing the initial density did not affect the density at equilibrium. In addition, starting from an initial configuration, which was different of the expected result, guaranteed independent predictions regarding possible deviations to ideality.

A cost-efficient estimate of V_i^P was tested by calculating the volume enclosed within the Connolly surface accessible to a hydrogen atom and noted V_i^H. This surface was sampled for several conformers by rolling around the solute a spherical probe with a radius comparable to a hydrogen atom. The enclosed volume was calculated by Delaunay tessellation.

4. Results and discussion

4.1. Typical desorption isotherms of plastic additives in ethanol

Typical desorption isotherms of plastic additives including light stabilizers, an antioxidant and a lubricant (see Table 1) are plotted in Fig. 2 for F=ethanol 95%. Several equilibriums were carried out by varying the volume of F in contact. Contact times were longer than 3 months to ensure a both a thermodynamical equilibrium even for large additives and to mimic the long term storage of food products. It is important to notice that all additives belonged to a same formulation of high density polyethylene and were consequently obtained in similar conditions. All isotherms appeared linear with an intercept close to 0. According to Eq. (1), the slope was proportional to the partition coefficient when b_i was negligible. Estimates of b_i were given by the intercept with $C_{i,F}\big|_{eq}$ and represented between 0 and 0.2 % of the initial content in additive. These values were roughly correlated to the melting point of the considered additive (Table 1) and were used to derive accurate confidence intervals on partition coefficients including biases as defined in Eq. (1).

Significant deviation to linearity occurred only for Erucamide. Its chemical affinity for F increased when the concentration in P at equilibrium increased. This effect was related to the poor compatibility of its unsaturated long chain carboxylic acid amide with polyethylene. The induced phase separation in polyethylene at high concentration is technologically used to modify the surface tension of polyolefins. The substance is indeed used as lubricant,

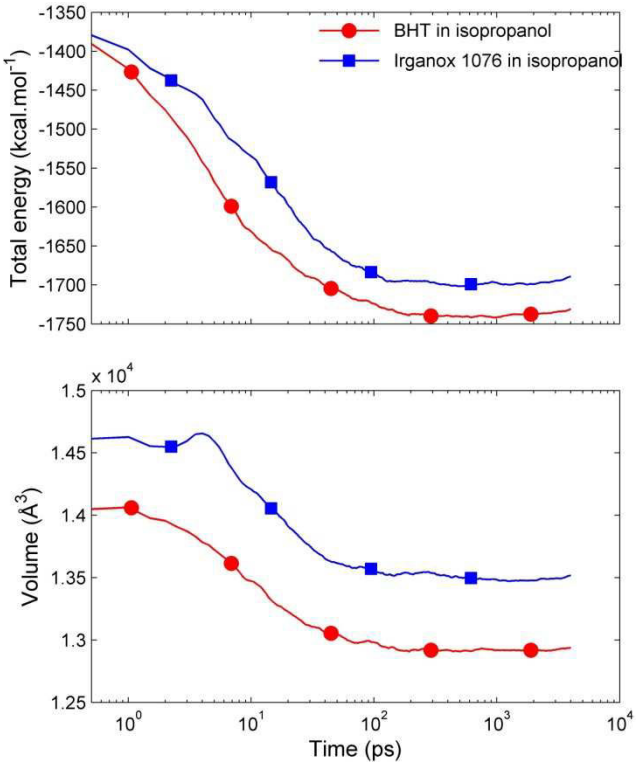

Fig. 3. Typical NPT MD runs at T=313 K and p=10^5 Pa in isopropanol. The number of molecules is N = 100 (isopropanol) +1 (solute). Total energy and volume are cumulated average.

antifogging or slip agent and is soluble in alcohols. Only the first linear part of the isotherm was considered to determine partitioning. On the opposite, Irgafos 168, which is used as peroxide decomposer, had the lowest chemical affinity for ethanol. The significant discrepancy between concentration measurements of Irgafos 168 in particular in F was attributed to the high reactivity of its trivalent phosphorus.

4.2. Required size of the cavity to insert a plastic additive in F

Fig. 3 presents typical runs of isobaric MD simulations at 313 K and 10^5 Pa to assess the volume at equilibrium of typical mixtures including a single additive and 100 molecules of F. The simulations started with initial configuration with a density lower than the one expected for ideal mixtures in targeted conditions of pressure and temperature. As a result, the systems underwent a contraction accompanied by a reduction in total potential energy caused by the progressive intensification of attractive interactions. The systems were on length scales ranged between 3 and 5 ns. Volumes of mixtures at equilibrium were obtained by averaging asymptotic values during the last nanosecond. To avoid particular initial configurations, all simulations were repeated on 5 different initial cells. It is underlined that starting for more condensed states led to similar results but generated higher instabilities in the explicit integration scheme due to higher energy barriers to update the configurational space of the simulated system.

The linear correlation between the volume of the mixture and the number of inserted solutes are plotted in Fig. 4. The overall consistence of MD results appeared as an intercept, which matched the volume of the pure considered simulant, whatever the considered solute and the number of F molecules in the cell. Furthermore, although fluctuations were noticed between repetitions, a satisfactory linearity was achieved between one and four solute insertions. It is worth to notice that regression lines obtained for a same solute and different simulants were almost parallel and would point out that the partial molar volume, V_i^P, would depend weakly on the considered simulant. This last assumption is analyzed in Fig. 5 by comparing V_i^P with common simple descriptors of simulant and solute properties.

From a geometrical point of view, when host molecules F were smaller, it could be thought that V_i^P of large additives should be smaller, with values possibly lower than their corresponding molar volumes, V_i^M. As shown in Fig. 5a, such a behavior was never observed and all V_i^P values were significantly greater than V_i^M ones and were either independent of F or decreased when the size of F increased. This last effect was well identified with solutes including a BHT pattern (BHT and Irganox 1076) and was approximately correlated to the electrical dipole moment of F with an increase V_i^P by 40% when isopropanol was replaced by water. These results showed

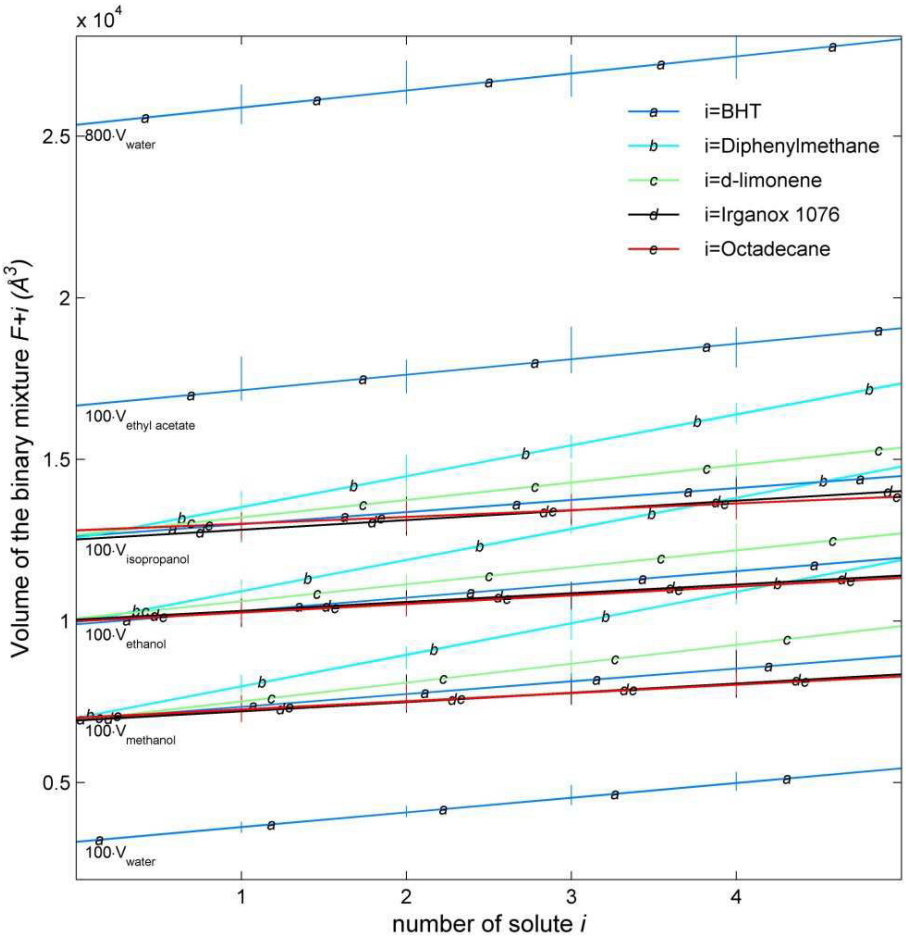

Fig. 4. Variations of binary systems solute+F with the number of solute molecules. The number of molecules F was 100 or 800. Vertical bars represent the spread of between 5 repetitions (all 30 values considered at equilibrium were plotted).

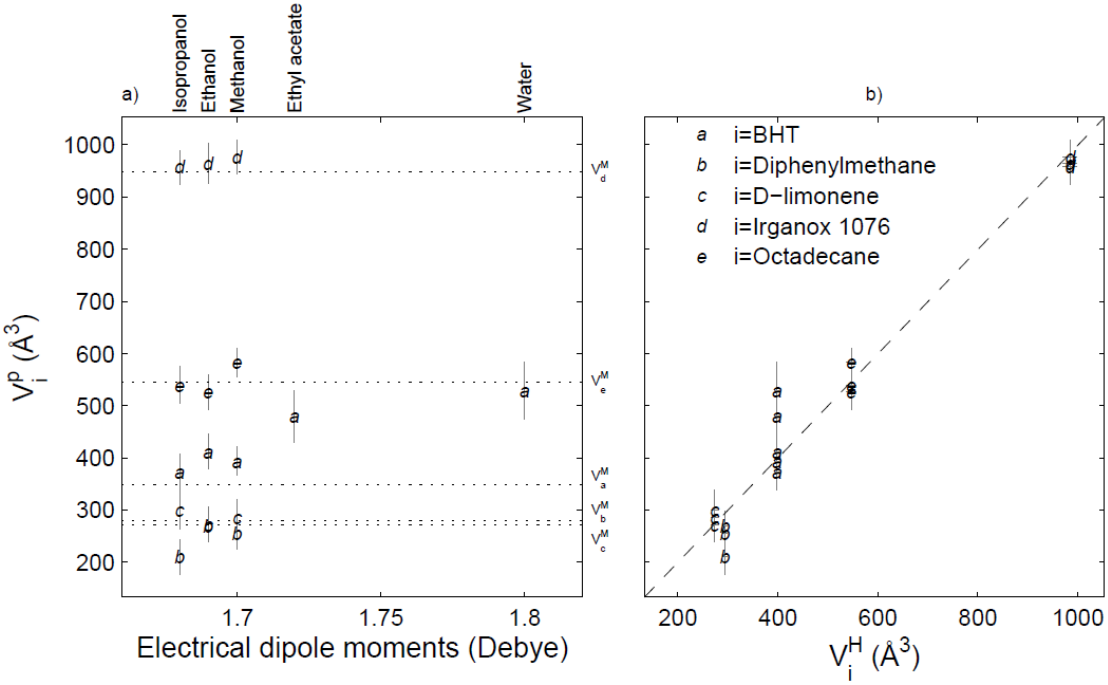

Fig. 5. Partial molar volumes of solutes *i* in different simulants, V_i^P, and their correlations with common properties of simulant and solute: a) electrical dipole moment of simulant and b) volume enclosed to the surface accessible to hydrogen atoms, V_i^M. Molar volumes of solutes appear as dotted horizontal lines in a).

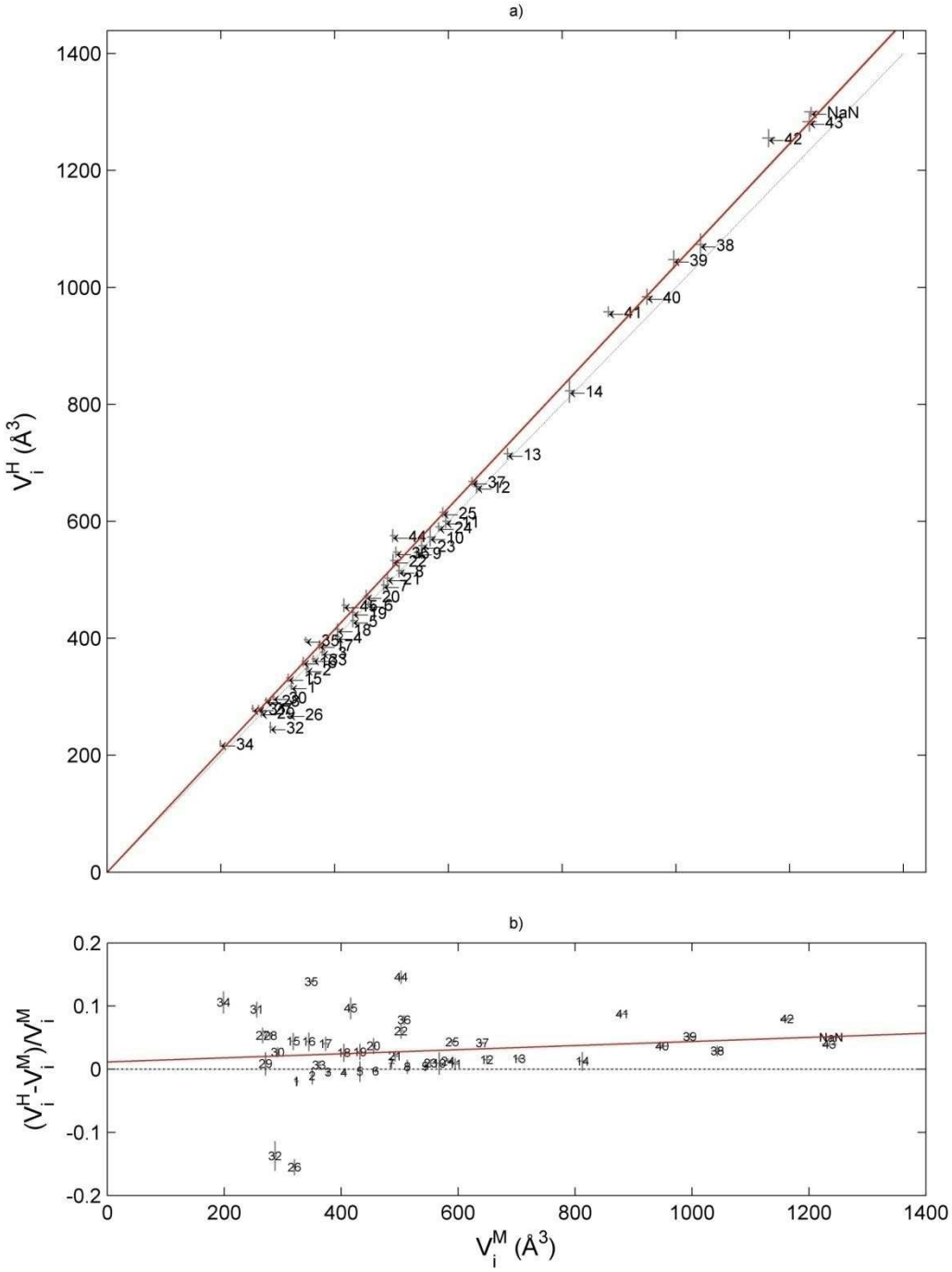

Fig. 6. Comparisons between V_i^H and for a large set of solutes *i=1..43*: a) linear correlation and comparisons with the bisection curve $V_i^H = V_i^M$ (dotted line) and the regression line intercepting zero (continuous line), b) relative deviation and comparisons with average deviation (dotted line) and the regression line (continuous line). 1: decane; 2: undecane; 3: dodecane; 4: tridecane; 5: tetradecane; 6: pentadecane; 7: hexadecane; 8: heptadecane; 9: octadecane; 10: nonadecane; 11 : eicosane; 12 : docosane; 13 : tetracosane; 14: octacosane; 15: decanol; 16: undecanol; 17: dodecanol; 18: tridecanol; 19: tetradecanol; 20: pentadecanol; 21: hexadecanol; 22: heptadecanol; 23: octadecanol; 24: nonadecanol; 25: eicosanol; 26: camphor; 27: diphenyl oxide; 28: diphenylmethane; 29: D-limonene; 30: DL-menthol; 31: eugenol; 32: isoamyl acetate; 33: linalyl acetate; 34: phenylethyl alcohol; 35: BHT; 36: Chimassorb 81; 37: erucamide; 38: Irgafos 168; 39: Irganox 1035; 40: Irganox1076; 41: Irganox 245; 42: Irganox 3114; 43: IrganoxPS802; 44: stearic acid; 45: Tinuvin 326.

that the volume of simulant molecules displaced by the insertion of a solute, $r_{i,F}^{-1}$, was controlled by the volume of the inserted solute and by a non-ideal effect related to the perturbation of the network of attractive interactions in F. In other

words, the large external surface of the solute hindered locally the creation of attractive electrostatic forces, which were responsible for a higher compaction and cohesion of molecules in pure F.

Because all investigated solutes were able to create only a few hydrogen bond donors, they were statistically in contact with atoms, which were the most abundant in F, that is hydrogen atoms. It was thus argued that V_i^P should be correlated with the volume enclosed within the solute external surface accessible to hydrogen atoms, V_i^H. A good agreement was observed for both small solutes and large additives. In addition, for antioxidants with simulated MD (BHT and Irganox 1076), the positive deviation between V_i^H and V_i^M (Fig. 6b) agreed the positive excess molar volumes in alcohols (Fig. 5a). In more polar simulants such as in water, results obtained on BHT (Fig 5a) suggested that the perturbation region around large additives should be thicker than a single hydrogen atom and V_i^H values should underestimate $r_{i,F}^{-1}$ and consequently $K_{i,F/P}$. Due to the high computational cost of V_i^P calculations by MD simulations, V_i^H values were used to assess partitioning via Eq. (2) or Eq. (5). This choice confirmed our first allegations[18], for which the large entropic contribution involved in the partitioning of plastic additives should be controlled by their large hardcore volume plus an interstitial volume that would be proportional to the surface exposed to F. According to this description, the interstitial volume was on average 9% larger when V_i^H was used instead of V_i^M as in[18]. For flexible solutes, variations in the interstitial volume were found according to the way conformers were sampled from molecular dynamics "in vacuum" (without intermolecular interactions) or in solution (with intermolecular interactions). As discussed further in sub-section 4.4, significant discrepancies were mainly observed for n-alkanes.

4.3. Biases associated to the sampling of pair contact energies for plastic additives

The sampling of intermolecular interactions between large hindered additives and themselves or with small simulant molecules raised several difficulties that did not emerge as saliently for smaller or linear solutes[18]. The main biases due to an overestimation of specific pair interactions are discussed in this sub-section and illustrated in Fig. 7.

Secondary polymeric antioxidants (or peroxide decomposer) are either phosphorous acid esters, which comprise Irgafos 168, or thioethers (also known as sulfides), which comprise Irganox PS802. Such molecules include a proton acceptor (a phosphorus or sulfur atom), which is always located close to the center of mass because the symmetry of large substituents. Besides, the rigidity of either ether or ester bond was responsible for the creation of an open cavity, which tended to be oversampled by smaller contact molecules, as previously discussed[18]. In presence of a hydrogen bond donor simulant (alcohols, water), our standard pair contact algorithm, which proceeded by an expansion of both centers of mass until the van-der-Waals surfaces of both molecules came in contact, tended to overestimate the contribution of the internal hydrogen bond with the simulant. This effect is depicted in Fig. 7a for a conformer of Irganox PS802 in contact with methanol. The corresponding distribution of "thermalized" contact energies (see the ensemble average operator defined in Eq. (3)) are plotted in Fig. 7b. To overcome such a difficulty, contraction methods were used instead of expansion ones and in combination with directions of translation, which were not collinear with centers-of-mass of both molecules.

Similar biases arose when the interactions between two phosphorous acid esters were sampled. The internal cavity was charged when the lateral groups were

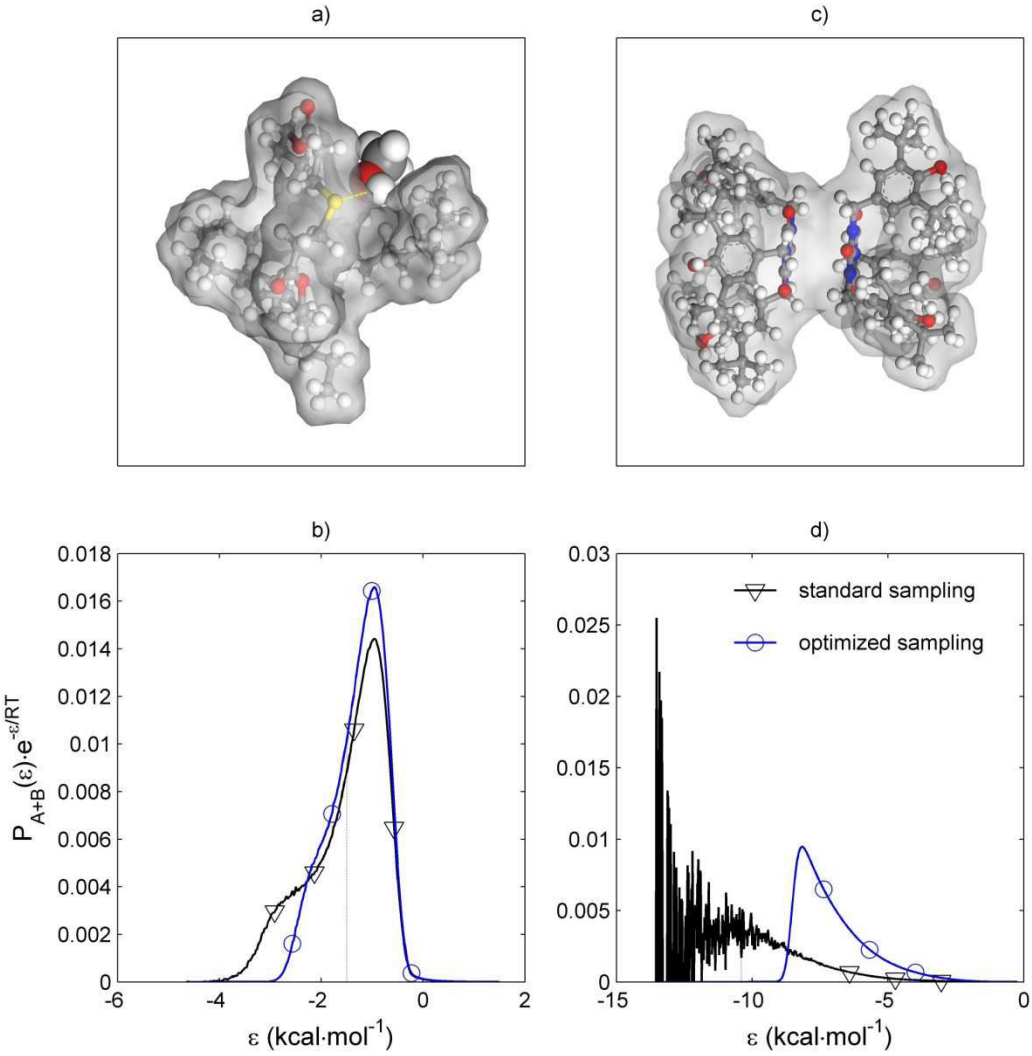

Fig. 7. Illustrations of biased sampling of contact energies involving large additives: a-b) sampling of contact energies between Irganox PS802 and methanol, c-d) sampling of contact energies between Irganox 3114 and itself. The configurations depicted in a) and c) have a minimal interaction energy. Sampled distributions of contact energies plotted in b) and d) are weighted with the corresponding Boltzmann factor at 313 K.

not. As a result, the dipole interactions between cavities were favored in a head of tail configuration. Such configurations depicted in Fig 7c had very low potential energies, as plotted in Fig. 7d, but they were very unlikely to represent the state of an ordered system at 313 K. Indeed, the melting point of Irganox 3114 is ranged between 219 and 226°C so that the pure substance is assumed to be crystalline at 313 K. The likely structure of the crystal would correspond to a stacking of molecules, where a convex surface (bulging outward) would be in contact with a concave one (bulging inward). Our optimized sampling took into account such considerations by an appropriate a posteriori weighting. Such refinements led to Flory interaction parameters in P, which were ranged between 0 and 3 (Table 3). Neglecting previous effects would yield much higher values, which would be unrealistic for molecules, which have by design a good solubility in P.

4.4. Predictions of partitioning with alcohols

Partition coefficients in alcohols were calculated by means of Eq. (2) and by assuming that $r_{i,F}^{-1}$ was equal to the ratio between V_i^H and the molar volume of F. The predictions were updated to account for the experimental temperature, either 313 K or 298 K. Corresponding $\chi_{i,F}$ and $\chi_{i,P}$ values are gathered in Table 3. They were finally compared to reference data used in

Table 3. Calculated Flory-Huggins interaction parameters at 313 K.

Solute	$\chi_{i,water}$	$\chi_{i,methanol}$	$\chi_{i,ethanol}$	$\chi_{i,isopropanol}$	$\chi_{i,P}$
Decane	/	5.89 ± 0.01 [c]	4.40 ± 0.01 [c]	3.28 ± 0.002 [c]	0.3 ± 0.05 [c]
Undecane	/	6.17 ± 0.005 [c]	4.65 ± 0.003 [c]	3.50 ± 0.001 [c]	0.30 ± 0.001 [c]
Dodecane	/	6.62 ± 0.001 [c]	5.06 ± 0.003 [c]	3.87 ± 0.001 [c]	0.31 ± 0.02 [c]
Tridecane	/	6.90 ± 0.005 [c]	5.31 ± 0.003 [c]	4.10 ± 0.01 [c]	0.30 ± 0.01 [c]
Tetradecane	/	7.26 ± 0.01 [c]	5.64 ± 0.01 [c]	4.38 ± 0.02 [c]	0.23 ± 0.003 [c]
Pentadecane	/	7.84 ± 0.02 [c]	6.16 ± 0.01 [c]	4.85 ± 0.01 [c]	0.24 ± 0.01 [c]
Hexadecane	/	8.03 ± 0.05 [c]	6.35 ± 0.05 [c]	5.03 ± 0.04 [c]	0.37 ± 0.04 [c]
Heptadecane	/	8.44 ± 0.05 [c]	6.72 ± 0.05 [c]	5.36 ± 0.04 [c]	0.28 ± 0.04 [c]
Octadecane	/	8.76 ± 0.05 [c]	7.01 ± 0.05 [c]	5.62 ± 0.04 [c]	0.44 ± 0.04 [c]
Nonadecane	/	8.82 ± 0.05 [c]	7.09 ± 0.05 [c]	5.66 ± 0.04 [c]	0.55 ± 0.04 [c]
Eicosane	/	9.15 ± 0.02 [c]	7.38 ± 0.02 [c]	5.93 ± 0.01 [c]	0.68 ± 0.01 [c]
Docosane	/	9.71 ± 0.02 [c]	7.91 ± 0.01 [c]	6.40 ± 0.01 [c]	0.11 ± 0.01 [c]
Tetracosane	/	9.96 ± 0.6 [c]	8.21 ± 0.06 [c]	6.68 ± 0.05 [c]	0.39 ± 0.05 [c]
Octacosane	/	10.87 ± 0.7 [c]	9.08 ± 0.6 [c]	7.48 ± 0.5 [c]	0.35 ± 0.5 [c]
Decanol	/	3.77 ± 0.05 [c]	2.49 ± 0.04 [c]	1.86 ± 0.04 [c]	0.79 ± 0.03 [c]
Undecanol	/	4.43 ± 0.05 [c]	3.03 ± 0.04 [c]	2.09 ± 0.04 [c]	0.77 ± 0.04 [c]
Dodecanol	/	5.29 ± 0.01 [c]	3.71 ± 0.005 [c]	2.47 ± 0.001 [c]	0.69 ± 0.002 [c]
Tridecanol	/	5.19 ± 0.04 [c]	3.77 ± 0.03 [c]	2.27 ± 0.03 [c]	0.68 ± 0.01 [c]
Tetradecanol	/	5.81 ± 0.03 [c]	4.35 ± 0.03 [c]	2.49 ± 0.03 [c]	0.40 ± 0.003 [c]
Pentadecanol	/	6.21 ± 0.02 [c]	4.80 ± 0.02 [c]	2.52 ± 0.01 [c]	0.46 ± 0.01 [c]
Hexadecanol	/	6.18 ± 0.06 [c]	4.92 ± 0.06 [c]	2.37 ± 0.05 [c]	0.54 ± 0.05 [c]
Heptadecanol	/	6.89 ± 0.06 [c]	5.62 ± 0.06 [c]	2.70 ± 0.05 [c]	0.47 ± 0.04 [c]
Octadecanol	/	6.76 ± 0.03 [c]	5.71 ± 0.03 [c]	2.34 ± 0.02 [c]	0.70 ± 0.02 [c]
Nonadecanol	/	7.22 ± 0.06 [c]	6.04 ± 0.06 [c]	2.49 ± 0.05 [c]	0.72 ± 0.05 [c]
Eicosanol	/	7.95 ± 0.02 [c]	6.68 ± 0.02 [c]	2.94 ± 0.01 [c]	0.76 ± 0.01 [c]
Camphor	/	-0.54 ± 0.005 [b]	-0.81 ± 0.005 [b]	-1.02 ± 0.005 [b]	0.67 ± 0.002 [b]
Diphenyl oxide	/	-1.05 ± 0.005 [b]	-0.78 ± 0.005 [b]	-0.55 ± 0.005 [b]	0.42 ± 0.002 [b]
Diphenylmethane	/	3.37 ± 0.02 [b]	2.73 ± 0.01 [b]	2.12 ± 0.01 [b]	-0.05 ± 0.01 [b]
D-limonene	/	5.12 ± 0.03 [b]	3.80 ± 0.01 [b]	2.73 ± 0.01 [b]	0.04 ± 0.01 [b]
DL-menthol	/	2.02 ± 0.03 [b]	1.55 ± 0.03 [b]	1.09 ± 0.03 [b]	0.56 ± 0.03 [b]
Eugenol	/	3.07 ± 0.02 [b]	2.59 ± 0.01 [b]	2.02 ± 0.04 [b]	0.43 ± 0.03 [b]
Isoamyl acetate	/	1.36 ± 0.02 [b]	0.71 ± 0.01 [b]	0.21 ± 0.01 [b]	0.49 ± 0.01 [b]
Linalyl acetate	/	2.40 ± 0.03 [b]	1.77 ± 0.02 [b]	1.19 ± 0.02 [b]	0.20 ± 0.02 [b]
Phenylethyl alcohol	/	1.62 ± 0.02 [b]	1.30 ± 0.01 [b]	0.93 ± 0.01 [b]	0.62 ± 0.01 [b]
BHT	30.45 ± 1.74 [c]	3.85 ± 0.003 [c]	3.12 ± 0.61 [c]	2.30 ± 0.1 [c]	0.51 ± 0.06 [c]
Chimassorb 81	33.84 ± 0.01 [a,c]	5.24 ± 0.15 [c]	4.40 ± 0.15 [a,c]	3.34 ± 0.15 [c]	1.12 ± 0.31 [c]
Erucamide	30.13 ± 0.02 [a,c]	6.05 ± 0.01 [c]	5.38 ± 0.05 [a,c]	4.81 ± 0.10 [c]	1.75 ± 0.19 [c]
Irgafos 168	44.17 ± 1.74 [a,c]	14.22 ± 0.1 [c]	12.77 ± 0.1 [a,c]	11.18 ± 0.1 [c]	0.12 ± 0.01 [c]
Irganox 1035	/	9.87 ± 0.61 [c]	9.49 ± 0.98 [c]	8.75 ± 0.1 [c]	1.38 ± 0.31 [c]
Irganox 1076	36.33 ± 0.12 [a,c]	8.65 ± 0.13 [c]	7.14 ± 0.48 [a,c]	6.03 ± 0.1 [c]	0.15 ± 0.1 [c]
Irganox 245	/	9.81 ± 1.09 [c]	8.48 ± 0.78 [c]	5.92 ± 0.1 [c]	2.44 ± 0.21 [c]
Irganox 3114	45.36 ± 0.98 [c]	15.56 ± 0.14 [c]	14.54 ± 0.09 [c]	13.07 ± 0.06 [c]	2.57 ± 0.13 [c]
Irganox PS802	/	15.21 ± 0.14 [c]	14.15 ± 0.14 [c]	12.33 ± 0.1 [c]	-0.31 ± 0.01 [c]
Stearic acid	/	4.58 ± 0.03 [c]	3.78 ± 0.08 [c]	2.80 ± 0.02 [c]	1.56 ± 0.03 [c]
Tinuvin 326	30.97 ± 0.93 [a,c]	4.25 ± 0.09 [c]	4.50 ± 0.09 [a,c]	4.63 ± 0.1 [c]	1.49 ± 0.07 [c]

[a]: values used also in ternary mixtures; [b]: values at 298K, [c]: values at 313K.

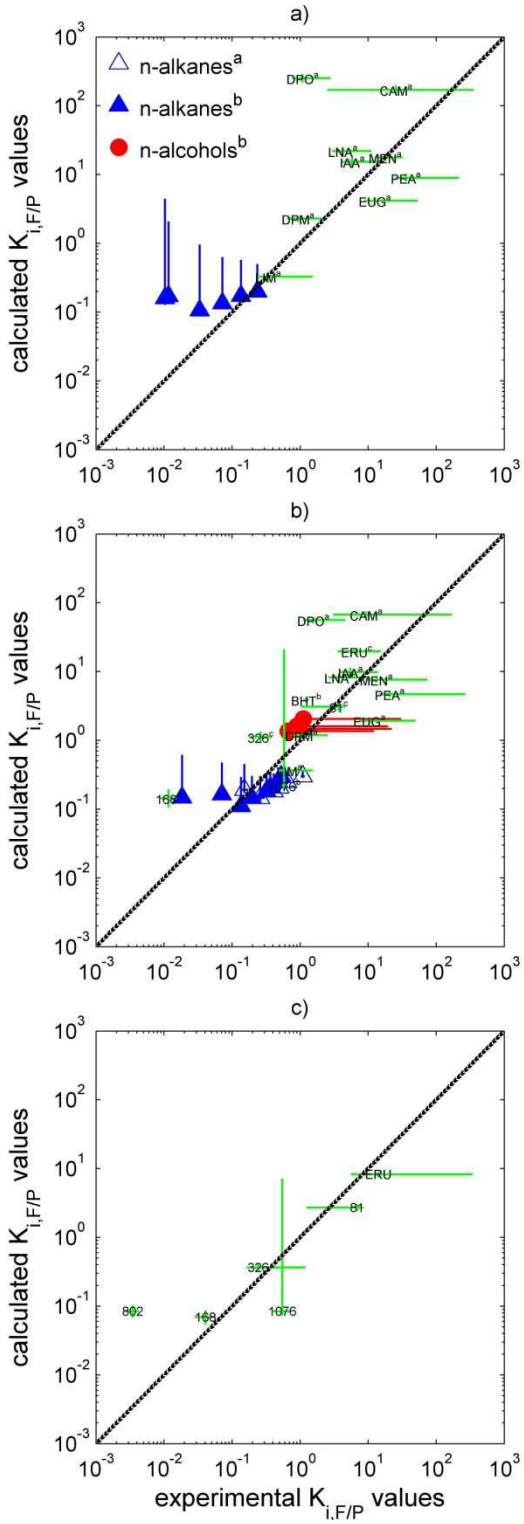

Fig. 8. Comparisons between predicted (Eq. 2) and experimental partition coefficients, $K_{i,F/P}$, between F=alcohols and P=amorphous regions of polyethylene: a) F=methanol, b) F= ethanol, c) F=isopropanol. 1076 = Irganox 1076; 168 = Irgafos 168; 326 = Tinuvin 326; 802 = Irganox PS802; 81 = Chimassorb 81; ERU = erucamide. [a] experimental values from Baner et al. at 298K[17]; [b] experimental values from Vitrac et al. at 313K[23]; [c] experimental values in Ethanol 95% at 313K.previous work[18] and to additional data generated by this study.

The comparisons are plotted crudely in Fig. 8 without applying any fitting procedure. The predictions were particularly satisfactory for plastic additives. For n-alkanes, different predictions were obtained according to V_i^H values were averaged on conformers interacting with F or not. Shrunk configurations were promoted in alcohols, because they minimized the number of broken hydrogen bonds. As such configurations in condition of poor solvent led to much better predictions for large alkanes, they confirmed indirectly the high sensitivity of partitioning of large solutes to positional entropy. Examples of configurations of decane extracted from isobaric MD simulations at 313 K and 10^5 Pa in methanol and in ethanol are depicted in Figs. 9a and 9c. The number of elbows tended to be larger in methanol (about 2) than in ethanol (about 1). Because the internal region of the elbow was inaccessible to simulant hydrogen atoms, the interstitial volume between the solute hardcore volume and F tended to be lower. As a rule of thumb, it was thus observed that 1 elbow contributed to make a C_nH_{2n+2} look like a $C_{n-2}H_{2n-2}$. The legitimacy of such a semi-empirical correction is analyzed in Figs. 9b and 9d by plotting the ratio, R_i, between $r_{i,F}^{-1}$ calculated from configurations "in vacuum" and its theoretical value derived from experimental partitioning data:

$$R_i = \frac{r_{i,F}^{-1}\Big|_{\text{no intermolecular interactions}}}{\left(\ln K_{i,F/P}\right) - \left(\chi_{i,P} - \chi_{i,F}\right)} \qquad (9)$$

The overestimation (R_i>1) was very significant above tetradecane and was higher in methanol.

Additional analyses of deviations between predictions and measurements were limited by the reliability of experimental protocols involving conventionally the contact of small pieces of a plastic material with a large volume of F. Such conditions applied to substances with a relative high chemical affinity for F

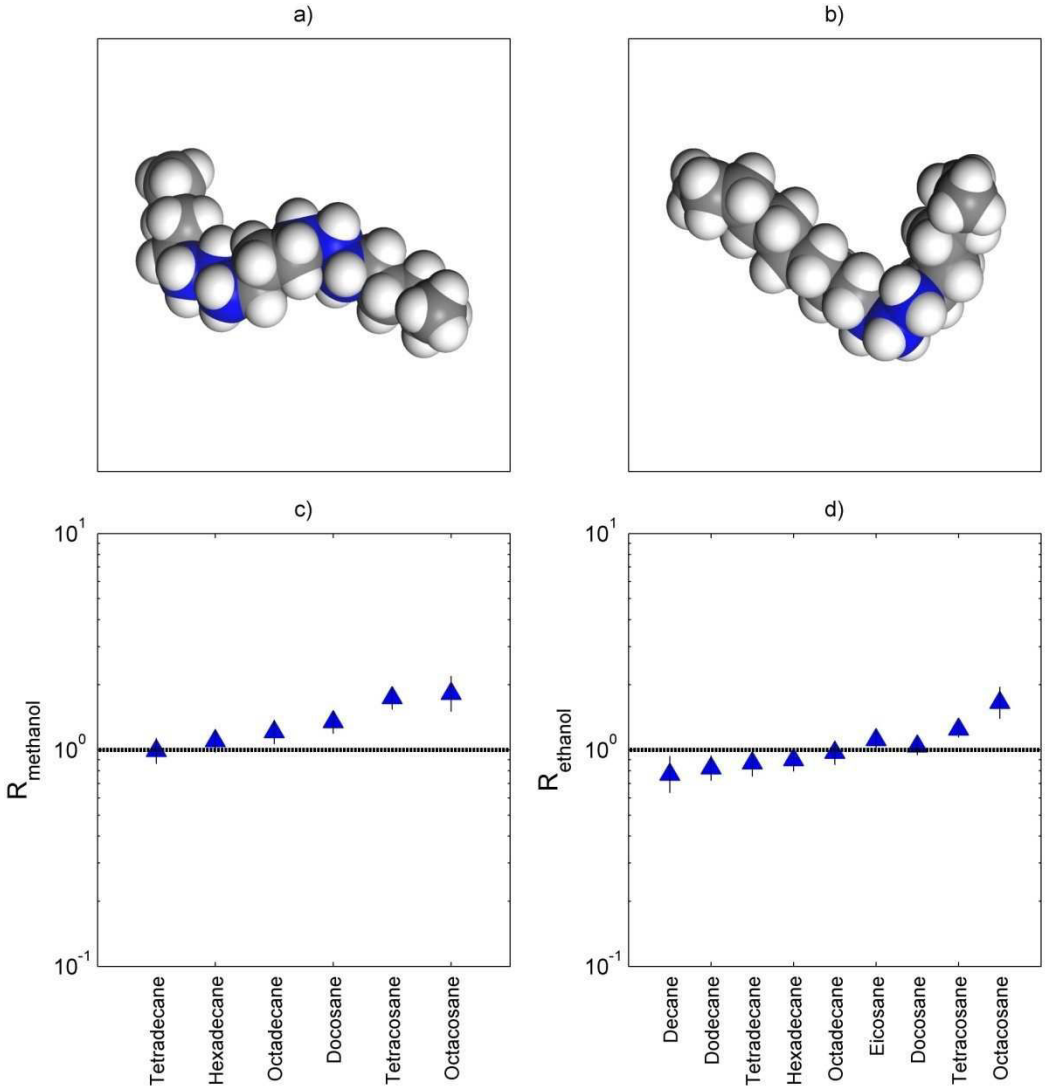

Fig. 9. Theoretical overestimation factor of $r_{i,F}^{-1}$ defined in Eq. (9), when V_i^H values are calculated from MD configurations sampled in vacuum instead of being sampled in solution: a-b) F=methanol, c-d) F=ethanol. Examples of expected configurations in a poor solvent are depicted in a) methanol and b) ethanol. Parts Surfaces inaccessible to F molecules are rendered in dark gray.

lead to a large uncertainties in the determination of $K_{i,\mathrm{F/P}}$ values caused by the difficulty to measure low residual concentrations in P at equilibrium.

4.5. Predictions of partitioning with ethanol-water mixtures

Previous analyses neglected the presence of water in ethanol and ethanol 95 % was falsely considered as a pure substance. This sub-section integrates explicitly the volume fraction of water in ethanol via Eqs. (5) and (7). Flory-Huggins theory applied to ternary mixtures predicts a nonlinear behavior of $\ln K_{i,F/P}$ with the resulting fraction of ethanol, $\phi_{ethanol}$. The origin of this behavior results from the virial expansion of the free energy for a ternary mixture. As expressed in Eq. (4), quadratic dependence of solute chemical potential with $\phi_{ethanol}$ was expected to result mainly from the pair interaction between the two major constituents, $\chi_{water,ethanol}$. Higher order dependence was expected to be caused either by ternary interactions, which were here neglected, or by significant variations of $\chi_{water,ethanol}$ with composition. Fig. 10 plots the predicted partitioning of typical plastic additives in water-ethanol mixtures when the cubic trend was included or not, along with

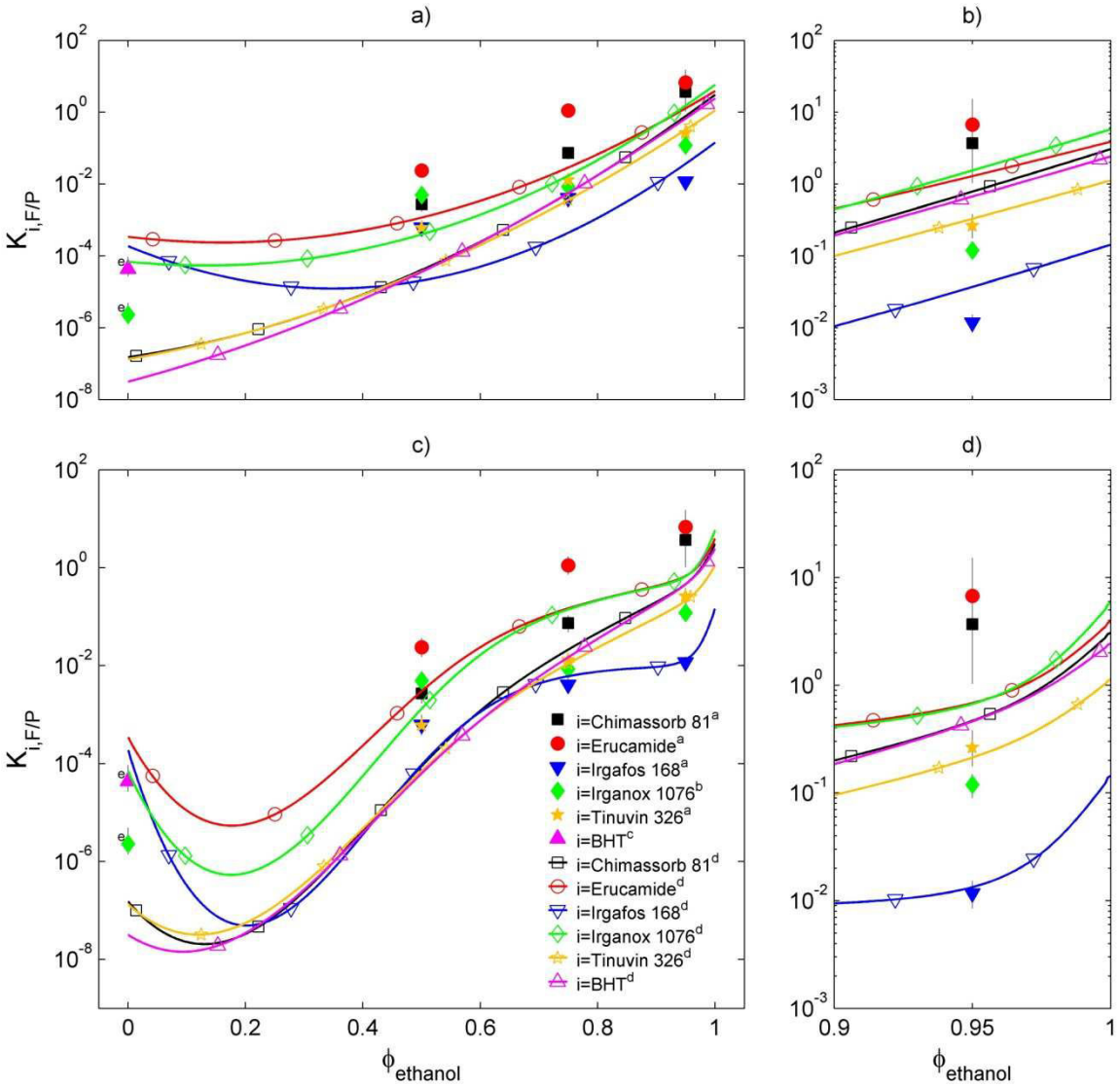

Figure 10. Predicted and experimental partition coefficients, $K_{i,F/P}$, in F=water-ethanol mixtures: a-b) predictions without cubic terms ($\chi_{water,ethanol}$=-2.04), c-d) predictions with cubic terms. Insets b) and d) are details of curves plotted in a) and c) respectively. [a]experimental values generated by this study; [b]: experimental values generated by this study, except values in pure water from[27]; [c]: experimental value from[27]; [d]: values predicted with Eq. (5).

experimental values. Sampled binary interaction parameters involved in Eq. (7) are tabulated in Table 3. Experimental values in pure water were reported by Gandek[27] from desorption kinetics. Although they were obtained without any theoretical consideration on the linearity of $\ln K_{i,F/P}$ with $\phi_{ethanol}$, they might be biased by the partial hydrolysis during the experiment.

The quadratic and cubic models of partitioning predicted both a change in curvature at low fractions in ethanol. The solute chemical affinity for F tended either to decrease much more slowly or even to increase when more water was added to the mixture. As a result, the lowest chemical affinity for F could be obtained for a mixture, which might not be pure water. This condition would correspond to a fraction in ethanol between 0.1 and 0.3, where the behavior of the water-ethanol mixture deviates the most from the ideality. Indeed, the van-Laar enthalpy, $\Delta H^{m}_{water+ethanol}$, is minimal for $\phi_{ethanol}$~0.3 [36]. This counter intuitive result was not possible to verify directly, because most of experiments were performed with a much

higher fraction in ethanol. Only a global validation based on bounds values at $\phi_{ethanol}$=0 and at $\phi_{ethanol}$=0.95, along with their variations between 0.5 and 0.95, was possible. It is underlined that the latter range corresponds to values, where $\chi_{water,ethanol}$ values were maximum (Fig. 1a) and where the expected nonlinearities were therefore minimal.

Assuming a constant $\chi_{water,ethanol}$ value equal to its average in Fig. 1a led to less accurate predictions but kept the ranking of solute according to their chemical affinity for F (Figs. 10a and 10b). Adding nonlinear effects increased significantly the accuracy, while providing further insight on the effect of the fraction in water (Figs. 10c and 10d). A significant underestimation was only obtained for Erucamide, whose desorption isotherm exhibited also significant deviations to Henry's law. For the other additives, it was shown that adding 5% v/v water in ethanol was accompanied by a sharp decrease in partitioning (Fig. 10d). This trend would explain why predicted $\ln K_{i,F/P}$ values in pure ethanol would overestimate the experimental values in 95% ethanol mixtures (Fig. 8b). The much less significant variation of $\ln K_{i,F/P}$ between $\phi_{ethanol}$=0.5 and $\phi_{ethanol}$=0.95 was well described. In pure water, the value of partitioning of Irganox 1076 was satisfactory predicted but the value of BHT was underestimated.

5. Conclusions

Because most of previous methods of estimations of partition coefficients between packaging materials and liquids depended on the availability of experimental data, a general framework for their prediction have been developed in a series of two papers[18]. Activity coefficients in both phases were approximated through a generalized off-lattice Flory-Huggins formulation applied to semi-crystalline materials, denoted P, and to interacting liquids simulating food products, denoted F, such as alcohols and water. The Flory-Huggins approximation introduced three features, which participated to the attractiveness and good predictions of the method. Firstly, the method sampled only contact interactions between pair molecules and did not require the explicit modeling of mixtures. Potential contact energies could be therefore calculated at low cost with an atomistic semi-empirical forcefield for any molecule with technological interest (polymer, food simulant, additive/residue). The distribution of interactions was straightforwardly averaged to any temperature. Secondly, the positional entropy, which was falsely neglected in previous studies applied to smaller solutes, could be derived independently from geometrical considerations. Finally, the same theory could be applied indifferently to binary and ternary mixtures.

The application to practical cases showed however that refinements or extensions were required to apply the general framework to "real" migrants such as oligomers or plastic additives. The main difficulties came from the sampling of interactions between molecules highly different in size and in shape. The configuration space was in addition significantly augmented by the presence of flexible molecules. Because these biases were analyzed in the first paper, this work focused on two extensions of the Flory-Huggins approach.

The first extension aims at improving the accuracy of the estimate of the size of cavity required to insert a large solute in F. In previous work[18], the volume for the insertion of alkanes was guessed to be close to their hardcore volumes whereas it was envisioned close to or greater than their molar volumes for large hindered molecules. Isobaric molecular dynamics simulations confirmed previous allegations by showing that different scenarios should be applied for flexible and stiff molecules. In addition, the volumes were found to be larger in water than in alcohols. To

maintain the calculations tractable for a wide range of substances, a reliable estimate was proposed as the volume to the surface accessible to hydrogen atoms. The interstitial volume between the solute and F was found proportional to the surface exposed to F and coincided with a region without attractive forces. In water, the thickness of this region was assessed 40% larger than in alcohols. For n-alkanes in alcohols, the exposed surface was associated to shrunk configurations of solute.

The second extension was less natural as it involved an intrinsic limitation of the Flory-Huggins approximation. Cooperative hydrogen bonding observed between more than two molecules of water could not be sampled by pair interactions. Indeed, on the contrary to alcohols, the number of neighbors around a water molecule and contact energies were correlated quantities. The ensemble average operator was modified accordingly to include the expected long lifetime tetrahedral coordination of liquid water at room temperature. This formal extension opened the way to the prediction of partitioning in water and in ethanol-water mixtures. In particular, it was found that a highly non linear variation of $\ln K_{i,F/P}$ should be expected with the fraction of ethanol. Such a behavior was related to the non-ideal properties of water-ethanol mixtures. To prevent additional artifacts, measured properties of binary water-ethanol mixtures were introduced. A similar treatment could be envisioned for other mixtures used as food simulants, such as ethyl acetate – isopropanol proposed as a substitute of olive oil.

From the sanitary point of view and because partitioning data in aqueous simulants or in ethanol 50% are missing in the literature, our predictive approach and predictions could be used to check the reliability of some simulant choices introduced in the EU regulation or to perform sanitary survey to plastic additives. Indeed, it is underlined that our parallel implementations on a 2.4 GHz bi-quad core personal computer made it possible to assess accurately up to 20 activity coefficients per day (i.e. potentially more than 10 partition coefficients). This capacity was very competitive to experiments, where weeks or months should be alternatively required.

As an illustration, the typical contamination of typical dairy product in contact with high density polyethylene with a crystallinity of 80% could be easily estimated by assuming that the food product could be replaced by a water-ethanol 50%, as recommended in[19]. For a ubiquitous antioxidant such as Irganox 1076 and according to Fig 10, $K_{i,F/P}$ is expected to be close to $5 \cdot 10^{-3}$, which corresponds to an apparent partition coefficient, as measured, of 10^{-3} from Eq. (1). For a food product of 500 ml packed within a 0.1 µm bottle, ones gets a volume ratio between the packaging material and the food product of about 1/60. For a likely concentration in additive of 10^3 mg·L^{-1}, the mass balance predicts a maximum possible contamination of food at thermodynamical equilibrium of 0.94 mg·L^{-1}. The obtained value is about 1 sixth the specific migration limit[14]. According to its diffusion coefficient[12], the thermodynamic equilibrium is expected to be reached in about one month at room temperature. The interested reader can find similar detailed derivations in[6,8].

As suggested in EU regulation[19], previous reasoning replaces a real food product by a so-called simulant. Replacing an almost fat in water emulsion (i.e. a diary product such as aromatized milk) by a water-ethanol mixture is not an intuitive approximation from the physicochemical point of view. In the former case, the solute is partitioned between three immiscible phases according a linear combination of partition coefficients between P and water, denoted $K_{i,water/P}$, and between P and fat, $K_{i,fat/P}$:

$$K_{i,F/P} = \frac{1}{L}\left[(1-fc)\cdot K_{i,water/P} + fc\cdot K_{i,fat/P}\right] \quad (10)$$

where L is the ratio volume between the packaging material and F; fc is the fat content expressed in volume fraction of F. The mixing rule in Eq. (10) is highly different from Eq. (5) for a miscible mixture, such as water-ethanol. From the point of view of consumer protection, Eq. (5) should replace Eq. (10) only when it overestimates the partition coefficient observed in emulsions. According to our estimates of partitioning in water and in water-ethanol mixtures, this condition could only be valid for food with very low fat content and would require additional verification. Similarly, the crude assessment of the contamination of food by phenolic antioxidants should be revised accordingly.

Acknowledgment

We would like to thank the Association de Coordination Technique pour l'Industrie Agroalimentaire and the Association Nationale pour la Recherche Technique for their financial support. We also want to thank the Centre Technique de la Conservation des Produits Agricoles and the Centre d'Appui et de Stimulation de l'Industrie par les Moyens de l'Innovation et de la Recherche for their help in generating generate new experimental partition coefficients.

References

(1) European Community. Regulation (EC) No 1935/2004 of the European Parliament and of the Council of 27 October 2004 on materials and articles intended to come into contact with food and repealing Directives 80/590/EEC and 89/109/EEC. *Off. J. Eur. Union* of 13.11.**2004**, L338, 4-17.

(2) European Community. Commission Directive 2002/72/EC of 6 August 2002 relating to plastic materials and articles intended to come into contact with foodstuffs. *Off. J. Eur. Communities* of 15.8.**2002**, L220, 18-58.

(3) European Commission. Substances listed in EU directives on plastics in contact with food. http://ec.europa.eu/food/food/chemicalsafety/foodcontact/eu_substances_en.pdf. 2008.

(4) European Community. Regulation (EC) No 1907/2006 of the European Parliament and of the Council of 18 December 2006 concerning the Registration, Evaluation, Authorisation and Restriction of Chemicals (REACH), establishing a European Chemicals Agency, amending Directive 1999/45/EC and repealing Council Regulation (EEC) No 793/93 and Commission Regulation (EC) No 1488/94 as well as Council Directive 76/769/EEC and Commission Directives 91/155/EEC, 93/67/EEC, 93/105/EC and 2000/21/EC. Off. J. Eur. Union of 30.12.2006, L396, 1-849.

(5) Vitrac, O.; Hayert, M. Risk assessment of migration from packaging materials into foodstuffs. *AIChE J.* **2005**, 51, 4, 1080-1095.

(6) Vitrac, O.; Challe, B.; Leblanc, J.-C; Feigenbaum, A. Contamination of packaged food by substances migrating from a direct-contact plastic layer: Assessment using a generic quantitative household scale methodology. *Food Addit. Contam*. **2007**. 24, 75-94.

(7) Vitrac, O.; Leblanc, J.-C. Exposure of consumers to plastic packaging materials: assessment of the contribution of styrene from yoghurt pots. *Food Addit. Contam*. **2007**, 24, 194–215.

(8) Vitrac, O.; Hayert, M. In *New trends chemical engineering research*, Berton, L.P., Ed.; Nova Science: New York, 2007; pp251-292.

(9) Beygley T., Castle L., Feigenbaum A., Franz R., Hinrinchs K., Lickly T., Mercea P., Milana M., O'Brien A., *Food Addit. Contam*. **2005**, 22, 73-90

(10) Reynier, A.; Dole, P.; Feigenbaum, A.; Humbel, S. Diffusion coefficients of additives in polymers. I. Correlation with geometric parameters. *J. Appl. Polym. Sci*. **2001**, 82, 2422-2433.

(11) Reynier, A.; Dole, P.; Feigenbaum, A.; Humbel, S. Diffusion coefficients of additives in polyolefins. II. Effect of swelling and temperature on the D = f(M) correlation. *J. Appl. Polym. Sci*. **2001**, 82, 2434-2443.

(12) Vitrac, O.; Lézervant, J.; Feigenbaum, A. Application of Decision Trees to the Robust Estimation of Diffusion Coefficients in Polyolefines. *J. Appl. Polymer Sci*. **2006**, 101, 2167-2186.

(13) Vitrac, O.; Hayert, M. Effect of the Distribution of Sorption Sites on Transport Diffusivities: a Contribution to the

Transport of Medium-Weight-Molecules in Polymeric Materials. *Chem. Eng. Sci*. **2007**, 62, 9, 2503-2521.
(14) European Commission. Food contact materials. A practical guide for users of European directives. http://ec.europa.eu/food/food/chemicalsafety/foodcontact/practical_guide_en.pdf. 2003
(15) Burman, L.; Albertsson, A.-C.; Höglund, A.; Solid-phase microextraction for qualitative and quantitative determination of migrated degradation products of antioxydants in an organic aqueous solution. *J. Chromat. A*. **2005**, 1080, 107-116.
(16) Piringer, O.G.; Baner A. L. Partition Coefficients. In "Plastic Packaging. Interactions with Food and Pharmaceuticals. 2nd Edition". Whiley-Vch, Weinheim, Germany, 2008, 89-121.
(17) Baner, A. L.; Piringer, O. G. Prediction of solute partition coefficients between polyolefins and alcohols using the regular solution theory and group contribution methods. *Ind. Eng. Chem. Res.* **1991**, 30, 1506-1515.
(18) Gillet, G; Vitrac, O.; Desobry, S. Prediction of solute partition coefficients between polyolefins and alcohols using a generalized Flory-Huggins approach. *Ind. Eng. Chem. Res.* submitted.
(19) European Community. Commission directive 2007/19/EC amending Directive 2002/72/EC relating to plastic materials and articles intended to come into contact with food and Council Directive 85/572/EEC laying down the list of simulants to be used for testing migration of constituents of plastic materials and articles intended to come into contact with foodstuffs. *Off. J. Eur. Union* of 12.4.**2007**, L97, 50-69.
(20) Bagnati, R.; Blanchi, G.; Marangin, E.; Zuccato, E.; Fanelli, R.; Davoli, E. Direct analysis of isopropylthioxanthone (ITX) in milk by high-performance liquid chromatography/tandem mass spectrometry. *Rapid Commun. Mass Spec.* **2007**, 21, 1998-2002.
(21) Sun, C.; Chan, S.H.; Lu, D.; Lee, H.M.W.; Bloodworth, B.C. Determination of isopropyl-9H-thioxanthen-9-one in packaged beverages by solid-phase extraction clean-up and liquid chromatography with tandem mass spectrometry detection *J. Chromatogr. A*. **2007**, 1143, 162-167.
(22) Saiz, L.; Padró J.A.; Guàrdia E. Dynamics and hydrogen bonding in liquid ethanol. *Mol. Phys*. **1999**, 97, 897-905.
(23) Jorgensed, W.L. Transferable Intermolecular Potential Functions for Water, Alcohols, and Ethers. Application to Liquid Water. *J. Am. Chem. Soc*., **1981**, 103, 335-340.
(24) Mahoney, M.W.; Jorgensen, W.L. A five-site model for liquid water and the reproduction of the density anomaly by rigid, nonpolarizable potential functions. *J. Chem. Phys*. **2000**, 112, 8910-8922.
(25) Mahoney, M.W.; Jorgensen, W.L. Diffusion constant of the TIP5P model of liquid water. *J. Chem. Phys*. **2001**, 114, 363-366.
(26) Vitrac, O.; Mougharbel, A.; Feigenbaum, A. Interfacial Mass Transport Properties Which Control the Migration of Packaging Constituents into Foodstuffs. *J. Food Eng*. **2007**, 79, 3,1048-1064.
(27) Gandek, T.P.; Alan Hatton T.; Reaid, R.C. Batch Extraction with Reaction: Phenolic Antioxidant Migration from Polyolefins to Water. 2. Experimental Results and Discussion. *Ind. Eng. Chem. Res.* **1989**, 28, 1036-1045
(28) Vitrac, O.; Lézervant, J.; Feigenbaum, A. Application of Decision Trees to the Robust Estimation of Diffusion Coefficients in Polyolefines. *J. Appl. Polymer Sci*. **2006**, 101, 2167-2186.
(29) Flory, P. J. Thermodynamics of high polymer solutions. *J. Chem. Phys.* **1941**, 9, 660-661.
(30) Huggins, M. L. Theory of Sulutions of high polymers. *J. AM. Chem. Soc*. **1942**, 64, 1712-1719.
(31) Flory P. J. Thermodynamics of high polymer solutions. *J. Chem. Phys*. **1942**. 10, 51-61.
(32) Huggins M. L. Derivation of Molecular Relaxation Parameters of an Isomeric Relaxation. *J. Chem. Phys*. **1942**, 46, 151-153.
(33) Flory, P.J. *Principles of Polymer Chemistry*; Cornell University: Ithaca, 1953.
(34) Pouchly, J.; Zivny, A.; Solc, K. Thermodynamics equilibrium in the system macromolecular coil-binary solvent. *J. Polym. Sci. C*, **1968**, 23, 245-256.
(35) Young, T.-H.; Chuang W.-Y. Thermodynamic analysis on the cononsolvency of poly(vinyl alcohol) in water–DMSO mixtures through the ternary interaction parameter. *J. Membrane Sci*., **2002**, 210, 349–359.
(36) Boyne J.A.; Williamson, A.G. Enthalpies of mixing of ethanol and water at 25°C. *J. Chem. Eng. Data*. **1967**, 12, 318.
(37) Lide, D. R. In *CRC Handbook of Chemistry and Physics*, CRC: Boca-Raton, 2005, pp15-41.
(38) Cruzan, J.D.; Braly, L.B.; Liu, K; Brown, M.G.; Loeser, J.G.; Saykally, R. J. Quantifying hydrogen bond cooperativity

in water: VRT spectroscopy of the water tetramer. *Science*, **1996**, 271, 59-62.
(39) Keutsch, F.N.; Saykally, R.J. Water clusters: Untangling the mysteries of the liquid, one molecule at a time, *Proc. Natl. Acad. Sci. U.S.A*. **2001**, 98, 10533-10540.
(40) Yang, J.; Peng, C.; Liu, H.; Hu, Y.; Jiang, J. A generic molecular thermodynamic model for linear and branched polymer solutions in a lattice. *Fluid Phase Equil*. **2006**, 244, 188-192.
(41) Coulier, L.; Kaal, E.R.; Tienstra, M.; Hankemeier, Th. Identification and quantification of (polymeric) hindered-amine light stabilizers in polymers using pyrolysis–gas chromatography–mass spectrometry and liquid chromatography–ultraviolet absorbance detection–evaporative light scattering detection. *J. Chromatogr. A*. **2005**, 1062, 227-238
(42) Garrido-López, Á.; Tena, M.T. Experimental design approach for the optimisation of pressurised fluid extraction of additives from polyethylene films. *J. Chromatogr. A*. **2005**, 1099, 75-83.

2. Développement d'une méthode rapide de déformulation d'un HDPE pour la vérification de la conformité vis-à-vis du contact alimentaire.

Dans la première partie, nous avons montré que les coefficients de partage sont très dépendants de la taille (contribution entropique) et de la structure chimique (contribution enthalpique) des additifs. L'effet de la taille en particulier avait été négligé dans les précédentes études. Les molécules de poids moléculaire élevé ont une meilleure affinité pour les solvants très polaires comme l'eau que ce qui était envisagé ultérieurement. Il a par ailleurs été montré que les modèles de prévision de coefficients de partage dans les mélanges eau/éthanol basés sur des modèles linéaires ne sont pas adaptés.

Un modèle de prévision de $K_{i,F/P}$ a été proposé dans les simulants constitué d'un ou deux liquides, permettant une utilisation plus efficace des modèles de prévision de la contamination des aliments et rendant possible une estimation robuste de $C_{i,P}\big|_{t=0}^{\max}$ (équation (1.8)). La conformité d'un matériau plastique est alors validée si l'on est sûr que chaque additif n'est pas présent dans le polymère à une concentration supérieure au $C_{i,P}\big|_{t=0}^{\max}$ correspondant. Il est ainsi possible pour le fournisseur de certifier que cette quantité n'est pas dépassée sans dévoiler la formulation exacte de son matériau. Dans le cas où le fournisseur refuse cette alternative, il faudra mesurer $C_{i,P}|_{t=0}$ par des méthodes expérimentales. La Figure 3.2 représente un arbre de décision simplifié pour rendre compte de ces éléments dans l'évaluation de la conformité.

Il apparaît nécessaire de disposer de méthodes permettant l'identification et la quantification des substances présentes dans les matériaux. La combinaison de techniques d'extraction et de séparation présentées en bibliographie peut être efficace, mais elle nécessite souvent un temps comparable à celui des tests de migration et présente donc un intérêt limité. La réalisation du spectre IRTF d'un film polymère ne prend quant à elle que quelques minutes. L'identification et la quantification des substances contenues dans le film à partir de ce spectre est possible avec des méthodes d'empreintes associant une bande caractéristique à chaque molécule. Toutefois, ces méthodes perdent rapidement en efficacité lorsque le nombre de molécules recherchées augmente car les bandes caractéristiques se superposent.

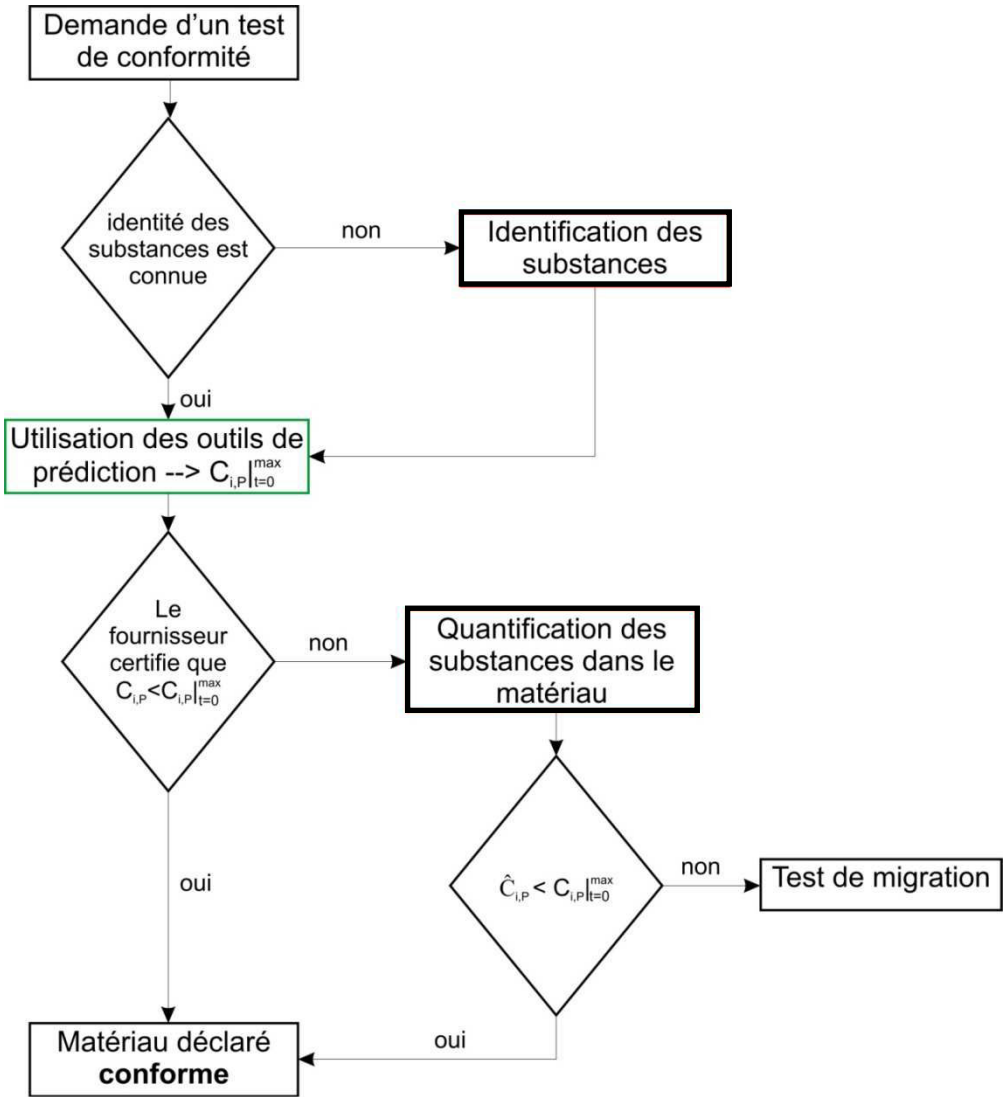

Figure 3.2. Arbre de décision simplifié pour valider la conformité d'un matériau plastique vis-à-vis du contact alimentaire. Les losanges représentent les questions, la flèche du bas correspond à une réponse "oui" et la flèche de droite à une réponse "non". Les cases en gras correspondent aux problématiques envisagées dans la seconde partie des résultats, présentée ci-après.

Nous avons donc choisi d'évaluer une méthode rapide d'identification et de quantification des substances contenues dans un PEHD basée sur la déconvolution du spectre complet du film ou d'un extrait. Ce travail a fait l'objet d'une publication, présentée ci-après, dans laquelle nous proposons une procédure de déconvolution semi-automatique permettant de travailler à partir de dictionnaires de substances (banque de données de spectres) larges et ouverts, c'est-à-dire permettant de considérer d'une part un grand nombre de substances connues simultanément et d'autre part des substances inconnues (dont les spectres n'existent pas dans la banque de données). Une analyse des biais et interactions possibles entre molécules a aussi été proposée.

A fast method to assess the composition of a polyolefin: an application to compliance testing of food contact materials

Guillaume Gillet[a,b], Olivier Vitrac[c*], Stéphane Desobry[b]

[a]: Laboratoire National de métrologie et d'Essais, Centre Energie, Matériaux et Emballage, 29 avenue Roger Hennequin, 78197 Trappes CEDEX, France.
[b]: Nancy Université, LSGA-ENSAIA-INPL, 2 avenue de la forêt de Haye, BP 172, 54505 Vandoeuvre lès Nancy, France.
[c]: Institut National de la Recherche Agronomique, UMR 1145 Génie Industriel Alimentaire, 1 avenue des Olympiades, 91300 Massy, France

[*]: correspondence to O. Vitrac (olivier.vitrac@agroparistech.fr)

ABSTRACT: For plastics materials intended to be in contact with food, recent EU regulations, 72/2002/EC and 1935/2004/EC, enforce the assessment of the migration of 502 substances of the 932 positively-listed substances. As mathematical modeling has been proposed to overcome such considerable effort in particular by providing maximum acceptable concentrations in the formulation, the compliance testing problem is efficiently reduced to the identification of substances and to their extent in initial materials. This work examines a fast identification and quantification procedure based on a semi-supervised deconvolution procedure of FTIR spectra of polymer extracts in dichloromethane. The inversion procedure was implemented as a Tikhonov least square problem and designed to work on large and open dictionary of substances by combining both spectra of reference additives and normalized responses of typical chemical functions. The sparsity of the overall solution was ensured by non-negativity constraints, while traces were detected by an iterative reweighting and stochastic resonance. The whole methodology was calibrated onto 21 typical additives of polyolefins and satisfactory tested on numerical examples and on extracts of processed films in high density polyethylene including up to eight unknown compounds. Maps of possible confusions and biases were generated for all tested substances. The mass balance for molecules with similar technological functions was particularly highlighted.

Key words: FT-IR, modeling, additives

INTRODUCTION

Along the food packaging chain, from raw materials up to finished products, the information and know-how is highly asymmetric between the different stakeholders: producers, converters, packaging fillers, retailers, enforcement laboratories, regulators, consumers… The resulting incompleteness on a global market limits the usability of predictive mathematical models to check the compliance of materials and articles intended to come in contact with food or to assess their traceability to facilitate the control, the recall of defective products, consumer information and the attribution of responsibilities, as encouraged by recent European regulations 2002/72[1] and 1935/2004[2]. In the case of thermoplastic materials used on the European market, the legislation, to which one of us participated, is particularly complex since it is both very detailed and it is still in the consolidation phase. Among the 937 substances

(including 340 monomers and 597 additives), which are positively listed in EU directives on plastics in contact with food[3], 502 substances (including 230 monomers and 272 additives) are thus subjected to specific migration limits (SML) due to toxicological concern. Substances, which are not authorized because they do not belong to the positive list, can also be used when they are located behind one or more layers, which prevents their migration into foods or food simulants above a detectable level[4]. This concept of relative barrier, so-called functional barrier, has been initially introduced to authorize the use of certain recycled materials for food contact applications. Although provisions are lacking or are divergent, this general principle tends today to be generalized to any multilayer structure and any substance including adhesives used in laminates, non-food contact material and printing inks. In the context, where the EU Regulation 2023/2006[5] lays also down the responsibility of business operators, the development of rapid methods to identify possible migrants and their amount in the initial materials is of significant concern. Indeed, each business operator should implement an effective quality management in order to select starting materials, which ensure compliance of the finished material or article. In absence of a certificate from the provider, which declares the compliance *a priori*, or for quality audit purposes, the extent of the migration of substances subjected to restrictions may be predicted via mathematical modeling, while avoiding unnecessary repetitions of time-consuming compliance studies. Modeling carried out in-house or outsourced has several benefits. It is an incremental procedure, which can handle several sources of uncertainty or variability (e.g. composition, geometry physicochemical properties, storage conditions…)[6], and, which can be used in real time to setup internal specifications: acceptable substances (e.g. molecular mass cutoff), acceptable concentrations[7].

The introduction of fingerprints in good manufacturing practice has been suggested in the early conclusions of the EU AIR research program CT94-1025[8], but the recommended technique, ^{1}H-magnetic resonance, is still not widely available. Conventional deformulation techniques have been reviewed by Bart[9]. They involve mainly wet chemistry rules on material extracts, while combining an ever-increasing order of sophistication in analytical ingenuity. Previous studies demonstrated that the burden remained on the identification of substances and not on the extraction step itself, which can be optimized by an appropriate choice of solvent and an accurate estimate of the extraction yield[10]. For the fast discrimination of extracts involving volatile compounds, electronic noses based on metal-oxide sensors have been proposed but their applications is still restricted to the detection off-odors and outgassing issues in thermo-plastics[9]. FT-Raman spectroscopy combining with CCD array detectors and near-infrared diode laser excitation could be an appealing alternative to tag *in situ* additives according to their vibrational spectra[11]. The method is however much less applied than infrared methods due to poor Raman scattering, insufficient reproducibility and the lack of specific Raman libraries[12]. By contrast, mid-infrared spectroscopy is one the most established analytical in the packaging industry and enforcement laboratories. In particular, Fourier transform infrared (FTIR) spectroscopy is supported by commercially available databases covering polymers and polymer additives, and it is suited for direct identification on either solid samples or extracts. Without being exhaustive, several studies[13-19] using mid-infrared techniques demonstrated the feasibility of the technique to trace the concentrations of minor constituents such as antioxidants in polyolefins. The usefulness of the technique to indentify the

formulation on commercial materials (i.e. blind materials) including more than 3 additives and possible unknown components (i.e. without reference spectrum) has however never been tested. Unique identification and corresponding quantification in mixtures is expected to be hindered by the inherent functional group identification, so that the spectra of large polymeric additives may be improperly assigned or the spectra of phosphorous acid esters used as hydroperoxide decomposers may be confounded with hindered phenolic antioxidants. In the latter case, the confusion may have a significant impact on the safety of the tested material, as the SML is of 60 $mg \cdot kg^{-1}$ for secondary antioxidants (hydroperoxide decomposers) against 6 $mg \cdot kg^{-1}$ for primary antioxidants (radical scavengers)[3].

Our objective was to design and discuss a general and robust framework to retrieve the identification and the quantification of major additives in commercial polyethylene materials by FTIR measurements for compliance testing purposes. The originality of the approach was to include in the study the most used additives (21 additives) for packaging applications, while integrating complex mixtures combining an unknown number of additives and possibly non-documented substances (not belonging to any positive list). It is underlined that handling unknown substances might help to prevent an accidental contamination of food products and subsequent crisis, such as the one generated by the contamination of baby milk[20] and other packaged drinks[21] by 2-isopropylthioxanthone. The paper is organized as follows. Section 2 describes the two-steps semi-supervised regression procedure, which was setup up for identification and quantification on mixtures including an unknown number of substances and possible unknown ones. The ill-posedness of the corresponding deconvolution problem was minimized by introducing constraints on the solution such as non-negativity and sparsity. Resulting biases were decomposed and analyzed in terms of false positives and quantification biases. Experiments are described in section 3. As additives are heterogeneously distributed in the material, the methodology was applied to spectra of extracts in dichloromethane. This method was found to be more convenient for routine analysis as it avoids the scattering problem in semi-crystalline polymers such as polyolefins. Results are presented in section 4 on either synthesized spectra or spectra of real extracts for four typical formulations of high-density polyethylene. Recommendations for compliance testing are summarized in section 5.

THEORY

Forward problem: decomposition of the spectrum of a mixture

For each measured wavenumber, λ, the FTIR absorption spectrum of a mixture (or an extract) in dichloromethane (DCM), S_{tot}^{λ}, was interpreted as a linear superposition of the spectra due to DCM, S_{DCM}^{λ}, n additives $\{A_i\}_{i=1..n}$ belonging to a dictionary (i.e. database) of spectra, $\{S_{A_i}^{\lambda}\}_{i=1..n}$, m chemical groups $\{U_j\}_{j=1..n}$ not assigned to $\{A_i\}_{i=1..n}$, $\{S_{U_j}^{\lambda}\}_{i=0..m}$, extracted oligomers and other polymer residues (fillers, pigments, coatings…), S_{PM}^{λ}, and finally a normal error with zero mean ε^{λ}:

$$S_{tot}^{\lambda} = S_{DCM}^{\lambda} + \sum_{i=1}^{n} S_{A_i}^{\lambda} + S_{PM}^{\lambda} + \sum_{j=1}^{m} S_{U_j}^{\lambda} + \varepsilon^{\lambda} \quad (1)$$

Except the spectrum of the background, all spectra were assumed to obey to the generalized Beer-Lambert law:

$$\begin{cases} S_{A_i}^{\lambda} = \alpha_{A_i}^{\lambda} \cdot C_{A_i} \\ S_{U_j}^{\lambda} = \alpha_{U_j}^{\lambda} \cdot \gamma_{U_j} \\ S_{PM}^{\lambda} = \alpha_{PM}^{\lambda} \cdot \gamma_{PM} \end{cases} \quad (2)$$

where $\left\{\alpha_k^{\lambda}\right\}_{k=A_i,U_j,PM}$ are the products of molar extinction coefficient of the k^{th} component at the wavenumber λ and the path length (i.e. the width of the cuvette which was a constant). $\left\{C_{A_i}\right\}_{i=..n}$, $\left\{\gamma_{U_j}\right\}_{j=1..m}$, γ_{PM} are the concentrations in A_i, U_i, PM respectively. By considering wavenumbers between 550 cm^{-1} and 4000 cm^{-1} (3451 values), Eqs. (1) and (2) lead to the following linear system:

$$\begin{bmatrix} S_{tot}^{\lambda_1} \\ S_{tot}^{\lambda_2} \\ \dots \\ S_{tot}^{\lambda_{3451}} \end{bmatrix} = \begin{bmatrix} S_{DCM}^{\lambda_1} \\ S_{DCM}^{\lambda_2} \\ \dots \\ S_{DCM}^{\lambda_{3451}} \end{bmatrix} + \begin{bmatrix} \varepsilon^{\lambda_1} \\ \varepsilon^{\lambda_2} \\ \dots \\ \varepsilon^{\lambda_{3451}} \end{bmatrix}$$

$$+ \begin{bmatrix} \alpha_{A_1}^{\lambda_1} & \dots & \alpha_{A_n}^{\lambda_1} & \alpha_{U_1}^{\lambda_1} & \dots & \alpha_{U_m}^{\lambda_1} & \alpha_{PM}^{\lambda_1} \\ \alpha_{A_1}^{\lambda_2} & \dots & \alpha_{A_n}^{\lambda_2} & \alpha_{U_1}^{\lambda_2} & \dots & \alpha_{U_m}^{\lambda_2} & \alpha_{PM}^{\lambda_2} \\ \dots & \dots & \dots & \dots & \dots & \dots & \dots \\ \alpha_{A_1}^{\lambda_{3451}} & \dots & \alpha_{A_n}^{\lambda_{3451}} & \alpha_{U_1}^{\lambda_{3441}} & \dots & \alpha_{U_m}^{\lambda_{3451}} & \alpha_{PM}^{\lambda_{3451}} \end{bmatrix} \cdot \begin{bmatrix} C_{A_1} \\ \dots \\ C_{A_n} \\ \gamma_{U_1} \\ \dots \\ \gamma_{U_m} \\ \gamma_{PM} \end{bmatrix} \quad (3)$$

which was written in a shorter form as:

$$\underline{S_{tot}} - \underline{S_{DCM}} = \underline{\underline{D}} \cdot \underline{C} + \underline{\varepsilon} \quad (4)$$

A graphical interpretation is given in Fig. 1 on a simple mixture. $\underline{S_{tot}} - \underline{S_{DCM}}$ is the spectrum associated to the mixture with the background associated to DCM subtracted. $\underline{\underline{D}}$ is the dictionary matrix or calibration matrix containing the normalized spectra of all available substances and the spectra of functional groups associated to functional groups. As the measured intensity for a given chemical group depends on the sensitivity and linearity of the detector, an optimal $\underline{\underline{D}}$ was obtained by generating the database on a same spectrometer instead of using a commercial database. An additional interest was to take into account possible interactions with DCM and to weight wavelengths according to the linearity of the detector. A realistic solution $\underline{C}$ must minimize the L^2-norm $\left\|\underline{\varepsilon}\right\|^2$ (variance of $\underline{\varepsilon}$) while ensuring $\underline{\varepsilon}$ has a zero mean. As the number of wavenumbers is much greater than the number of unknown compounds, the linear system was extensively overdetermined. To avoid additional confusion between bands present in documented additives (i.e. in A_i) with generic bands (i.e. in U_j), generic bands were associated to bump functions, which guaranteed smooth cutoffs (see Fig. 1a).

Eq. (3) was relaxed to optimal wavelengths by introducing a weighting 3451×3451diagonal matrix, $\underline{\underline{W}}$, whose main diagonal elements were ranged between 0 and 1:

$$\underbrace{\underline{\underline{W}} \cdot \left(\underline{S_{tot}} - \underline{S_{DCM}}\right)}_{\underline{\Sigma}} = \underbrace{\underline{\underline{W}} \cdot \underline{\underline{D}}}_{\underline{\underline{\Delta}}} \cdot \underline{C} + \underline{\underline{W}} \cdot \underline{\varepsilon} \quad (5)$$

The relative weight of each wavenumber was determined from the determination coefficient, $\left\{r_{\lambda,i}^2\right\}_{i=1..n}$, derived from the calibration curve of binary mixtures DCM+A_i obtained for 5 different concentrations. As a heuristic (semi-supervised regression), a weight of 1 at λ was assigned when one of the three following properties was fulfilled:

i) all $\left\{r_{\lambda,i}^2\right\}_{i=1..n}$ values were greater than 0.7 with at least one value above 0.9;

ii) at least one $\left\{\alpha_{A_i}^{\lambda}\right\}_{i=1..n}$ was higher than the 70$^{\text{th}}$ percentile values of the whole spectra $\left\{\alpha_{A_i}^{\lambda}\right\}_{\lambda=\lambda_1..\lambda_{3541}}$;

iii) at least one $\left\{\alpha_{U_j}^{\lambda}\right\}_{j=1..m}$ is significantly higher than 1.

To increase the signal-to-noise ratio a smooth spline cutoff was applied to adjacent wavenumbers with a cutoff of 5 cm^{-1} and a transition width of 3 cm^{-1}. It was verified that this low cost procedure was almost equivalent to a filtering step with zero phase low pass band filter of

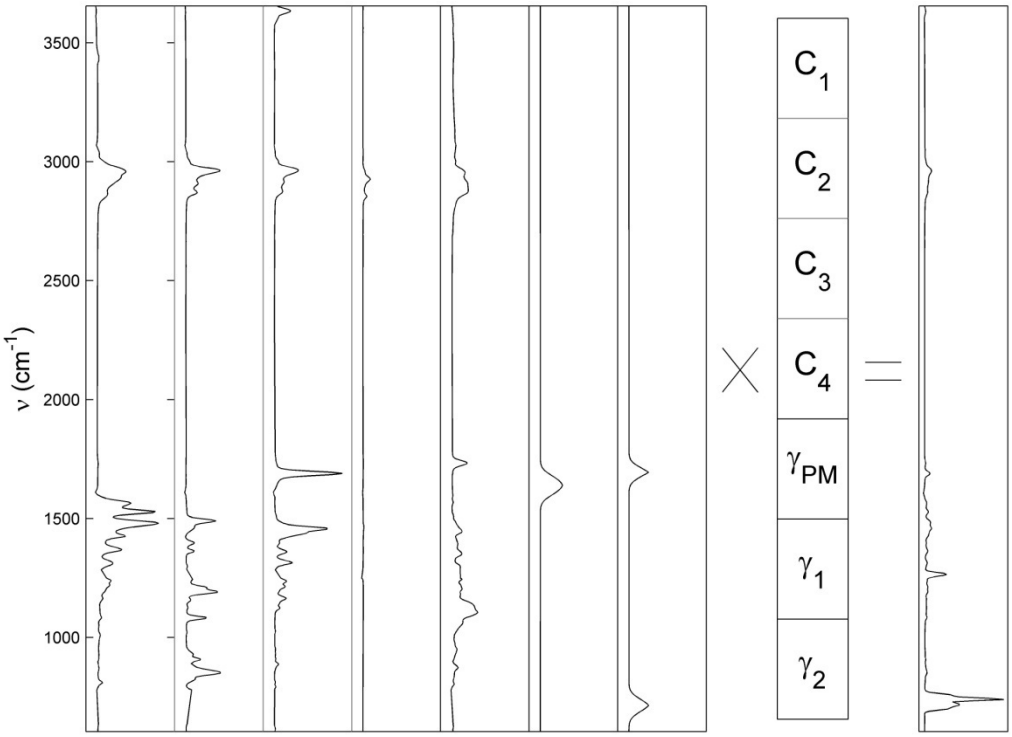

Figure 1. Graphical interpretation of the normal equation (5), $\underline{\underline{\Delta}} \cdot \underline{C} = \underline{\Sigma}$, for a mixture including Irganox 1076 (concentration C_1), Irgafos 168 (concentration C_2), erucamide (concentration C_3) and Chimassorb 944 (concentration C_4) in polyethylene (concentration γ_{PM}). γ_1 and γ_2 stand for the concentrations in simple chemical functions (respectively), whose normalized spectra are plotted in columns 6 and 7 of $\underline{\underline{\Delta}}$.

bandwidth 10 cm^{-1}. At the end, for the 21 considered additives and 15 additional chemical groups, 354 wavenumbers had a weight equal to 1.

The contribution of the polymer was obtained similarly from the calibration curve obtained for five different virgin polymer extracts. Since the substances were unknown, $\left\{\gamma_{U_j}\right\}_{j=1..m}$ and γ_{PM} were expressed in arbitrary units.

Inversion problem: finding concentrations of unknown compounds

Linear system (5), written as $\underline{\Sigma} = \underline{\underline{\Delta}} \cdot \underline{C}$, was poorly conditioned due to significant correlations between the FTIR spectra of additives with close chemical formula or including repeated patterns. The practical consequence was that the large null-space of $\underline{\underline{B}}$ dominated the solution vector, $\underline{C}$, of the standard least-square problem $\underline{C} = \arg\min \left\| \underline{\Sigma} - \underline{\underline{\Delta}} \cdot \underline{C} \right\|^2$. Indeed, any vector of the null-space, $\underline{\Delta C}$, could be added to calculate a new solution of $\underline{\Sigma} = \underline{\underline{\Delta}} \cdot \underline{C}$. Without correction, this method would give concentration estimates highly sensitive to noise measurements as well as numerous false positives and erroneous quantifications. To reduce such artifacts, a ridge regression was used instead and implemented as the following Tikhonov regularization problem[22]:

$$\underline{C} = \arg\min \left\| \underline{\underline{\Delta}} \cdot \underline{C} - \underline{\Sigma} \right\|^2 + \xi^2 \cdot \left\| \underline{\underline{\Delta_\Gamma}} \cdot \underline{C} \right\|^2$$

$$= \arg\min \left\| \begin{bmatrix} \underline{\underline{\Delta}} \\ \xi \cdot \underline{\underline{\Delta_\Gamma}} \end{bmatrix} \cdot \underline{C} - \begin{bmatrix} \underline{\Sigma} \\ \underline{0} \end{bmatrix} \right\|^2 \qquad (6)$$

$$\text{subjected to } \left\{ C_i \geq 0 \right\}_{i=1...n+m+1}$$

where $\underline{\underline{\Delta_\Gamma}}$ is a (n+m+1)×(n+m+1) diagonal matrix, where the diagonal term is zero when the concentration component is not subjected to any restriction (it may be present) and 1 otherwise, when its content is expected to be minimal. In other words, the sparsity of the solution (absence of certain compounds) was enforced by

adding additional constraints, which prevented the apparition of false positive for unexpected compounds. This constraint was systematically introduced for bands applied to unknown compounds $\{U_j\}_{j=1..m}$ to enhance the identification of substances included in the dictionary. The tradeoff between the minimization of the fitting error and the constraint was controlled by a positive constant ξ, so-called Tikhonov constant. As recommended by Hansen[23], ξ for a given problem was set to homogenize variances between measurements and predictions:

$$\xi^2 = \frac{\mathrm{var}\left(\underline{S_{tot}} - \underline{S_{DCM}}, \mathrm{diag}(\underline{\underline{W}})\right)}{\mathrm{var}\left(\underline{C}, \mathrm{diag}(I)\right)} \qquad (7)$$

where $\mathrm{var}(\underline{u},\underline{v})$ is the variance of $\underline{u}$ relatively to weights $\underline{v}$, $\mathrm{diag}(\underline{\underline{w}})$ is the main diagonal of $\underline{\underline{w}}$ and I is the identity matrix. As $\underline{C}$ is not known *a priori*, an iterative procedure is applied starting with ξ =0 (unregularized problem) in Eq. (6). Under these assumptions, the calculated solution is the most likely according to available measurements and the available database. To restrict solutions to feasible ones, a positivity constraint was added to Eq. (6). They were efficiently handled using an iterative inversion procedure method based on the interior-reflective Newton method described in[24]. The method was started from the solution calculated without constraint from the truncated singular value decomposition of $\left[\underline{\underline{\Delta}} \quad \xi \cdot \underline{\underline{\Delta_\Gamma}}\right]^T$.

The whole strategy prevented noise components in the null space (due to mainly overlapping regions in spectra) to propagate significantly in the approximated concentration vector. When disambiguation needed to be verified or when quantification should be improved due to non-assigned residual bands in $\underline{\underline{W}} \cdot \underline{\varepsilon}$, $W_{\lambda\lambda}$ components with non-zero values were replaced by $1/|\varepsilon_\lambda|$. Although the convergence was not guaranteed, such a modified analysis focused on spectrum components, for which the variance could be the best explained. This last refinement ensured the applicability of the method to any mixtures and polymer samples even if some peaks could not be recognized. To check whether the concentrations of some substances might be overestimated, the previous procedure could be modified by assigning a null weight to wavenumbers, where ε_λ were significantly above 0.

Biases associated to identification and quantification

Difficulties in assessing the composition of even simple mixtures are illustrated in Fig. 2. In this theoretical example, an additive with a 2 bands spectrum was mixed with an unknown substance including, according to the considered scenario: no common band (Fig. 2a), one common band (Fig. 2a), two common bands (Fig. 2c). The objective was to retrieve the true concentration of the additive (here 3 in arbitrary units), C_A, when only the spectra of the mixture, $\underline{\Sigma}$, and of the additive, $\underline{S_A}$, were known. The ratio between the known and unknown substances was set to 2/3. In this simple example, the Moore-Penrose pseudoinverse was $0.1252 \cdot \underline{S_A}^T$ and the solution corresponding to the theoretical normal equation, $\underline{\Sigma} = \underline{S_A} \cdot C_A$, was $0.1252 \cdot \underline{S_A}^T \cdot \underline{\Sigma}$. This crude approach, which neglected the unknown substance, led to C_A values equal to 3, 3.75 and 4.02 when no, one and two common bands were present. Because adding 20% white noise to $\underline{S_A}$ and $\underline{\Sigma}$ gave 2.92, 3.74 and 3.97 respectively, the C_A estimates were almost insensitive to noise but results were biased when a non-indexed substance was present. The overestimation observed, when at least one common band was present, was caused by the indiscernibility of the response for some wave numbers. As previously suggested, increasing the

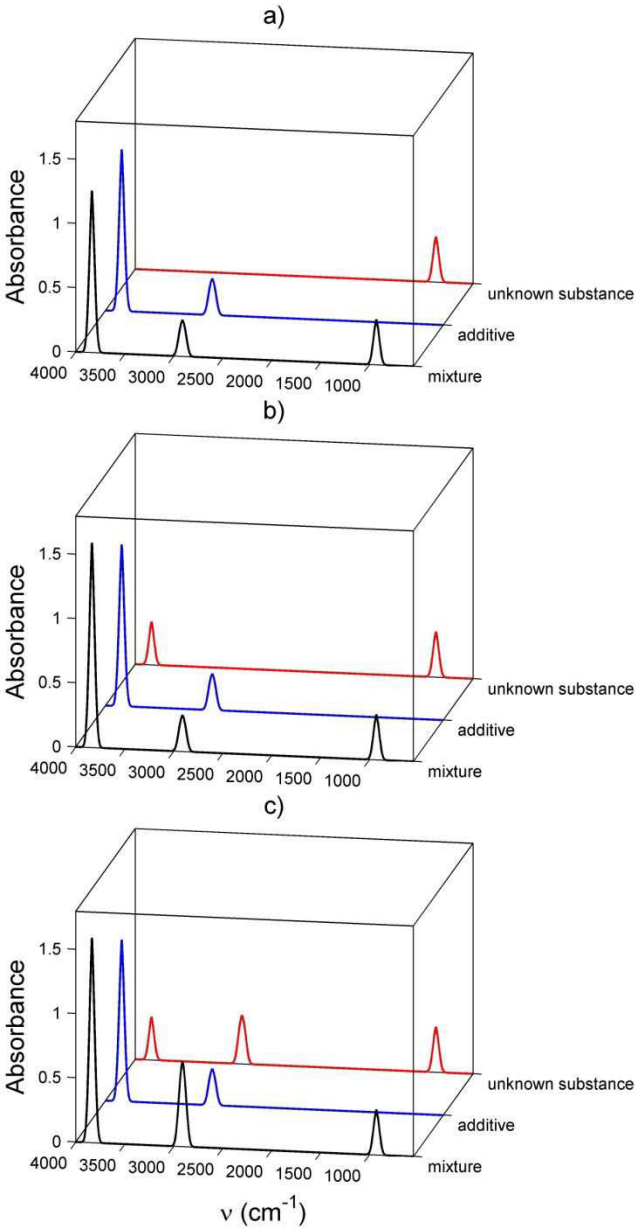

Figure 2. Theoretical example including an additive with a known spectrum (including three bands) and an unknown substance or residue with: a) no common band, b) one common band, c) two common bands.

weight of wave numbers where the predicted spectrum was underestimated could help to reduce the bias. In absence of noise, the corrected estimates were 3, 3 and 3.8 respectively. In presence of noise, the correction was much less efficient due to significant confidence intervals on predictions, which hindered the identification of the spectrum regions, where the predictions overestimated the measures. On real samples, bands that looked homothetic exhibited subtle differences, which were expected to increase the well-posedness of the mathematical attribution of bands.

The biases associated to an erroneous attribution of bands were calculated systematically by analysis all the 21×20/2 binary mixtures, mixing a substance X and a substance Y with $X \neq Y$. The overall objective was to retrieve a table of possible pairs, which might yield a false identification of the substance, a poor detection level, an erroneous quantification, etc. when the whole dictionary of known substances (21) was used for the identification. For a given pair, the total bias, β_{tot}, was decomposed as:

$$\begin{aligned}\beta_{tot} &= \left\langle \hat{C}_Y^{all} - C_Y \right\rangle_Y \\ &= \beta_{00} + \left\langle \beta_{X0}^{XY} \right\rangle_X + \left\langle \beta_{X0}^{all} \right\rangle_X + \left\langle \beta_{X0}^{XY} \right\rangle_Y \\ &+ \left\langle \beta_{X0}^{all} \right\rangle_Y + \left\langle \beta_{0Y} \right\rangle_Y + \left\langle \beta_{XY}^{XY} \right\rangle_{X,Y} + \left\langle \beta_{XY}^{all} \right\rangle_{X,Y}\end{aligned} \quad (8)$$

where $\hat{C}_Y^{all}$ is the estimated concentration in Y when the whole inversion procedure was applied, C_Y is the "true" concentration in Y in the mixture. For each pair X and Y, a normalized range of concentrations including 11 levels for C_X and C_Y (11×11 combinations) was used to evaluate the biases. To get realistic estimates a 10% white noise was added to the spectrum of each mixture. $\langle\ \rangle_L$ is the average operator over all realizations, which verifies the subset of rules L. β_{00} is the systematic bias related to noise.

β_{00} is the systematic bias due to identification irrespectively to the considered substances. $\left\langle \beta_{X0}^{XY} \right\rangle_X$ and $\left\langle \beta_{X0}^{all} \right\rangle_X$ assess the non-specific false detection level associated to the substance X when no other substance is added to the mixture, respectively when the dictionary is reduced to substances X and Y, and when all known substances are incorporated. $\left\langle \beta_{X0}^{XY} \right\rangle_Y$ and $\left\langle \beta_{X0}^{all} \right\rangle_Y$ assess the false detection level on Y related to the

Table 2. Composition of processed high density polyethylene films.

Additive name	PE1 (mg/kg)	PE2 (mg/kg)	PE3 (mg/kg)	PE4 (mg/kg)
Irganox 1076	467 ± 23	/	156 ± 3	159 ± 27
Irgafos 168	2497 ± 167	/	626 ± 40	/
Erucamide	3436 ± 116	/	1523 ± 152	/
Chimassorb 81	/	3293 ± 370	668 ± 46	/
Chimassorb 944	/	3327 ± 237	/	545 ± 26
Tinuvin 622	/	3416 ± 960	/	427 ± 120
Irganox 3114	/	/	463 ± 42	/
Tinuvin 326	/	/	626 ± 61	/
Irganox PS 802	/	/	/	502 ± 17
Triethylphosphite†	969 ± 10	969 ± 10	969 ± 10	969 ± 10

†Substance added to the extract, with a concentration expressed as it was present in the processed film.

incorporation of any substance *X*, respectively when the dictionary is reduced to substances *X* and *Y*, and when all known substances are incorporated.

$\langle \beta_{0Y} \rangle_Y$ is the bias of quantification associated to *Y* alone, when no other substance is added to the mixture. This bias was different of 0 only when the whole dictionary was used. $\langle \beta_{XY}^{XY} \rangle_Y$ and $\langle \beta_{XY}^{all} \rangle_Y$ assess the biases associated interaction between *X* and *Y*, respectively when the dictionary is reduced to substances *X* and *Y*, and when all known substances are incorporated.

EXPERIMENTAL

Formulation of samples

To test the whole identification and quantification methodology on real samples, four high density polyethylene with typical formulations were formulated at semi-industrial scale. Formulations are detailed in Table 1, they include antioxidants, light stabilizers, surface agents, swelling agent. Chemical structures of additives are represented in Table 2. They include most of typical chemical groups absorbing in FTIR: alcohol, aldehyde, ketone, aromatic circle, tertiobutyl, ester, thio-ester, phosphite, amine, amide, benzotriazine, benzotriazol. Plastic additives were provided by Ciba (Switzerland) except Erucamide, which was obtained from Croda (Italy), and calcium stearate, which was obtained from Merck (Germany). Virgin high density polyethylene was obtained from ATOCHEM (France). Polymer flakes were formulated during a first extrusion step prior to final processing at semi-industrial scale as 150 mm wide and 0.2 mm thick ribbons by a second extrusion and subsequent calendering. Both extrusion steps were performed at 200°C and polymer flakes were dried during 4h at 40°C between formulation and final processing. The final density and the melting point were of 940 $kg \cdot m^{-3}$ and 136°C respectively. The crystallinity was evaluated to 70% by differential scanning calorimetry.

Extraction of additives from samples

Extraction of additives from films was performed by soxhlet extraction in DCM (ACROS organics, Belgium). Ten grams of films cut in 5 mm × 5 mm pieces were placed in contact with 100 ml of DCM 40 h at 40°C. To prevent the degradation of additives during the extraction, 100µL/L of tri-ethylphosphite (Sigma-Aldrich, USA) was added to DCM. Long-term extraction was required to get accurate reference estimates of the formulation of processed films. For compliance testing or rapid screening, this constraining procedure could be replaced by a 40 minutes pressurized solid-liquid extraction.

Table 1. Substances tested and listed in the dictionary for identification and quantification.

Distance rank†	Commercial name	Chemical name	Technological function	CAS number	M ($g \cdot mol^{-1}$)	Chemical structure
1	BHT	Butylated hydroxytoluene	radical scavenger	000128-37-0	220	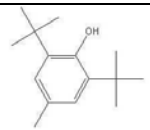
2	Irganox 1330	1,3,5-Trimethyl-2,4,6-tris(3,5-di-tert-butyl- 4-hydroxybenzyl)benzene	radical scavenger	01709-70-2	774	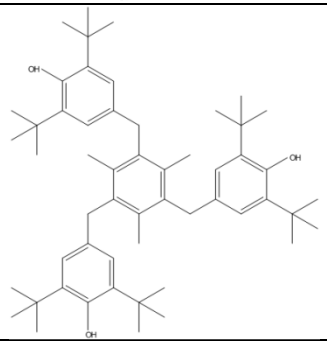
3	Irganox 1076	Octadecyl 3-(3,5-di-tert-butyl-4-hydroxyphenyl) propionate	radical scavenger	2082-79-3	530	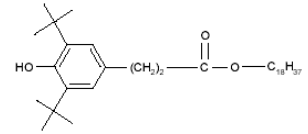
4	Irganox PS800	Thiodipropionic acid, didodecyl ester	hydroperoxide decomposer	00128-26-4	515	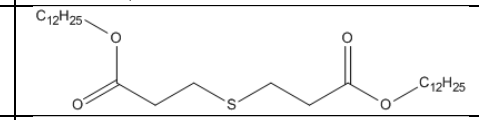
5	Irganox PS802	dioctadecyl Thiodipropionate	hydroperoxide decomposer	00693-36-7	683	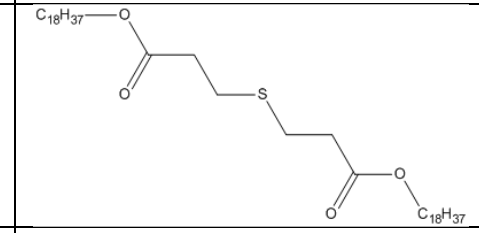
6	Irganox 1520	2,4-Bis(octylthiomethyl)-6-methylphenol	hydroperoxide decomposer	110553-27-0	424	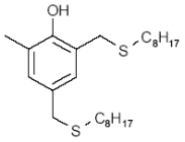

Distance rank†	Commercial name	Chemical name	Technological function	CAS number	M ($g \cdot mol^{-1}$)	Chemical structure
7	Atmer 163	N,N-Bis(2-hydroxyethyl)alkyl(C8-C18)amine	antistatic agent	71786-60-2	285-309	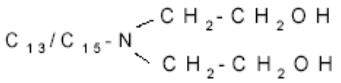
8	Stearic acid	Octadecanoic acid	lubricant	00057-11-4	268	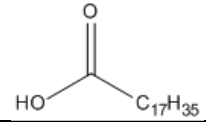
9	Erucamide	Cis-13-docosenoamide	slip agent	00112-84-5	337	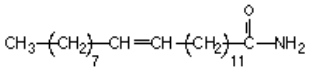
10	Tinuvin 326	2-(2-Hydroxy-3-tert-butyl-5-methylphenyl)-5-chlorobenzotriazole	light stabilizer	03896-11-5	316	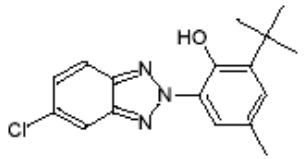
11	Tinuvin 770	Bis(2,2,6,6,-tetramethyl-4-piperidyl)sebaceate	light stabilizer	52829-07-9-	481	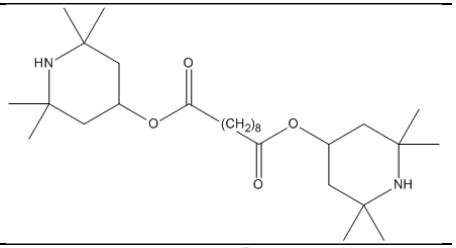
12	Irganox 1035	Thiodiethanol bis(3-(3,5-di-tert-butyl-4-hydroxyphenyl) propionate)	radical scavenger	41484-35-9	642	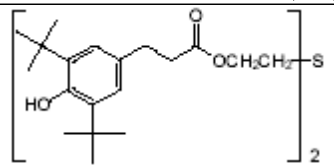
13	Irganox 245	Triethyleneglycol bis(3-(3-tert-butyl-4-hydroxy-5-methylphenyl) propionate)	radical scavenger	036443-68-2	586	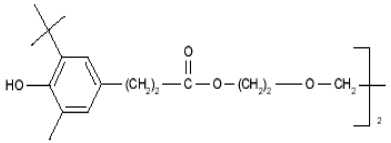

Distance rank†	Commercial name	Chemical name	Technological function	CAS number	M ($g \cdot mol^{-1}$)	Chemical structure
14	Irganox 3052	2-(1,1-dimethylethyl)-6-[3-(1,1-dimethylethyl)-2-hydroxy-5-methylphenyl] methylphenyl acrylate	radical scavenger	61167-58-6	394	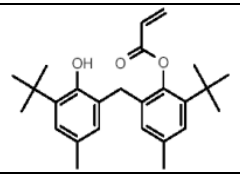
15	Tinuvin 622	1-(2-Hydroxyethyl)-4-hydroxy-2,2,6,6-tetramethyl piperidine-succinic acid, dimethyl ester, copolymer	light stabilizer	65447-77-0	3100-4000	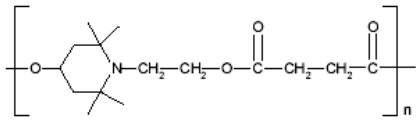
16	Irgafos 168	Phosphorous acid, tris(2,4-di-tert-butylphenyl) ester	hydroperoxide decomposer	31570-04-4	647	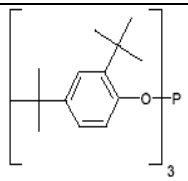
17	Chimassorb 81	2-Hydroxy-4-n-octyloxybenzophenone	light stabilizer	01843-05-6	326	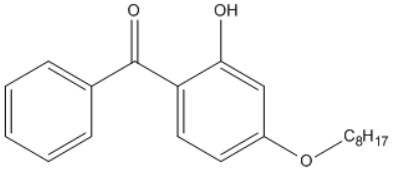
18	Chimassorb 944	Poly[6-[(1,1,3,3-tetramethylbutyl)amino]-1,3,5-triazine-2,4-diyl]-[(2,2,6,6-tetramethyl- 4-piperidyl)-imino]hexamethylene[(2,2,6,6 -tetramethyl-4-piperidyl)imino]	light stabilizer	71878-19-8	1200-3100	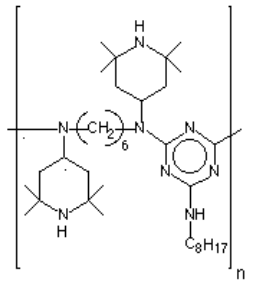

Distance rank†	Commercial name	Chemical name	Technological function	CAS number	M ($g \cdot mol^{-1}$)	Chemical structure
19	Irganox 3114	1,3,5-Tris(3,5-di-tert-butyl-4-hydroxybenzyl)- 1,3,5-triazine-2,4,6(1H,3H,5H-)trione	radical scavenger / light absorber	27676-62-6	784	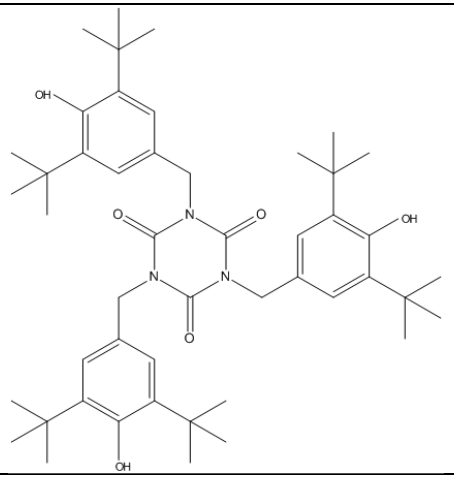
20	Irganox 1010	Pentaerythritol tetrakis(3-(3,5-di-tert-butyl-4-hydroxyphenyl)propionate)	radical scavenger	06683-19-8	1178	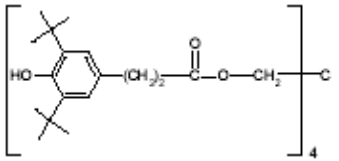
21	Triethylphosphite	triethylphosphite	peroxide decomposer	/	166	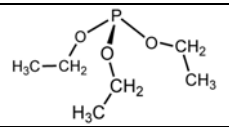
22	PE	polyethylene	/	/	16n+2	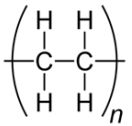

†rank corresponding to the Euclidian distance between normalized spectra as depicted in Fig. 5b.

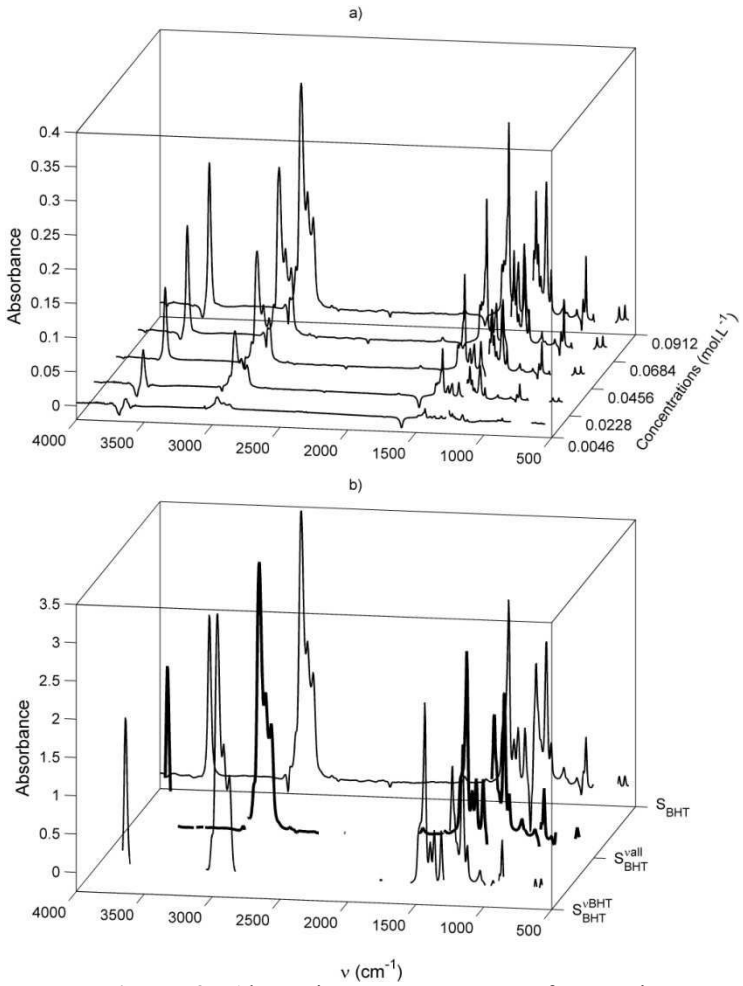

Figure 3. Absorption FTIR spectra of BHT in DCM with background subtracted: a) raw spectra at different concentrations, b) spectra regions with a relative weight of 1 according the number of additives considered in the dictionary: BHT alone ($S_{BHT}^{\nu,BHT}$), BHT with the full database ($S_{BHT}^{\nu,all}$).

Reference concentration measurements

Reference concentrations were measured by High Performance Liquid Chromatography (HPLC) associated to an UV Diode Array Detector (DAD) and an Evaporative Light Scattering Detector (ELSD) in series. The HPLC protocol was similar to the one described by Garrido-López et al.[25]. The HPLC system consisted in a Waters 717plus autosampler, a Waters 600 controller equipped with a thermostatted column compartment and an in-line degasser AF (Waters, USA). Separation was achieved on a Xterra C8 column (150mm×3.0mm; 5µm particles; Waters , USA) operated at 60°C.

FTIR spectra acquisition

Absorption spectra of extracts in DCM were acquired between 4000 to 550 cm^{-1} in a 100 µm thick cuvette (model moni-cell, Eurolab, Germany) located in a Fast Fourier Transform infrared spectrometer (model spectrum One, Perkin-Elmer, USA) at 23°C. Reference spectra of additives at different concentrations, ranging between X and X, were acquired similarly in DCM.

As previously discussed, to increase the sensitivity to small differences, a white noise, ranged between 0.1% and 1%, smaller than the repetition error, was added to measured spectra before applying the deconvolution. This procedure was repeated until to achieve a convergence of concentration estimates.

RESULTS AND DISCUSSION

FTIR spectra of a typical BHT pattern

Absorption spectra of a typical additive pattern, BHT, are plotted in Fig. 3 when the contribution of the solvent DCM was removed. The linear increase of the band absorption with concentration was used to identify specific mid-infrared bands of BHT. The proposed assignation of bands relied on the analysis proposed in[26]. The fundamental vibrations in the 3700-3600 cm^{-1} region were due to O-H stretching of the phenol group. The broad band between 3100 and 3000 cm^{-1} was associated to C-H attached to the aromatic ring. The 1500-650 cm^{-1} region with a forest of bands was referred as the finger print region, which revealed the signature of most bending and skeletal vibrations. It is worth to notice that the vibrational response of DCM perturbed some bands in this region, so that the subtracted spectra appeared discontinuous at some wavenumbers (Fig. 3a).

Our automatic weighting procedure recognized robustly the major bands and in particular the signature of the random reorientation of both tertio-butyl groups. By combining the information of all tested 21 additives (Table 2), it was obvious that most of the available degree of freedoms

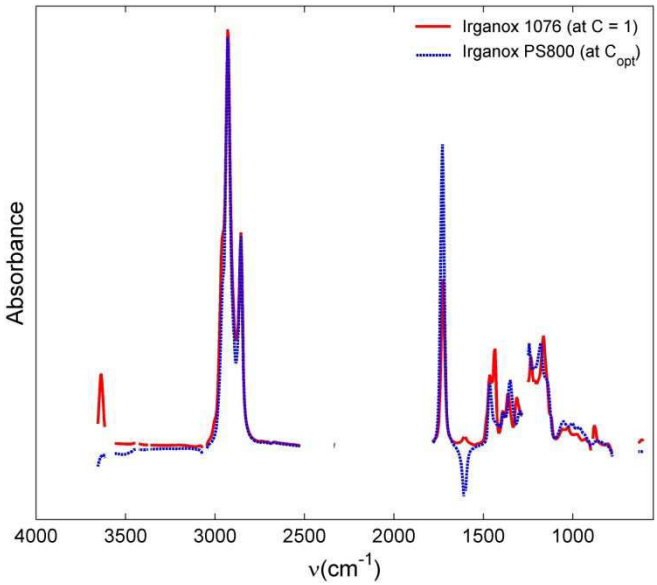

Figure 4. Spectra of Irganox 1076 and Irganox PS800 normalized to maximize the similitudes: a) whole range of wavenumbers, b) details in the fingerprint region.

for the identification came from the fingerprint region and were controlled by the lateral hindering groups. The alcohol band and the rigid C-H bands were much less specific as most of antioxidants included a phenol group. Only the terminal part of the 1830-1650 cm^{-1} region of carbonyl group was incorporated in the full analysis. Secondary amine groups stretching, usually observed between 3400 and 3300 cm^{-1}, was also selected for Atmer, Cimassorb 944 and Tinuvin series. The aromatic C-N stretching, the aliphatic C-N stretching and the N-H wagging band were also present respectively at 1360-1250 cm^{-1},1220-1020 cm^{-1} and around 715 cm^{-1}. The aliphatic P-O stretching and the thioether function included in secondary antioxidants were merged in the middle of the finger print region at 1450-1430 cm^{-1} and at 700-600 cm^{-1} respectively. Finally, C–H stretching bands from aliphatic domains, which occur in the range 3000–2850 cm^{-1}, was also introduced to derive the contribution of oligomers in the mixture.

Degrees of similitude between the FTIR spectra of tested additives

The presence of similar chemical groups for molecules with similar technological function complicated the identification of those substances. This effect is illustrated in Fig 4. by comparing the normalized spectra of additives, Irganox 1076 and Irganox PS800, with dissimilar chemical structures but with close signatures. The concentration ratio, which maximized the resemblance between both additives, was determined from the right-singular vectors of $\underline{\underline{\Delta}}$restricted to the two columns corresponding to the two tested additives. The C-H stretching band from aliphatic segments in the range 3000-2850 cm^{-1} dominated the response of both molecules. The carbonyl stretching in the 1830-1650 cm^{-1} region was highly recognizable but not enough specific to separate both molecules. Tenuous differences appeared along the whole fingerprint region. Although they contributed to about 21% of the overall mean square difference between both spectra, they were much more specific.

To assess the importance of the fingerprint region in the separation of substances, the former comparison was applied to all 22×22 pairs including the 21 additives and the polymer itself. The Euclidian distances between all spectra, assembled as a similarity matrix, were used to reconstruct a theoretical map of proximities between tested substances in a low dimensional space. The scatter was maximized by projecting the distances onto a three-dimensional space with an average distance error of 16% and a maximum error up to 60%. The same similarity matrix was used to obtain a hierarchical classification of the proximity of spectra based on the averaged distances between groups of substances. Distance maps and dendrograms are plotted in Fig. 5 when the whole spectra or the fingerprint regions were used. They confirmed that only few substances could be identified undoubtedly, among them: Tinuvin 622, Irganox 1010, Triethylphosphite, Chimassorb 944. The analysis of the fingerprint region increased globally the discrimination, with significant

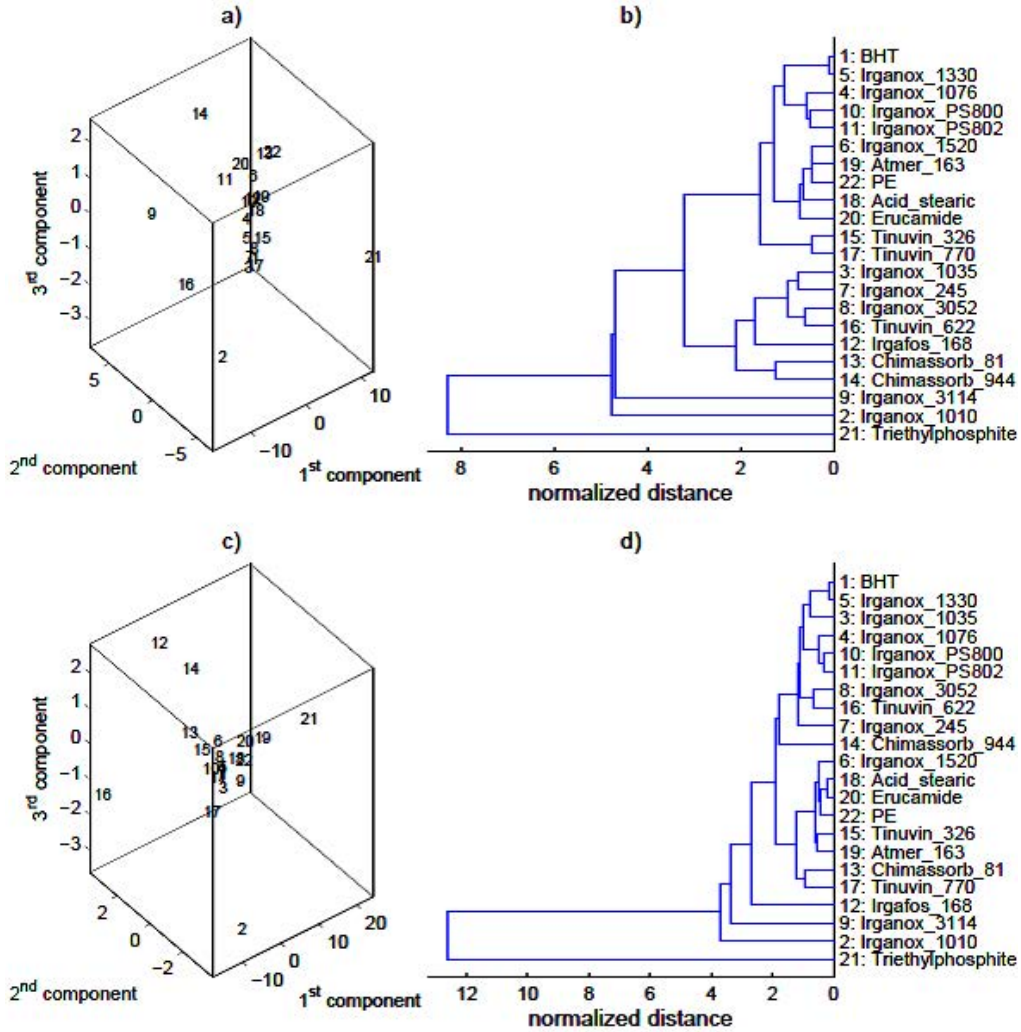

Figure 5. Distance map between spectra of tested substances: a-b) whole spectra, c-d) fingerprint region.

improvements for Irgafos 168 and Chimassorb 81. On one hand, the small distances generally observed between spectra confirmed the mathematical ill-posedness of the inversion of Eq. (6). On the other hand, the distances maps suggested that clustering of molecules with spectra a normalized threshold distance (e.g. 0.5), could help to identify the number of some typical chemical patterns present in the mixture. Thus, although BHT, Irganox 1330, Irganox 1035 and Irganox 1076 had very similar spectra, the concentration in BHT patterns could be guessed from their responses in the fingerprint region as they were almost proportional to the number of embedded BHT, respectively 1, 4, 2 and 1.

Biases estimates on binary mixtures

Previous considerations were based on well-defined spectra of molar extinction coefficients and not on crude spectra of mixtures. In addition, they did not take into account and the cutoff distance introduced by the inversion procedure itself. Biases associated to the similarities among the 21 additives were calculated by applying the whole procedure to all combinations of binary mixtures. A white noise level of 5 % was added to all mixtures and the concentrations were sampled from 500 repetitions. The biases were linearly decomposed according to Eq. (8). To assess the relevance of non-negativity constraints, detection biases were calculated according to unconstrained solutions of Eq. (6). The systematic bias, β_{00}, was found not significant. The other

Figure 6. Identification biases on Y for binary mixtures X+Y as defined in Eq. (8) when Y is not present in the mixture: a-b) average false detection level generated by all substances X listed in the dictionary, $\left\langle \beta_{X0}^{XY} \right\rangle_Y$ and $\left\langle \beta_{X0}^{all} \right\rangle_Y$ **;** c-d) average false detection levels generated by the substance X on all possible Y listed in the dictionary, $\left\langle \beta_{X0}^{XY} \right\rangle_X$ and $\left\langle \beta_{X0}^{all} \right\rangle_X$; e) false detection associated to a specific substance X. Biases in a and c were calculated with dictionaries containing only molecules X and Y whereas they were calculated with all 21 additives in b, d and e. Signed biases were obtained by removing non-negativity constraints in Eq. (6). Substances are ordered according to the distances between spectra plotted in Fig. 6b.

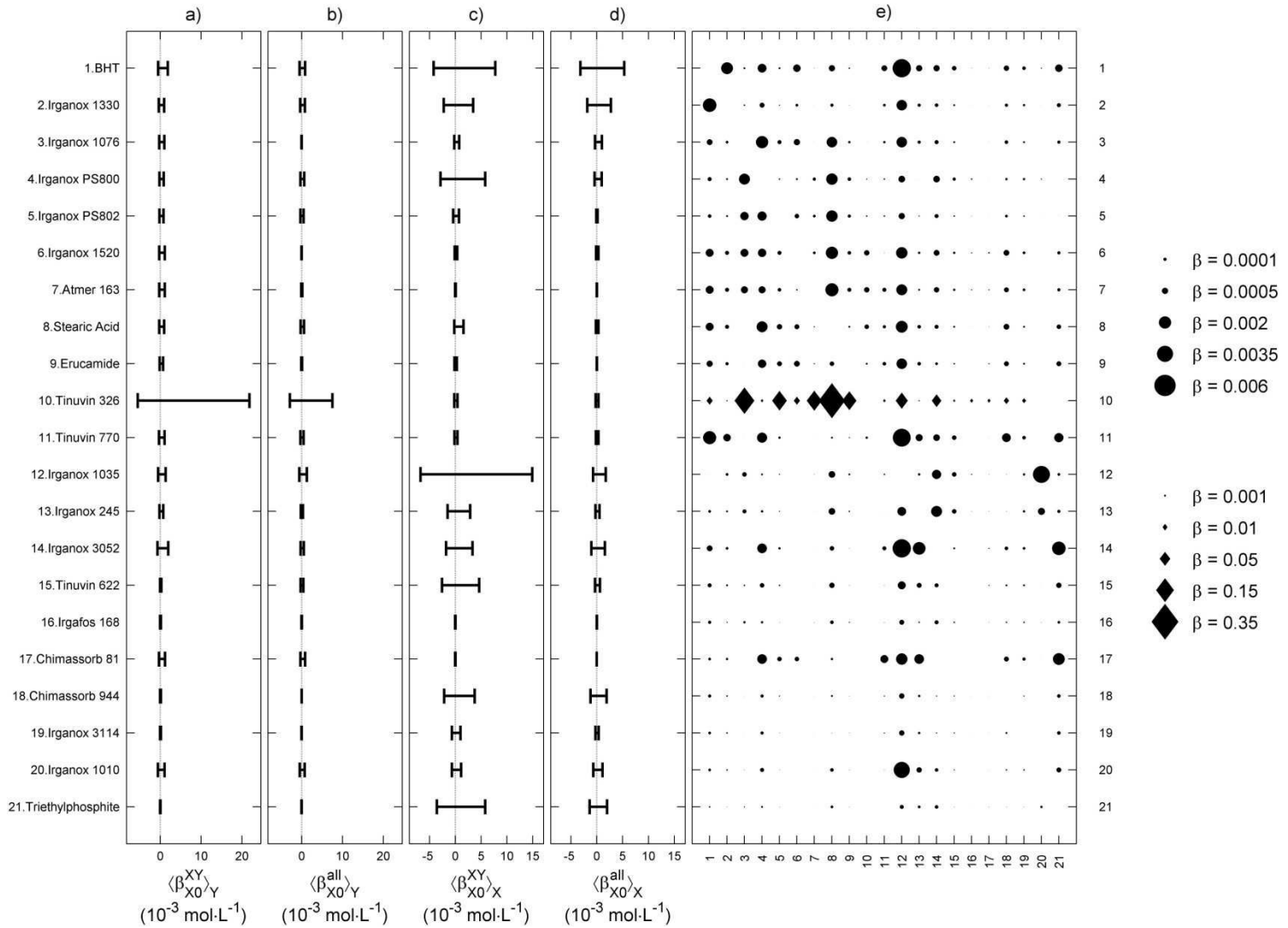

Figure 7. Quantification biases on Y concentration for binary mixtures X+Y as defined in Eq. (8): a) biases associated to Y alone when no W was added, $\langle \beta_{0Y} \rangle_Y$; b-c) average biases associated to increasing concentrations in X for all possible X; d) biases associated to a specific substance X. Biases in b were calculated with dictionaries containing only molecules X and Y whereas they were calculate with all 21 additives in a, c and d.

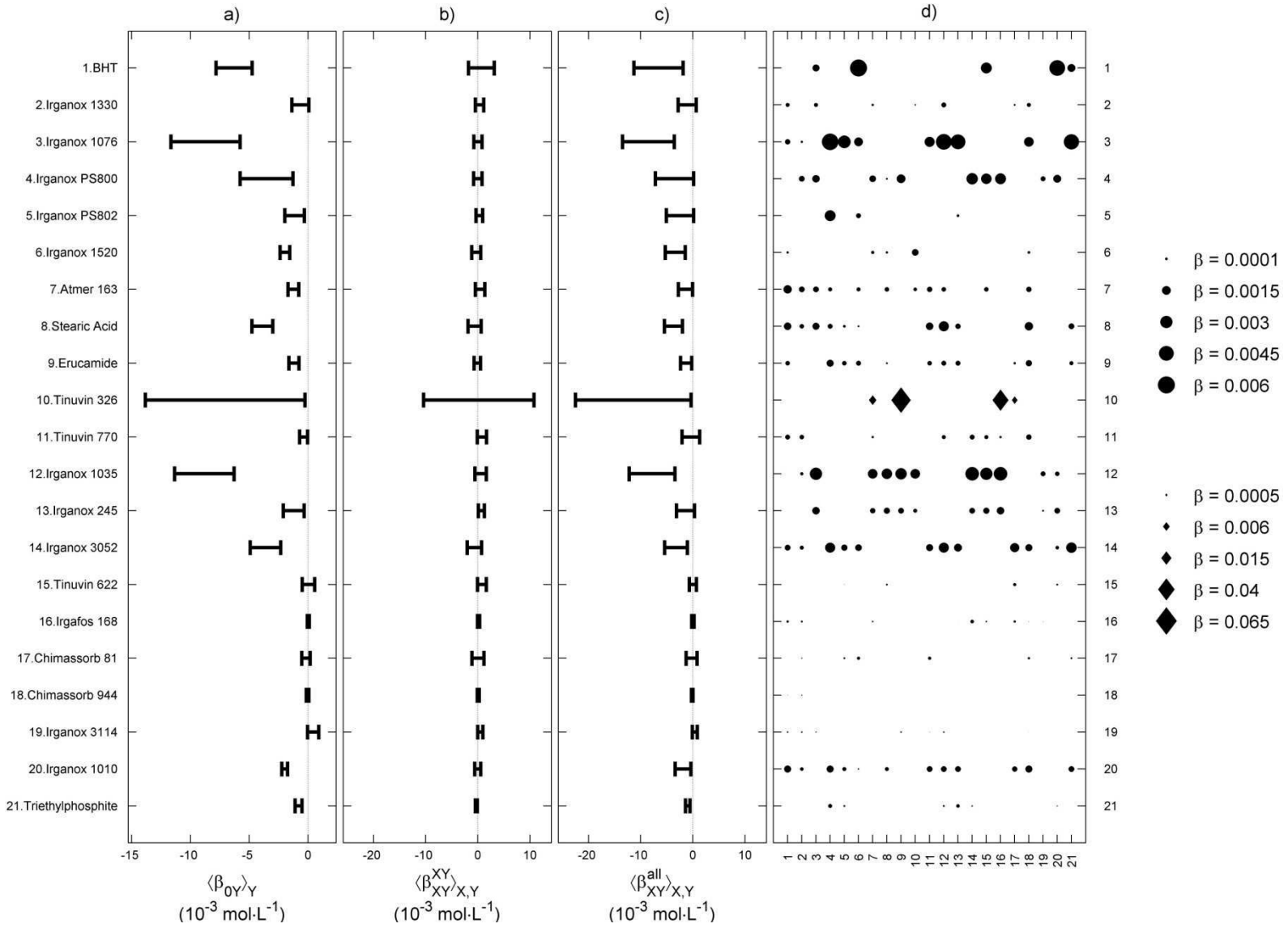

biases related to identification and quantification are summarized in Figs. 6 and 7 respectively for a dictionary including only the two tested molecules or the whole set of additives. All molecules were indexed according to the overall distances between spectra plotted in dendrogram 6b to highlight the correlations between biases and spectra closeness.

The disruptor character of a given substance in a mixture was assessed by a $\left\langle \beta_{X0}^{XY} \right\rangle_X$ or $\left\langle \beta_{X0}^{all} \right\rangle_X$ value different from 0 (Figs. 6a and 6b). Only Tinuvin 326, a ultraviolet absorber, including amines functions and a BHT pattern, acted as a "chimera" and hindered the detection of several substances with partial resemblance. Its signature was however unique and it was always detected, when it was present. Molecules subjected to an elevated risk of false positive were revealed by a significant positive bias $\left\langle \beta_{X0}^{XY} \right\rangle_Y$ or $\left\langle \beta_{X0}^{all} \right\rangle_Y$ (Figs 6c and 7d). On the opposite, molecules with high detection threshold were identified by a negative bias. Working with a large set of substances in the database reduced both risks by spreading the total variance on more degrees of freedom (i.e. more substances). The confusion matrix (Fig. 6e) revealed that all substances including a significant pattern such as BHT or several amine functions were subjected to significant detection threshold, as they might be replaced by molecules with a similar pattern. In practice, large spots in the confusion matrix read column-wise should be interpreted as falsely detected molecules susceptible to mask the one indicated on the row title. The masking intensity was expressed as the expected molar concentration in the true substance. Reciprocally, the same matrix read row-wise gave the underestimation factor due to a false assignment to other substances.

Quantification biases took into account the interactions between pairs of additives. Since these interactions were associated to confusion between substances, they were mainly negative. The true concentrations were on average lowered by a value $\left\langle \beta_{0Y} \right\rangle_Y$ when only the measured substance was present in the mixture (Fig. 7a). As expected from previous behaviors, the negative deviation was maximal for Tinuvin 326 and molecules including a BHT pattern. The introduction of a second substance increased the previous trend with an additional deviation $\left\langle \beta_{XY}^{all} \right\rangle_Y$ mostly negative (Fig. 7c). The confusion matrix extended to quantifications (Fig. 7d) assessed the average amount, which should be related to the molecule read row-wise.

Deconvolution of theoretical complex mixtures

In practice, mixtures are expected to contain more than two unknown substances and a significant amount of oligomers and other residues from the polymer, denoted PE. In addition some substances can be missing in the dictionary. To assess the performance of the identification procedure defined by Eq. (6), three typical situations were theoretically constructed from the individual spectrum of each substance:

- extract A: 5 substances with low binary biases and PE; all substances are indexed in the dictionary;
- extract B: 3 substances with significant binary biases and PE; all substances are indexed in the dictionary;
- extract C: 5 substances and PE; 3 substances are not indexed in the dictionary (3 columns are removed from $\underline{\underline{\Delta}}$);

To match real extracts, the concentration in PE was set to contribute to 15 % to the whole variance of the measured spectrum. The inversion procedure was applied on the synthesized spectra including 5 % of white noise. To retrieve a reliable statistics (5% and 95% percentiles), the whole process was reiterated 500 times. All determinations relied on a large dictionary,

Figure 8. Identification and quantification capabilities on three typical synthesized mixtures including 5% white noise: a) extract A, b) extract B, c) extract C. Spectra include the synthesized spectrum, *S*, the calculated spectrum after identification, S_{calc}, and the residues, ε. Calculated concentrations in DCM are gathered as intervals for all listed species in the dictionary. Each interval represents the 95% confidence intervals based over 500 repetitions. Zeroed concentrations in the solution have an signed value equal to the theoretical detection limit (DL). True concentrations appeared as open triangles. Chemical functions are reported only when their concentrations were determined non null.

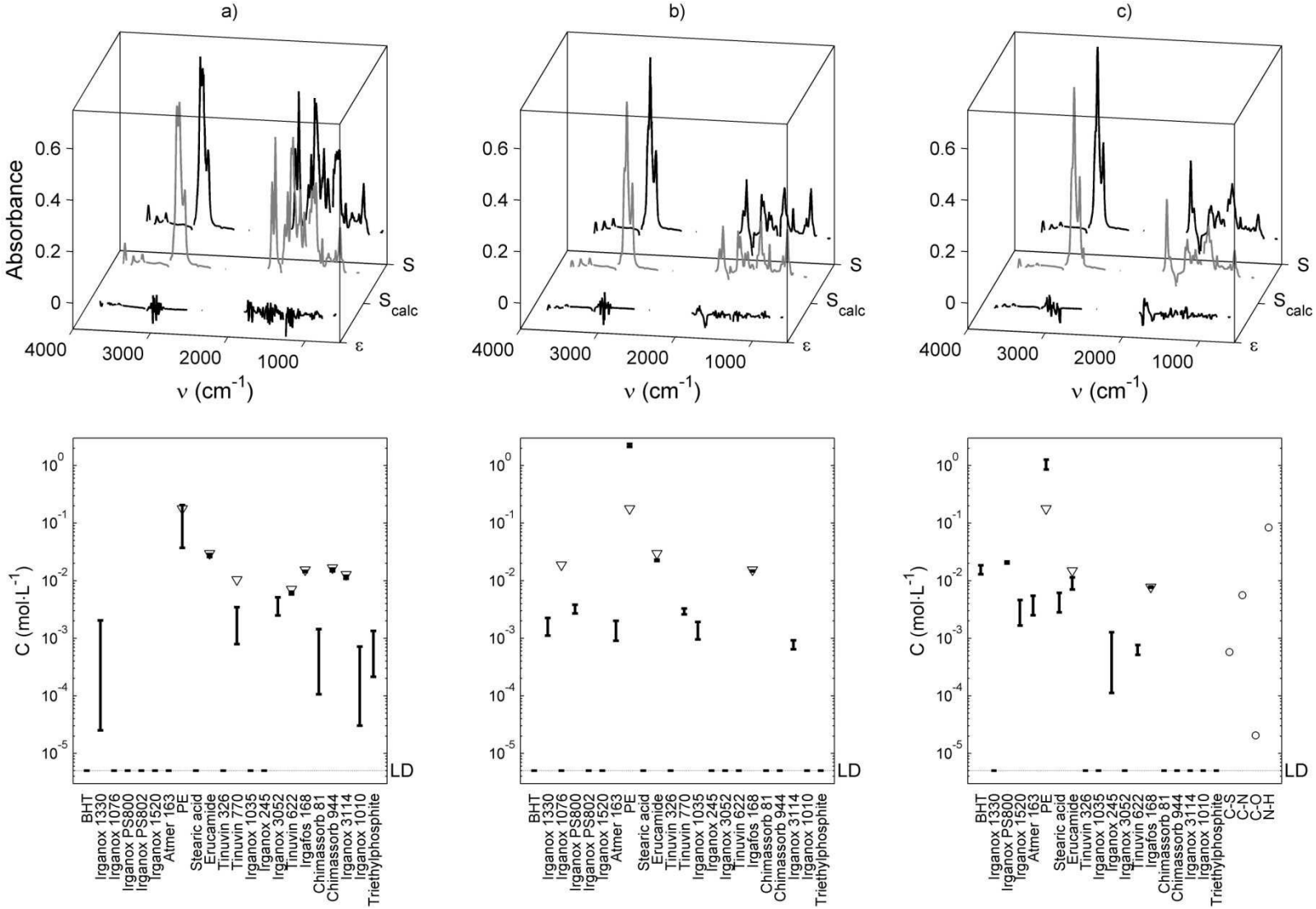

Figure 9. Identification and quantification capabilities on four real extracts from high density polyethylene films: a) PE1, b) PE2, c) PE3, d) PE4. The data are expressed as in Fig. 9 except the concentrations are reported in the initial processed films instead of in the extracts.

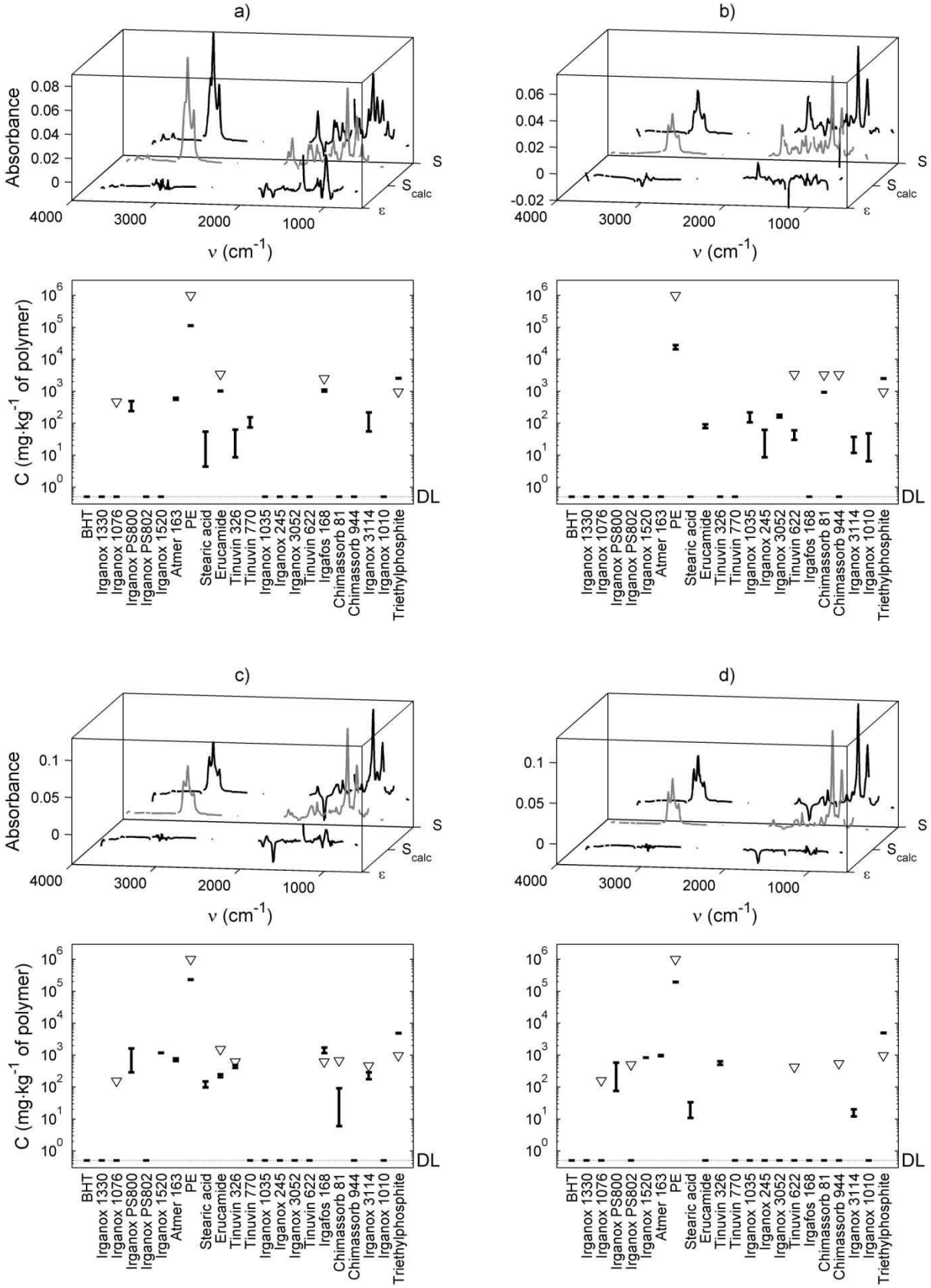

including 21 substance accessions, except for extract C where only 18 entries were considered, and including 4 chemical group accessions: C-S, C-N, C-O and N-H. Residues spectra and identified concentrations for all molecules and chemical groups presented in the database are plotted in Fig. 8. To help the identification a possible false assignation of substances, the molecules were ordered according to the overall distances between spectra as plotted in Fig. 5b. It is thus highlighted that a concentration attributed to a given substance could be also shared with molecules in the neighborhood. As concentrations were molar concentrations, the mass balance between homologous molecules could be determined.

In extract A, all molecules were well identified with predicted concentrations in good agreement with theoretical ones (Fig 8a). Due to the presence of some false positive, the concentrations tended to be underestimated. False positive were easily separated from real additives as they concentrations were one magnitude order much lower. In real processed materials, they would appear with concentrations much lower than those recommended by the industry. It is underlined that the solution remained mainly sparse and that no additional functional group was introduced by the resolution algorithm. As they are subjected to different specific migration limits, the separation between primary antioxidants (Irganox 1076, Irganox 1010, Irganox 3114), secondary antioxidants (Irgafos 168) and light stabilizer (Chimassorb 944) was particularly remarkable.

A similar behavior was observed in extract B (Fig. 8b). Irganox 1076 was however not identified and was replaced by a false positive Irganox PS800 with very a similar absorption spectrum (Fig 4). The surface agent Atmer 163 tended to be mistaken for polyethylene residues. Besides, as Irganox 1076 presented an aliphatic group similar to octadecane, it led to a significant overestimation of polyethylene residues contribution.

Mixture C was a complex case, where Irganox 1076, Irganox PS802 and Tinuvin 770 were present in the mixture with respective concentrations of 20 $mol \cdot L^{-1}$, 7 $mol \cdot L^{-1}$ and 10 $mol \cdot L^{-1}$ but missing in the dictionary $\underline{\underline{\Delta}}$. Under constraints of non-negativity, the total variance could not be explained by the listed substances alone and four additional functions were additionally identified. Although its spectrum was unknown, Irganox 1076 was substituted in a consistent manner by BHT and Irganox PS800 with a very similar spectrum (Fig. 4). The introduction of C-S and N-H functions were a reliable signatures of molecules belonging to the family og Irganox PS802 and Tinuvin 770 respectively. As the spectra of such functions were idealized, they could not be used for quantification.

Examples follow-up drove some practical conclusions. Phosphorous acid esters such as Irgafos 168 were well identified and quantified. Chimassorb 944, Tinuvin 622 and Irganox 3114 were well quantified but subjected to false positive. Erucamide was identified but its concentration was underestimated. Irganox 1076 because was never identified, whatever it was present or not, and was systematically replaced by Irganox PS800. Removing Irganox PS800 from $\underline{\underline{\Delta}}$ corrected the situation but it was not a reliable choice on commercial samples. The overall approach was enough robust to propose additional functions were a compound in the mixture exhibited a spectrum sufficiently different from those recorded. The procedure can be easily enriched by the introduction of new substances.

Deconvolution of the extracts of real formulations

In previous examples, the deconvolution was applied to mixtures were each compound was introduced with nominal concentrations. Within a real mixture the deconvolution was complicated by a

contribution to the total variance, which was highly inhomogeneous. In order to get multi-scale deconvolution procedure either on major and minor substances, the following two-pass deconvolution procedure was applied to four different real formulations of HDPE, denoted $\{PE_i\}_{i=1..4}$:

1) application of normal weights, W, to all wavenumbers and identification;
2) reweighting W according to $1/|\varepsilon_\nu|$ from previous step and identification restricted to the non fingerprint region (above 1500 cm^{-1});
3) reweighting W according to $1/|\varepsilon_\nu|$ from previous step and identification restricted to nitrogen-containing compounds between 1500 and 2500 cm^{-1} and beyond 3200 cm^{-1};
4) all previous steps were reiterated by starting from step 3 down to step 1.

The concentrations of minor compounds, which explained less than 20% of the total variance, were defined as the maximum the six determinations. The concentrations of other compounds were derived from step 1 alone to prevent additional biases due to non-linear approximations of spectra deviations. The two-pass deconvolution in forward and reverse order with iterative reweighting ensured that details in the non-fingerprint region, which supports most of the variance, could be revealed without introducing a large numbers of false-positive. The overall sparsity of the solution was controlled thanks to non-negativity constraints applied to all steps. Spectra obtained at step 1 and final concentrations after the two-pass deconvolution are plotted in Fig. 9. The concentration results are expressed in the usual manner for compliance testing in $mg \cdot kg^{-1}$ of polymer. An arbitrary threshold of 0.1 $mg \cdot kg^{-1}$ was applied to all unidentified substances. Confidence intervals were obtained by adding 5% white noise to the measured spectrum and by repeating the whole procedure 500 times. This protocol contributed via stochastic resonance to enhance the response of the deconvolution procedure to small contributions.

Although the identification was not exact for all substances, the magnitude orders agreed well the real contents. False positives appeared at much lower concentrations (traces) or involved molecules with very close spectra and/or with close chemical structure. As a rule of thumb, most of false positive were reliably identified by large confidence intervals over about one magnitude order. Exceptions appeared for linear molecules easily confused with polymer residues such as Atmer 163 and for molecules including presenting several BHT patterns. Due to false positives, the concentrations of most identified substances were underestimated.

In details, PE1 had a composition close to the previous extract B and exhibited a very similar behavior. Irganox 1076 was replaced by Irganox PS800 and in a less extent by Tinuvin 770. Triethylphosphite and Erucamide were well identified. According to Fig. 7e, the underestimation would be caused by 1076, Erucamide and triethylphosphite. PE2 contained ultraviolet 3 light absorbers and two detected. Chimassorb 81was reliably detected whereas Chimmassorb 944 was mistaken with very similar polymeric antioxidants Irganox 3114 and Irganox 1010 as predicted by Fig. 7e. Similarly, the Tinuvin 622 extent was partly replaced by an amount of Irganox 3052. PE3 and PE4 were very realistic formulations of polyethylene including primary antioxidants, secondary antioxidants and light stabilizers. The method identified either the right substance or the immediately adjacent substances. The analyses were highly convincing in PE3 while they were more difficult to interpret in PE4. Two substances or analogous ones were however not identified in PE4: Irgafos 168 and Tinuvin 622. As both additives are polymeric and highly reactive, they might be identified as smaller additives with similar chemical

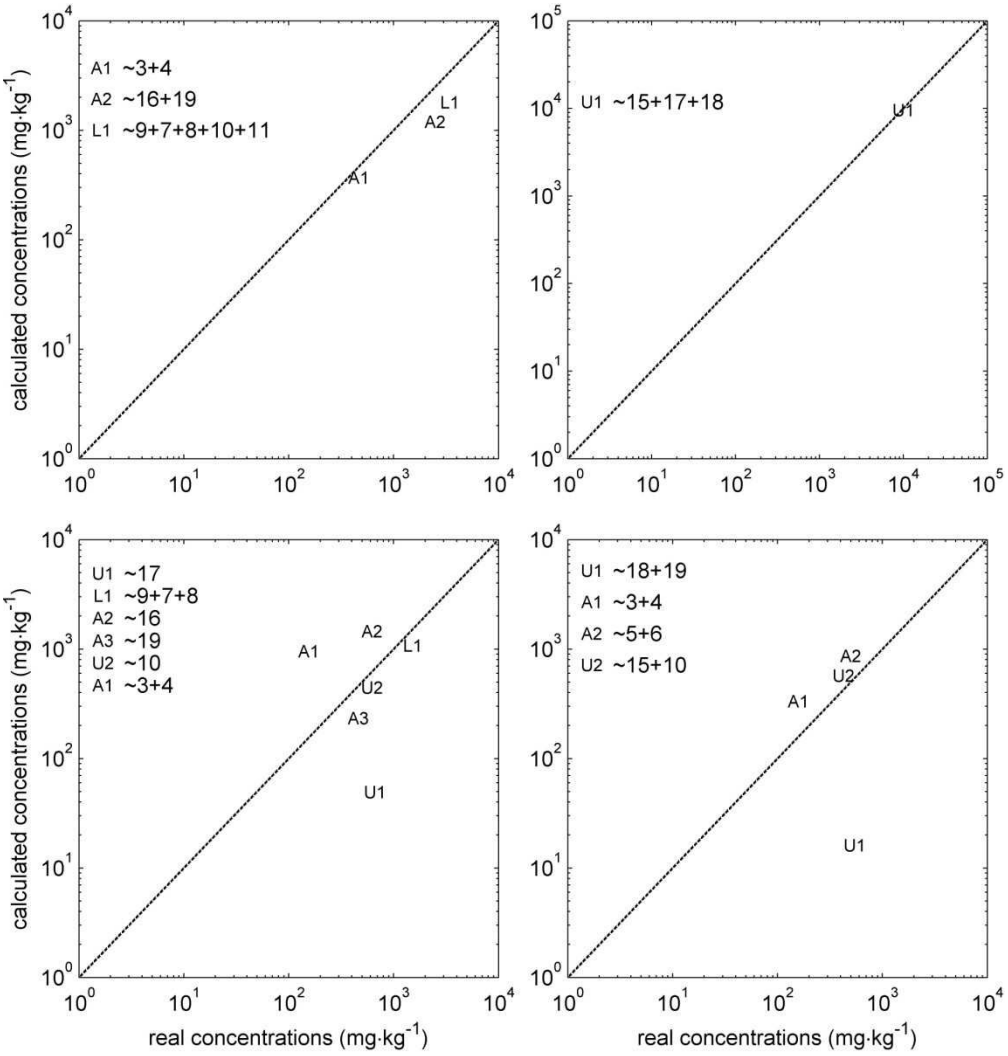

Figure 10. Mass balance in substances with similar technological functions against the theoretical extent in processed films: a) PE1, b) PE2, c) PE3 and d) PE4 plotted in Fig. 10.

formula. Tinuvin 326 could thus replace Tinuvin 622. The last poorly identified substance, Erucamide, was replaced consistently by Atmer 163.

The ability of the whole approach to predict the lumped concentration of additives with a similar technological function is presented in Fig. 10 by plotting the calculated lumped concentrations against the real ones. This approach made it possible to merge reconstructions from substances with tangled spectra. The predictions were in well agreement for primary and secondary antioxidants, ultraviolet light absorbers. Significant underestimation occurred only for surface modifiers.

Separation of additives by their chemical functions

As tested phenolic antioxidants additives were polymeric and could be confused with other hindered molecules such as light stabilizer, their absolute identification was a stiff mathematical problem. As an example, the ubiquitous Irganox 1076 was commonly mistaken with a less common antioxidant Irganox PS800. A possible strategy to identify robustly Irganox 1076 and to contribute to separate antioxidants between several alternatives was to obtain a signature of the two patterns characteristic of Irganox 1076: the BHT head and the complementary tail, including an ester function and an octadecane

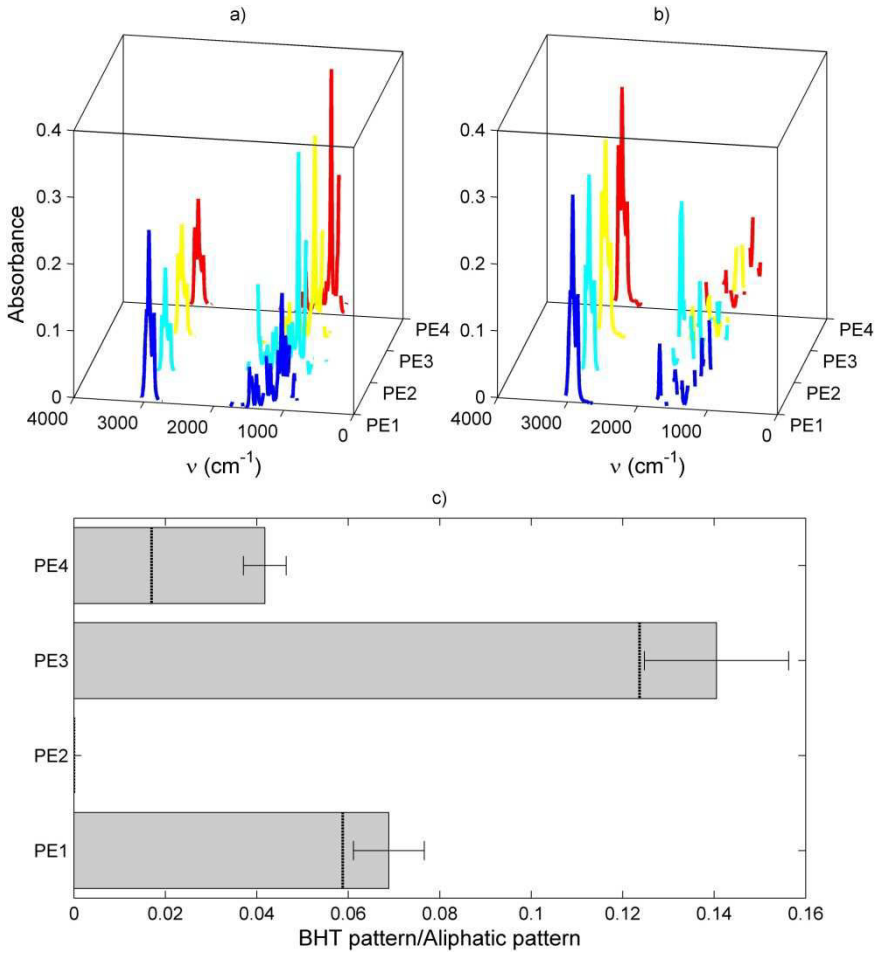

Figure 11. Absorption spectra of extracts of processed films by considering: a) nominal weights for the BHT pattern, b) nominal weights for an aliphatic pattern similar to the Irganox 1076 tail; ratio of concentrations between previous patterns.

pattern. Because PS800 does not include any BHT pattern, the presence of Irganox 1076 could be very likely as soon as the ratio between the number of BHT head pattern and the number of tail pattern would be significantly greater than 0. On the opposite, a value closer to unity would reveal the presence of a significant amount of polymeric hindered phenolic antioxidants. Values greater than 1 were by contrast very unlikely as the signature of the tail was common several additives. The signature of the tail in Irganox 1076 was retrieved by subtracting the BHT contribution from the molar spectrum of Irganox 1076. Optimal wave numbers weighting for each pattern was derived by studying the linearity of the spectrum with concentration. The molar concentration ratios inferred from specific deconvolutions of previous extracts are summarized in Fig. 11. The exact ratio, which accounted all linear molecules, is also plotted for comparison.

Although the ratio did not sign any substance, it supported unambiguously that PE2 did not contain any phenolic antioxidant and that the composition in phenolic antioxidants in PE3 was significantly different from PE1 and PE4 with a likely presence of a polymeric antioxidant. It confirmed thus the presence of Irganox 3114 including three BHT patterns in PE3 (Fig. 9c). By contrast, the lower ratio in PE4 confirmed the presence of a significant amount of aliphatic thioethers, identified as Irganox PS802 (Fig. 9d). The predictions of this ratio were highly reliable and provided an additional framework to choose between several alternatives.

Other ratios were found to be valuable to improve predictions presented in Fig. 9 at least qualitatively. Table 3 present the

relative concentrations in some specific patterns as they were identified. Among them, the acid pattern found in PE1 was related to stearic acid, which was poorly identified with the global procedure. The piperidinyl group typical of Tinuvin 770, Tinuvin 622 and Chimassorb 944 was accurately detected in PE2 and PE4 where as none of them were initially detected. Other patterns such as the ester function and ring patterns in Irganox 1330 and 3114 were not identified, as they were either not accurately calibrated by successive subtractions of spectra or not supported by a significant variance in the measured spectra.

CONCLUSIONS

A semi-supervised deconvolution procedure of FTIR spectra based on a ridge regression procedure has been described to identify and quantify the concentrations of plastics additives in polymer extracts. The methodology was designed to work obtained on complex mixtures including several compounds with either known or unknown compounds. The proposed formulation offered a consistent weighting procedure to derive sparse solutions focused either on substances, chemical functions or a combination of both. This strategy was particularly suited to polymeric additives including a repeated pattern. The automatic switch between a global or a local solution was performed using an iteratively re-weighted least square criterion, which either zoomed or unzoomed on unexplained spectra residues. As the added non-negativity constraints acted as a Wiener filter, they avoided false positives while imposing a sensory threshold to small contributions involving 1% or less of the total variance in the measured spectrum. This inherent limitation was partly corrected by invoking systematically stochastic resonance effects by Monte-Carlo sampling. Adding randomly a white noise to the measured spectrum caused low signal intensities to cross more often the identification threshold and offered statistics to our non-linear identification technique.

The whole technique has been implemented within a specific Matlab toolbox (Mathworks, USA), so-called ACTIA-LNE, and calibrated on 21 common additives of polyolefins and 4 chemical functions typical of possible non-listed substances. As the calibration method took into account the linearity and detection limit of the spectrophotometer, the generated dictionary of spectra and related optimal weights depended on the experimental device and could not be transposed to commercially available FTIR spectra databases. However, although the method has been applied to extracts in dichloromethane, it could be directly applied to processed films in transmission mode or in attenuated total reflectance. The only difficulty came from the ability to subtract the background. In our extracts, the background was both related to the intense bands of dichloromethane and to polymer residues (oligomers mainly). Since the olymer background could not be known a priori, three commercial virgin flakes of high density polyethylene were used to assign a normalized spectrum to polymer residues. The theoretical concentration associated to these residues was therefore an additional unknown in the inversion problem.

The ill-posedness of the general deconvolution problem was assessed by calculating the distances between spectra, the identification and quantification biases for all possible binary mixtures. A table of confusion was generated to support the interpretation of false positives, masking effects and possible sources of underestimations. The whole procedure was applied to 4 theoretical and 4 real mixtures including up to 8 compounds. In all cases, the method provided valuable conclusions by either identifying the right substances or substances which were chemically close. The determination of the lumped concentration of substances with a similar technological function

(antioxidants, light stabilizers, surface agents) was as reliable as techniques involving a physical separation such as chromatographic techniques. In real conditions, the "absolute" identification of additives was possible only for some substances. Appropriate identification and quantification were revealed by low confidence intervals and values in agreement with good manufacturing practice. Poorly identified or quantified analysis required an additional interpretation of spectra based on specific chemical functions.

Although some fuzziness may remain after deconvolution, the identification of possible migrants and of their amounts in a packaging material is of prime importance to start an assessment of its compliance with EU regulations. Indeed for most additives and contact applications, abacuses or softwares are available to calculate the maximum amount in the polymer, which could permit to demonstrate the compliance with mathematical modeling[7]. Due to inherent uncertainty in physic-chemical properties, these approaches do not claim to predict the real migration rate but an overestimate instead with sufficient safety margin. As a result, the subsequent steps should focus only on situations (substances and concentrations) for which the compliance could not be demonstrated with the previous approach. Next steps might include a discussion with the provider or complementary measurements with conventional techniques. A companion work aims at integrating databases, simulation tools and fast identification by FTIR methods to design automated decision tools to assist enforcement and control laboratories in identifying non compliant plastics materials intended to be in contact with food. As a rule of thumb and in case of doubt on the real substance, it is worth to notice that a polymeric additive including n sub-units can be always replaced by a migrant consisting in a single unit at a concentration n times higher. The question for compliance testing is then: "Which value of n could demonstrate the compliance?". When the calculated n is suspected to be too small, a validation by or with the provider is required.

As the methodology was proven to be quantitative at least for lumped additives, it might be also envisioned to monitor desorption rates during standard migration tests.

ACKNOWLEDGEMENTS

The authors are grateful for the financial support received from the Association de Coordination Technique pour l'Industrie Agroalimentaire and the Association Nationale pour la Recherche Technique. The authors would also like to thank D. Tissier (Centre d'Appui et de Stimulation de l'Industrie par les Moyens de l'Innovation et de la Recherche, France) for her technical assistance.

REFERENCES

1. European Commission Directive *Official J* 2002, L220, 18.
2. European Commission Regulation *Official J* 2004, L338, 4.
3. European Commission. Substances listed in EU directives on plastics in contact with food. http://ec.europa.eu/food/food/chemicalsafety/foodcontact/eu_substances_en.pdf. 2008.
4. European Commission. COMMISSION DIRECTIVE 2007/19 *Official J Eur Union* 2007, L97, 50.
5. European Commission. COMMISSION DIRECTIVE 2023/2006 *Official J Eur Union* 2007, L384, 75.
6. Vitrac, O.; Hayert, M. *AIChE J* 2005, 51, 4, 1080-1095.
7. Vitrac, O.; Hayert, M. In *New trends chemical engineering research*, Berton, L.P., Ed.; Nova Science: New York, 2007; pp251-292.
8. Feigenbaum A., Scholler D., Bouquant J., Brigot G. , Ferrier D., Franz R. , Lillemark L. , Riquet A. M., Petersen J. H. , Van Lierop B., Yagoubi N. *Food Add Contam* 2002, 19, 184-201.
9. Bart, J. C. J. *Additives in polymers: Industrial analysis and applications*; John Wiley & Sons: Chichester, 2005.
10. Choller D., Vergnaud J. M., Bouquant J., Vergallen H., Feigenbaum A. *Packag Technol Sci* 2003, 16, 209-220.

11. Bart, J. C. J. *Plastics Additives: Advanced Industrial Analysis*; Ios Pr Inc.: Amsterdam. 2006.
12. Hummel D. O. *Atlas of Plastics Additives: Analysis by Spectroscopic Methods*. Springer-Verlag : Berlin. 2002.
13. Vigerust, B.; Kolset, K.; Nordenson, S; Henriksen, A.; Kleveland, K. *Appl Spectrosc* 1991, 45, 173-177.
14. Norman S. Allen, Simon J. Palmer, G. P. Marshall, Jean Luc-Gard. *Polym Degrad Stabil* 1997, 56, 265-274.
15. Zehnacker, S.; Marcha, J. *Polym Degrad Stabil* 1994, 45, 435-439.
16. Möller, K.; Gevert, T.; et Holmström, A. *Polym Degrad Stabil* 2001, 73, 69.
17. Földes, E.; Maloschik, E.; Kriston, I.; Staniek, P.; Putanszky, B. *Polym Degrad Stabil* 2006, 91, 479.
18. Yagoubi, N.; Denuzière, A.; Pellerin, F.; Ferrier, D. *Ann Phar Fr* 1996, 54, 126.
19. Vitali, M. *Polym Test* 2001, 20, 741.
20. Bagnati, R.; Blanchi, G.; Marangin, E.; Zuccato, E.; Fanelli, R.; Davoli, E. *Rapid Commun Mass Spec* 2007, 21, 1998-2002.
21. Sun, C.; Chan, S. H.; Lu, D.; Lee, H. M. W.; Bloodworth, B. C. *J Chromatogr A* 2007, 1143, 162-167.
22. Tikhonov, A.N.; Arsenin, V. *Solution of ill-posed problems*; Wiley: New-York, 1977.
23. Hansen, C. *Numer Algorithms* 1994, 6, 1-35.
24. Coleman, T.F.; Li, Y. SIAM *J Optimiz* 1996, 6, 1040-1058.
25. Garrido-López, Á.; Tena, M.T. *J Chromatogr A* 2005, 1099, 75-83.
26. Stuart, B. *Infrared Spectroscopy: fundamentals and applications*. John Wiley and Sons: Hoboken. 2004

3. Approche complète de vérification de la conformité des matériaux destinés au contact alimentaire

Une méthode rapide d'identification et de quantification des additifs contenus dans un PEHD ($C_{i,P}|_{t=0}$) a été proposée. La comparaison de ces $C_{i,P}|_{t=0}$ avec les $C_{i,P}|^{max}$ permet de prendre une décision rapide quant à la conformité du matériau pour le contact alimentaire (Figure 3.2).

Dans une logique d'aide à la décision, il paraît intéressant de combiner les deux approches, prédictive et expérimentale, développées dans les deux parties précédentes. Différents scénarios peuvent être envisagés selon le degré de connaissance du matériau et des paramètres nécessaires à la modélisation (additifs présents, quantités connues, disponibilité de valeurs robustes de $D_{i,P}$ et/ou $K_{i,F/P}$). Un grand nombre de valeurs expérimentales de $D_{i,P}$ sont aujourd'hui disponibles pour les PEs. Nous avons par ailleurs choisi d'utiliser le modèle de prévision basé sur les descripteurs géométriques des molécules pour les substances non étudiées expérimentalement. Les valeurs de $K_{i,F/P}$ peuvent être déterminées en utilisant les modèles développés en partie 1. Lorsqu'une donnée est supposée manquante dans le scénario, un surestimateur est utilisé (modèle de Piringer pour $D_{i,P}$; 1000 pour $K_{i,F/P}$). Trois cas différents peuvent se présenter dans les scénarios pour la $C_{i,P}|_{t=0}$: i) elle est connue et utilisée ; ii) elle est inconnue et un surestimateur est utilisé (quantité maximale conseillée par le fabricant de la substance) ; iii) elle est inconnue et une valeur de $C_{i,P}|^{max}$ est recherchée à partir des données connues.

Ainsi, nous nous proposons dans une troisième partie de combiner les approches pour établir des règles de décision. Ces travaux ont fait l'objet d'une publication, soumise à *Food Additives and Contaminants*, dans laquelle des exemples sont étudiés pour 7 migrants potentiels, dont des additifs des matériaux plastiques et un photo-initiateur d'encres d'impression. Dix scénarios sont envisagés selon le degré de connaissance du matériau et des paramètres décris dans le paragraphe précédent. Une discussion est proposée dans le but de sélectionner les expérimentations justes nécessaires pour démontrer la conformité des matériaux (plutôt que de prévoir la migration exacte de substances dans les aliments).

Development of decision tools to assess the migration from plastic materials in contact with food

G. Gillet[a,b], O. Vitrac[1c], D. Tissier[d], P. Saillard[e], S. Desobry[b]

[a] *Centre Energie, Matériaux et Emballage, Laboratoire National de métrologie et d'Essais, 29 avenue Roger Hennequin, 78197 Trappes CEDEX, France;* [b] *Laboratoire de science et génie alimentaires, Nancy Université-INPL, 2 avenue de la forêt de Haye, BP 172, 54505 Vandoeuvre lès Nancy, France;* [c] *UMR 1145 Génie Industriel Alimentaire, Institut National de la Recherche Agronomique , Agroparistech site de Massy, 1 avenue des Olympiades, 91300 Massy, France;* [d] *Pôle emballage, Centre d'Appui et de Stimulation de l'Industrie par les Moyens de l'Innovation et de la Recherche, 24 avenue des Landais, BP 154, 63173 Aubières CEDEX France.* [e] *Service Sécurité et Qualité des Emballages, Centre Technique de la Conservation des Produits Agricoles, Rue Henri de Boissieu, 01060, Bourg en Bresse, France*

Abstract

Testing the specific migration limits of all substances intentionally added to polymer material according to European Union (EU) regulation is a tedious and expensive task. Although mathematical modeling offers an interesting alternative, it fails to predict the migration in situations, which are less conservative than those encountered with simulant D. In addition, its application is of little use for end-users or enforcement laboratories, which do not have access to the formulation. This paper revises the paradigm of migration modeling by combining modeling with deformulation experiments and iterative modeling in the framework of decision theory. The complete approach is illustrated on polyolefins in contact with 50% ethanol for eight typical migrants, including hindered phenolic antioxidants and low molecular weight surrogates. Results of the national RA 05.22 ACTIA project on the identification of formulation fingerprints and on the prediction of partition coefficients with alcoholic and aqueous simulants were in particular considered. When the true migration was close but still lower than the limit of concern, the proposed compact decision tree, including up to four sources of uncertainty, showed that the chance of demonstrating compliance was about 3:4 in presence of one source of uncertainty, whereas it fell below 2:4 and 1:4 with two and three sources of uncertainty respectively. The recommendations for further sanitary surveys and future developments are discussed in the last section.

Key words: food contact materials, migration modeling, compliance testing, sanitary survery.

Introduction

For the last three decades, consumer exposure to chemicals from food packaging materials has attracted much public attention and interest of European regulation authorities. Thus, although the EU regulation is still in a consolidation phase, 502 substances (including 230 monomers and 272 additives) among the 937 which are positively listed in EU directives on plastics in contact with food (European Commission, 2008), are subjected to specific migration limits (SML) due to toxicological concern. The recent authorization of substances not belonging to the positive list, when they are located behind one or more layers, which prevents their migration into foods or food simulants above a detectable level (European Commission, 2007), complicated the assessment of compliance testing and requirements of traceability (European Commission, 2004). The introduction of modeling in directive 2002/72/EC (European Commission, 2002) as an alternative to time consuming migration testing was an appropriate

[1] Corresponding author.
Email: olivier.vitrac@agroparistech.fr

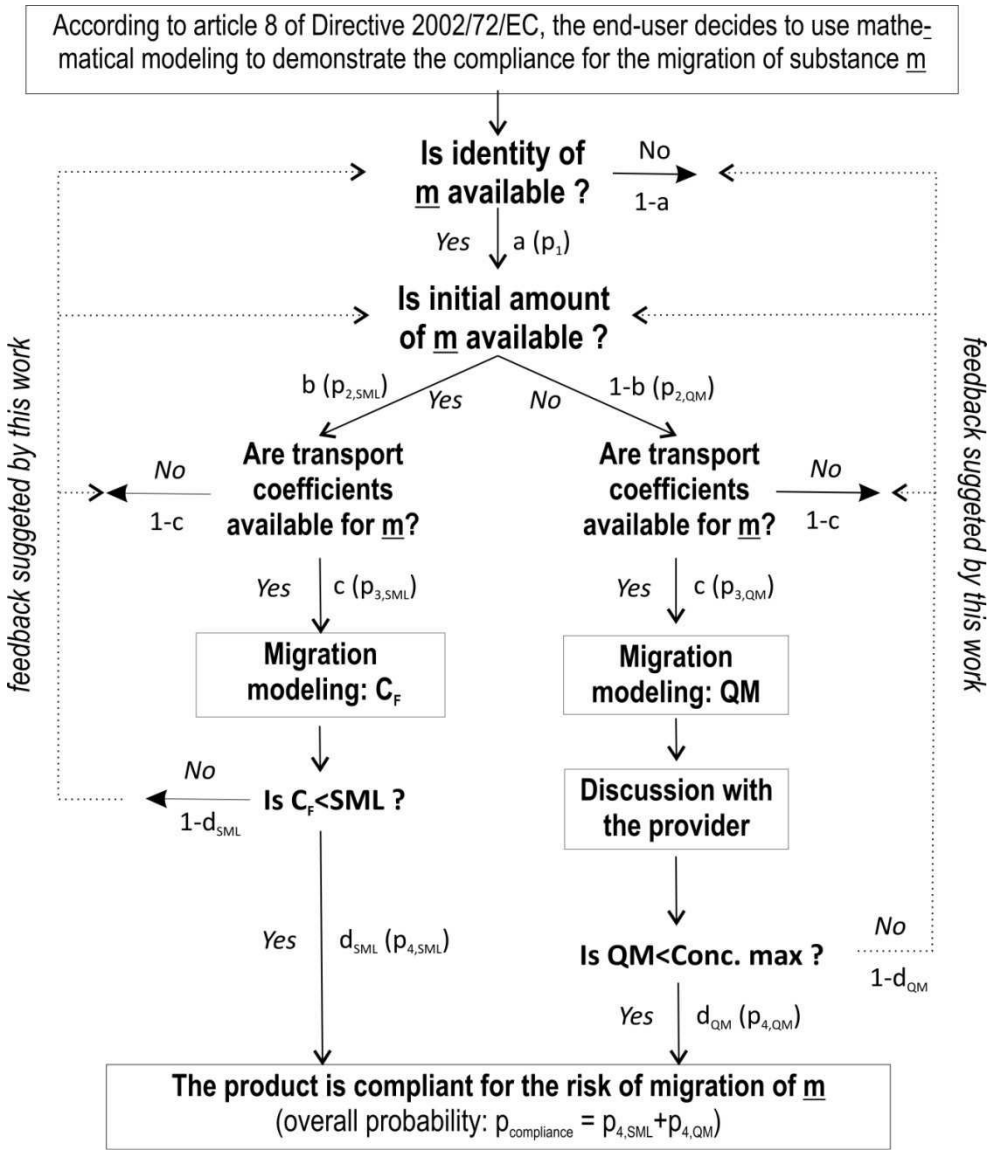

Figure 1: Decision diagram to demonstrate the compliance of plastic materials according to article 8 of directive 2002/72/EC. Current and modified transition probabilities of acceptation are gathered in table 1. Additional improvements via iterative modeling appeared as dotted lines.

response to the increasing sophistication of plastics materials on the market including multilayer materials, active or intelligent packaging, recycled polymers, nanocomposites… Despite significant collaborative works on the collection of diffusion coefficients (Begley *et al.*, 2005; Dole *et al.* 2006), the whole approach remains highly semi-empirical and insufficiently described in the literature according to their context of application. Most of studies are focused on punctual demonstrations that predictions based on worst-case scenarios overestimate the real migration (Franz and Welle, 2008). As a result, in the current framework, either worst-case modeling does demonstrate the compliance or migration testing must be performed. In practice, the highly asymmetric know-how and information along the food-packaging chain from producer batch to consumer fork is responsible for a strong uncertainty on consumer side, which lessen drastically the interest of modeling for end-users, enforcement authorities (Petersen *et al.* 2005) and sanitary survey authorities.

The very low utility of current predictive approaches, expressed as a probability to demonstrate the compliance, is illustrated

Table I. Transition and overall probabilities of the decision tree plotted in Figure 1. The final probability to demonstrate the compliance is denoted $p_{compliance}$. The values obtained with the current methodologies used at LNE (Laboratoire National de métrologie et d'Essais) and the expected values with the new proposed paradigm are compared.

	Notations	Current state at LNE	Expected value with the new methodology
Transition probabilities	a	5%	50%
	b	50%	75%
	c	10%	80%
	d_{SML}	90%	90%
	d_{QM}	50%	50%
Overall probabilities	$p_1 = a$	5%	50%
	$p_{2,SML} = a \cdot b$	2.5%	37.5%
	$p_{3,SML} = a \cdot b \cdot c$	0.25%	30%
	$p_{4,SML} = a \cdot b \cdot c \cdot d_{SML}$	0.20%	27%
	$p_{2,QM} = a \cdot (1-b)$	2.5%	12.5%
	$p_{3,QM} = a \cdot (1-b) \cdot c$	0.25%	10%
	$p_{4,QM} = a \cdot (1-b) \cdot c \cdot d_{QM}$	0.13%	5%
	$p_{compliance} = p_{4,SML} + p_{4,QM}$	0.33%	32%

as a decision diagram in Figure 1, where a probability of acceptation is associated to each alternative. Reference probabilities, gathered in Table I, were assigned according to the expertise obtained at the Laboratoire National de métrologie et d'Essais (LNE) and at the Institut National de la Recherche Agronomique (INRA). The current utility for a national reference laboratory as LNE is estimated lower than 3:1000 for most of monolayer cases. The main limiting factors are the identity of substances and their amounts in the starting materials. Additional limitations arise from the lack of realistic estimates of transport coefficients (diffusion coefficients and partition coefficients) in the conditions of storage. The combined effect of several sources of uncertainty including on composition and transport coefficients has been studied extensively for monolayer materials (Vitrac and Hayert, 2005) and extended to multilayer materials and multimaterials (Vitrac and Hayert, 2007) via a stochastic description of the contamination of food and an interval approach, respectively. They showed that the expected utility collapsed rapidly as soon as more than two sources of uncertainty were combined. Full modeling approaches independent on specific experiments has been applied on finished food products on the market (Vitrac *et al.*, 2007) and on consumer exposure (Vitrac and Hayert, 2007) only in rare occasions where a significant expertise on physicochemical properties of packaging materials was available.

This paper proposes to revise the paradigm of migration modeling by introducing modeling along with deformulation experiments and refined prediction scenarios, recently made available. The main objective was to combine several rapid experimental and numerical techniques to improve the expected utility value up to 1:3 (Table I),

in order to justify the additional costs induced by modeling (software licenses, training…). The final approach will be integrated in an expert system developed by INRA including databases and simulation tools. In this new framework, the issue is not to minimize the deviation between the predicted value and the real one, but determining the fastest decision path among possible alternatives to demonstrate the compliance in the first place. The demonstration relies either on a predicted value lower than SML or to a maximum value in the polymer (QM), acknowledged by the supplier to be higher than the true amount (Figure 1). The proposed four steps algorithm is particularly comprehensive for monolayer materials as few input parameters, x_i, are involved:

- Step 1: finding the most influencing set of inputs, $X = [x_1\ x_2\ \ldots x_n]$ for the considered conditions of migration (food packaging geometry, contact time and temperature…).
- Step 2: finding the optimal set x°, which leads to migration = SML (idem with QM).
- Step 3: for all inputs in the set, finding all conditions "$x_i<x_i°$" or "$x_i>x_i°$" to guarantee migration<SML.
- Step 4: check whether all conditions are likely according to values available in databases, additional modeling or to experiments.

The first step is the most critical because the number of influencing inputs, *n*, and their identities are not a priori known. Our objective was to analyze all four steps for polyolefins in contact with 50% ethanol as simulant of dairy products (European Commission, 2007). This situation was of significant concern as polyolefin materials represent nearly one third of all food packaging applications and currently no guidance exists to predict the migration in such a food simulant. Additional interest in such semi-crystalline materials was triggered by the recent validation of several alternatives to conventional migration testing. Overestimates (Begley *et al.*, 2005) and likely estimates (Vitrac *et al.*, 2006) of diffusion coefficients have been published for all substances, which do not cause blooming effects. The French national project ACTIA RA 0522 "decision tools for compliance testing" (ACTIA, 2005) contributed to generate missing steps in the predictive approach of the migration from polyolefins starting from the diagram depicted in Figure 1: i) rapid deformulation of materials from Fourier Transform Infrared spectroscopy (FTIR) absorption spectra of polymer extracts (Gillet *et al.*, 2008c), ii) prediction of partitioning between polyolefins and most simulants (alcohols, water and water-ethanol mixtures) from molecular simulations of molecular pair interactions (Vitrac and Gillet, 2008; Gillet *et al.*, 2008a and 2008b). The importance of deformulation to identify possible migrants and their extent has been already discussed in the conclusions of the EU AIR research program CT94-1025 (Feigenbaum *et al.*, 2002). For polymeric additives based on the repetition of a similar pattern, such as hindered phenolic antioxidants, FTIR offers additional worst-case scenarios based on an equivalent amount of high-diffusing free patterns. The direct calculation of activity coefficients at atomistic scale for both flexible and hindered migrants in various food simulants and in polyolefins widens dramatically the range of applicability of modeling for monolayer and multilayer materials. As the approach was validated in 51 different conditions and did not require any fitting procedure, it would replace advantageously both rough estimations suggested in the "practical guide" to European Directives (European Commission, 2003) and the semi-empirical group contribution devised for the partitioning of volatile substances (Baner and Piringer, 1991). Besides, direct calculations provided two important insights at molecular scale, which were

underestimated in previous works. On one hand, polymeric additives have a higher chemical affinity than their constitutive patterns for simulants. This entropic effect, which does not depend on chemical composition effects, was related to the increased number of micro-configurations to recreate simulant-simulant interactions (e.g. hydrogen bonding) when a large guest molecule was inserted among smaller host ones. The practical consequence is that the partitioning of large additives cannot be extrapolated from volatile substances. On the other hand, strong deviations from ideality in water-ethanol mixtures were found to be responsible for highly non-linear variations of partitioning with the volume fraction in ethanol, and where in contradiction from prior extrapolations in pure water. The practical consequence is that the lowest chemical affinity for the simulant is expected to be obtained with 20%-30% ethanol rather than in pure water.

The paper is organized as follows. The second section details the methodologies, assumptions and scenarios to assess the compliance according to the decision tree depicted in Figure 1 and the proposed four steps algorithm. As a quantification of the initial amount may be required, a fast extraction technique under pressure was compared with the conventional reflux method on a typical high density polyethylene (HDPE). Eight typical migrants of polyolefins were particularly considered. The photo-initiator used in printing inks, 2-isopropylthioxanthone (2-ITX), was included because it was recently found in several food products including dairy ones in spite of not being authorized in EU (Bagnati *et al.*, 2007; Sun *et al.*, 2007; Rothenbacher *et al.*, 2007). The main experimental and simulated results are presented in the third section. Biases due to possible incomplete extractions of semi-crystalline polymers, which are insoluble in solvents, were tabulated according to the number of extraction steps as suggested by Choller *et al.* (2003). The effect of inputs on migration and on the ability to demonstrate the compliance was analyzed by ranking all prediction scenarios. Important insights on other migrants can be easily replicated by simple geometric constructions. The findings and provides recommendations for its generalization in good manufacturing practices and quality auditing purposes are summariezd in the last section.

Materials and methods

Tested substances

Tested substances are listed in Table II. They were chosen to be representative of most technological functionalities in polyolefins. Irganox 1330 and Irganox 3114 were proposed as typical polymeric phenolic hindered antioxidants. As they include three BHT patterns, they can be easily mistaken with dispersed BHT molecules in FTIR spectroscopy, with an equivalent concentration assessed three times higher than the true one. Erucamide is an unsaturated long chain carboxylic acid amide used as slip agent, anti-fogging, or lubricant in plastic films. As it is only partly compatible with polyethylene, its migration does not obey to Fickian diffusion and migration modeling cannot be applied. As a result, it was only used in extraction experiments as a prototype of substance poorly dispersed in polyolefins. Two typical low molecular weights surrogates, which are not intentionally added substances into plastics, were also included: 2-ITX and diphenylmethane. The latter was introduced as partitioning data have already been published by Baner and Piringer (1991).

Evaluation of extraction methods

Extraction methods were evaluated on HDPE films formulated with Irganox 1076, Irgafos 168 and Erucamide. Dried polymer flakes were formulated during a first extrusion step prior to final processing at a semi-industrial scale. Both extrusions were performed at 200°C in a bi-screw

Table II. List of tested substances.

Category	Code	Chemical name	Function	CAS number	M ($g \cdot mol^{-1}$)	SML ($mg \cdot kg^{-1}$)	Chemical structure
Plastic additives	Irganox 1076	Octadecyl 3-(3,5-di-tert-butyl-4-hydroxyphenyl) propionate	radical scavenger	2082-79-3	530	6	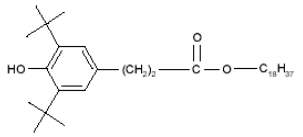
	Irgafos 168	Phosphorous acid, tris(2,4-di-tert-butylphenyl) ester	hydroperoxide decomposer	31570-04-4	647	60	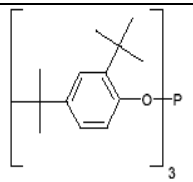
	Erucamide	Cis-13-docosenoamide	slip agent	00112-84-5	337	60	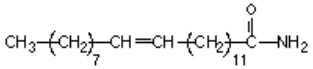
	BHT	Butylated hydroxytoluene	radical scavenger	000128-37-0	220	3	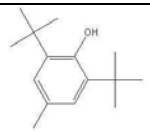
	Irganox 1330	1,3,5-Trimethyl-2,4,6-tris(3,5-di-tert-butyl- 4-hydroxybenzyl)benzene	radical scavenger	01709-70-2	774	60	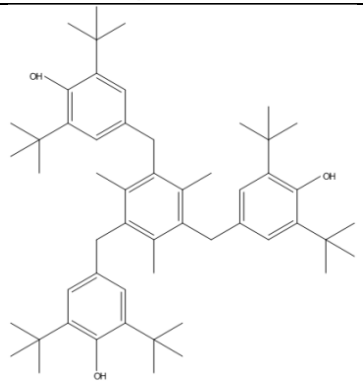

Category	Code	Chemical name	Function	CAS number	M ($g \cdot mol^{-1}$)	SML ($mg \cdot kg^{-1}$)	Chemical structure
	Irganox 3114	1,3,5-Tris(3,5-di-tert-butyl-4-hydroxybenzyl)-1,3,5-triazine-2,4,6(1H,3H,5H-)trione	radical scavenger / light absorber	27676-62-6	784	5	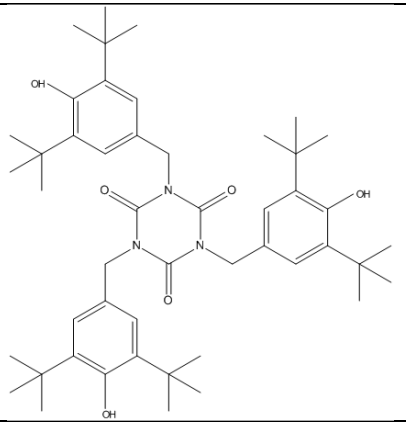
Low molecular weight contaminants	2-ITX	2-(1-methylethyl)-9H-Thioxanthen-9-one	Printing ink photoinitiator	5495-84-1	254	10^{-2} ‡	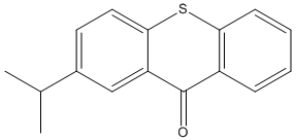
	DPM	diphenylmethane	reference†	101-81-5	168	10^{-2} ‡	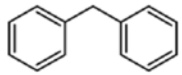

† experimental partition coefficient between HDPE and ethanol is available (Baner *et al.,* 1991).

‡ threshold value corresponding to the migration of an authorized below the detection level through a functional barrier as described in article 10 of directive 2007/19/EC (EC, 2007).

extruder (model BC-21 Clextral, France) and the material was finally calendered as 0.15 m wide ribbons. The final density and the crystallinity were of 940 kg·m^{-3} and 70 % respectively, with a melting point of 136°C. Plastic additives were provided by CIBA (Basel, Switzerland) except for Erucamide, which was obtained from CRODA (Vimodrone, Italy). Raw HDPE was obtained from ATOCHEM (Paris, France).

Two common extraction methods were considered: a conventional 40 h reflux extraction method in dichloromethane and a 40 min pressurized solid-liquid extraction (model ASE 200, Dionex, USA) in a 75:25 v/v mixture of isopropanol-dichloromethane at 105°C and 10.3 MPa. The latter conditions were similar to ones described by Coulier *et al.* (2005) and were applied to 600 mg of samples mixed with sand in 11 ml extraction cells. Two static cycles of 15 min each were applied to achieve complete extraction. To prevent the degradation of additives during extraction, 100 µL·L^{-1} of tri-ethylphosphite (Sigma-Aldrich, USA) was added to solvents for both methods.

Determination of concentrations in extracts was done by high-performance liquid chromatography (HPLC) with diode array and evaporative light scattering detection. The HPLC system consisted in a Waters 717plus autosampler, a Waters 600 controller equipped with a thermostatted column compartment and an in-line degasser AF (Waters, USA). The protocol described by Garrido-López (2005) was used. Separation was achieved on a Xterra C8 column (150mm×3.0mm; 5µm particles; Waters , USA) operated at 60°C.

Migration modeling

Migration modeling was performed under the same assumptions described by Vitrac and Hayert (2006) and by Vitrac *et al.* (2007) for similar applications. Migration in food or in a food simulant was assumed to be one-dimensional without any reaction and mass losses with surroundings. The material was considered to be homogeneous and the relaxation of polymer chains was assumed unaffected by the desorption process. The concentration profile in substance i, $C_i(Fo,x)$, along the packaging thickness, with SI units in kg·m^{-3}, evolved therefore with the dimensionless diffusion time, denoted Fo, as:

$$\frac{\partial C_i(Fo,x)}{\partial Fo} = \frac{\partial^2 C_i(Fo,x)}{\partial x^2} \qquad (1)$$

where $Fo = D_{i,P} \cdot t / l_P^2$ and x is the dimensionless position between 0 and 1 within the film. $D_{i,P}$ is the diffusion coefficient with SI units in m^2·s^{-1} ; l_P is the packaging thickness and t is the contact time. Only a pervious contact is assumed on food side, at x=1:

$$\left.\frac{\partial C_F}{\partial Fo}\right|_{Fo} = -\left.\frac{\partial C_i}{\partial x}\right|_{x=1,Fo} = Bi \cdot \left[K_{i,F/P} \cdot C_i(x=1,Fo) - C_F(Fo)\right] \qquad (2)$$

where Bi is the mass Biot number assigned to 10^3 to prevent a significant mass transfer resistance at the interface, as the liquid simulant was stirred. $K_{i,F/P} = C_{i,F}(Fo \to \infty) / C_{i,P}(x=1, Fo \to \infty)$ is the partition coefficient between the food product or food simulant, denoted F, and the packaging material, denoted P. The concentration in food or in food simulant, $C_F(Fo)$, was obtained from the mass balance t=0 and t by assuming a uniform initial concentration profile equal to $C_{i,P}^0$:

$$L_{F/P} \cdot C_F(Fo) = C_{i,P}^0 - \int_0^1 C_i(x,Fo) \cdot dx \qquad (3)$$

where $L_{F/P} = V_F / (A \cdot l_p)$ is the volume dilution ratio. V_F and A are respectively the volume of F and the contact surface area between P and F. Equations 1-3 were integrated in time using a finite volume technique documented and implemented online in QSPR-MS tools of the Safe Food Packaging Portal (INRA 2008). All simulations results were exported as datasheets to be further interpreted.

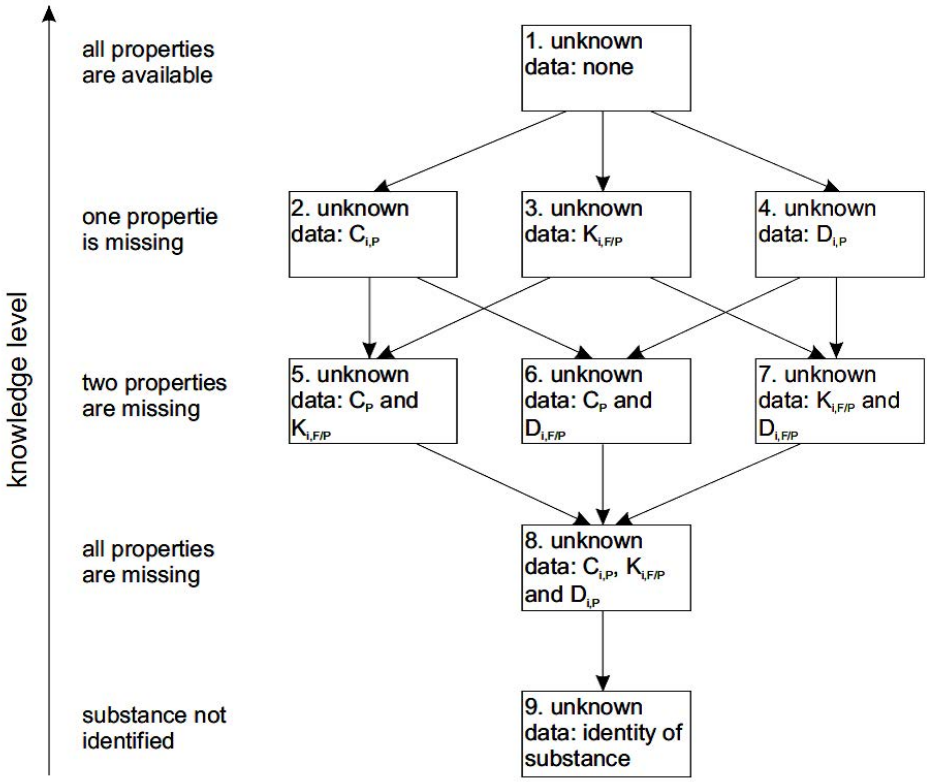

Figure 2. Influence diagram relating all nine scenarios involved in the assessment of compliance when migration modeling and deformulation experiments are combined together.

Migration scenarios

Nine scenarios with different sources of uncertainty were considered for five additives as plotted in Figure 2. For each quantity X required for modeling, two values were considered: a likely value $\bar{X}$ and a robust overestimate X^+ such that $\bar{X} < X^+$. The corresponding values are gathered in Table III for each substance and in Table V for each scenario. A similar $\bar{D}_{i,P}$ value was assigned to Irganox 1330 and Irganox 3114 as they had a very similar chemical structure and as the expected difference is lower than the common experimental error as assessed in (Vitrac *et al.* 2006). Parameters required to calculate $\bar{K}_{i,F/P}$ values in the framework of a generalized Flory-Huggins theory at atomistic scale are presented in Table IV. They were either extracted from molecular simulations (Vitrac and Gillet, 2008; Gillet *et al.* 2008a) or thermodynamical data for water-ethanol properties (Gillet *et al.* 2008b). Desorption was assumed to occur in water-ethanol (50:50 v/v) to simulate a contact with a dairy product (European Commission 2007). As a possible worst case of packaging materials in contact with a dairy product, additives were assumed to be used in a rigid container of 200 µm thickness and in contact with a low volume of food of 100 mL. The conditions of test corresponded to a contact of 10 days at 40°C. By contrast, low molecular weight contaminants were assumed to be located in thin 50 µm liner in contact with a product of 1 L. To simulate more realistic conditions in the latter case, a contact with a dairy product at 4°C during 90 days was assumed.

The scenarios numbered from 1 to 8 were located at the vertices of a cube. The face 1,4,7,3 corresponded to uncertainties on transport properties. The opposite face 2,6,8,5 combined in addition uncertainty on composition, $C^0_{i,P}$. In absence of a transport property, a robust overestimate was used instead. As no recommendation has been specifically proposed for 50% ethanol used as simulant, an upper bound of 10^3 was chosen for $K^+_{i,F/P}$ instead of the unitary value recommended for simulant D

Table III. List of inputs used to predict the migration from a polyolefin to a 50:50 v/v water-ethanol simulant.

		Low molecular weight contaminants		Plastic additives		
Migrant		2-ITX	DPM	BHT	Irganox 1330	Irganox 3114
Homologous migrant†		not available	not available	not available	BHT (3)	BHT (3)
Polymer		LDPE††	LDPE††	HDPE†††	HDPE†††	HDPE†††
PARAMETER	**notation (unit)**					
Thickness	l_P (µm)	50	50	200	200	200
Volume dilution ratio	$L_{F/P}$ (-)	360	360	50	50	50
Biot mass number	Bi (-)	10^3	10^3	10^3	10^3	10^3
Contact Time	t (days)	90	90	10	10	10
Temperature	(°C)	4	4	40	40	40
Likely initial concentration[a]	$\overline{C}^0_{i,P}$ [a] (mg·kg^{-1})	100 ± 10	100 ± 10	10^3± 100	10^3± 100	10^3± 100
Conservative initial concentration[b]	$\left(C^0_{i,P}\right)^+$ [b] (mg·kg^{-1})	300	300	$3\cdot10^3$	$3\cdot10^3$	$3\cdot10^3$
Likely diffusion coefficient[c]	$\overline{D}_{i,P}$ [c] (m^2.s^{-1})	$8.4\cdot10^{-16}$ [$7.6\cdot10^{-16}$ $9.2\cdot10^{-16}$]	$7.3\cdot10^{-14}$ [$6.7\cdot10^{-14}$ $8.0\cdot10^{-14}$]	$2.7\cdot10^{-13}$ [$2.5\cdot10^{-13}$ $2.9\cdot10^{-13}$]	$1.6\cdot10^{-15}$ [$1.5\cdot10^{-15}$ $1.8\cdot10^{-15}$]	$1.6\cdot10^{-15}$ [$1.5\cdot10^{-15}$ $1.8\cdot10^{-15}$]
Conservative diffusion coefficient[d]	$D^+_{i,P}$ [d] (m^2.s^{-1})	$3.9\cdot10^{-14}$	$1.1\cdot10^{-13}$	$4.4\cdot10^{-12}$	$3.6\cdot10^{-14}$	$3.4\cdot10^{-14}$
Likely partition coefficient[e]	$\overline{K}_{i,F/P}$ (-)	$1.4\cdot10^{-9}$ [$3.7\cdot10^{-10}$ $5.1\cdot10^{-9}$]	$1.2\cdot10^{-4}$ [$3.4\cdot10^{-5}$ $4.6\cdot10^{-4}$]	$2.1\cdot10^{-4}$ [$5.7\cdot10^{-5}$ $7.7\cdot10^{-4}$]	2.9 [0.77 10]	0.013 [$3.5\cdot10^{-3}$ 0.048]
Conservative partition coefficient	$K^+_{i,F/P}$ (-)	10^3	10^3	10^3	10^3	10^3

† molecule which gives a similar IR absorption spectrum with a molar ratio indicated between brackets.

††density = 0.899, crystallinity = 30%; †††density = 0.959, crystallinity = 70%.

[a] chosen to fit real concentrations for a similar packaging material.

[b] three times the likely value (matched the maximal recommended values for Irganox 1330 and Irganox 3114).

[c] robust estimate according from Vitrac *et al.* (2006) and available on the SAFE FOOD PACKAGING PORTAL (INRA, 2008), 95% confidence intervals in brackets include the overall uncertainty on $D_{i,P}$ and its activation energy for this class of substance.

[d] from the overestimate model described in Beygley *et al.* (2005).

[e]calculated from the generalize Flory-Huggins approach described by Gillet *et al.* (2008b) for water-ethanol mixtures, all inputs required from thermodynamical and Molecular simulations are listed in Table 3. 95% confidence intervals based on a sensitivity analysis are indicated between brackets.

Table IV. List of inputs used to calculate $\overline{K}_{i,F/P}$ between a polyethylene and a 50:50 v/v water-ethanol simulant within the framework of the Flory-Huggins theory as described in Gillet *et al.* (2008b) and in Gillet *et al.* (2008c). By noting F_1=water and F_2=ethanol, the analytical expression while accounting the non-idealities of the water-ethanol mixture is:

$$\ln\left[\frac{K_{i,(F_1+F_2)/P}}{1-c}\right] = -2\frac{V_i^{vdw}}{V_{F_2}^P}\frac{\partial\chi_{F_1,F_2}}{\partial\phi_{F_2}}\cdot\phi_{F_2}^3 + \frac{V_i^{vdw}}{V_{F_2}^P}\cdot\left(\chi_{F_1,F_2}+3\frac{\partial\chi_{F_1,F_2}}{\partial\phi_{F_2}}\right)\cdot\phi_{F_2}^2 + \left(\frac{V_i^H}{V_{F_2}}-\frac{V_i^H}{V_{F_1}}+\chi_{i,F_1}-\frac{V_i^{vdw}}{V_{F_2}^P}\chi_{i,F_2}+\frac{V_i^{vdw}}{V_{F_2}^P}\chi_{F_1,F_2}-\frac{V_i^{vdw}}{V_{F_2}^P}\frac{\partial\chi_{F_1,F_2}}{\partial\phi_{F_2}}\right)\cdot\phi_{F_2}+\frac{V_i^H}{V_{F_1}}+\chi_{i,P}-\chi_{i,F_1}$$

Parameter	Physical meaning (units)	Low molecular weight migrants		Additives		
		2-ITX	DPM	BHT	Irganox 1330	Irganox 3114
c	Polymer crystallinity (-)	0.3		0.7		
V_i^{vdw}	Van-der-Waals volume of migrant *i* (Å^3)	241 ± 4	179 ± 4	251 ± 7	889 ± 10	849 ± 12
V_i^H	Volume enclosed within the surface accessible to hydrogen atoms of migrant *i* (Å^3)	386 ± 5	294 ± 5	398 ± 5	1300 ± 9	1256 ± 15
V_{F_1}	Molar volume of water (Å^3)	29.9				
V_{F_2}	Molar volume of ethanol (Å^3)	99				
$V_{F_2}^P$	Partial molar volume of ethanol in water (Å^3)	96				
$\chi_{i,P}$	Binary Flory-Huggins interaction parameter between migrant *i* and polymer (-)	0 - 0.3	0 - 0.3	0 - 0.5	0 - 0.5	0 - 0.5
$\chi_{i,water}$	Binary Flory-Huggins interaction parameter between migrant *i* and water (-)	44.1	30.1	30.5	39.3	43.4
$\chi_{i,ethanol}$	Binary Flory-Huggins interaction parameter between migrant *i* and ethanol (-)	11.2	2.75	3.13	12.6	7.5
$\left.\frac{\partial\chi_{F_1,F_2}}{\partial\phi_2}\right\|_{\phi_2=0.5}$	Non ideal behavior of the water ethanol mixture (-)	-1.476				
Φ_2	Volume fraction in ethanol (-)	0.5				

Table V. Combination of input values associated to each scenario. The index i in scenarios 1..8 corresponds to an identified substance, whereas the index h in scenarios 9..10 corresponds to an homologous molecule (BHT for antioxidants) with a similar mid-infrared vibrational spectrum (Gillet *et al.*, 2008c).

Scenario	$C^0_{i,P}$ value	$K_{i,F/P}$ value	$D_{i,P}$ value
1	$\overline{C}^0_{i,P}$	$\overline{K}_{i,F/P}$	$\overline{D}_{i,P}$
2	$\left(C^0_{i,P}\right)^+$	$\overline{K}_{i,F/P}$	$\overline{D}_{i,P}$
3	$\overline{C}^0_{i,P}$	$K^+_{i,F/P}$	$\overline{D}_{i,P}$
4	$\overline{C}^0_{i,P}$	$\overline{K}_{i,F/P}$	$D^+_{i,P}$
5	$\left(C^0_{i,P}\right)^+$	$K^+_{i,F/P}$	$\overline{D}_{i,P}$
6	$\left(C^0_{i,P}\right)^+$	$\overline{K}_{i,F/P}$	$D^+_{i,P}$
7	$\overline{C}^0_{i,P}$	$K^+_{i,F/P}$	$D^+_{i,P}$
8	$\left(C^0_{i,P}\right)^+$	$K^+_{i,F/P}$	$D^+_{i,P}$
9	$\overline{C}^0_{h,P}$ †	$\overline{K}_{h,F/P}$	$\overline{D}_{h,P}$
10	$\left(C^0_{h,P}\right)^+$ ‡	$\overline{K}_{h,F/P}$	$\overline{D}_{h,P}$

† 852 mg·kg^{-1} in BHT to match an equivalent concentration in BHT patterns included in Irganox 1330 and Irganox 3114. ‡ 3000 mg·kg^{-1}.

(olive oil) in the "Practical Guide" (European Commission 2003) as extreme worst case. This choice was consistent with experimental $K_{i,F/P}$ values found higher than 1 between polyolefins and ethanol (Vitrac *et al*. 2007, Gillet *et al.* 2008b). In absence of data on initial concentrations, maximum values recommended by the providers were used. For low molecular weight contaminants, a value in agreement with the extensive study of Rothenbacher *et al.* (2007) was used. Scenarios 9 and 10 are a special case where the identity of the substance i is unknown. In this work, an unknown antioxidant was replaced by a smaller molecule with a similar mid-infrared vibrational spectrum and with a conservative migration rate. As Irganox 1330 and Irganox 3114 included 3 BHT patterns (Table I), they were replaced by an equivalent amount in BHT patterns (Table IV).

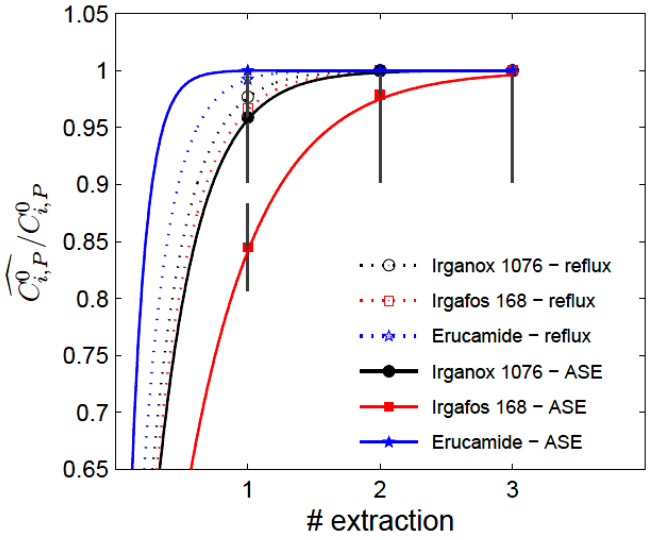

Figure 3. Estimated concentrations in HDPE, $\widehat{C^0_{i,P}}$, of three additives against the number of extraction steps. All concentrations were normalized according the value after 4 extractions and denoted $C^0_{i,P}$.

Results and discussion

Extraction yields

A compilation of list of potential migrants to food is required before starting any assessment of specific migration limit. Though this approach is not limited to additives, it is mainly suitable for substances, which are intentionally added to materials in contact with food. The information on the composition, types of molecules and extent, is a heavy obligation on declaration of compliance and can be obtain either by partial disclosure of confidential information or by deformulation. For practical cases taken in consideration by the Laboratoire National d'Essais in France, the information is transmitted for less than 5% of tested samples (Table I). As a result, deformulation appears currently as the most robust approach to start the decision tree depicted in Figure 1. To be cost efficient, the deformulation must be rapid and predictive. The difficulty arises with semicrystalline materials such as polyolefins, which cannot be dissolved in solvents. Figure 3 presents the estimated concentration in P after successive extractions during a long-term extraction by reflux (extraction time 48 h) and using a

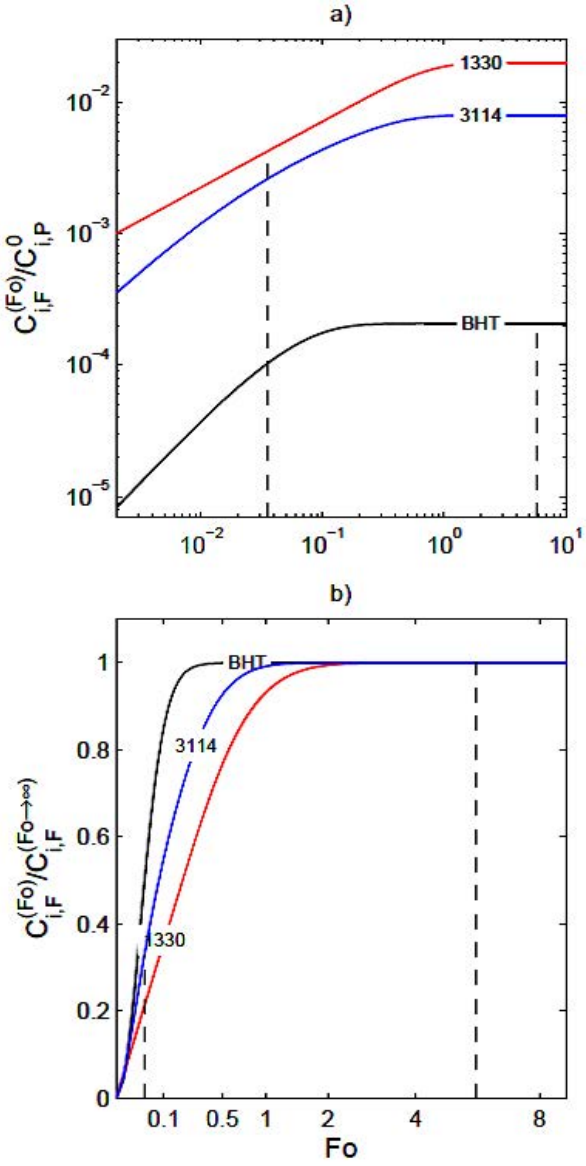

Figure 4. Dimensionless migration kinetics of BHT, Irganox 1330 and Irganox 3114 corresponding to likely input values in Table 2: a) kinetics on a log-log scale, b) kinetics against the square root of time. Dimensionless contact times corresponding for each migrant to contact times of 10 days are also depicted.

pressurized cell (extraction time 40 min). The data were obtained for two typical antioxidants, Irganox 1076 and Irgafos 168, well dispersed in the bulk and a slip agent, Erucamide, mainly located at the external surface of *P*.

Differences between methods and substances (including 3 extractions×3 concentrations measurements) were almost insignificant. As only leaching was required to extract Erucamide from HDPE, the extraction was complete in one step. For additives dispersed in the bulk, 95 % extraction was reached after the first step. The bias related to a single extraction was therefore minimal. Although the extraction bias (systematic error) could be corrected with the extraction yield, the experimental error (random error) was much higher. The overall relative experimental error was assessed up to 20 % and did not decrease with the considered number of extraction steps, since the extracted amounts were cumulated and not averaged. The magnitude of the extraction error was directly correlated to the accuracy of sampling and concentration measurements.

Migration kinetics

Figure 4 plots the dimensionless kinetics corresponding to the most complete scenario (i.e. with the lowest uncertainty), ranked 1 in Figure 2, for three antioxidants initially included in a 200 µm thick film in contact with 50% ethanol ($L_{F/P}$=50) at 40°C. The dimensionless diffusion time corresponding to a conventional contact time of 10 days at 40°C, denoted Fo_{10}, is also depicted. Although most of decision-makers would not start with this scenario, it is particularly useful to illustrate the migrant based reasoning. Diffusion behavior of BHT was highly distinct of polymeric additives with a Fo_{10} value close to 6 against a value of $4 \cdot 10^{-2}$ for Irganox 1330 and Irganox 3114. Concentration values at equilibrium, $C_{i,F}^{(Fo\to\infty)}$, given by the overall mass balance defined in Equation 4, were also highly different:

$$C_{i,F}^{(Fo\to\infty)} = \frac{1}{L_{F/P} + 1/K_{i,F/P}} \cdot C_{i,P}^{0} \qquad (4)$$

As a same dilution ratio, $L_{F/P}$, and a same initial concentration, $C_{i,P}^{0}$, were applied to all migrants, the differences were only related to partitioning in 50% ethanol, $K_{i,F/P}$. Despite all migrants consisted in the repetition of same BHT pattern, their chemical affinity for 50% ethanol varied significantly with their size. This size effect was related to a much higher dispersion of chemical interactions between the migrant and the simulant

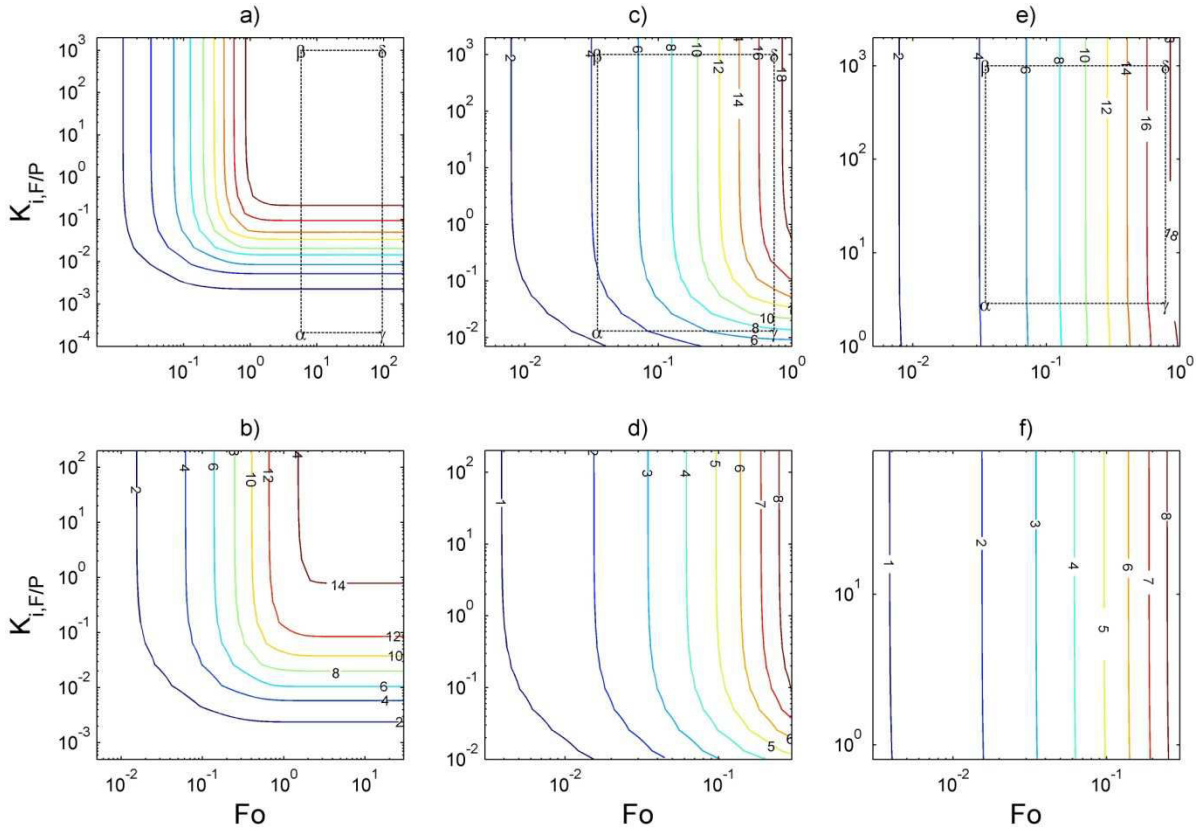

Figure 5. Isocontours of $10^3 \cdot C_{i,F}^{(Fo)} / C_{i,P}^0$ against Fo and $K_{i,F/P}$ for a,c,e) $L_{F/P}$=50) and b,d,f) $L_{F/P}$=83: a-b) BHT, c-d) Irganox 3114, e-f) Irganox 1330. Scenarios 1..8 are also represented as α (scenarios 1 and 2), β (scenarios 3 and 5), γ (scenarios 4 and 6), δ (scenarios 7 and 8).

when the migrant was larger. Indeed, a large molecule as Irganox 3114 consisting in 3 BHT patterns exposed a much lower specific surface to simulant than a single BHT molecule and consequently perturbed less the cooperative network of hydrogen bonds in water-ethanol mixtures. This effect has been extensively studied in Gillet *et al.* (2008a and 2008b) and has been proposed to explain the relative high chemical affinity of large additives for mixtures consisting in much smaller molecules. Similar considerations are detailed by Fill and Bromberg (2003). It is underlined that the current approach neglects possible reactions, which could reduce the size of migrants and which could modify accordingly the chemical affinity of fragments for the simulant.

In details, the migration of large additives, Irganox 1330 and Irganox 3114, was controlled by both the migrant chemical affinity for 50% ethanol (which favors the migration comparatively to BHT) and by the limiting diffusion in the film (Figure 4b). However, as the corresponding migration rates, $C_{i,F}^{(Fo=10)} / C_{i,F}^{(Fo\to\infty)}$, were sufficiently close to unity, with values larger than 0.4, partitioning appeared to be the main source of uncertainty to predict $C_{i,F}^{(Fo_{10})}$. It is worth to notice that such a very low partitioning (Table III) with the simulant requires a particular care in the writing of the boundary condition (Equation 2) and in the resolution of the complete set of transport equations. It is in particular expected that the requested time to reach the equilibrium is lower when the chemical affinity is very low for *F*. In simple words, the equilibrium was reached all the more rapidly than the amount of migrant to be desorbed to reach the equilibrium was lower. In absence of chemical affinity of the simulant, the macroscopic equilibrium would be thus obtained instantaneously as soon as a single molecule would have left the

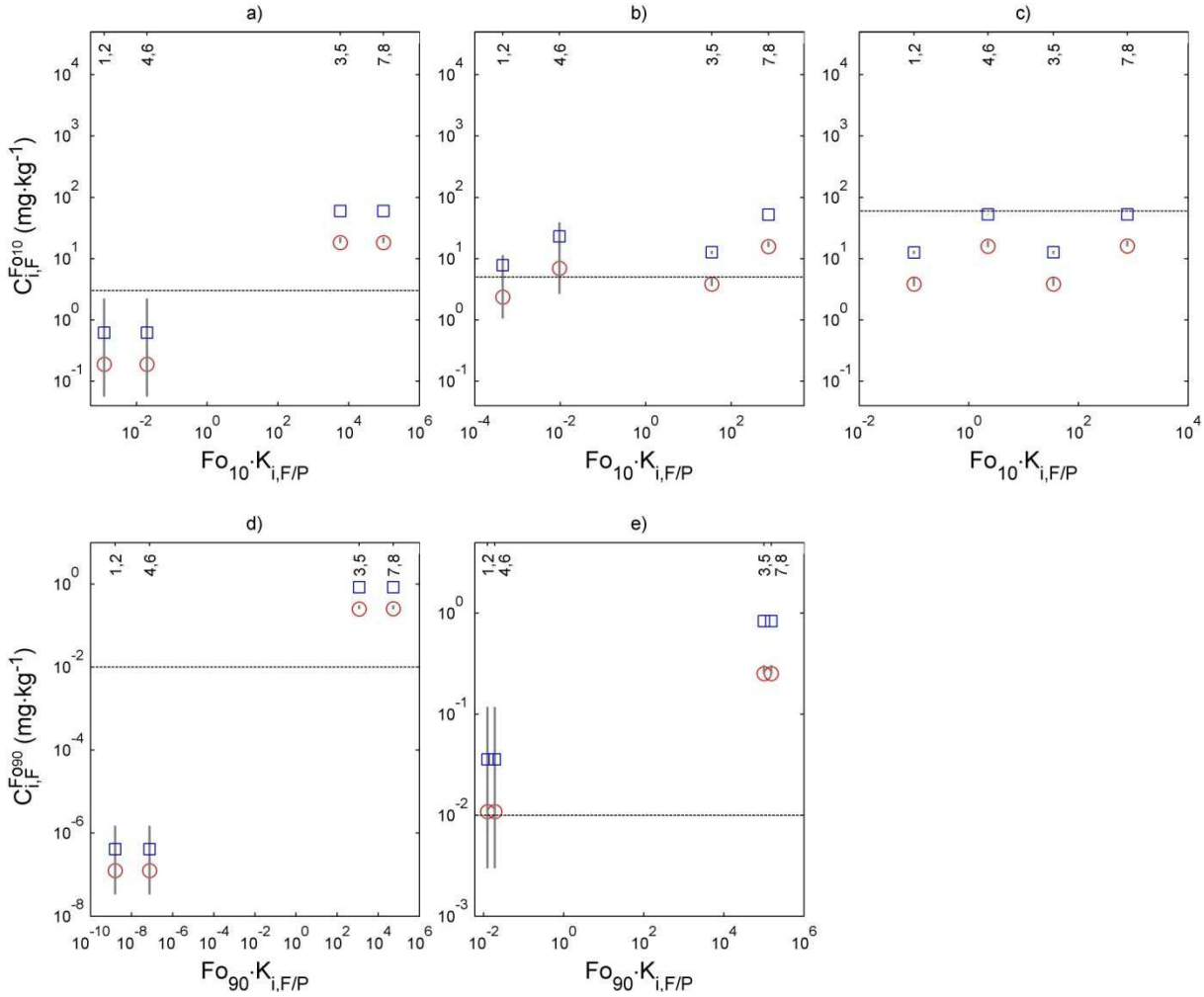

Figure 6. Sensitivity diagram of $C_{i,F}^{(Fo)}$ against all unknowns: a) *i*=BHT, b) *i*=Irganox 3114, c) *i*=Irganox 1330, d) *i*=2-ITX, e) *i*=DPM. Error bars represent 95% confidence intervals on estimates. The limit of concern appears as a dashed line. Scenarios including $\overline{C}_{i,P}^{0}$ and $\left(C_{i,P}^{0}\right)^{+}$ are plotted as circles and squares respectively.

polymer. These features, which may appear counterintuitive, are discussed by Vitrac and Hayert (2006).

The practical consequence was that the falsely identification in FTIR of Irganox 1330 as BHT, with a three times higher molar concentration (note that the mass concentration would remain unchanged), would not be necessarily a worst case as the affinity of Irganox 1330 for the simulant would be also higher.

Sensitivity diagrams to uncertainty

Introducing uncertainty on transport coefficients as it could be in the real practices blurred the initial description of the migration. The effects of mistaken $K_{i,F/P}$ and $D_{i,P}$ values corresponding to Figure 4 are illustrated as isocontours of $10^{3}\cdot C_{i,F}^{(Fo)}/C_{i,P}^{0}$ in Figure 5 for two dilution ratios: $L_{F/P}$=50 and $L_{F/P}$=83. The ratio matched the conventional assumption used in conservative consumer exposure assessment in EU (European Commission 2002): 1 kg on food in contact with 6 dm^2 of packaging material. In Figure 5, scenarios numbered from 1 to 8 are plotted at the vertices of a rectangle. The extents of variations represent the effects of overestimations when one or two input values are missing. For a small migrant, only overestimating the partitioning changed the concentration in food simulant up to the maximum value permitted by the maximum concentration in HDPE. The overestimation factor reached up two decades. The behavior was opposite for large antioxidants and isocontours

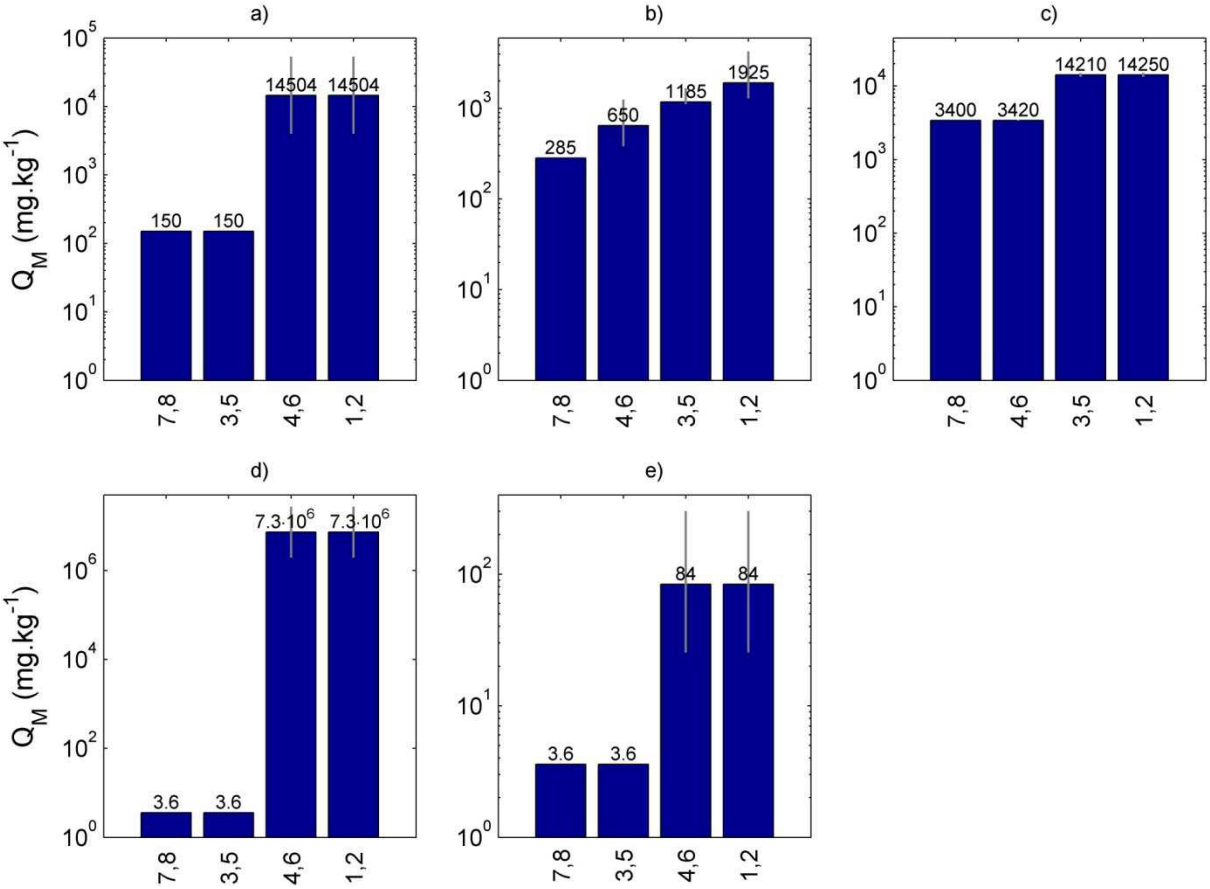

Figure 7. Decision diagrams expressed as ordered Q_M values for scenarios 1..8: a) *i*=BHT, b) *i*=Irganox 3114, c) *i*=Irganox 1330, d) i=2-ITX, e) i=DPM.

appeared mainly parallel to $K_{i,P}$ axis and with a maximum overestimation factor of 5. According to Equation 4, decreasing $K^{+}_{i,F/P}$ from 1000 down to 1 (worst case recommended in "practical guide" (2003)) did not change previous conclusions as $L_{F/P}$ values higher than 10 led to almost complete extraction for any $K^{+}_{i,F/P} \geq 1$.

The additional effect induced by $L_{F/P}$ was related to two complementary contributions: i) lowering the effect of a poor chemical affinity for simulant at high $L_{F/P}$ values and ii) increasing the dilution of the amount of migrated substances. Depending on the units used to express the specific migration limit (SML), in mg·dm^{-2} of packaging or mg·kg^{-1} of packaging, the one or the other led to a conservative assumption. As we expressed SML in mg·kg^{-1}, $L_{F/P}$=50 was chosen in the remainder of the work as a worst case assumption. The conventional assumption 1 kg in contact with 6 dm^2 would lead to a concentration in food simulant down to twice lower.

The effect of cumulating up to three sources of uncertainty made the utility of some scenarios questionable according to the expected migration limit of concern (SML or detection limit). To generate a practical sensitivity diagram depicting all combined sources of uncertainty, a simplified descriptor, derived from Equation 2, $Fo_{10} \cdot K_{i,F/P}$ was used instead of isocontours. For low molecular weight contaminants with a contact time of 90 days (Table III), a similar descriptor was proposed: $Fo_{90} \cdot K_{i,F/P}$. Values of $C_{i,F}^{(Fo=Fo_{10},Fo_{90})}$ against the previous criteria are plotted in Figure 6 for $\bar{C}^0_{i,P}$ and $\left(C^0_{i,P}\right)^+$. Confidence intervals caused by uncertainties on transport properties, $\overline{K}_{i,F/P}$ and $\overline{D}_{i,P}$, are also presented to highlight that the decision of compliance should not be taken

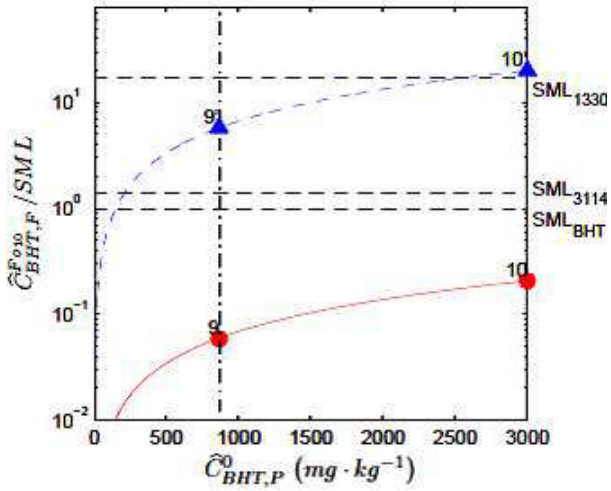

Figure 8. Decision diagram when Irganox 1330 or Irganox 3114 is replaced by a similar concentration in BHT patterns, $\hat{C}^{Fo_{10}}_{BHT,F}$, with the properties of BHT (see Table 2). Scenarios 9 and 10 are calculated with $\overline{D}_{BHT,P}$ and $\overline{K}_{BHT,F/P}$ wheras scenarios 9' and 10' are equivalent scenarios calculated with $D^{+}_{BHT,P}$ and $K^{+}_{BHT,F/P}$. The decision is taken by comparing $\hat{C}^{Fo_{10}}_{BHT,F}/SML_{BHT}$ with one. The corresponding limit for the real additives are also depicted.

necessarily at the predicted value but should include an additional safety margin.

Combining several sources of uncertainty showed that the hierarchy of scenarios to demonstrate the compliance was not intuitive as it depended on the considered case.. Scenarios involving $K^{+}_{i,F/P}$ values (3,5,7,8), as generally recommended for migration modeling, were able to demonstrate the compliance only when the migration limit was as high as the overall migration limit in EU regulation, 60 mg·kg^{-1}, that is for Irganox 1330. By contrast, refined scenarios 1,2,4,6 involving at least one likely transport properties were always applicable to demonstrate compliance. Irganox 3114 and DPM were special cases, where compliance could not be determined when more than one source of uncertainty was included.

Decision diagrams in QM

The usability of previous sensitivity diagrams by end-users, having not access to the initial formulation of their materials, was improved by replacing the concentration in food simulant by the equivalent maximum concentration in the packaging material, Q_M, which matches the limit of concern. It was calculated as:

$$Q_M = \frac{C^{0}_{i,P}}{C^{(Fo)}_{i,F}} \cdot \text{limit of concern} \qquad (5)$$

Q_M values are more practical as they can be calculated *a priori* for a given food packaging application and they can be compared subsequently with formulation data derived from general manufacturing practices or from a partial formulation disclosure (Figure 1). The interesting feature is that the provider needs only to acknowledge that it uses the substance at a lower concentration than Q_M. To make robust conclusions, the uncertainty associated to each Q_M estimates must be accounted. Q_M values corresponding to Figure 6 are plotted in Figure 7 in increasing order. When implemented as decision diagram, each bin represents a condition node: is the initial concentration higher than the value above each bin? If the answer is yes, the question must be repeated with the next bin on the right. If the answer is no, the compliance is demonstrated. For large additives, the Q_M values were progressively increasing as the migration model was sensitive to all sources of uncertainty. For low molecular weight contaminants and additives, changes between values were most abrupt. Ordering scenarios *a priori* guaranteed the decision-maker that acquiring new information will improve the decision. A strict improvement is obtained by merging scenarios with similar values. As it is physically expected, $\overline{K}_{i,F/P}$ was the most valuable information for small migrants while it was $\overline{D}_{i,P}$ for large polymeric additives.

Decision diagrams for phenolic antioxidants mistaken with BHT

When the identity of the substance was not known as it might occur in FTIR

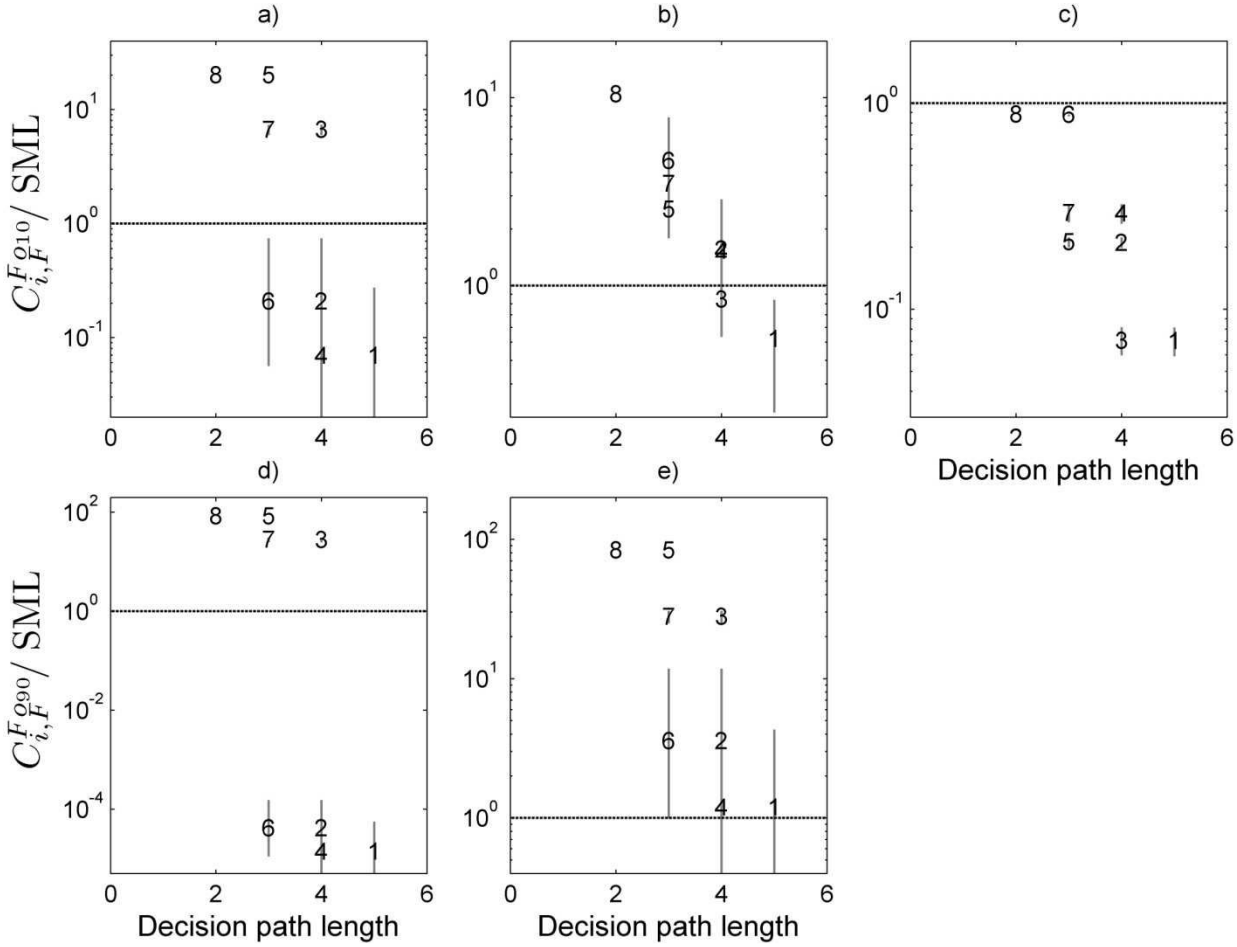

Figure 9. Decision diagrams expressed as minimum path lengths in the influence diagram depicted in Figure 1 (the decision process is started with scenario 10): a) *i*=BHT, b) *i*=Irganox 3114, c) *i*=Irganox 1330, d) *i*=2-ITX, e) *i*=DPM.

deformulation, a large molecule (in this work a large hindered phenolic antioxidant) was replaced by much smaller one (BHT). This approximation suited particularly for Irganox 1330 and Irganox 3114. Nevertheless two additional difficulties appeared: the initial concentration was expressed in equivalent concentration in BHT patterns and the limit of concern was assumed to be the SML of BHT. The reliability of such assumptions to demonstrate the compliance is depicted in Figure 8. As the SML of BHT was much lower than the one of real additives, the approximation guaranteed a conservative decision limit. By introducing the expected transport properties of BHT, $\overline{D}_{BHT,P}$ and $\overline{K}_{BHT,F/P}$, and an equivalent concentration in BHT pattern, the predictions of scenarios 9 and 10 were close to those of scenarios 1 and 2 respectively (Figure 5). As a result, the compliance could be demonstrated easily with scenario 9 and 10.

The proposed approximation seemed valid when BHT replaces molecules based on the repetition of several BHT patterns. It should not be generalized to any series of additives. A more general estimate based on $D^{+}_{BHT,P}$ and $K^{+}_{BHT,F/P}$ was tested and plotted as scenarios 9' and 10' in Figure 8. As it led to equivalent Q_M values lower than 200, it was not suitable for antioxidants, which are conventionally used at concentrations much higher.

Shortest paths to demonstrate the compliance

From the point of view of decision-maker, the dependence diagram depicted in Figure 2 should be started in the reverse order with the lowest knowledge level. For antioxidants, it could be started with

scenarios 9 and 10 as a homologous molecule was available. For other molecules, it should be started with the scenario 8. The best scenario was the one, which made it possible to demonstrate the compliance and was connected with shortest path length (decision path length) to the initial scenario. In other words, the optimal scenario should minimize the extent of additional information necessary to demonstrate the compliance.

All scenarios were ranked according to their equivalent decision path length in Figure 9. The so-defined diagram highlighted that several scenarios, though they generated distinct predictions, should be seen similar by the decision maker: they demonstrated the compliance at the lowest cost. Except when the SML was as high as the global migration limit (Irganox 3114), a path of length 4 was required, which indicated that no more than two sources of uncertainty should be combined. On one hand, it could be argued, as a rule of thumb, that when partial formulation disclosure is not accepted or available, at least one transport property must be known with enough accuracy. On the other hand, when the initial concentration is available, conventional overestimates, although inaccurate, are expected to be able to demonstrate the compliance not in all cases but with a significant expectation, between 50% and 75%.

For polyolefins (one third of total food contact applications), the current state of the art suggests that scenario 2 and possibly scenario 1 should be nearly available for all practical cases, while minimizing the risk of false negative (considered as "not able to demonstrate the compliance" when it is compliant). In addition, the risk of false positives would be very low while appropriate safety margin on likely transport properties are included in the decision.

Conclusions and prospects

This paper addresses a general framework to combine migration modeling and experiments into a same decision tool to demonstrate the compliance of thermoplastics materials in contact with food. The objective was to select the necessary experiments and simulation scenarios among several alternatives to make a decision: "it is compliant" or "the compliance cannot be demonstrated with this approach". Comparatively to conventional approaches used in migration modeling, the ambition was neither to assess the real migration nor to overestimate all uncontrolled factors but to increase drastically the usability of modeling-based compliance testing. The improvements consisted mainly in designing an end user-oriented approach, which was:

- more efficient under uncertainty (more robust, it takes less time to accomplish the demonstration, it requires fewer assumptions, formulation disclosure is not systematically required…);
- easier to learn (based on simple diagrams, include a robust physical reasoning based in particular on minimal number of dimensionless quantities);
- more satisfying to use (the method toggles when required from empirical models of transport properties to more sophisticated ones based on a molecular simulation).

The method was tested in complicated cases involving the migration of low molecular weight contaminants and hindered phenolic antioxidants into the simulant proposed for dairy products, 50% ethanol, for which the possibilities of modeling had not yet been examined. Although the current results might find an application in the previous 2-ITX crisis, the finality was mainly methodological. All nine scenarios incorporating up to three sources of uncertainty has been incorporated into an on line semi-supervised software on the SAFE FOOD PACKAGING PORTAL (INRA 2008). It

generates all proposed diagrams in less than 3 minutes so that the overall decision tree can be easily integrated along with the process of identification and quantification of substances and along with the audit of the provider.

Apart from the decision tool concept, this work brought two important insights for both compliance testing and future sanitary survey. The migration of large additives such antioxidants is mainly controlled by the resistance of material to diffusion, while their chemical affinity for simulant or food consisting in much smaller molecules is higher than the one for smaller migrant with similar chemical composition. As an example of consequence, long time contacts and heating should lead to higher contamination of food products by large additives than by smaller ones. As this description neglects a possible hydrolysis of additives, a dedicated experimental verification is encouraged. Finally, the results highlighted that the crude assumptions recommended in the current "Practical Guide" (2003) for modeling, based mainly on simulant D and strong overestimates of diffusion coefficients, failed to deserve the demonstration of compliance for intentionally added substances in most of tested cased. As modeling combined with fast deformulation techniques appear to be the mainly independent approach to audit the compliance, further extension of this work to other polymers and multilayer materials is highly desirable.

Acknowledgment

We would like to thank the Association de Coordination Technique pour l'Industrie Agroalimentaire and the Association Nationale pour la Recherche Technique for their financial support. We also want to thank the Institut National des Sciences Appliquées from Lyon, and particularly Hervé Perrier-Camby, for processing the studied polymer materials.

References

Bagnati R, Blanchi G, Marangin E, Zuccato E, Fanelli R, Davoli E. 2007. Direct analysis of isopropylthioxanthone (ITX) in milk by high-performance liquid chromatography/tandem mass spectrometry. Rapid Commun. Mass Spec. 21:1998-2002.

Baner AL, Piringer OG. 1991. Prediction of solute partition coefficients between polyolefins and alcohols using the regular solution theory and group contribution methods. Ind Eng Chem Res. 30:1506-1515.

Beygley T, Castle L, Feigenbaum A, Franz R, Hinrinchs K, Lickly T, Mercea P, Milana M, O'Brien A, Rebre S, Rijk R, Piringer O. 2005. Evaluation of migration models that might be used in support of regulations for food-contact plastics. Food Addit Contam. 22:73-90

Colerangle JB, Roy D. 1997. Profound effects of the weak environmental estrogen-like chemical bisphenol A on the growth of the mammary gland of noble rats. J Steroid Biochem Mol Biol. 60:153-160.

Coulier L, Kaal ER, Tienstra M, Hankemeier Th. 2005. Identification and quantification of (polymeric) hindered-amine light stabilizers in polymers using pyrolysis–gas chromatography–mass spectrometry and liquid chromatography–ultraviolet absorbance detection–evaporative light scattering detection. J Chromatogr A. 1062:227-238

Choller D, Vergnaud JM, Bouquant J, Vergallen H, Feigenbaum A. 2003. Safety and quality of plastic food contact materials. Optimization of extraction time and extraction yield, based on arithmetic rules derived from mathematical description of diffusion. Application to control strategies. Pack Technol Sci. 16(5):209-220.

Dole P, Feigenbaum A, De la Cruz C, Pastorelli S, Paseiro P, Hankemeier T, Voulzatis Y, Aucejo S, Saillard P, Papaspyrides C. 2006. Typical diffusion behaviour in packaging polymers-application to functional barriers. Food Addit Contamin. 23: 202-211.

European Commission, Health & Consumer Protection Directorate-General (EC-DGSANCO-D3). 2002. Conclusions of the

workshop CANCO: Can coatings for direct food contact. EU-QLAM-2001-00066, Brussels, Belgium: EC.

European Commission. 2002. Directive2002/72/EC. Off J Eur Union. L220:18-58.

European Commission. 2003. Food contact materials. A practical guide for users of European directives. http://ec.europa.eu/food/food/chemicalsafety/foodcontact/practical_guide_en.pdf.

European Commission. 2004. Regulation 1935/2004/EC. Off J Eur Union. L338:4-18.

European Commission. 2007. Directive 2007/19/EC amending Directive 2002/72/EC relating to plastic materials and articles intended to come into contact with food and Council Directive 85/572/EEC laying down the list of simulants to be used for testing migration of constituents of plastic materials and articles intended to come into contact with foodstuffs. Off J Eur Union of 12.4.2007. L97:50-69.

European Commission. 2008. Substances listed in EU directives on plastics in contact with food. http://ec.europa.eu/food/food/chemicalsafety/foodcontact/eu_substances_en.pdf.

Fantoni L, Simoneau C. 2001. Contamination of baby food by epoxydised soybean oil. Proceedings of 6th International Symposium of Food Authenticity and Safety; Nov. 28–30; Nantes, France.

Feigenbaum A, Scholler D, Bouquant J, Brigot G, Ferrier D, Franz R, Lillemark L, Riquet AM, Petersen JH, Van Lierop B, Yagoubi N. 2002. Safety and quality of food contact materials. Part 1: Evaluation of analytical strategies to introduce migration testing into good manufacturing practice. Food Addit Contamin.19:184-201.

Fill KA, Bromberg S. 2003. Molecular driving forces : statistical thermodynamics in chemistry and in biology. New-York: Garland Science. Chapter 31, p. 593-608.

Franz R, Welle F. 2008. Migration measurement and modelling from poly(ethylene terephthalate) (PET) into soft drinks and fruit juices in comparison with food simulants. Food Addit Contam. 25:1033-1046.

Garrido-López Á, Tena MT. 2005. Experimental design approach for the optimisation of pressurised fluid extraction of additives from polyethylene films. J Chromatogr A. 1099:75-83.

Gillet G, Vitrac O, Desobry S. 2008. Prediction of solute partition coefficients between polyolefins and alcohols using a generalized Flory-Huggins approach. Accepted in Ind Eng Chem Res.

Gillet G, Vitrac O, Desobry S. 2008. Prediction of partition coefficients of plastic additives between packaging materials and food simulants. Submitted to Ind Eng Chem Res.

Gillet G, Vitrac O, Desobry S. 2008. Fast method to assess the composition of a polyolefin: an application to compliance testing of FCM. Submitted to J Appl Pol Sci.

Harison H. 1988. Migration of plasticizers from cling-film. Food Addit Contam. 5:493-499.

Institut National de la Recherche Agronomique: SAFE FOOD PACKAGING PORTAL: a site dedicated to the developement of decision tools based on numerical simulation and databases for the food industry. Retrieved 30 september 2008. Available from http://h29.univ-reims.fr/.

International Agency for Research on Cancer (IARC). 2000. IARC Monographs on the Evolution of Carcinogenic Risks to Humans to Some Industrial Chemicals, Vol. 77. Lyon, France: IARC Press.

Nielsen T J. 1994. Limonene and micrene sorption into refillable polyethylene teriphthalate bottles, and washing effects on removal of sorbed compounds. J Food Sci. 53: 253–257.

Petersen JH, Breindahl T. 2000. Plasticizers in total diet samples, baby food and infant formulae. Food Addit Contam. 17: 133-141.

Petersen JH, Trier XT, Fabech B. 2005. Mathematical modelling of migration : A suitable tool for the enforcement authorities? Food Addit Contam. 22:938-944.

Rothenbacher T, Baumann M., Fügel D. 2007. 2-isopropylthioxanthone (2-ITX) in food and food packaging materials on the German market. Food Addit Contamin. 24:438-444.

Sanches-Silva A, Pastorellis S, Cruz JM, Simoneau C, Castanheira I, Paseiro-Losada P. 2008. Development of a method to study the migration of six photoinitiators into powdered milk. J Agric Food Chem. 56:2722-2726.

Sharman M, Readn WA, Castle L, Gilbert J. 1994. Levels of di-(2-ethylhexyl) phthalate and total phthalate esters in milk, cream, butter and cheese. Food Addit Contam. 11:375-385.

Simoneau C, Theobald A, Wiltschko D, Anklam E. 1999. Estimation of intake of BADGE from canned fish consumption in Europe and migration survey. Food Addit Contam. 16:457-463.

Sun C, Chan SH, Lu D, Lee HMW, Bloodworth BC. 2007. Determination of isopropyl-9H-thioxanthen-9-one in packaged beverages by solid-phase extraction clean-up and liquid chromatography with tandem mass spectrometry detection J Chromatogr A. 1143:162-167.

Vitrac O, Challe B, Leblanc JC, Feigenbaum A. 2007. Contamination of packaged food by substances migrating from a direct-contact plastic layer: Assessment using a generic quantitative household scale methodology. Food Addit Contam. 24:75-94.

Vitrac O, Gillet G. 2008. Prediction of partition coefficients between food simulants and packaging materials. In "18th European Symposium on Computer Aided Process Engineering", Ed. B. Braunschweig and X. Joulia. Amsterdam: Elsevier. pp811-816.

Vitrac O, Hayert M. 2005. Risk assessment of migration from packaging materials into foodstuffs. AIChE J. 51(4):1080-1095.

Vitrac O, Hayert M. 2006. Identification of diffusion transport properties from desorption/sorption kinetics: an analysis based on a new approximation of Fick equation during solid-liquid contact. Ind Eng Chem Res. 45:7941-7956.

Vitrac O, Lézervant J, Feigenbaum A. 2006. Application of decision trees to the robust estimation of diffusion coefficients in polyolefines. J Appl Polymer Sci. 101:2167-2186.

Vitrac O, Mougharbel A, Feigenbaum A. 2007. Interfacial mass transport properties which control the migration of packaging constituents into foodstuffs. J Food Eng. 79(3):1048-1064.

4. Extensions possibles des méthodes développées

La combinaison des approches prédictives et expérimentales permet une prise de décision rapide quant à la conformité d'un matériau à condition que des données de référence de $D_{i,P}$ et/ou $K_{i,F/P}$ soient disponibles. La connaissance de l'un de ces deux paramètres n'est pas nécessaire lorsque la migration est très fortement contrôlée par l'autre paramètre ($D_{i,P}$ limitant pour l'Irganox 1330, $K_{i,F/P}$ limitant pour le BHT). Plus les informations disponibles sur le matériau et les additifs qui y sont ajoutés sont importantes, c'est-à-dire moins de facteurs de sécurité (surestimateurs) sont utilisés, plus la valeur de $C_{i,P}|^{max}$ augmente et plus il est simple de valider la conformité du matériau sur la seule base de résultats de prévision. La contamination peut aussi être évaluée dans le cas ou une identification de motifs chimiques présents est réalisée plutôt qu'une identification stricte des substances.

Les méthodes développées au cours de ce travail sont a priori généralisables aux autres polymères, substances et simulants. Nous avons toutefois identifié un certain nombre de limites à l'extension des méthodes, présentées dans le Tableau 3.1.

Tableau 3.1. Identification des limites à l'extension des méthodes proposées et solutions possibles imaginées. Les solutions soulignées seront testées dans la suite du travail.

Limite identifiée	Problème posé	Solution envisagée
$\chi_{i,P} \sim 0$ pour tous les polymères	Prévision de $K_{i,F/P}$ facilitée si cet effet est vérifié	Comparaison de coefficients de partages expérimentaux obtenus pour des polymères différents
Spectre IRTF du matériau brut présente une absorption forte dans une large gamme de nombres d'onde	Méthode de déconvolution des spectres inappropriée pour l'identification et la quantification des substances présentes dans le matériau	Utilisation de méthodes spectroscopiques alternatives (Raman par exemple)
Extraction lente des substances du matériau (polymères vitreux par exemple)	Compétitivité de l'extraction des substances (pour identification et quantification en vue d'appliquer les modèles prédictifs) avec le test de migration	Développer une méthode d'extraction rapide pour les matériaux concernés
Substances engendrant une séparation de phase dans un des milieux (lubrifiants par exemple)	Sous-évaluation possible de la contamination	Négliger l'effet cinétique
Plastifiants : modification des propriétés du matériau au cours de la migration	Variation du coefficient de diffusion avec le temps. Surévaluation de la contamination.	Développement de modèles de migration spécifiques
Limites de solubilité des additifs dans l'eau	Précipitation possible dans un des milieux, sous-évaluation de la contamination si précipitation	Tenir compte des quantités précipitées dans l'évaluation de la contamination
Substances réactives : équilibre continument déplacé	Contamination par des substances non présentes initialement dans le matériau	Identification et quantification des produits néoformés et intégration dans l'estimation de la contamination

Nous avons choisi de nous intéresser en particulier au PS, polymère vitreux, totalement amorphe, dont le comportement devrait donc être très différent de celui du PE, semi-cristallin. Des extensions concernant les méthodes analytiques et prédictives au PS sont développées dans les parties qui suivent. L'intégration des coefficients de solubilité dans un cadre plus large est aussi discutée.

4.1. Extension aux autres matériaux : cas du polystyrène

Concernant le PS en particulier, très peu de travaux ont été effectués à ce jour sur les méthodes d'extraction ou sur la mesure de coefficients de partage. La séparation des additifs extraits peut quant à elle se faire de la même manière quelque soit le matériau de départ à condition que les solvants d'extraction soient suffisamment similaires. Le Tableau 3.2 résume les conclusions auxquelles nous avons abouti pour le PEHD et les hypothèses complémentaires que nous avons souhaité vérifier pour le PS.

Tableau 3.2. Applications possibles des résultats précédents au cas du PS.

Conclusions faites pour le PE	**Hypothèses à vérifier sur le PS**
Migration des gros additifs forte dans les solvants de petite taille	$K_{i,F/P}$ dépend peu des propriétés du polymère
$\chi_{i,PE} \sim 0$	
Prévision robuste de $K_{i,F/PE}$ pour des simulants complexes (eau/éthanol)	On peut prévoir $K_{i,F/PS}$ pour des simulants complexes
Identification et quantification des additifs d'un matériau à partir d'un spectre IRTF de l'échantillon	Ces méthodes sont transposables au PS
Extraction totale des additifs d'un PE en deux extractions successives par reflux ou ASE	

4.1.1. Extraction des additifs d'un polystyrène

Les méthodes d'extraction à reflux et ASE ont été utilisées avec succès sur le PE. La méthode d'extraction la plus largement utilisée pour le PS est la dissolution/reprécipitation. Celle-ci présente un biais à nos yeux du fait que l'on ne contrôle pas la quantité d'additifs piégés dans le matériau au cours de sa reprécipitation. Nous avons donc souhaité appliquer une autre méthode d'extraction au PS et nous nous sommes en particulier intéressés au développement d'une méthode par ASE, plus rapide. La quantification des additifs dans les simulants a été réalisée grâce à la méthode CLHP utilisée pour les extraits de PEHD.

Dans un premier temps, le choix d'un solvant d'extraction adéquat s'est avéré nécessaire. Le PS est en effet soluble dans les solvants les plus courants (DCM, THF, etc.) et nous en avons cherché un qui permette une bonne extraction (gonflement élevé du matériau

correspondant à un écartement des chaines de polymère) des additifs sans dissoudre l'échantillon. Les résultats des tests de gonflement sont présentés sur la Figure 3.3. Les alcools étant généralement utilisés pour reprécipiter le PS dissous, nous avons testé des mélanges contenant 75% d'IPA et 25% d'un solvant apte à dissoudre le PS.

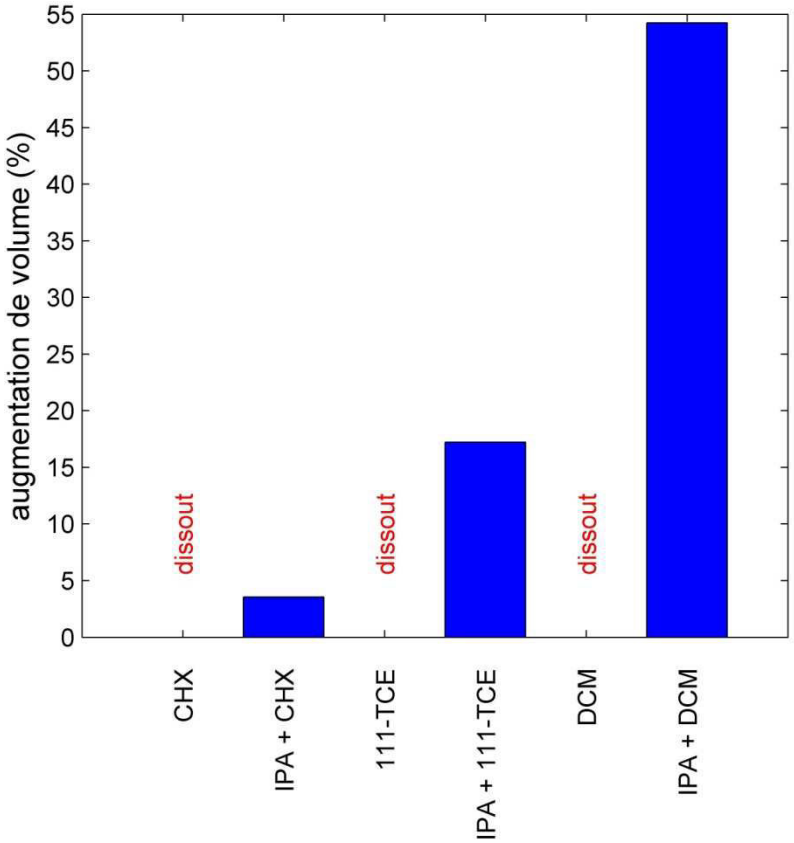

Figure 3.3. Gonflement du polystyrène en fonction du solvant ou mélange de solvant utilisé, après 24h de contact à 40°C. IPA = isopropanol, CHX = cyclohexane, 111-TCE = 1,1,1-trichloroéthane, DCM = dichlorométhane. Les mélanges sont constitués de 75% d'IPA (v/v).

Le mélange IPA/DCM (75:25, v/v) présente les propriétés de solvant recherchées et a été sélectionné pour réaliser les extractions d'additifs du PS.

Dans le cas d'extractions successives des substances d'un échantillon, une extrapolation mathématique des premières extractions permettant de déduire la quantité totale a été démontrée et appliquée avec succès à la CPG à espace de tête (Kolb et Ettre, 1991 ; Maucourt, 1991).

$$C_{tot} = \frac{(C_1)^2}{C_1 - C_2} \tag{3.1}$$

Ou C_1 est la quantité extraite au cours de la première extraction, C_2 est la quantité extraite au cours de la seconde extraction et C_{tot} est la quantité extraite après extraction totale. Le

modèle présenté par l'équation (3.1) est a priori applicable à tous types d'extraction à condition que les équilibres soient atteints à chaque étape. Il suppose une décroissance exponentielle des quantités extraites. L'extraction totale des additifs du PS nécessite un grand nombre d'extractions successives pour les substances de taille importante. Les fortes contraintes (pression et température élevées) appliquées au matériau lors d'extractions par ASE permettent par ailleurs d'atteindre rapidement les équilibres.

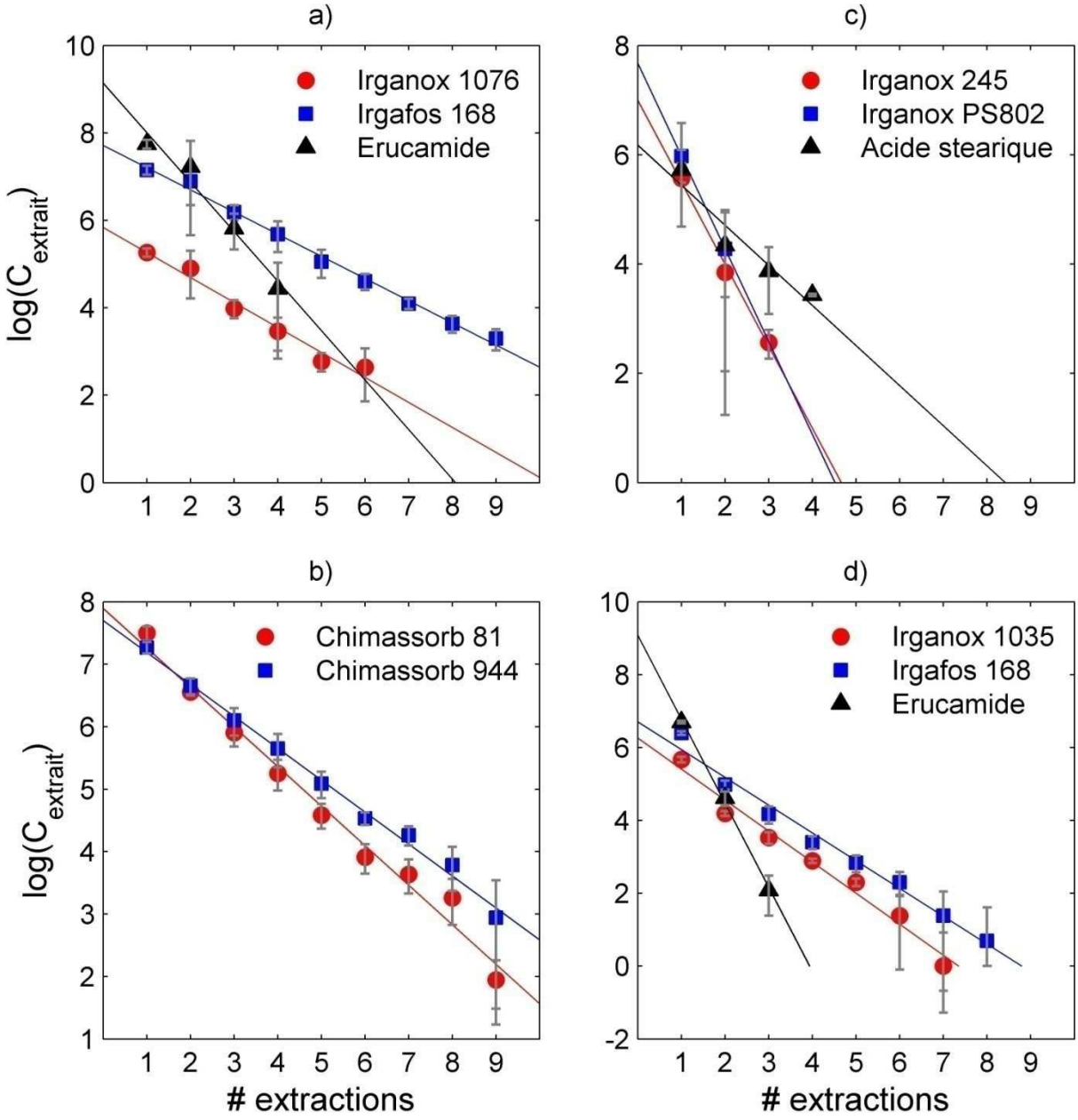

Figure 3.4. Quantités extraites de films PS formulés au cours de 9 extractions successives. Chaque expérience et chaque dosage ont été répétés 3 fois, de sorte que chaque point est la moyenne de 9 résultats.

La Figure 3.4 présente les résultats de 9 extractions successives appliquées à quatre échantillons formulés de PS et permet de vérifier la décroissance exponentielle des quantités

extraites. La méthode semble donc applicable. La Figure 3.5 présente par ailleurs une comparaison entre les concentrations estimées grâce à deux extractions successives par ASE et l'équation (3.1) d'une part et la quantité cumulée des 9 extractions successives (extraction totale).

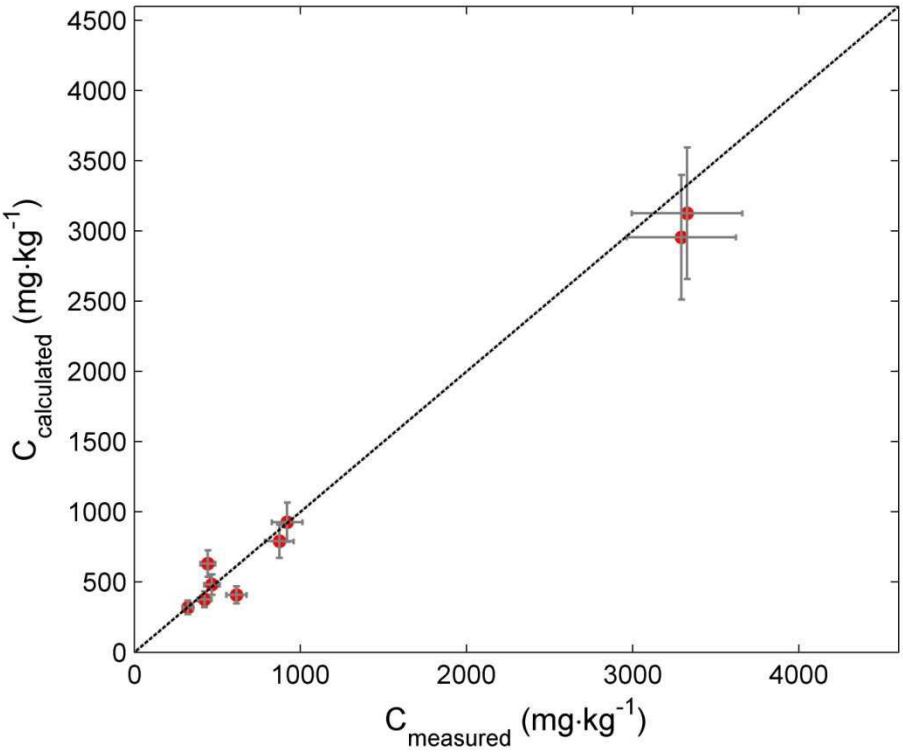

Figure 3.5. Comparaison entre les quantités extraites par reflux jusqu'à extraction totale cumulées et la quantité estimée à partir de deux extractions ASE et de l'équation (3.1).

Les résultats sont satisfaisants. Les écarts observés entre les valeurs mesurées et observées ne dépassent pas en moyenne l'erreur liée à la mesure. Une quantification des additifs présents dans un PS peut donc être obtenue rapidement grâce à seulement deux extractions successives par ASE.

4.1.2. Effet des propriétés du polymère sur la prévision des coefficients de partage

Les résultats obtenus pour le PE montrent une faible dépendance des coefficients de partage estimés aux propriétés du polymère ($\chi_{i,PE} \approx 0$). En appliquant l'équation (1.26) au PEHD et au PS, le rapport des coefficients de partage s'écrit :

$$\frac{K_{i,F/PE}}{K_{i,F/PS}} = \frac{\left[\left(1-c\right)\cdot\dfrac{\hat{C}_{i,F}\Big|_{eq}}{\dfrac{1}{a_i}\cdot\hat{C}_{i,P}\Big|_{eq} - b_i\cdot C_{i,P}\Big|_{t=0}}\right]_{PE}}{\left[\dfrac{\hat{C}_{i,F}\Big|_{eq}}{\dfrac{1}{a_i}\cdot\hat{C}_{i,P}\Big|_{eq}}\right]_{PS}} = \left(1-c\right)\cdot\frac{\left[\dfrac{\hat{C}_{i,F}\Big|_{eq}}{\hat{C}_{i,P}\Big|_{eq} - \dfrac{b_i}{a_i}\cdot C_{i,P}\Big|_{t=0}}\right]_{PE}}{\left[\dfrac{\hat{C}_{i,F}\Big|_{eq}}{\hat{C}_{i,P}\Big|_{eq}}\right]_{PS}} \tag{3.2}$$

En considérant que b_i est très petit devant a_i ($\frac{b_i}{a_i} \to 0$), on en déduit :

$$\frac{K_{i,F/PE}}{K_{i,F/PS}} \approx \left(1-c\right)\cdot\frac{\widehat{K}_{i,F/PE}}{\widehat{K}_{i,F/PS}} \tag{3.3}$$

Soit, si les $K_{i,F/P}$ prévus sont égaux :

$$c \approx 1 - \frac{\widehat{K}_{i,F/PS}}{\widehat{K}_{i,F/PE}} \tag{3.4}$$

Ainsi, si les coefficients de partage ne dépendent pas du polymère, les coefficients de partage d'une substance entre un simulant et divers polymères devraient être les même au facteur de cristallinité près. Une comparaison des coefficients mesurés expérimentalement pour le Chimassorb 81 entre divers simulants et un PEHD ou un PS est représentée sur la Figure 3.6.

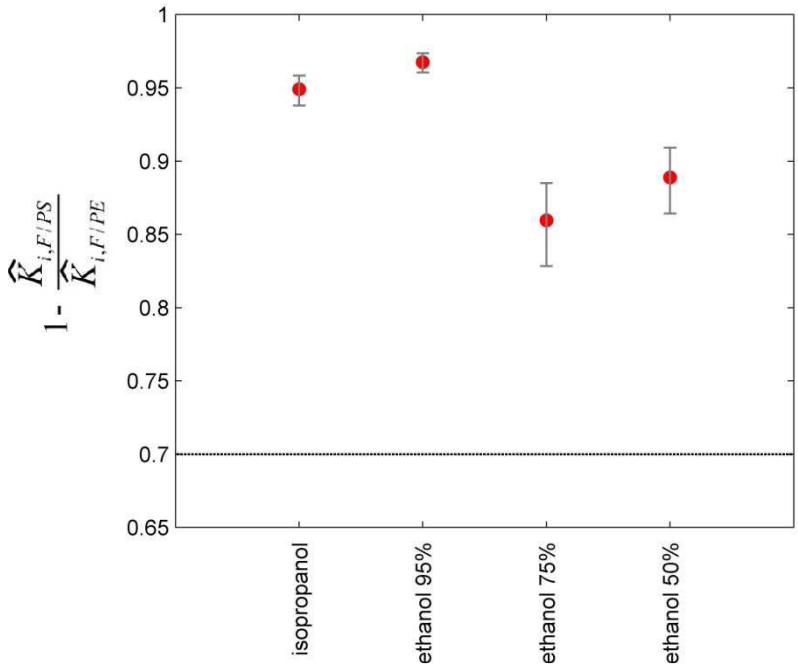

Figure 3.6. Effet des propriétés du polymère sur les coefficients de partage. La ligne pointillée représente la valeur de la cristallinité du PEHD étudié.

Le rapport des coefficients de partage mesurés ne correspond pas à la cristallinité du PEHD même si la tendance est la bonne (rapport inférieur à 1). Une réserve sera tout de même émise sur les valeurs de $\widehat{K}_{i,F/PS}$ car la concentration résiduelle dans le polymère a été estimée en utilisant la technique de dissolution/reprécipitation pour l'extraction des substances résiduelles. Par ailleurs les barres d'erreurs indiquées ont été calculées à partir des répétitions de mesure des coefficients de partage et ne tiennent donc pas compte des erreurs de mesure de la cristallinité du PEHD.

Le modèle des coefficients de partage a ensuite été appliqué aux additifs pour lesquels un coefficient a été mesuré dans l'isopropanol (Figure 3.7) et dans les mélanges eau/éthanol (Figure 3.8).

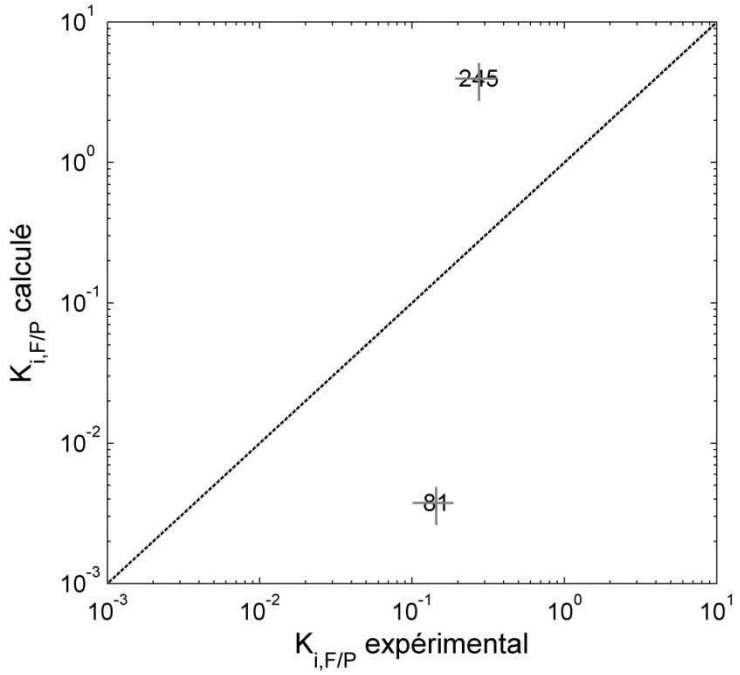

Figure 3.7. Coefficients de partage prévus et expérimentaux, $K_{i,F/P}$ entre l'isopropanol et le PS, pour l'Irganox 245 et le Chimassorb 81. Les additifs sont représentés par leur numéro.

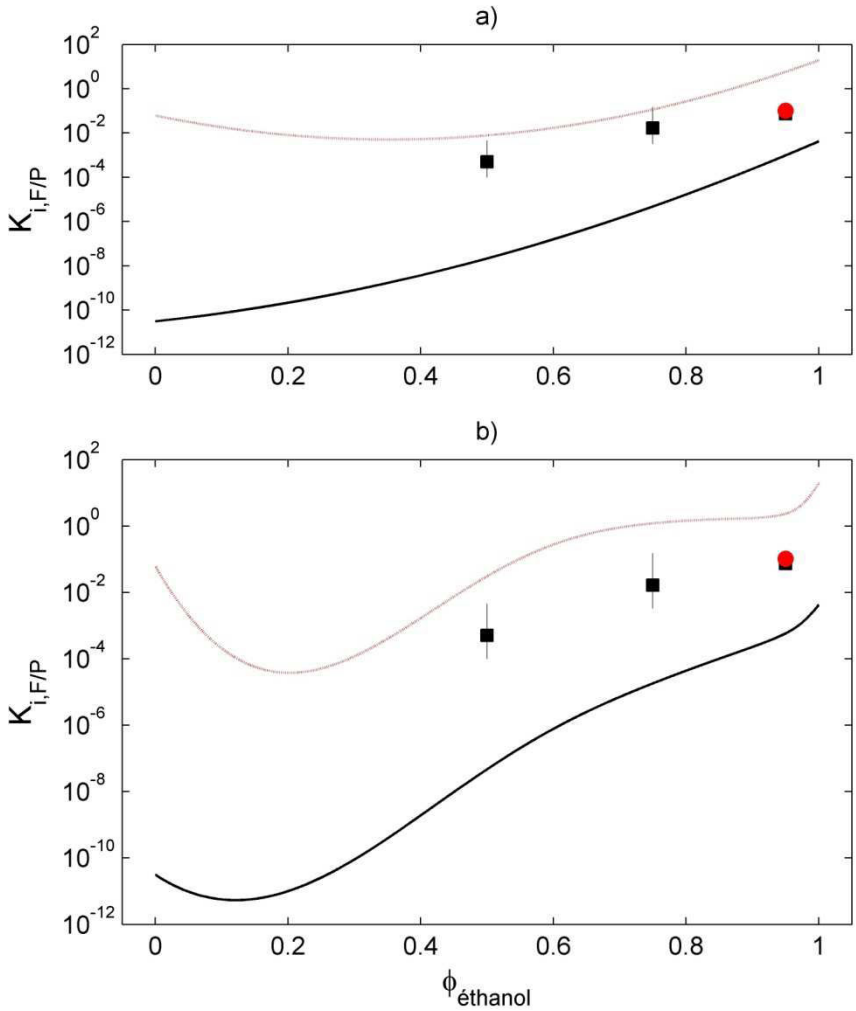

Figure 3.8. Coefficients de partage prévus et expérimentaux, $K_{i,F/P}$: a) A = mélange eau/éthanol, prévision sans les termes d'ordre 3, ($\chi_{eau,éthanol}$=-2.04), b) A = mélange eau/éthanol, prévision avec les termes d'ordre 3. Le modèle continue correspond aux valeurs prévues pour le Chimassorb 81 (■). Le modèle pointillé correspond aux valeurs prévues pour l'Irganox 245(●).

La Figure 3.8 présente les valeurs expérimentales et prévues de $K_{i,F/P}$ dans les mélanges eau/éthanol. Les résultats sont similaires à ceux obtenus pour les PEs. Les courbes de valeurs calculées sont cohérentes avec les propriétés des modèles associés : modèle du second degré à dérivée strictement positive pour la Figure 3.8a et modèle du troisième degré pour la Figure 3.8b. Sur cette dernière, l'allure particulière des courbes est due à la variation de $\chi_{eau,éthanol}$, lui-même corrélé aux enthalpies de mélange (équation (2.5)). Il faut noter que peu de valeurs sont disponibles à ce jour pour évaluer complètement la méthode sur ce matériau. La méthode de prévision semble toutefois applicable.

4.1.3. Conclusion partielle sur le PS

Une méthode rapide d'extraction ainsi qu'un solvant adéquat ont été proposés. L'identification et la quantification des additifs présents dans un PS sont ainsi réalisables en un temps compatible aves l'utilisation des outils de prédiction.

Le modèle de prévision des coefficients de partage a été appliqué au PS avec succès sur les quelques données expérimentales disponibles. Il n'a par ailleurs pas été démontré que les propriétés du polymère n'ont pas d'influence sur la valeur de $K_{i,F/P}$ prévue.

4.2. Effet des limites de solubilité dans l'eau

Si l'on considère le point de vue de la thermodynamique des phénomènes irréversibles, on peut décrire le système à l'équilibre de la manière suivante (Figure 3.9).

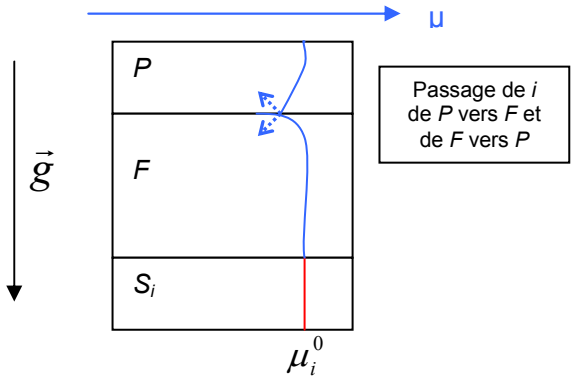

Figure 3.9. Schéma d'un système aliment (*F*) / emballage plastique (*P*), ce dernier contenant initialement une substance *i*. Une phase constituée de la substance *i* solide (S_i) est aussi envisagée. Cette dernière est supposée être un précipitât, qui se dépose par gravité.

A tout moment dans *F* et *P*, on a :

$$\mu_i = \mu_i^0 + R.T.\ln a_i \leq \mu_i^0 \qquad (3.5)$$

D'après l'équation, les potentiels chimiques ne vont pas dans le sens de la création du précipitât, au contraire. C'est l'intervention de la convection solutale et du flux thermique qui permet la formation du précipité (force de gravitation et flux thermique). On en déduit que tout matériaux formulé en deçà de sa limite de solubilité ne fera pas de S_i. Les limites de solubilités des migrants dans les simulants en général et dans l'eau en particulier ne seront donc dépassées au cours de la migration, engendrant la précipitation du migrant, que si le polymère au contact est formulé au delà de sa propre limite de solubilité.

Conclusion

Les coefficients de partage de contaminants de faibles poids moléculaires et d'additifs des matériaux plastiques ont été prévus en utilisant une représentation à grille de type Flory-Huggins dans les deux compartiments, aliment et polymère. Ce modèle de prévision prend en compte une contribution entropique non configurationelle qui était négligée dans les modèles précédemment proposés et peut être simplement dérivée de considérations purement géométriques. Il a été montré que cette contribution peut être évaluée rapidement à partir des volumes des migrants accessibles aux atomes d'hydrogène. Notre modèle ne tient compte que des interactions entre proches voisins, ne nécessitant donc ni une représentation détaillée de tout le polymère, ni des capacités de calcul élevées (un ordinateur personnel peut être suffisant). Les biais liés à l'échantillonnage des énergies paires à paires ont par ailleurs été largement étudiés et des corrections proposées pour éviter notamment le sur-échantillonnage de configuration particulières dûes à l'enroulement des molécules linéaires. L'approche a été étendue à l'eau et aux mélanges eau/éthanol, intégrant la non idéalité du mélange. Une repondération des énergies de contact ainsi que l'introduction de propriétés tabulées des mélanges eau/éthanol sont proposées pour lever les limitations intrinsèques de l'approximation de Flory-Huggins à intégrer les liaisons hydrogènes. Il a été montré en particulier que l'évolution de $K_{i,F/P}$ est non linéaire en fonction de la fraction volumique en éthanol. L'erreur commise sur les valeurs prévues est proche de celle commise sur les valeurs expérimentales.

Une méthode rapide d'identification et de quantification basée sur une procédure semi-automatique de déconvolution de spectres infrarouge d'extraits de polymère dans le dichlorométhane a été développée. La procédure d'inversion est implémentée comme un problème itératif des moindre carrés re-pondéré à chaque étape et optimisée pour travailler sur un dictionnaire de substances ouvert (toutes les substances ne sont pas connues) en combinant des spectres de référence des additifs et des spectres d'absorption normalisés de fonctions chimiques typiques. La méthode a été calibrée pour 21 additifs typiques et testée avec succès sur 3 mélanges théoriques et 4 extraits de PEHD contenant jusqu'à 8 substances. Une identification par motif est aussi proposée lorsque l'identification stricte des additifs n'est pas possible. La méthode complète a été implémentée dans une toolbox Matlab (Mathworks, USA) nommée ACTIA-LNE.

Un processus de décision complet a été proposé pour des PEs au contact d'un mélange eau/éthanol (50:50, v/v), intégrant les étapes de déformulation et les valeurs prévues de $K_{i,F/P}$. La démonstration de la conformité peut être réalisée sans disposer de toutes les informations sur le matériau. L'approche permet notamment de calculer rapidement pour chaque substance

une quantité maximale autorisée dans le matériau sans risquer de dépasser la LMS et de la faire valider par le fabricant.

Ce travail a par ailleurs montré que malgré l'affinité naturelle des additifs pour les polymères, ceux-ci présentent aussi une affinité forte pour les solvants polaires constitués de petites molécules du fait de la contribution entropique (effet de taille). Ceci nous amène à prévoir des taux de migration dans les aliments élevés à des températures où la diffusion et la solubilité ne sont plus limitantes. Une conséquence pratique est que, dans le cas de contacts prolongés à température élevée, la contamination par des molécules de masses moléculaires élevées sera plus importante que la contamination par des molécules de faibles masses moléculaires.

Une première extension des méthodes développées pour des PEs a été est proposée sur le PS. Une méthode rapide d'extraction des substances par ASE a été développée et les outils de prévisions de $K_{i,F/P}$ ont été appliqués. L'utilisation de méthodes rapides semble bien applicable à des matériaux de structure cristalline différente. Une extension plus généralisée des méthodes proposées à d'autres matériaux, simulants et substances est fortement souhaitable pour généraliser une procédure rapide de validation de la conformité des matériaux d'emballes plastiques vis-à-vis du contact alimentaire.

L'application de l'approche Flory-Huggins peut être étendue a priori à tous les matériaux, tous les simulants et tous les contaminants potentiels. Elle peut être étendue à d'autres mélanges binaires de solvants utilisés comme simulants alimentaires alternatifs de l'huile d'olive (isopropanol/acétate d'éthyle par exemple). Il sera toutefois difficile de valider l'applicabilité de l'approche à des matériaux autres que les polyoléfines du fait du manque de données expérimentales. Générer ces données est une première priorité dans les études futures pour pouvoir ensuite valider les modèles de prévision. L'application aux matériaux vitreux en particulier pourra être testée sur le PS ou le PET.

La méthode de déconvolution de spectres IRTF ne peut raisonnablement pas être étendue à tous les matériaux. Le PS, par exemple, présente des bandes d'absorption très importantes sur l'ensemble des gammes de longueurs d'onde étudiées, rendant l'application de la méthode très difficile. Des applications à d'autres techniques de spectrométries, telle que la spectrométrie Raman, sont à envisager dans ce cas là. Par ailleurs, la méthode n'a pas pour but de prévoir les concentrations exactes des substances mais plutôt de fournir des surestimateurs de ces concentrations. La surestimation ne permettant pas toujours de conclure

à la conformité d'un matériau, il sera utile de développer des approches complémentaires pour prévoir plus précisément les concentrations dans ce cas là. En appliquant la technique à des solutions de simulants plutôt qu'à des extraits dans le dichlorométhane, il pourrait aussi être envisagé d'appliquer cette méthode au suivi de cinétiques de désorption/migration des additifs dans des solvants ou des simulants.

Enfin, une extension du processus complet d'évaluation de la conformité à d'autres matériaux et d'autres simulants est souhaitable. Couplée à un transfert du processus aux utilisateurs finaux des emballages et aux laboratoires de contrôle, elle leur permettrait de réaliser rapidement l'évaluation des matériaux pour démontrer leur conformité.

Bibliographie

AKTS. 2008. AKTS-Thermokinetics software. Accès le 30 Septembre 2008. http://www.akts.com/sml-diffusion-migration-multilayer-packaging/download-diffusion-prediction-software.html.

Arab Tehrany, E.; Desobry, S. 2004. Partition coefficient in food/packaging systems : a review. *Food Additives and Contaminants.* 2004, Vol. 21, pp. 1186-1202.

Arab Tehrany, E. 2005. *Modelling of molecular partition coefficient in food-packaging systems.* Thèse de doctorat de l'Institut National Polytechnique de Lorraine.

Arab Tehrany, E.; Fournier, F.; Desobry, S. 2006. Simple method to calculate partition coefficient of migrants in food stimulant/Polymer system. *Journal of Food Engineering.* vol. 77 pp. 135-139.

Arab Tehrany, E.; Desobry, S. 2007. Determination of partition coefficient of migrants in food simulants/polymers systems. *Journal of Food Chemistry*. vol. 10 pp. 1714-1718.

Arab Tehrany, E.; Mouawad, C.; Desobry, S. 2007. Determination of partition coefficient of migrants in food simulants by the PRV method. *Journal of Food Chemistry*. vol. 105, pp. 1571-1577

Arpino, P.J.; Dilettato, D.; Nguyen, Khoa; Bruchet, A. 1990. Investigation of antioxydants and UV stabilizers from platics. Part I : comparison of HPLC and SFC ; preliminary SFC/Ms study. *Journal of High resolution Chromatography.* 1990, Vol. 13, pp. 5-12.

Ashraf-Khorassani, M.; Levy, J.M. 1990. Quantitative analysis of polymer additives in low density polyethylene using supercritical fluid extraction/supercritical fluid chromatography. *Journal of High Resolution Chromatography.* 1990, Vol. 13, pp. 742-747.

Ashraf-Khorassani, M.; Hinman, S.; Taylor, T. 1999. A unified sample preparation system for extraction of various anlyte/matrix combinations. *Journal of High Resolution Chromatography.* 1999, Vol. 22, pp. 271-275.

Baner, A. L.; Brandsch, J.; Frantz, R.; Piringer, O. 1996. The application of a predictive migration model for evaluationg the compliance of plastic materials with European food regulations. *Food Additives and Contaminants.* 1996, Vol. 13, pp. 587-601.

Baner, A.L. et Piringer, O.G. 1991. Prediction of solute partition coefficients between polyolefins and alcohols using the regular solution theory and group contribution methods. *Industrial and Engineering Chemistry Research.* 1991, Vol. 30, pp. 1506-1515.

Bart, J.C.J. 2005. *Additives in polymers : Industrial analysis and applications.* Chichester : John Wiley & Sons, 2005.

Barton, A.F.M. 1983. *CRC Handbook of Solubility Parameters and Other Cohesion Parameters.* Boca Raton : CRC, 1983.

Battum, D.; van et Lierop, J.B.H. 1997. *Materials and articles in contact with foodstuffs, Guide for examination of plastic food contact materials.* s.l. : CEN TC 194/SCI/WG2 document N118, 1997.

Bawendi, M.G.; Freed, K.F. 1988. Systematic corrections to Flory-Huggins theory: Polymer-Solvent-Void systems and Binary Blend-Void Systems. *Journal of Chemical Physics.* 1988, Vol. 88, pp. 2741-2756.

Bawendi, M.G.; Freed, K.F.; Mohanty, U. 1987. A Lattice Field Theory for Polymer Systems with Nearest-Neighbor Interaction Energies. *Journal of Chemical Physics.* 1987, Vol. 87, pp. 5534-5540.

Bawendi, M.G.; Freed, K.F.; Mohanty, U. 1986. A Lattice Model for Self-Avoiding Polymers with Controlled Length Distributions. II. Corrections to Flory-Huggins Mean Field. *Journal of Chemical Physics.* 1986, Vol. 84, pp. 7036-7047.

Begley, T.H. 1997. Methods and approaches used by FDA to evaluate the safety of food packaging materials. *Food Additives and Contaminants.* 1997, Vol. 14, pp. 545-553.

Begley, T.; Castle, L.; Feigenbaum, A.; Frantz, R.; Hinrichs, K.; Liclmy, T.; Mercea, P.; Milana, M.; O'Brien, A.; Rebre, S.; Rijk, R.; Piringer, O. 2005. Evaluation of migration models that might be used in support of regulations for food-contact plastics. *Food Additives and Contaminants.* 2005, Vol. 22, pp. 73-90.

Ben-Naim, A. 2006. *Molecular Theory of Solutions.* Oxford : Oxford university, 2006.

Bermudez, M.-D.; Carrion-Vilches, F.-J.; Martinez-Nicolas, G.; Pagan, M. 2002. Supercritical carbon dioxide extraction of a liquid crystalline additive from polystyrene matrices. *Journal of Supercritical Fluids.* 2002, Vol. 23, pp. 59-63.

Boulougouris, G.C.; Economou, I.G.; Theodorou, D.N. 2001. Calculation of the chemical potential of chain molecules using the staged particle deletion scheme. *Journal of Chemical Physics.* 2001, Vol. 115, pp. 8231-8237.

Boyne, J.A.; Williamson, A.G. 1967. Enthalpies of mixing of ethanol and water at 25°C. *Journal of Chemical Engineering Date.* 1967, Vol. 12, p. 318.

Brandsch, J.; Mercea, P.; Ruter, M.; Tosa, V.; Piringer, O. 2002. Migration modelling as a tool for quality assurance of food packaging. *Food Additives and Contaminants.* 2002, Vol. 19 (sup), pp. 29-41.

Breen, C.; Last, P. M.; Taylor, S.; Komadel, P. 2000. Synergic chemical analysis – the coupling of TG with FTIR, MS and GC-MS 2. Catalytic transformation of the gases evolved

during the thermal decomposition of HDPE using acid-activated clays. *Thermochimica Acta.* 2000, Vol. 363, pp. 93-104.

Brydson, J.A. 1999. *Plastics materials.* 7th Edition. Oxford : Butterworth-Heinemann, 1999. p. 920.

Buchalla, R.; Boess, C.; Bögl, K.W. 2000. Analysis of volatile radiolysis products in gamma-irradiated LDPE and polypropylene films by thermal desorption-gas chromatography-mass spectrometry. *Applied Radiation and Isotopes.* 2000, Vol. 52, pp. 251-269.

Buchalla, R.; Boess, C.; Bögl, K.W. 1999. Characterization of volatile radiolysis products in radiation-sterilized plastics by thermal desorption-gas chromatography-mass spectrometry : screening of six medical polymers. *Radiatoin Physics and Chemistry.* 1999, Vol. 56, pp. 353-367.

Bueche, F. 1968. Diffusion of Polystyrene in Polystyrene: Effect of Matrix Molecular Weight. *Journal of Chemical Physics.* 1968, Vol. 48, pp. 1410-1411.

Bücherl, T.; Gruner, A.; Palibroda, N. 1994. Rapid analysis of polymer homologues and addiives withSFE/SFC-MS coupling. *Packaging Technology and Science.* 1994, Vol. 7, pp. 139-154.

Burman, L.; Albertsson, A.-C. 2005. Chromatographic fingerprinting - a tool for classification and for predicting the degradation state of degradable polyethylene. *Polymer Degradation and Stability.* 2005, Vol. 89, pp. 50-63.

Burman, L.; Albertsson, A.-C.; Höglund, A. 2005. Solid-phase microextraction for qualitative and quantitative determination of migrated degradation products of antioxydants in an organic aqueous solution. *Journal of Chromatography A.* 2005, Vol. 1080, pp. 107-116.

Caceres, A.; Ysambertt, F.; Lopez, J.; Marquez, N. 1996. Analysis of photstabilizer in high density polyethylene by reverse- and normal-phase HPLC. *Separation Science and Technology.* 1996, Vol. 31, pp. 2287-2298.

Camacho, W.; Karlsson, S. 2001. Quality-determination of recycled plastic packaging waste by identification of contaminants by GC-MS after microwave assisted extraction (MAE). *Polymer Degradation and Stability.* 2001, Vol. 71, pp. 123-134.

Carlsson, D.J.; Krzymien, M.E.; Deschênes, L.; Mercier, M.; Vachon, C. 2001. Phosphite additives and their transformation products in polyethylene packaging for G-irradiation. *Food Additives and Contaminants.* 2001, Vol. 18, pp. 581-591.

Carrega, M. 2005. *Aide-mémoire : Matières plastiques.* Paris : Dunod, 2005.

Carrott, M.J.; Joens, D.C.; Davidson, G. 1998. Identification and analysis of polymer additives using packed-column supercritical fluid chromatography with APCI mass spectrometric detection. *Analyst.* 1998, Vol. 123, pp. 1827-1833.

Commission Européenne. 2002. Directive 2002/72/CE. *Journal officiel des communautés européennes L 220 du 15 août 2002.* 2002, pp. 18-58.

Commission Européenne. 2004. Règlement 1935/2004. *Journal officiel des communautés européennes L 338 du 13 novembre 2004.* 2004, pp. 4-17.

Commission Européenne. 2005. *Synoptic Document.* 2005.

Commission Européenne. 2007. Directive 2007/19/CE. *Journal officiel des communautés européennes L 91 du 31 Mars 2007.* 2007.

Chatwin, P.C.; Katan, L.L. 1989. The role of mathematics and physics in migration predictions. *Packaging Technology and Science.* 1989, Vol. 2, pp. 75-84.

Coulier, L.; Kaal, E.R.; Tienstra, M.; Hankemeier, Th. 2005. Identification and quantification of (polymeric) hindered-amine light stabilizers in polymers using pyrolysis–gas chromatography–mass spectrometry and liquid chromatography–ultraviolet absorbance detection–evaporative light scattering detection. *Journal of Chromatography A.* 2005, Vol. 1062, pp. 227-238.

Crank, J. 1975. *The mathematics of diffusion.* 2nd Ed. Oxford : Oxford University, 1975. p. 414.

Crine, J.P.; Haridoss, S.; Cole, K.C. 1988. Determination of the nature and content of antioxydant and antioxydant synergist in polyethylene and crosslinked polyethylene in cables. *Polymer engineering and science.* 1988, Vol. 28, pp. 1445-1449.

Cussler, E.L. 1997. *Diffusion, mass transfer in fluids systems.* 2nd Ed. Cambridge : Cambridge university, 1997.

De Gennes, P.G. 1971. Reptation of a polymer chain in presence of fixed obstacles. *Journal of Chemical Physics.* 1971, Vol. 55, pp. 572-579.

Deschesnes, A.; Vanden Bout, D.A. 2001. Single-molecule studies of heterogeneous dynamics in polymer melts near the glass transition. *Science.* 2001, Vol. 292, pp. 255-258.

Doi, M.; Edwards, S.F. 1978. Dynamics of concentrated polymer systems. Part 1. Brownian motion in the equilibrium state. *Journal of the Chemical Society, Faraday Transactions.* 1978, Vol. 74, pp. 1789-1801.

Dopico-Garcia, M.S.; López-Vilariño, J.M.; Gonz, M.V. 2003. Determination of antioxidant migration levels from low-density polyethylene films into food simulants. *Journal of Chromatography A.* 2003, Vol. 1018, pp. 53-62.

Downes, T.W. 1987. Practical and theoretical considerations in migration. [éd.] J.E Gray, B. Harte et J. Miltz. *Food Product-Package compatibility.* 1987, pp. 44-58.

Ehrenstein, G.W.; Montagne, F. 2000. *Matériaux polymères : structure, propriétés et applications.* Paris : HERMES science publication, 2000.

Einstein, A. 1905. Über die von der molekularkinetischen Theorie der Wärme geforderte Bewegung von in ruhenden Flüssigkeiten suspendierten Teilchen. *Annals of Physics.* 1905, Vol. 17, pp. 549–560.

Elbro, H.S.; Fredenslund, A.; Rasmussen, P. 1990. A new simple equation for the prediction of solvent activities in polymer solutions. *Macromolecules.* 1990, Vol. 23n, pp. 4707-4714.

Ezquerro, O.; Pons, B.; Tena, M.T. 2003. Direct quantitation of volatile organic compounds in packaging materials by headspace solid-phase microextraction–gas chromatography–mass spectrometry ; Oscar Ezquerro, Begona Pons, Marıa Teresa Tena. *Journal of chromatography A.* 2003, Vol. 985, pp. 247-257.

FABES. 2008. Analytik und Bewertung von Stoffürbeganger. Accès le 2 Novembre 2008. http://www.fabes-online.de/software.php?lang=de&mode=migratest

Feigenbaum, A.; Petersen, J.H.; Binderup, M.L.; Lillemark, L.; Van Lierop, B.; Brigot, G.; Vergnaud, J.M.; Ferrier, D.; Ygoubi, N.; Frantz, R.; Bouquant, J. 1997. *EU DG XII Research Programme AIR 941025 : Safety and quality contrôle of plastics materials for food contact.* 1997.

Flick, E.W. 2002. *Plastics Additives, an Industrial guide.* Norwich, New York : Noyes publication, William and Andrew Publishing, 2002.

Flory, P.J. 1953. *Principles of Polymer Chemistry.* Ithaca : Cornell University, 1953.

Földes, E.; Maloschik, E.; Kriston, I.; Staniek, P.; Putanszky, B. 2006. Efficiency and mechanism of phophorous antioxydants in Phillips type polyethylene. *Polymer Degradation and Stability.* 2006, Vol. 91, pp. 479-487.

Font, R. Aracil, I.; Fullana, A.; Conesa, J.A. 2004. Semivolatile and volatile compounds in combustion of polyethylene. *Chemosphere.* 2004, Vol. 57, pp. 615-627.

Franz, R., Huber, M., Piringer, O. 1997. Presentation and experimental verification of a physico-mathematical model describing the migration across functional barrier layers into foodstuffs. *Food Additives and Contaminants.* 1997, Vol. 14, pp. 627-640.

Fredenslund, A.; Gmehling, J.; Rasmussen, P. 1977. Computerized design of multicomponent distillation columns using the UNIFAC group contribution method for

calculation of activity coefficients. *Industrial and Engineering Chemistry.* 1977, Vol. 16, pp. 450–462.

Frenkel, D.;Smit, B. 2002. *Understanding molecular simulation. From algorithms to applications.* New York : Academic press, 2002. Vol. 1.

Frisina, G.; Busi, P.; sevini, F. 1979. Gas chromatographic analysis of fatty acid amides in polyolefins. *Journal of chromatography A.* 1979, Vol. 173, pp. 190-193.

García, R.S.; Sanches silva, AT.; Losada, P.P. 2004. Determination of diphenylbutadiene by liquid chromatography–UV–fluorescence in foodstuffs ; Raquel Sendón García, Ana Teresa Sanches Silva, Perfecto Paseiro Losada. *Journal of Chromatography A.* 2004, Vol. 1056, pp. 99-103.

Garrido-Lopez, Á.; Tena, M.T. 2005. Experimental design approach for the optimisation of pressurised fluid extraction of additives from polyethylene films. *Journal of chromatography A.* 2005, Vol. 1099, pp. 75-83.

Garrido-López, Á.; Esquiu, V.; tena, M.T. 2007a. comparison of three chromatography methods for the determination of slip agents in polyethylene films ; Álvado Garrido López, Vanesa Esquiu, María Teresa Tena. *Journal of Chromatographt A.* 2007, Vol. 1150, pp. 178-182.

Garrido-López, Á.; Cancet, I.; Montaño, P.; González, R.; Tena, M.T. 2007b. Microwave-assisted oxidation of phosphite-type antioxidant additives in polyethylene film extracts. *Journal of Chromatography A.* 2007, Vol. 1175, pp. 154-161.

Gavara, R.; Hernandez, R.J.; Giacin, J. 1996. Methods to determine partition coefficients of organic compounds in water/polystyren system. *Journal of Food Science.* 1996, Vol. 61, pp. 947-952.

Goujot, D.; Vitrac O. 2008. Exact solutions to mass diffusion in complex cases. Solutions for nonlinear isotherms. Submitted to *AiCHE J.*

Gilbert, S.; Miltz, J.; Giacin, J.R. 1980. Transport considerationsof potential migrants from food packaging materials. *Journal of Food Processing and Preservation.* 1980, Vol. 4, pp. 27-49.

GPF, Groupe. 2005. Publications de la commission enseignement du groupe français d'étude et d'applications des polymères. [En ligne] 2005. http://gfp.asso.fr/.

Haider, N.; Karlsson, S. 1999a. A rapid ultrasonic extraction technique to identify and quantify additives in poly(ethylene) ; Nadejzda Haider and Sigbritt Karlsson. *Analyst.* 1999, Vol. 124, pp. 797-800.

Haider, N.; Karlsson, S. 1999b. Migration and release profile of Chimassorb 944 from low-density polyethylene film (LDPE) in simulated landfills. *Polymer Degradation and Stability.* 1999, Vol. 64, pp. 321-328.

Haider, N.; Karlsson, S. 2001. Loss of Chimassorb 944 from LDPE and identification of additive degradation products after exposure to water, air and compost ; Nadejzda Haider, Sigbritt Karlsson. *Polymer Degradation and Stability.* 2001, Vol. 74, pp. 103-112.

Haider, N.; Karlsson, S. 2002. Loss and transformation products of the aromatic antioxydants in MDPE film under long-term exposure to biotic and abiotic conditions. *Journal of Applied Polymer Science.* 2002, Vol. 85, pp. 974-988.

Hansen, C.M. 2007. *Hansen solubility parameters. A user's handbook.* 2nd Ed. Boca Raton : CRC, 2007.

Harison, H. 1988. Migration of plasticizers from cling-film. *Food Additives and Contaminants.* 1988, Vol. 5, pp. 493-499.

Helmroth, E.; Rijk, R.; Dekker, M.; Jongen, W. 2002. Predictive modelling of migration from packaging materials into food products for regulatory purposes. *Trends in Food Science and Technology.* 2002, Vol. 13, pp. 102-109.

Helmroth, E., Varekamp, C. et Dekker, M. 2005. Stochastic modelling of migration from polyolefins. *Journal od the Science of Food and Agriculture.* 2005, Vol. 85, pp. 909-918.

Hernandez-Munoz, P., Catala, R. et Gavara, R. 2001. Food aromapartition between packaging materials and food simulants. *Food Additives and Contaminants.* 2001, Vol. 18, pp. 673-682.

Hildebrand, J.H. et Scott, R.L. 1936. *The Solubility of Non-Electrolytes.* New York : Reinhold, 1936.

Hines, A.L. et Maddox, R.N. 1985. *Mass transfer: fundamentals and applications.* New Jersey : Prentice Hall, 1985.

Hinrichs, K.; Piringer, O. (editors). 2002. *Evaluation of migration models tu used under Directive 90/128/EEC. Final report contract SMT4-CT98-7513.* s.l. : EUR 20604 EN (Brussels: European commission, Directorate Deneral for Research), 2002.

Hodgeman, D.K.C. 1981. Analyis of 2-hydroxybenzophenone and 2'-hydroxyphenylbenzotriazole UV stabilisers by high performance liquid chromatography. *Journal of Chromatography.* 1981, Vol. 214, pp. 237-242.

Hoy, K.L. 1985. *The Hoy Tables of Solubility Parameters.* South Charleston : Union Carbide Corp., 1985.

Hsiao, S.T.; Tseng, M.C.; Chen, Y.R.; Her, G.R. 2001. Analysis of polymer additives by matrix-assisted laser desorption ionization/time of flight mass spectrometer using delayed extraction and collision induced dissociation. *Journal of the Chinese Chemical Society.* 2001, Vol. 48, pp. 1017-1027.

INRA. 2008. Safe Food Packaging Portal : a site dedicated to the developement of decision tools based on numerical simulation and databases for the food industry. Accès le 30 Septembre 2008. http://h29.univ-reims.fr/.

ISO. 2004. Norme ISO 1183-1:2004. Plastiques -- Méthodes de détermination de la masse volumique des plastiques non alvéolaires -- Partie 1: Méthode par immersion, méthode du pycnomètre en milieu liquide et méthode par titrage.

Jordan, S.L.; Taylor, L.T. 1997. HPLC separation with solvent elimination FTIR detection of polymer additives. *Journal of Chromatographic science.* 1997, Vol. 35, pp. 7-13.

Jost, W. 1960. Diffusion in solids, liquids, gases. [auteur du livre] E.M. Loebl. *Physical chemistry vol. 1.* New York : Academis press inc., 1960.

Kaal, E.R.; Alkema, G.; Kurano, M.; Geissler, M.; Janssen, H.-G. 2007. On-line size exclusion chromatography-pyrolysis-gas chromatography-mass spectrometry for copolymer characterisation and additive analysis. *Journal of Chromatography A.* 2007, Vol. 1143, pp. 182-189.

Karstang, T.V.; Henriksen, A. 1992. Infrared spectroscopy and multivariate calibration used in quantitative analysis of additives in high-density polyethylene ; T. V. Karstang, A. Henriksen. *Chemometrics and Intelligent Laboratory System.* 1992, Vol. 14, pp. 331-339.

Kausch, H.H.; Heymans, N.; Plummer, C.J.; Decroly, P. 2001. *Traité des Matériaux - volume 14 - Matériaux polymères : propriétés mécaniques et physiques.* Lausanne : Presse Polytechnique et Universitaires Romandes, 2001.

Kinigakis, P.; Miltz, J.; Gilbert, S.G. 1987. Partition of VCM in plasticized PVC/food simulant systems. *Journal of Food Processing and Preservation.* 1987, Vol. 11, pp. 247–255.

Kirwan, M.J.; Strawbridge, J.W. 2003. Plastics in food packaging. [éd.] R. Coles, D. McDowell et M.J. Kirwan. *Food Packaging technology.* s.l. : Blackwell publishing, CRC Press, 2003, pp. 174-241.

Kithinji, J.P.; Bartle, K.D.; Raynor, M.W.; Clifford, A.A. 1990. Rapid analysis of polyolfin antioxydants and light stabilisers by supercritical fluid chromatography. *Analyst.* 1990, Vol. 115, pp. 125-128.

Klenin, V.J. 1999. *Thermodynamics of systems containing flexible-chain polymers.* Amsterdam : Elsevier Science, 1999. p. 826.

Kolb, B.; Ettre, L.S. 1991. Theory and practice of multiple headspace extraction. *Chromatographia.* 1991, Vol. 32, pp. 505-513.

Koros, W.J.; Hopfenberg, H.B. 1979. Scientific aspects of migration of indirect additives from plastics to food. *Food Technologist.* 1979, Vol. 33, pp. 56-60.

Koszinowski, J. 1986a. Diffusion and Solubility of n-Alkanes in Polyolefins. *Journal of Applied Polymer Science.* 1986, Vol. 31, pp. 1805-1826.

Koszinowski, J. 1986b. Diffusion and Solubility of Hydroxy Compounds in Polyolefins. *Journal of Applied Polymer Science.* 1986, Vol. 31, pp. 2711-2720.

Koszinowski, J.; Piringer, 0. 1990. Diffusion und relative Loslichkeit von Riechstoffen in Polyolefinen. *Verpackungs-Rundschau.* 1990, Vol. 41, pp. 15-17.

Kovarski, A.L. 1997. *Molecular dynamics of additives in polymers.* Utrecht : VSP, 1997.

Kramer, R. 1998. *Chemometric techniques for quantitative analysis.* New York : CRC, 1998.

Krzymien, M.E.; Carlsson, D.J.; Deschênes, L.; Mercier, M. 2001. Analysis of volatile transformation products from additives in gamma-irradiated polyethylene packaging. *Food Additives and Contaminants.* 2001, Vol. 18, pp. 739-749.

Lachenal, G. 1998. Analyse par spectroscopie proche infrarouge (PIR) et applications aux polymères. *Analusis Magazine.* 1998, Vol. 26, pp. M20-M29.

Lau, O.W.; Wong, S.K.; Leung, K.S. 1995. A mathematical model for the migration of naphthalene from the atmosphere into milk drink packaged in polyethylene bottles. *Packaging Technology and Science.* 1995, Vol. 8, pp. 261-170.

Lau, O.W.; Wong, S.K. 1997. Mathematical model for the migration of plasticisers from food contact materials into solid food. *Analytica Chimica Acta.* 1997, Vol. 347, pp. 249-156.

Lau, O.W.; Wong, S.K. 2000. Contamination in food from packaging material. *Journal of Chromatography A.* 2000, Vol. 882, pp. 255-270.

Leepipatpiboon, N.; Sae-Khow, O.; Jayanta, S. 2005. Simultaneous determination of bisphenol-A-diglycidyl ether, bisphenol-F-diglycidyl ether, and their derivatives in oil-in-water and aqueous-based canned foods by high-performance liquid chromatography with fluorescence detection. *Journal of Chromatography A.* 2005, Vol. 1073, pp. 331-339.

Leselier, E.; Tchapla, A. 1993. Sequential optimisation of the separation of a complex mixture of plastics additives by HPLC with a quaternary gradient and a dual detection. *Chromatographia.* 1993, Vol. 36, pp. 135-143.

Li, Y.; Yang, S.; Wang, J.; Gu, B.; Liu, F. 1999. Simultaneous determination of multicomponents in air toxic organic compounds using artificial neural networks in FTIR spectroscopy. *Spectroscopy Letters.* 1999, Vol. 32, pp. 421-429.

Lickly, T.D.; Lehr, K.M.; Welsh, G.C. 1995. Migration of styrene from polystyrene foam food-contact articles. *Food and Chemical Toxycology.* 1995, Vol. 33, pp. 475-481.

Limm, W.; Hollifield, H.C. 1996. Modelling of additive diffusion in polymers. *Food Additives and Contaminants.* 1996, Vol. 13, pp. 949-967.

Lindvig, T.; Michelsen, M.L.; Kontogeorgis, G.M. 2002. A Flory-Huggins model based on the Hansen solubility parameters. *Fluid Phase Equilibria*. 2002, Vol. 203, pp. 247-260.

Lodge, T.P. 1999. Reconciliation of the Molecular Weight Dependence of Diffusion and Viscosity in Entangled Polymers. *Physical Review Letters.* 1999, Vol. 83, pp. 3218-3221.

Luettmer-Strathmann, J.; Schoenhard, J.A.; Lipson, J.E.G. 1998. Thermodynamics of n-alkane mixtures and polyethylene-n-alkane solutions: comparison of theory and experiment. *Macromolecules.* 1998, Vol. 31, pp. 9231-9237.

Lundbäck, M.; Strandberg, C.; Albertsson, A.-C.; Hedenqvist, M.S.; Gedde, U.W. 2005. Loss of stability by migration and chemical reaction of Santonox R in branched polyethylene under anaerobic and aerobic conditions. *Polymer Degradation and Stability.* 2005, Vol. 91, pp. 1071-1078.

Macko, T.; Furtner, B.; Lederer, K. 1996. Analysis of aromatic antioxydants and ultraviolet stabilizers in polyethylene using high-temperature extraction with low boiling solvent. *Journal of Applied Polymer Science*. 1996, Vol. 62, pp. 2201-2207.

Manabe, N.; Toyoda, T.; Yokota, Y. 1999. Determination of a hindered phenol-type antioxidant by pyrolysis-GC/MS in the presence of tetramethyl ammonium hydroxyde. *Bunseki Kagaru.* 1999, Vol. 48, pp. 449-456.

Marcato, B.; Fantazzii, C.; Sevini, F. 1991. Determination of polymeric hindered amine light stabilizers in polyolefins by high performance liquid chromatography. *Journal of Chromatography.* 1991, Vol. 553, pp. 415-422.

Marcato, B.; Vianello, M. 2000. Microwave-assisted extraction by fast sample preparation for the systematic analysis of additives in polyolefins by high-performance liquid chromatography. *Journal of Chromatography A*. 2000, Vol. 869, pp. 285-300.

Marcato, B.; Guerra, S.; Vianello, M.; Scalia, S. 2003. Migration of antioxydants additives from various polyolefinic materials into oleaginous vehicles. *International Journal of Pharmaceutics.* 2003, Vol. 257, pp. 217-225.

Masaro, L.; Zhu, X.X. 1999. Physical models of diffusion for polymer solutions, gels and solids. *Progress in Polymer Science.* 1999, Vol. 24, pp. 731-775.

Matuska, R.; Preisler, L.; Sedlar, J. 1992. Determination of the polymeric light stabilizer chimassorb 944 in polyolfins by isocratic high-performance liquid chromatography. *Journal of Chromatography.* 1992, Vol. 606, pp. 136-140.

Maucourt, M. 1991. La migration des substances résiduelles des emballages dans les produits laitiers. Diplôme d'ingénieur de l'École Nationale Supérieur d'Agronomie et des Industries Alimentaires.

Mauritz, K.A.; Storey R.F.; George S. E. 1990. A General Free Volume Based Theory for the Diffusion of Large Molecules in Amorphous Polymers above Tg. 2. Molecular Shape Dependence. *Macromolecules*, 1990, Vol. 23, pp. 2033-2038.

Medick, P.; Vogel, M.; Rössler, E. 2002. Large angle jumps of small molecules in amorphous matrices analysed by 2D exchange NMR. *Journal of Magnetic Resonance.* 2002, Vol. 159, pp. 126-136.

Molander, P.; Haugland, K.; Hegna, D.R.; Ommundsen, E.; Lundanes, E.; Greibrokk, T. 1999. Determination of low levels of an antioxydant in polyolefins by large-volume injection temperature-programmed packed capillary liquid chromatography. *Journal of chromatography A.* 1999, Vol. 864, pp. 103-109.

Möller, K.; Gevert, T.; Holmström, A. 2001. Examination of a low density polyethylene (LDPE) film after 15 years of service as an air and water vapour barrier. *Polymer Degradation and Stability.* 2001, Vol. 73, pp. 69-74.

Mougharbel, A. 2007. Etude des phénomènes de transfert aux interfaces emballage-aliment ; modification des propriétés de surface par traitement plasma. Thèse de Doctorat de l'Université de Reims Champagne-Ardenne.

Multon, J.F., Lepâtre, F.; Babusiaux, C. 1992. *Additifs et auxiliaires de fabrication dans les industries agro-alimentaires.* Paris : Tes et Doc-Lavoisier, 1992.

Nath, S.K.; Banaszak, B.J.; de Pablo, J.J. 2001. Simulation of ternary mixtures of ethylene, 1-hexene, and polyethylene. *Macromolecules.* 2001, Vol. 34, pp. 7841-7848.

Nerin, C.; Salafranca, J.; Cacho, J.; Rubio, C. 1995. Separation of polymer and on-line determination of several antioxydants and UV-stabilizers by coupling size-exclusion and normal-phase high-performance liquid chromatography columns. *Journal of chromatography A.* 1995, Vol. 690, pp. 230-236.

Nielson, R.C. 1991. Extraction and quantitation of polyolefin aditives. *Journal of liquid Chromatography.* 1991, Vol. 14, pp. 503-519.

Nielson, R.C. 1993. Recent advances in polyolefin additive analysis. *Journal of liquid Chromatography.* 1993, Vol. 16, pp. 1625-1638.

O'Brien, A.P.; Cooper, I.; Tice, P.A. 1997. Correlation of specific migration (Cf) of plastics additives with their initial concentration in the polymer (Cp). *Food Additives and Contaminants.* 1997, Vol. 14, pp. 705-719.

Pacáková, V.; Leclercq, P.A. 1991. Gas chromatography-mass spectrometry and high-performance liquid chromatographic analyses of thermal degradation products of common plastics. *Journal of Chromatography.* 1991, Vol. 555, pp. 229-237.

Paik, J.S.; Tigani, M.A. 1993. Application of regular solution theory in predicting equilibrium sorption of flavor compounds by packaging polymers. *Journal of Agricultural and Food Chemistry.* 1993, Vol. 41, pp. 806–808.

Park, D.W.; Hwang, E.Y.; Kim, J.R.; Choi, J.K.; Kim, Y.A.; Woo, H.C. 1999. Catalytic degradation of polyethylene over solid acid catalysts. *Polymer Degradation and Stability.* 1999, Vol. 65, pp. 193-198.

Petersen, J.H.; Breindhal, T. 2000. Plasticizers in total diet samples, baby food and infant formulate. *Food Additives and Contaminants.* 2000, Vol. 17, pp. 133-141.

Philo, M.R.; Fordham, P.J.; Damant, A.P.; Castle, L. 1997. Measurement of Styrene Oxide in Polystyrenes, Estimation of Migration to Foods, and Reaction Kinetics and Products in Food Simulants. *Food and Chemical Toxicology.* 1997, Vol. 35, pp. 821-826.

Piao, M.; Chu, S.; Zheng, M.; Xu, X. 1999. Characterization of the combustion products of polyethylene. *Chemosphere.* 1999, Vol. 39, pp. 1497-1512.

Piringer, O.G.; Baner, A.L. 2000. *Plastic Packaging Materials for Food: Barrier Function, Mass Transport, Quality Assurance, and Legislation.* Weinheim : Wiley-VCH, 2000.

Piringer, O.G.; Baner, A.L. 2008. *Plastic packaging : interactions with food and pharmaceuticals. Second edition.* Berlin : Wiley-Vch, 2008.

Pushpa, S.A., Goonetilleke, P. et Billingham, N.C. 1996. Solubility of antioxidants in rubber. *Rubber Chemistry and Technology.* 1996, Vol. 69, pp. 885–896.

Raoult-Wack, A.-L. 2001. *Dis-moi ce que tu manges.* Paris : Gallimard, 2001.

Raynor, M.W.; Bartle, K.D.; Davies, I.L.; Williams, A.; Clifford, A.A. 1988. Polymer additive characterization by capillary supercritical fluid chromatography/Fourrier transform infrared microspectrometry. *Analitical Chemistry.* 1988, Vol. 60, pp. 427-433.

Reyne, M. 1998. *Technologie des plastiques.* Paris : HERMES, 1998.

Reynier, A.; Dole, P.; Feigenbaum, A.; Humbel, S. 2001a. Diffusion coefficients of additives in polymers. I. Correlation with geometric parameters. *Journal of Applied Polymer Science.* 2001, Vol. 82, pp. 2422-2433.

Reynier, A.; Dole, P.; Feigenbaum, A.; Humbel, S. 2001b. Diffusion coefficients of additives in polyolefins. II. Effect of swelling and temperature on the D = f(M) correlation. *Journal of Applied Polymer Science.* 2001, Vol. 82, pp. 2434-2443.

Risch, S.J. 1988. Migration of toxicants, flavours and odour-active substances from flexible packaging materials to food. *Food Technologist.* 1988, Vol. 7, pp. 95-102.

Roduit, B.; Borgeat, C.H.; Cavin, S.; Fragnière, C.; Dudler, V. 2005. Application of finite element analysis (FEA) for the simulation of release of additives from multilayer polymeric packaging structures. *Food Additives and Contaminants.* 2005, Vol. 22, pp. 945-955.

Rosca, I.D.; Vergnaud, J.-M. 2006. Approach for a testing system to evaluate food safety with polymer packages. *Polymer Testing.* 2006, Vol. 25, pp. 532-543.

Rouse, P.E. 1953. A theory of the linear viscoelastic properties of dilute solutions of coiling polymers. *Journal of Chemical Physics.* 1953, Vol. 21, pp. 1272-1280.

Ryan, T.W.; Yocklovich, S.G.; Watkins, J.C.; Levy, E.J. 1990. Quantitative analysis of additives in polymers using coupled supercritical fluid extraction-supercritical fluid chromatography. *Journal of Chromatography.* 1990, Vol. 505, pp. 273-282.

Sagiv, A. 2001. Exact solution of mass diffusion into a finite volume. Journal of Membrane Science. 2001, Vol. 186, pp. 231-237.

Sagiv, A. 2002. Theoretical formulation of the diffusion through a slab – theory validation. *Journal of Membrane Science.* 2002, Vol. 199, pp. 125-134.

Salafranca, J.; Battle, R.; Nerín, C. 1999. Use of solid-phase microextraction for the analysis of bisphenol A and bisphenol A diglycidyl ether in food simulants. *Journal of Chromatography A.* 1999, Vol. 864, pp. 137-144.

Sariban, A.; Binder, K. 1987. Critical Properties of the Flory–Huggins Lattice Model of Polymer Mixtures. *Journal of Chemical Physics.* 1987, Vol. 86, pp. 5859-5873.

Schabron, J.F.; Fenska, L.E. 1980. Determination of BHT, Irganox 1076, and Irganox 1010 antioxidant additives in polyethylene by hign performance liquid chromatography. *Analytical Chemistry.* 1980, Vol. 52, pp. 1411-1415.

Schaefer, A.; Küchler, T.; Simat, T.J.; Steinhart, H. 2003. Migration of lubricants from food packagings Screening for lipid classes and quantitative estimation using normal-phase

liquid chromatographic separation with evaporative light scattering detection. *Journal of Chromatography A.* 2003, Vol. 1017, pp. 107-116.

Schunk, T.C.; Balke, S.T.; Cheung, P. 1994. Quantitative polymer composition characterization with a liquid chromatography-Fourier transform infrared spectrometry-solvent evaporation interface. *Journal of Chromatography A.* 1994, Vol. 661, pp. 227-238.

Schweizer, K.S.; Curro, J.G. 1988. Microscopic Theory of the Structure, Thermodynamics, and Apparent χ Parameter of Polymer Blends. *Physical Review Letters.* 1988, Vol. 60, pp. 809-812.

Sharman, M.; Readn, W. A.; Castle, L.; Gilbert, J. 1994. Level of di-(2-ethylhexyl)phtalate and total phtalate esters in milk, cream, butter and cheese. *Food Additives and Contaminants.* 1994, Vol. 11, pp. 375-385.

Sheftel, V.O. 2000. *Indirect Food Additives and Polymers, migration and toxicology.* s.l. : CRC Press, 2000.

Sherwood, T.K.; Pigford, R.L.; Wilke, C.R. 1975. *Mass transfert.* New York : MsGraw Hill, 1975.

Simal-Gandara, Jesus, Damant, Andrew P. et Castle, Laurence. 2002. The use of LC-MS in studies of migration from food contact materials : a review of present applications and future possibilities. *Analytical chemistry.* 2002, Vol. 32, pp. 47-78.

Singh, R.P.; Heldman, D.R. *Introduction to food engineering.* New-York : Academic Press.

Skelland, A. 1974. *Diffusional mass transfer.* New York : London Wiley Interscience, 1974.

Skjevrak, I.; Due, A.; Gjerstad, K.O.; Herikstad, H. 2003. Volatile organic components migrating from plastic pipes (HDPE,PEX and PVC) into drinking water. *Water Research.* 2003, Vol. 37, pp. 1912-1920.

Smith, S.H. 1998. *Extraction of Additives from Polystyrene and Subsequent Analysis.* Blacksburg, Virginia : s.n., 1998. rapport de master.

Somsen, G.W.; Rozendom, E.J.E.; Gooijer, C.; Velthorst, N.H.; Brinkman, U.A.Th. 1996. Polymer analysis by column liquid chromatography coupled semi-on-line with fourrier transform infrared spectrometry. *Analyst.* 1996, Vol. 121, pp. 1069-1074.

Tan, S.; Tatsuno, T.; Okada, T. 1988. Gas chromatographic determination of calcium stearate in polyethylene food packaging sheets. *Journal of Chromatography.* 1988, Vol. 447, pp. 198-201.

Tawfik, M.S.; Huyghebaert, A. 1999. Interaction of packaging materials and vegetable oils : oil stability. *Food Chemistry.* 1999, Vol. 64, pp. 451-459.

Till, D.E.; Reid, R.C.; Schwartz, P.S.; Sidman, K.R.; Valentine, J.R.; Whelan, R.H. 1982. Plasticizer migration from polyvinyl chloride film to solvents and foods. *Food and Cosmetics Toxicology.* 1982, Vol. 20, pp. 95-104.

Torres-Lapasió, J.R.; García-Álvarez-Coque, M.C. 2006. Levels in the interpretive optimisation of selectivity in high-performance liquid chromatography: A magical mystery tour ; J.R. Torres-Lapasió, M.C. García-Álvarez-Coque. *Journal of Chromatography A.* 2006, Vol. 1120, pp. 308-321.

Van der Vegt, F.F.A.; Briels, W.J. 1998. Efficient sampling of solvent free energies in polymers. *Journal of Chemical Physics.* 1998, Vol. 109, pp. 7578-7582.

Van Krevelen, D. W. et Hoftyzer, P. J. 1976. *Properties of Polymers: Their Estimation and Correlation with Chemical Structure.* Amsterdam : Elsevier, 1976.

Vandenburg, H.J.; Clifford, A.A.; Bartle, K.D.; Carlson, R.E.; Carrol, J.; Newton, I. D. 1999. A simple solvent selection method for accelerated solvent extraction of additives from polymer. *Analyst.* 1999, Vol. 124, pp. 1707-1710.

Vargo, J.D.; Olson, K.L. 1986. Characterization of additives in plastics by liquid chromatography-mass spectrometry. *Journal of Chromatography.* 1986, Vol. 353, pp. 215-224.

Vergnaud, J.M. 1993. *Controlled Drug Release of Oral Dosage Forms.* Boca Raton : CRC, 1993.

Vitali, M. 2001. Development of a semi-quantitative attenuated total reflection infrared spectroscopy analysis method for the study of compatibility of hindered amine stabilizers in polyethylene films. *Polymer Testing.* 2001, Vol. 20, pp. 741-748.

Vitrac, O.; Hayert, M. 2007. Effect of the Distribution of Sorption Sites on Transport Diffusivities: a Contribution to the Transport of Medium-Weight-Molecules in Polymeric Materials. *Chemical Engineering Science.* 2007, Vol. 62, pp. 2503-2521.

Vitrac, O.; Lezrvant, J.; Feigenbaum, A. 2006. Decision trees as applied to the robust estimation of diffusion coefficients in polyolefins. *Journal of Applied Polymer Science.* 2006, Vol. 101, pp. 2167-2186.

Vitrac, O.; Hayert, M. 2007. Design of safe food packaging materials under uncertainty. [auteur du livre] Leon P. Berton. *Chemical Engineering Research Trends.* New York : Nova, 2007, pp. 251-292.

Vitrac, O.; Joly, C. 2008. Contact Alimentaire : évaluation de la conformité. Partie 1. Techniques de l'Ingénieur – Sciences Fondamentales – Physique Chimie – Chimie des Interfaces, AF 6930, 1-22.

Voutsas, E.C.; Tassios, D.P. 1997. Analysis of the UNIFAC-type group-contribution models at the highly dilute region. 1. Limitations of the combinatorial and residual expressions. *Industrial and Engineering Chemistry Research.* 1997, Vol. 36, pp. 4965–4972.

Wallis, M.D.; Bhatia, S.K. 2007. Thermal degradation of high density polyethylene in a reactive extruder. *Polymer Degradation and Stability.* 2007, Vol. 92, pp. 1721-1729.

Wang, F.C.-Y.. 2000. Polymer additive analysis by pyrolysis–gas chromatography IV. Antioxidants. *Journal of Chromatography A.* 2000, Vol. 891, pp. 325-336.

Wang, F.C.-Y.; Buzanowski, W.C. 2000. Polymer additive analysis by pyrolysis–gas chromatography III. Lubricants. *Journal of Chromatographie A.* 2000, Vol. 891, pp. 313-324.

Widom, B. 1963. Some topics in the theory of fluids. *Journal of Chemical Physics.* 1963, Vol. 39, pp. 2808-2812.

Wiebolt, R.C.; Kempfert, K.D.; Dalrymple, D.L. 1990. Analysis of antioxidants in polyethylene using supercritical fluid extraction/ supercritical fluid chromatography and infrared detection ; R.C. Wieboldt, K.D. Kempfert, D.L. Dalrymple. *Applied Spectroscopy.* 1990, Vol. 44, pp. 1028-1034.

Yagoubi, N.; Denuzière, A.; Pellerin, F.; Ferrier, D. 1996. Caractérisation et dosage simultannés des polymères et des additifs constitutifs d'un matériau plastique multicouches à usage pharmaceutique, par IRTF. *Annales Pharmaceutiques Françaises.* 1996, Vol. 54, pp. 126-130.

Young, T.-H.; W.-Y., Chuang. 2002. Thermodynamic analysis on the cononsolvency of poly(vinyl alcohol) in water–DMSO mixtures through the ternary interaction parameter. *Journal of Membrane Science.* 2002, Vol. 210, pp. 349-359.

Zhou, L.Y.; Ashraf-Khorassani, M.; Taylor, L.T. 1999. Comparison of methods for quantitative analysis of additives in low-density polyethylene using supercritical fluid and enhanced solvent extraction. *Journal of Chromatography A.* 1999, Vol. 858, pp. 209-218.

Zweifel, H. 2000. *Plastics Additives Handbook.* 5th edition. Munich : Hanser Publishers, 2000.

Annexes

Annexe 1 : codes utilisés pour les substances dans les figures relatives aux méthodes de dosage, d'identification et d'extraction.

code	substance
1	BHA
2	DBP
3	BHT
4	Irganox 1010
5	Ethanox 330
6	Irgafos 168
7	Irganox 1076
8	HAS-C
9	HAS-P
10	Irganox MD1024
11	BMP
12	Irgafos 126
13	HP 136
14	Irganox 3114
15	Tinuvin 328
16	Irganox 1330
17	Tinuvin 770
18	Tinuvin 622
19	Chimassorb 119
20	Chimassorb 944
21	Chimassorb 2020
22	Chimassorb 81
23	Santonox R
24	acide stéarique
25	stéarate de butyle
26	stéarate de zinc
27	oléate de butyle
28	palmitate de butyle
29	stéaramide
30	EBS
31	Irganox 1035
32	Cyasorb UV-5411
33	Irganox 1425
34	Irganox 565
35	Irganox PS802
36	Irganox 245
37	Tinuvin 327
38	Tinuvin 440

code	substance
39	Tinuvin 1130
40	Hydroxy-methoxy-benzophénone
41	Topanol CA
42	Cyasorb UV-1164
43	Erucamide
44	Oléamide
45	BHEB
46	Isonox 129
47	Palmitamide
48	Irganox 1098
49	Santowhite powder
50	Lowinox
51	Irganox 259
52	Tinuvin P
53	Tinuvin 144
54	Tinuvin 320
55	Tinuvin326
56	Vulkanox BKF
57	Tinuvin 120
58	Vulkanox NKF
59	Irganox PS800
60	2,4-Dihydroxybenzophénone
61	Cyasorb UV-9
62	Cyasorb UV-24
63	Cyasorb UV-207
64	Cyasorb UV-284
65	Irganox 2246
66	Cyasorb UV-1084
67	Tinuvin 234
68	Cyasorb UV-3346
69	Ionol 220
70	Tinuvin 292
71	Irganox MD1025
72	Stéarate de calcium
73	palmitate de n-hexadecyle
74	palmitate de cholesteryle
75	tripalmitate de glycérol
76	1,3-dipalmitate de glycérol

code	substance
77	1,2-dipalmitate de glycérol
78	monopalmitate de glycérol
79	paraffine
80	ester méthylique de l'acide stéarique
81	hexadécanol
82	cholestérol
83	diphenylbutadiène
84	Sandostab P-EPQ
85	MM 6549/072
86	Irganox 1222
87	Tinuvin 312
88	Tinuvin 350
89	Wytox 312
101	acétone
102	acide acétique
103	butanal
104	3-méthylbutanal
105	pentanal
106	toluène
106	toluène
107	2,4-pentanedione
108	hexanal
109	acide pentanoique
110	3-heptanone
111	cyclohexanone
112	heptanal
113	2-éthylhexanal
114	acide hexanoique
115	décane
116	octanal
117	undecane
118	nonanal
119	dodecane
120	decanal
121	undecanal
122	dodecanal
123	acétate de butyle
124	hexanoate d'éthyle
125	acétate d'hexyle
126	hexanoate de propyle

code	substance
127	hexanoate de butyle
128	octanoate d'éthyle
129	butanoate d'hexamethyle
130	acetate d'isobornyle
131	hexanoate d'hexyle
132	decadienoate d'éthyle
133	diisobutyrate de 2,2,4-trimethyl-1,3-pentanediol
134	2-decanone
135	2-undecanone
136	2-dodecanone
137	alpha pinene
138	delta carene
139	Limonene
140	alpha terpinolene
141	alpha farnesene
142	benzène
143	ethyl benzene
144	m-pyrene
145	p-xylene
146	o-xylene
147	isopropyl benzène
148	n-propyl benzène
149	ethyl methyl benzène
150	1,3,5-trimethyl benzène
151	1,2,4-trimethyl benzène
152	p-isopropyl toluène
153	naphtalène
201	7,8-oxyde de styrène
202	4,4'dibutylazobenzène
203	styrène
301	2,4-ditertbutylphénol
302	2,6-ditertbutyl-p-benzoquinone
303	Acide 3,5-diterbutyl-4-hydroxyphénylpropionique
304	2,6 ditertbutyl-4-methoxyphénol
305	Acide 3,5-ditertbutyl-4-hydroxybenzoique
306	Triphenyl phosphate
307	Tri-p-tolyl phosphate
308	Diphenyl phosphate

Annexe 2 : figures complètes relatives aux méthodes d'identification et de dosage.

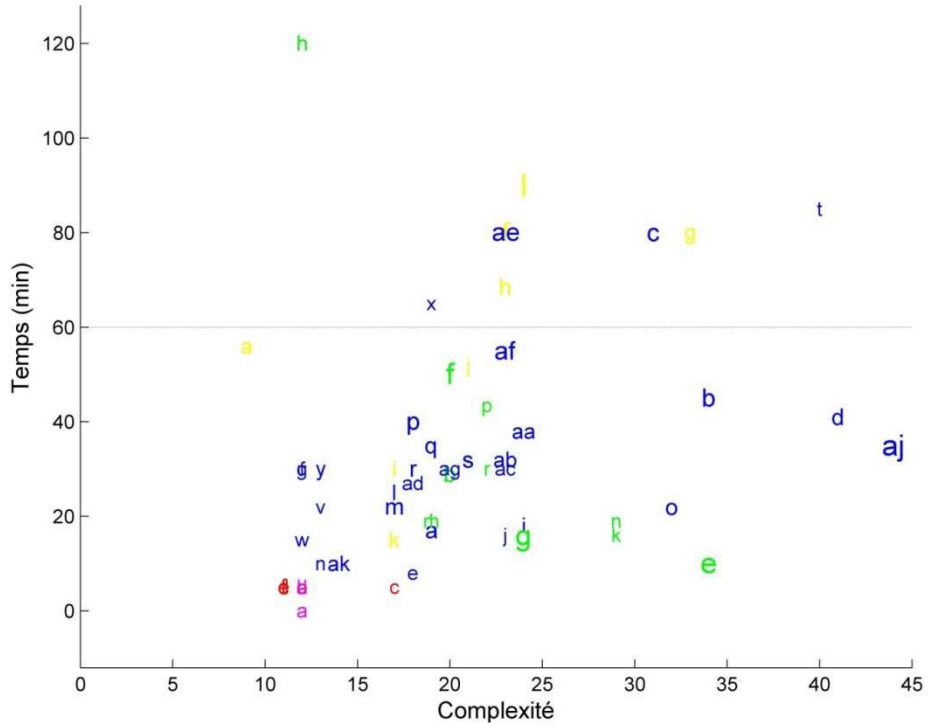

Figure 1.6. Temps nécessaire aux différentes méthodes référencées. Noir = CFS (F), bleu = CLHP (L), vert = CPG (G), rouge = IR (R), violet = UV (U). La taille du texte est proportionnelle au nombre de substances analysées par la méthode.

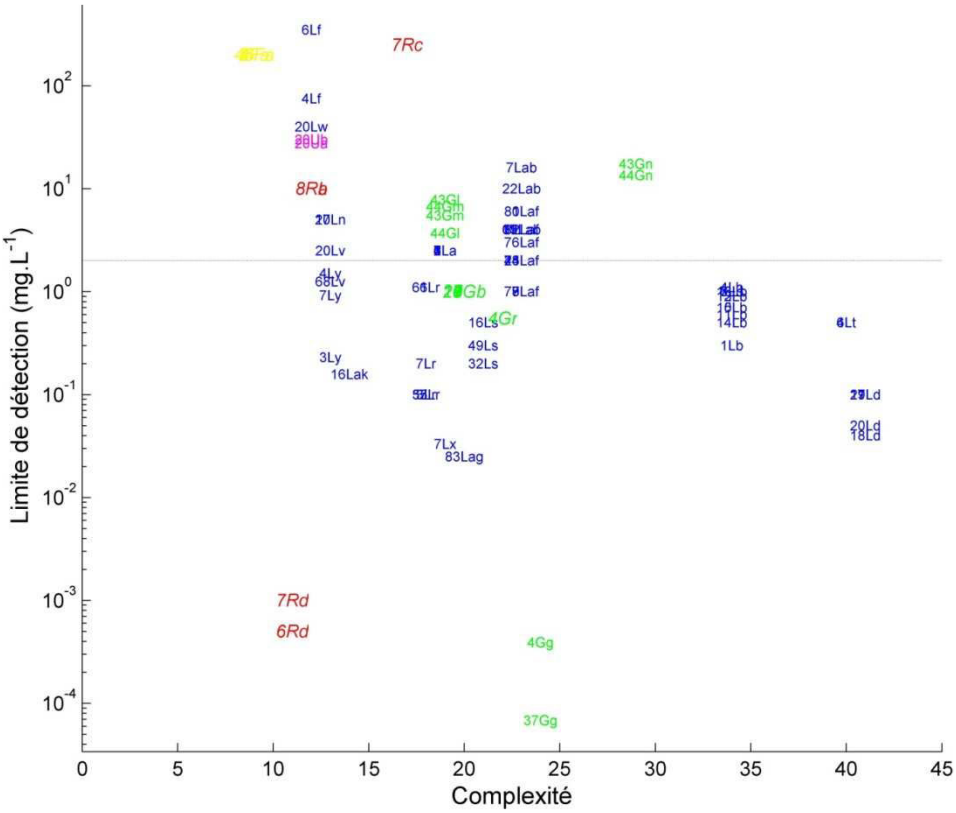

Figure 1.7. Limites de détection des additifs (cf annexe 1 pour les codes relatifs aux additifs). Les limites de détections dans les matériaux sont indiquées en gras et en italique. Noir = CFS (F), bleu = CLHP (L), vert = CPG (G), rouge = IR (R), violet = UV (U).

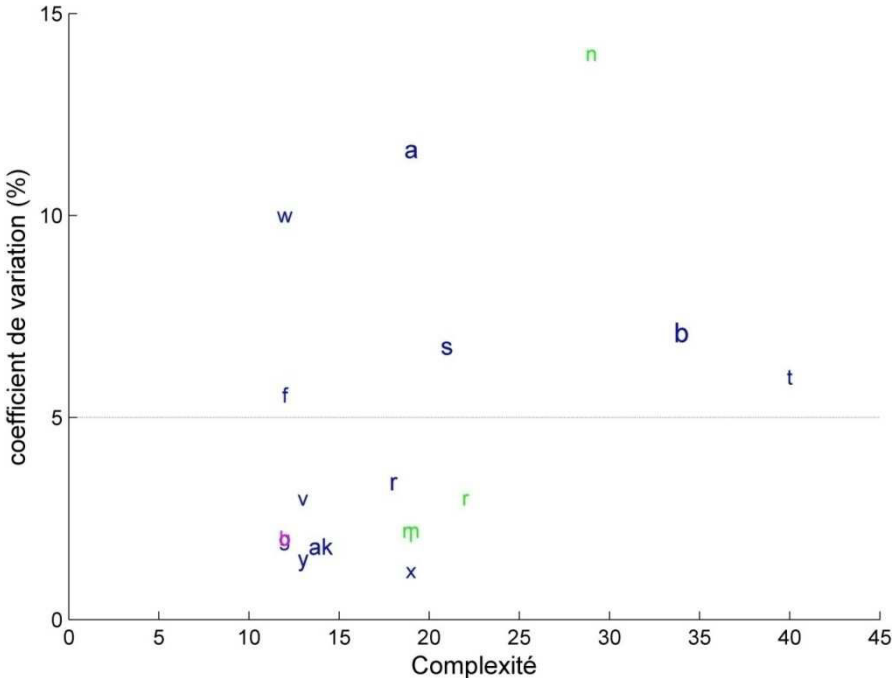

Figure 1.10. Coefficients de variation des méthodes. Noir = CFS (F), bleu = CLHP (L), vert = CPG (G), rouge = IR (R), violet = UV (U). La taille du texte est proportionnelle au nombre de substances analysées par la méthode.

Annexe 3 : liste et données des molécules étudiées.

Type de molécule	code	Nom chimique	Fonction technologique	N° CAS	LMS ($mg \cdot kg^{-1}$)	M ($g \cdot mol^{-1}$)	Structure chimique
Additif	BHT	Butylated hydroxytoluene	radical scavenger	000128-37-0	3	220	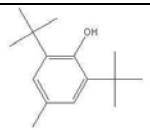
Additif	Irganox 1330	1,3,5-Trimethyl-2,4,6-tris(3,5-di-tert-butyl- 4-hydroxybenzyl) benzene	radical scavenger	01709-70-2	60	774	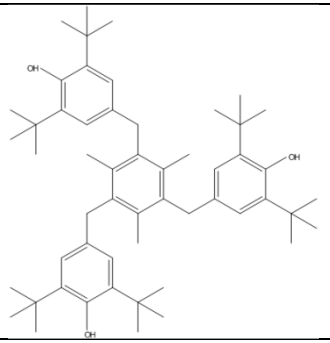
Additif	Irganox 1076	Octadecyl 3-(3,5-di-tert-butyl-4-hydroxyphenyl) propionate	radical scavenger	2082-79-3	6	530	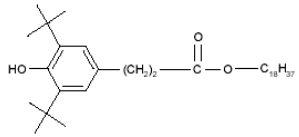
Additif	Irganox PS800	Thiodipropionic acid, didodecyl ester	hydroperoxide decomposer	00128-26-4	60	515	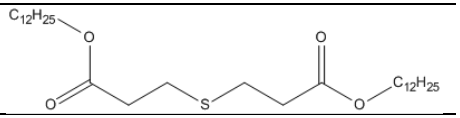
Additif	Irganox PS802	dioctadecyl Thiodipropionate	hydroperoxide decomposer	00693-36-7	5	683	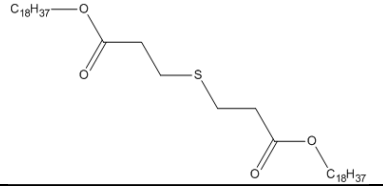
Additif	Irganox 1520	2,4-Bis(octylthiomethyl)-6-methylphenol	hydroperoxide decomposer	110553-27-0	60	424	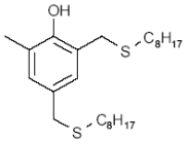

Type de molécule	code	Nom chimique	Fonction technologique	N° CAS	LMS ($mg \cdot kg^{-1}$)	M ($g \cdot mol^{-1}$)	Structure chimique
Additif	Atmer 163	N,N-Bis(2-hydroxyethyl)alkyl(C8-C18)amine	Agent antistatique	71786-60-2	60	285-309	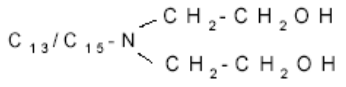
Additif	Acide stéarique	Octadecanoic acid	lubrifiant	00057-11-4	60	268	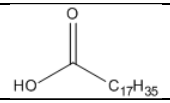
Additif	Erucamide	Cis-13-docosenoamide	Agent glissant	00112-84-5	60	337	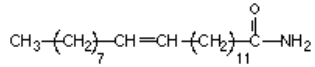
additif	Tinuvin 326	2-(2-Hydroxy-3-tert-butyl-5-methylphenyl)-5-chlorobenzotriazole	Stabilisant à la lumière	03896-11-5	30	316	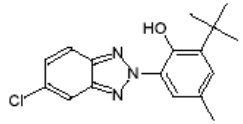
Additif	Tinuvin 770	Bis(2,2,6,6,-tetramethyl-4-piperidyl)sebaceate	Stabilisant à la lumière	52829-07-9-	60	481	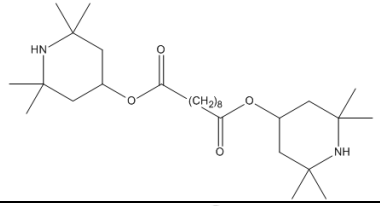
Additif	Irganox 1035	Thiodiethanol bis(3-(3,5-di-tert-butyl-4-hydroxyphenyl) propionate)	Fixateur de radicaux libre	41484-35-9	2.4	642	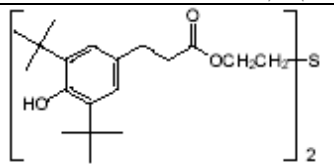
Additif	Irganox 245	Triethyleneglycol bis(3-(3-tert-butyl-4-hydroxy-5-methylphenyl) propionate)	Fixateur de radicaux libre	036443-68-2	9	586	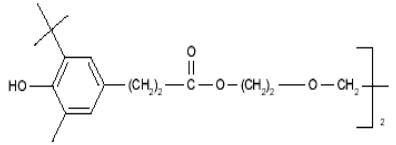
Additif	Irganox 3052	2-(1,1-dimethylethyl)-6-[3-(1,1-dimethylethyl)-2-hydroxy-5-methylphenyl] methylphenyl acrylate	Fixateur de radicaux libre	61167-58-6	60	394	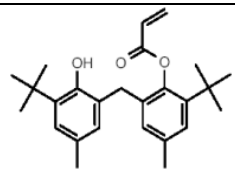

Type de molécule	code	Nom chimique	Fonction technologique	N° CAS	LMS ($mg \cdot kg^{-1}$)	M ($g \cdot mol^{-1}$)	Structure chimique
Additif	Tinuvin 622	1-(2-Hydroxyethyl)-4-hydroxy-2,2,6,6-tetramethyl piperidine-succinic acid, dimethyl ester, copolymer	Stabilisant UV	65447-77-0	30	3100-4000	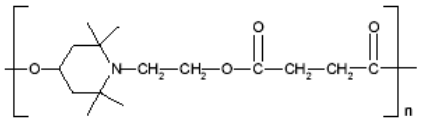
Additif	Irgafos 168	Phosphorous acid, tris(2,4-di-tert-butylphenyl) ester	Décomposeur d'hydro-peroxyde	31570-04-4	60	647	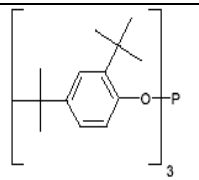
Additif	Chimassorb 81	2-Hydroxy-4-n-octyloxybenzophenone	Stabilisant UV	01843-05-6	6	326	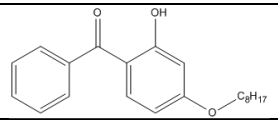
Additif	Chimassorb 944	Poly[6-[(1,1,3,3-tetramethylbutyl)amino]-1,3,5- triazine-2,4-diyl]-[(2,2,6,6-tetramethyl- 4-piperidyl)-imino]hexamethylene[(2,2,6,6 -tetramethyl-4-piperidyl)imino]	Stabilisant UV	71878-19-8	3	1200-3100	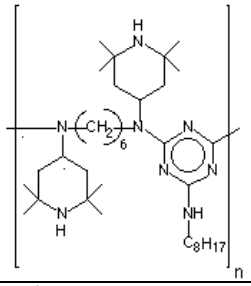
Additif	Irganox 3114	1,3,5-Tris(3,5-di-tert-butyl-4-hydroxybenzyl)-1,3,5-triazine-2,4,6(1H,3H,5H-)trione	Fixateur de radicaux libre / absorbeur UV	27676-62-6	5	784	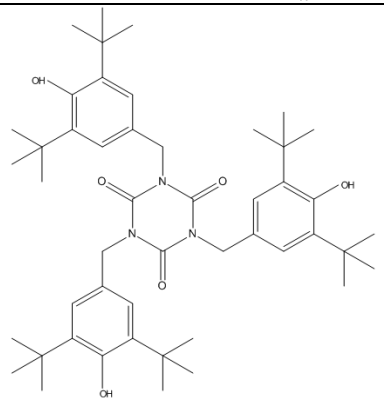

Type de molécule	code	Nom chimique	Fonction technologique	N° CAS	LMS ($mg \cdot kg^{-1}$)	M ($g \cdot mol^{-1}$)	Structure chimique
Additif	Irganox 1010	Pentaerythritol tetrakis(3-(3,5-di-tert-butyl-4-hydroxyphenyl)propionate)	Fixateur de radicaux libre	06683-19-8	60	1178	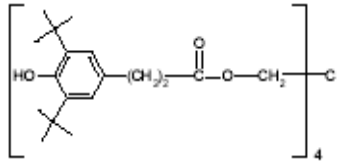
Contaminant de faible poids moléculaire	2-ITX	2-(1-methylethyl)-9H-Thioxanthen-9-one	Photoinitiateur d'encre d'impression	5495-84-1	10^{-2} †	254	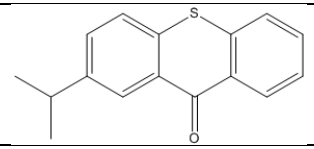
Contaminant de faible poids moléculaire	DPM	diphenylmethane	‡	101-81-5	10^{-2} †	168	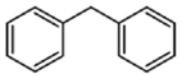
Contaminant de faible poids moléculaire	Camphre	1,7,7-riméthylbicyclo-[2,2,1]-heptan-2-one	‡	76-22-2	10^{-2} †	152	
Contaminant de faible poids moléculaire	DPO	Oxyde de diphényle	‡	101-84-8	10^{-2} †	152	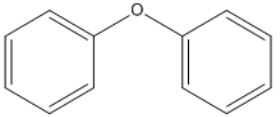
Contaminant de faible poids moléculaire	D-limonene (LIM)	1-méthyl-4-prop-1-èn-2-yl-cyclohexène	‡	5989-27-5	10^{-2} †	136	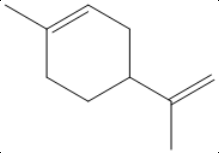
Contaminant de faible poids moléculaire	DL-menthol (MEN)	5-Methyl-2-(1-methylethyl) cyclohexanol	‡	89-78-1	10^{-2} †	156	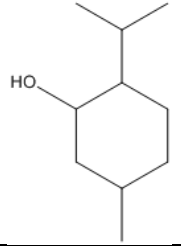

Type de molécule	code	Nom chimique	Fonction technologique	N° CAS	LMS ($mg \cdot kg^{-1}$)	M ($g \cdot mol^{-1}$)	Structure chimique
Contaminant de faible poids moléculaire	Eugénol (EUG)	4-allyl-2-méthoxyphénol	‡	97-53-0	10^{-2} †	164	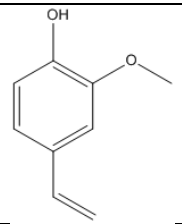
Contaminant de faible poids moléculaire	Isoamyl acetate (IAA)	3-methylbutyl ethanoate	‡	123-92-2	10^{-2} †	148	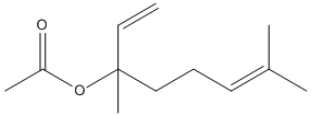
Contaminant de faible poids moléculaire	Linalyl acetate (LAA)	3,7-Dimethylocta-1,6-dien-3-yl acetate	‡	115-95-7	10^{-2} †	196	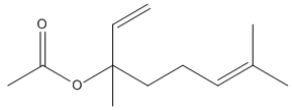
Contaminant de faible poids moléculaire	Phenylethyl alcohol (PEA)	2-Phenylethanol	‡	60-12-8	10^{-2} †	122	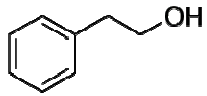

†: en supposant une contamination à travers une barrière fonctionnelle, comme décrit dans l'article 10 de la directive 2007/19/EC (CE, 2004) (CE, 2007); ‡: molécule introduite précédemment dans une étude de Baner *et al.* (Baner, et al., 1991).

INSTITUT NATIONAL
POLYTECHNIQUE
DE LORRAINE

AUTORISATION DE SOUTENANCE DE THESE
DU DOCTORAT DE L'INSTITUT NATIONAL
POLYTECHNIQUE DE LORRAINE

o0o

VU LES RAPPORTS ETABLIS PAR :
Madame Nathalie GONTARD, Professeur, Université de Montpellier II, Montpellier
Monsieur Bernard ROUSSEAU, Chargé de Recherche, Université Paris-Sud, Orsay

Le Président de l'Institut National Polytechnique de Lorraine, autorise :

Monsieur GILLET Guillaume

NANCY BRABOIS
2, AVENUE DE LA
FORET-DE-HAYE
BOITE POSTALE 3
F - 54501
VANDŒUVRE CEDEX

à soutenir devant un jury de l'INSTITUT NATIONAL POLYTECHNIQUE DE LORRAINE, une thèse intitulée :

"Prédiction de la conformité des matériaux d'emballage par intégration de méthodes de déformulation et de modélisation du coefficient de partage"

en vue de l'obtention du titre de :

DOCTEUR DE L'INSTITUT NATIONAL POLYTECHNIQUE DE LORRAINE

Spécialité : **« Procédés biotechnologiques et alimentaires »**

Fait à Vandoeuvre, le 04 novembre 2008
Le Président de l'I.N.P.L.,
F. LAURENT

TEL. 33/03.83.59.59.59
FAX. 33/03.83.59.59.55

Résumé

Les matériaux plastiques contiennent des additifs, qui ne sont pas fixés dans la matrice polymère et risquent migrer dans les aliments. La directive européenne 2002/72 a introduit la possibilité de démontrer l'aptitude au contact alimentaire de ces matériaux à partir d'approches prédictives, dont l'application est limitée par la disponibilité de données de formulation et de physico-chimie. Ces travaux visent à adapter et développer des approches analytiques rapides pour identifier et quantifier les substances majoritaires contenues dans les plastiques et à développer une approche générique de prédiction des coefficients de partage entre des polymères et les simulants de l'aliment.

Des méthodes conventionnelles d'extraction par solvant et de quantification en CLHP-UV-DEDL et CPG-DIF ont été comparées pour quatre formulations modèles de PEHD et PS. Une méthode rapide de déconvolution de spectres infrarouge d'extraits de PEHD a été développée pour identifier et quantifier les additifs.

Un modèle prédictif des coefficients d'activité dans les PE et les simulants est proposé. Les contributions enthalpique et entropique non configurationnelle sont évaluées à partir d'un échantillonnage des énergies de contact paire à paire. Il est démontré que la contribution entropique configurationnelle est indispensable à la description de l'affinité de molécules de grande taille dans les simulants polaires ou non constitués de petites molécules.

Des arbres de décision combinant approche expérimentale et modèle sont finalement discutés dans la logique de démonstration de la conformité et de veille sanitaire.

Abstract

Plastic packagings are formulated with additives, which can migrate from materials into foodstuffs. According to European directive 2002/72/EC, the ability of plastic materials to be used in contact with food can be demonstrated using modelling tools. Their use is however limited due to availability of some data, like the formulation of materials and partition coefficients of substances between plastics and food. On the one hand this work aims to develop the ability of laboratories to identify and quantify the main substances in plastic materials, and on the other hand it aims to develop a new method to predict partition coefficients between polymers and food simulants.

Four formulations of both HDPE and PS were chosen and used during the work. Standard extraction methods and quantification methods using HPLC-UV-ELSD and GC-FID were compared. A new deconvolution process applied on infrared spectra of extracts was developed to identify and quantify additives contained in HDPE.

Activity coefficients in both phases were approximated through a generalized off-lattice Flory-Huggins formulation applied to plastic materials and to liquids simulating food products. Potential contact energies were calculated with an atomistic semi-empirical forcefield. The simulations demonstrated that plastic additives have a significant chemical affinity, related to the significant contribution of the positional entropy, for liquids consisting in small molecules.

Finally, decision trees, which combine both experimental and modelling approaches to demonstrate the compliance of plastic materials, were discussed.